Master's thesis

NTNU
Norwegian University of Science and Technology
Faculty of Natural Sciences
Department of Physics

Jonas Halse Rygh

Study of the Quasiparticle Excitation Spectrum for the Ultracold, Two-Component, Synthetically Spin-Orbit Coupled, Weakly Interacting Bose Gas Residing on a Bravais Lattice

Master's thesis in MSPHYS
Supervisor: Asle Sudbø
May 2020

NTNU
Norwegian University of
Science and Technology

Jonas Halse Rygh

Study of the Quasiparticle Excitation Spectrum for the Ultracold, Two-Component, Synthetically Spin-Orbit Coupled, Weakly Interacting Bose Gas Residing on a Bravais Lattice

Master's thesis in MSPHYS
Supervisor: Asle Sudbø
May 2020

Norwegian University of Science and Technology
Faculty of Natural Sciences
Department of Physics

NTNU
Norwegian University of
Science and Technology

Master's Thesis

Study of the Quasiparticle Excitation Spectrum for the Ultracold, Two-Component, Synthetically Spin-Orbit Coupled, Weakly Interacting Bose Gas Residing on a Bravais Lattice

Jonas Halse Rygh

supervised by
Prof. Asle Sudbø

May 15, 2020

Abstract

This Master's thesis deals with the study of the two-component, synthetically spin-orbit coupled, weakly interacting Bose gas at ultra cold temperatures on a Bravais lattice. By way of mean-field theory and the Bose-Hubbard model, the excitation spectrum of the emerging quasiparticles in reciprocal space is obtained, valid in the superfluid phase. The excitation spectrum is then used to create a phase diagram, which is compared with the phase diagram for a pure condensate. Furthermore, the possibility of a superfluid critical velocity is investigated, and expressions for the chemical potentials and condensate densities are numerically analyzed.

Sammendrag

Denne masteroppgaven omhandler studiet av en to-komponent, syntetisk spin-bane koblet, svakt vekselvirkende Bose gass ved ultra kalde temperaturer bundet til et Bravais gitter. Gjennom en middelfeltstilnærming og Bose-Hubbard modellen vil eksitasjonsspektra til kvasipartiklene i det resiproke rom gis, gyldig for superfluid fasen. Disse eksitasjonsspektrene blir brukt til å generere et fasediagram som inkluderer eksitasjoner, og vil sammenliknes med fasediagrammet for et rent kondensat. I tillegg vil mulighetene for en superfluid kritisk hastighet studert, og uttrykkene for de kjemiske potensialene og kondensat-tetthetene analysert numerisk.

Preface

"All we have to decide is what to do with the time that is given to us." - Gandalf

I have spent the last 5 years of my life studying physics. This thesis can be seen as a culmination of the work laid down over the years, however, my joy for physics and mathematics will prevail beyond the submission of this thesis. Working on this thesis has been very experiential, and I have learned that hard work and determination is a key ingredient of working on any project. I have also learned the value of learning and seeking knowledge from others that know more than you do. I would like to thank my fellow student and friend Kristian Mæland for many valuable, if not necessary, discussions. I would also like to thank my supervisor Asle Sudbø, for always asking critical questions and being motivating.

A special thanks to my friends and family, and to my girlfriend for reminding me of the submission date.

Jonas Halse Rygh
Trondheim, Norway
May, 2020

Table of Contents

List of Tables

List of Figures

Chapter 1

Introduction

The first theory of a Bose-Einstein condensate dates back to more than 80 years ago, when Einstein considered a gas of non-interacting, massive bosons. He found that below a certain temperature T_c, a non-zero fraction of the bosons resided in the single-particle ground state of the system [15],[16][1]. Later, in 1938 Fritz London proposed the connection between the superfluid phase of liquid 4He, discovered experimentally in [1] and [34], and Bose-Einstein condensation [41], [42].

Bose-Einstein condensation (BEC) in dilute gases was first experimentally realized in 1995, sparking an interest in the study of ultra-cold quantum gases [44]. The first experiments used vapor of rubidium [3], sodium [12], and lithium [9]. In the first experiment, rubidium-87 atoms was confined by magnetic traps and cooled evaporatively. The vapor had to be cooled to the ultra-cold temperature of 170 nanokelvin before Bose-Einstein condensation could occur, with a number density of 2.5×10^{12} per cubic centimeter and could exist for more than 15 seconds. They observed a narrow peak in the thermal velocity distribution around zero, and as they lowered the temperature of the sample, the fraction of atoms in the vecinity of this peak increased abruptly. Bosons have integer spin [23]. The wave function for a system with identical bosons is symmetric under the interchange of spin and coordinates of any two particles [17]. Because of this, unlike fermions which have half-integer spin, bosons are able to occupy the same single-particle state. A way of estimating the transition temperature for Bose-Einstein condensation to occur, is to compare the mean particle spacing which is of order $n^{-1/3}$, where n is the average particle density, to the thermal deBroglie wavelength λ_T which is defined by [44]:

$$\lambda_T = \sqrt{\frac{2\pi}{mkT}}\hbar \tag{1.1}$$

One way to invision the thermal deBroglie wavelength is the "extent" of the wavefunction for each particle. In the classical regime, where the temprature T is large, the thermal deBroglie wavelength is small and not comparable to the mean particle spacing. Hence, there is negligible

[1] Einstein followed the work of Bose regarding the statistics of photons [8], for which the total number of photons is not a fixed quantity. Bose sent his work to Einstein, for which Einstein recoqnized the importance and translated and submitted it for publication. Consequently, Einstein included the case of *massive* bosons.

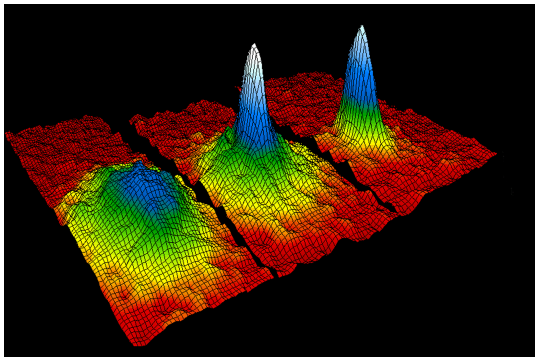

Figure 1.1: The velocity-distribution for a gas of rubidium atoms for the experiment in 1995, confirming the first Bose-Einstein condensate. In these three images in time, atoms cooled to ultra cold temperatures condensed from less dense areas on the left (red, yellow, and green) to very dense areas at the mid and right image (blue and white). Image credit: NIST/JILA/CU-Boulder.

overlap between the wavefunctions. For an ideal gas, Bose-Einstein condensation occurs when the deBroglie wavelength is comparable to the mean particle spacing [14]. Thus, one can in this limit invision the wavefunctions overlapping to form a coherent wavefunction, experiencing long rage correlations.

The *dilute* quantum gas is different from the classical gas, liquid or solid, which will be illustrated in the following. The typical condensate density in a Bose-Einstein condensed quantum gas is around $10^{13}\,\mathrm{cm}^{-3}$ to $10^{15}\,\mathrm{cm}^{-3}$. In everyday surroundings however, the density of air molecules at room temperature and atmospheric pressure is around $10^{19}\,\mathrm{cm}^{-3}$. In liquids and solid the density is around $10^{22}\,\mathrm{cm}^{-3}$, while in atoms the density of the nuclei is as at a staggering $10^{38}\,\mathrm{cm}^{-3}$. We are therefore dealing with *low-density* systems. To observe *quantum phenomena* in such low-density systems, the temperature of the system must be very low, in order of $10^{-5}\,\mathrm{K}$ or less. In contrast, for quantum phenomena to be observed for electrons in metals the temperature has to be less than the Fermi temperature, which is around $10^{4}\,\mathrm{K}$ to $10^{5}\,\mathrm{K}$, and for helium liquids the temperature must be around $1\,\mathrm{K}$.

The experiments in 1995, yielding the first BECs, exploited a technique devised in the mid 1970s for cooling alkali metal atoms using lasers. The laser-cooling had to be supported by an evaporative cooling stage, since the laser alone did not produce high enough densities and sufficiently low temperatures to create a Bose-Einstein condensate. The evaporative cooling stage then removed atoms with energies above a certain threshold, in effect cooling the less energetic atoms.

One can further confine the atoms in an optical lattice. A standing-wave laser [40] sets up a periodic potential in space, due to the fact that the electric field $\boldsymbol{E}$ is periodic in space. Thus by superimposing many lasers in one, two or three dimensions one can effectively trap the atoms in the emerging lattice. This is the physical idea behind optical lattices. The suggestion that light can be used to confine the motion of atoms is due to Letekhov [52] in 1968. As the features of the lattice is controlled externally, they offer unique tunability in modelling crystalline lattices. Lattice constants such as, potential wells and barrier walls strengths, hopping parameters etc.

may be controlled by adjusting the e.g. laser intensity [40]. Therefore optical lattices with cold atoms have often been used as a 'testing ground' for theories studying strongly correlated condensed-matter systems. As an example, we may study the Bose-Hubbard model which is the goal of this thesis.

Studying quantum gases allows us to explore quantum phenomena in great detail. In a BEC, all the atoms are essentially in the same ground state, and we may use mean-field theory to describe the system. Even though the gases are dilute, interactions play an important role as a consequence of the low temperature, causing overlap of atomic wavefunctions.

1.1 Spin-Orbit Coupling

Spin-Orbit Coupling (SOC) is a relativistic effect coupling the momentum of a particle to its quantum mechanical spin [27]. A particles spin is quantized, taking the values of $\pm\hbar/2$, commonly referred to as spin up or spin down. The spin degree of freedom has no classical counterpart, making it an important feature for a wide variety of quantum materials such as quantum magnets [5] and topological insulators [25]. This thesis will focus on ultracold atoms with *synthetic* SOC.

SOC requires *symmetry breaking*, since the coupling strength is related to the momentum as measured in a referance frame [20]. SOC thus originates from relativistic quantum mechanics, where the spin of the electrons are an essential ingredient in the equations of motion, which are given by the Dirac equation [24]. Taking the non-relativistic limit of the Dirac equation yields the Schrödinger equation, with relativistic corrections. One of these corrections couples the particles orbital angular momentum $\boldsymbol{L}$ to the quantum mechanical spin $\boldsymbol{S}$ via the term $\boldsymbol{L}\cdot\boldsymbol{S}$. This can be understood in terms of the usual $-\boldsymbol{\mu}\cdot\boldsymbol{B}$ Zeeman interaction, coupling the particles magnetic moment $\boldsymbol{\mu}$ parallel to the spin $\boldsymbol{S}$ to the effective magnetic field $\boldsymbol{B}$ present in the referance frame of the electron. SOC is most familiar in atomic physics, where it gives rise to a fine-structure splitting in the energy levels of hydrogen [39], acquiring its name: an electrons spin coupled to its orbital angular momentum about the nucleus. The electric field of the charged nucleus gives rise to an effective magnetic field in the referance frame of the electron, leading to a momentum-dependent Zeeman interaction.

This momentum dependence is particularly clear in materials. For example, Maxwells equations says that a static electric field $\boldsymbol{E} = E_0\hat{\boldsymbol{z}}$ in the laboratory frame (x, y, z) gives rise to a spin-orbit magnetic field

$$\boldsymbol{B}_{\mathrm{SO}} = \frac{E_0\hbar}{mc^2} \times (k_x\hat{\boldsymbol{y}} - k_y\hat{\boldsymbol{x}}) \tag{1.2}$$

present in the referance frame for particles moving with momentum $\hbar\boldsymbol{k}$. The resulting Zeeman interaction is on the form $-\boldsymbol{\mu}\cdot\boldsymbol{B} \approx \sigma_x k_y - \sigma_y k_x$, which is known as Rashba SOC [11], the type we will study in this thesis.[2] SOC effects are found everywhere in solids, and have been known to exist for a long time. The ongoing research and rapid development of spintronics [30], have advanced the study of these systems. This interest was motivated by a number of proposals for spintronic devices. SOC systems does not only have practical implications, but also displays many new and strange quantum mechanical fenomena, for exemple: spin-Hall effects [46],[35], topological insulators [25], and Majorana [45] and Weyl fermions [10].

[2] Here, σ_x and σ_y are the Pauli matrices. There also exist other types of SOC. See for example Dresselhaus SOC.

1.1.1 Synthetic Spin-Orbit Coupling

In an ordinary material, the intrinsic electric field generates an effective magnetic field in the referance frame of a moving electron, causing SOC. However, to get a significant SOC, this field must be extremly large. This makes it impractical for the laboratory, and one must turn to other methods. This is where *synthetic* SOC comes into play, using two-photon Raman transitions. The effect of Raman scattering was studied extensively by George Stokes prior to quantum mechanics, and observed experimentally by Sir Chandrasekhar Vankata Raman in 1928. An excited atom may not always return to its initial state after the emission of a photon; it may return to a higher or lower energy state [38],[26]. Raman scattering occurs when the scattering of incident light is *inelastic*, as opposed to Rayleigh scattering which is *elastic*. We consider a cold gas of atoms with two hyperfine states $|\downarrow\rangle$ and $|\uparrow\rangle$ with an energy difference of $\hbar w_0$, and also an excited state $|e\rangle$. Two laserbeams with momentum $\hbar \boldsymbol{k}_1$ and $\hbar \boldsymbol{k}_2$, with frequencies w_1 and w_2, are directed at the gas. The first beam is polarized such that it couples to the first state $|\downarrow\rangle$ and the excited state $|e\rangle$, and the second beam is polarized such that it couples to the second state $|\uparrow\rangle$ and the excited state $|e\rangle$. Both beams have a detuning Δ from the excited state $|e\rangle$, to supress transitions to this state. Instead, the beams scatter *inelastically* to an intermediary state, causing Raman transitions between the two states $|\uparrow\rangle$ and $|\downarrow\rangle$. This transition is made momentum dependent by a small detuning $\delta = (w_1 - w_2) - w_0$ from w_2 and $|\uparrow\rangle$. The momentum dependence of this detuning is caused by the Doppler effect; the frequencies of the incoming light are shifted in the rest frame of the atoms. In addition, the momentum dependence is furthered by the momentum transfer imparted by the photons in the collision. Hence, this experimental setup can simulate a momentum-dependent transition between two states, exactly as real spin-orbit coupling, where the states are spin states. See fig. 1.2 for a sketch of the process. We

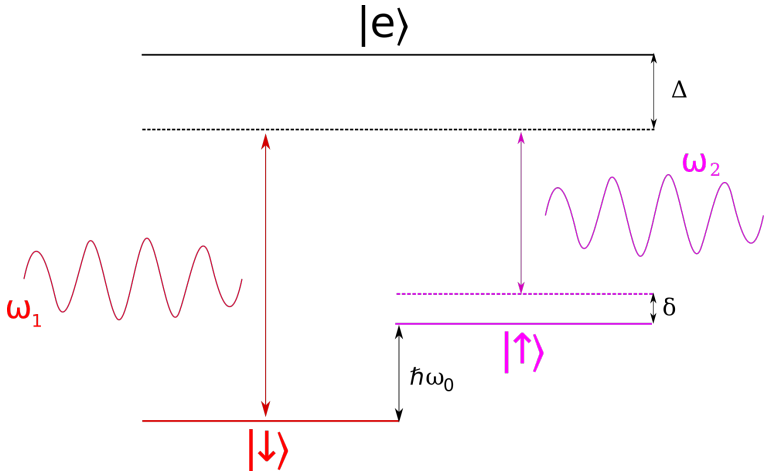

Figure 1.2: A schematic for the two-photon raman transitions.

will refer to the two hyperfine states as pseudo-spin up for $|\uparrow\rangle$ and pseudo-spin down for $|\downarrow\rangle$. Consequently, introducing spin-orbit coupling forces us to include *two* states in the description of the system.

1.2 Goal and Outline of Thesis

The work in this thesis is a continuation of the master's thesis by A.T.G Janssønn [32]. We will study the two-component, synthetically spin-orbit coupled, weakly interacting Bose gas on a Bravais lattice in great detail, utilizing diagonalization procedures and numerical methods. In Janssønns thesis, only the case of a *pure* condensate was considered, neglecting influence from excitations of the condensate. We will in this thesis also include excitations, and derive the excitation spectra for the emerging quasiparticles of the system. We will also construct a *phase diagram* for the emerging phases when going to momentum space, reproducing the case of a pure condensate which agrees with the literature, especially [21], and additionally including the case of excitations. In addition, as the Bose gas is weakly interacting, we will employ *mean-field* theory, and deduce expressions for the chemical potentials of the two pseudo-spin components, and the associated condensate densities. We will also investigate the possibility of a superfluid, which is revealed when studying the excitation spectra in the vicinity of a global minimum.

The thesis is structured as follows. Chapter 2 outlines the theoretical background for the work required, and also presents the Bose-Hubbard model in both position and momentum space, including the off-diagonal terms originating from spin-orbit coupling. In chapter 3 we treat firstly the spin-orbit coupled Bose gas without interactions, then the *one*-component weakly interacting Bose gas and finally the combined *two*-component, synthetically spin-orbit coupled, weakly interacting, Bose gas on a square lattice, which was the main focus of Janssønns master's thesis. In the same chapter, an effective method for diagonalizing bilinear Bose systems is presented, and a method for calculating the free energy, and numerically minimize its parameters, is outlined. Furthermore, we will review the case of a *pure* condensate, and give configurations for the momentum phases introduced by mean-field theory, namely, the PZ, NZ, PW, SW and LW phases. In chapters 4-8, we will treat each momentum phase in detail, diagoalizing the associated Hamiltonian and calculate the corresponding excitation spectrum. The accompanying chemical potentials and condensate densities will be explored, and the possibility of a superfluid is also studyied. In chapter 7, a phase diagram including excitations is provided. Lastly, we will discuss results and suggest future work. In the appendix, various formulas are provided, and a method for dealing with *linear* excitation operators is outlined[3].

[3]The term linear excitation operator will be explained later in the thesis.

Chapter 2

Theoretical framework

2.1 Notations and Conventions

The following list gives the notations and conventions used in this thesis

- Vectors are written in bold e.g $\boldsymbol{k}$. There will be exceptions to this, and it will be made clear when this is so.

- Lattice sites and condensate momenta are labeled by Latin lower indices such as i and j. Pseudo-spin states are labeled by greek letters such as α and β. Exceptions to this rule will be clear from the context.

- The Pauli spin matrices are σ_i, $i \in (x, y, z)$. With the convential definition

$$\sigma_x = \begin{pmatrix} 0 & 1 \\ 1 & 0 \end{pmatrix}, \quad \sigma_y = \begin{pmatrix} 0 & -i \\ i & 0 \end{pmatrix}, \quad \sigma_z = \begin{pmatrix} 1 & 0 \\ 0 & -1 \end{pmatrix} \tag{2.1}$$

  When labeled $\sigma_i^{\alpha\beta}$, where α and β are pseudo-spin indices, the elements of the Pauli matrices are

$$\sigma_i = \begin{pmatrix} \sigma_i^{\uparrow\uparrow} & \sigma_i^{\uparrow\downarrow} \\ \sigma_i^{\downarrow\uparrow} & \sigma_i^{\downarrow\downarrow} \end{pmatrix} \tag{2.2}$$

2.2 Bose-Einstein condensation

We consider a gas of non-interacting bosons with Hamiltonian given as a sum over single-particle states

$$H = \sum_{\nu} H_\nu \tag{2.3}$$

where ν is a set of quantum numbers specifying the state of the system. Let ϵ_ν be the energy of the single-particle state ν[1], and let n_ν be the occupation number for the same state. The grand-canonical partition function $\mathcal{G}$ is given by [2]

$$\mathcal{G} = \Pi_\nu \left(1 - e^{(\epsilon_\nu - \mu)/kT}\right)^{-1} \tag{2.4}$$

where k is Boltzmann's constant, T is the temperature of the system and μ is the chemical potential, associated with controlling the average number of particles in the system. Further, the average number of particles is given by

$$\begin{aligned} \langle N \rangle &= kT \frac{\partial}{\partial \mu} \ln \mathcal{G} \\ &= \sum_\nu \frac{1}{e^{(\epsilon_\nu - \mu)/kT} - 1} \end{aligned} \tag{2.5}$$

such that the mean number of particles for state ν is given by the Bose distribution function

$$\langle n_\nu \rangle = f^0(\epsilon_\nu) = \frac{1}{e^{(\epsilon_\nu - \mu)/kT} - 1} \tag{2.6}$$

We see that for f^0 to be positive, the chemical potential must be less than the ground state energy of the system, which we denote by ϵ_0. For a free particle in a box with volume V, the ground state has energy 0 such that $\mu < 0$ for all T. At high temperatures, we expect physically that the mean occupation number for state ν is much less than one. This means that, on average, we expect to find bosons spread out in the energy spectrum. To achive this we must have $e^{(\epsilon_\nu - \mu)/kT} - 1 \gg 1$, and the distribution function in eq. (2.6) is approximately given by the Boltzmann distribution,

$$f^0(\epsilon_\nu) \approx e^{-(\epsilon_\nu - \mu)/kT} \tag{2.7}$$

The fact that we get the Boltzmann distribution makes physical sense, as we in the high temperature limit expect quantum effects to become negligible. Hence this limit is often reffered to as the *classical limit*. However, we see that when T is large, μ must be chosen appropriately to achieve this. Specifically, we must have $\mu \ll \epsilon_0 - kT$ in this limit. Lets for a second imagine a gas of bosons at a high temperature. The deBroglie wavelength is tiny, such that the bosons are basically point particles. As the temperature decreases, the chemical potential rises from below and the mean occupation number for state ν increases. The chemical potential cannot exceed the value ϵ_0, as f^0 in this case is negative, which is unphysical. The mean occupation number for state ν therefore has a upper limit at the value

$$\frac{1}{e^{(\epsilon_\nu - \epsilon_0)/kT} - 1} \tag{2.8}$$

This expression blows up if $\epsilon_\nu \to \epsilon_0$. If the total number of particles in the excited states is less than N, the rest of the particles must reside in the ground state of the system, where the occupation number can be arbitrarily large. Thus the system has a Bose-Einstein condensate.

[1]The above Hamiltonian can include a trapping potential. This makes no difference for the distribution function in (2.6), where ϵ_ν is the energy spectrum with the trapping potential - i.e the energies in a harmonic oscillator. See [44], chapter 2, for details.

The number of particles N_0 in the BEC is the total number of particles N minus the number of particles in the excited states N_{ex}. The possibly finite temperature at which all the particles can be accomodated in the excitated states is referred to as the critical temperature T_c. Below the critical temperature, a large fraction of the total number of particles are found in the ground state of the system.

2.3 Second quantization

In this thesis we will use the "second quantization" formalism to describe a many-particle system, rather than the familiar first quantization [17]. This means that instead of using many-particle wave-functions $\Psi(x_1, x_2...x_n)$, we use the *occupation number representation*. In this representation, the essential information lies in the occupation number n_ν for single-particle state ν and the symmetry/anti-symmetry after the exchange of two particles. Bosons are symmetric under exchange of two particles, and the occupation number for state ν can as a consequence take any value $n_\nu = 0, 1..., \infty$, as apposed to fermions which have $n_\nu = 0, 1$. We write a state containing n_1 particles in state 1, n_2 particles in state 2 and so forth, as

$$|n\rangle = |n_1 n_2 \dots n_m\rangle \tag{2.9}$$

The total number of states is m. The bosonic creation and annihilation operators $b_\nu^\dagger$ and b_ν respectively creates and destroys a particle in state ν, and are defined as

$$b_\nu^\dagger |\dots n_\nu \dots\rangle = \sqrt{n_\nu + 1}\, |\dots n_\nu + 1 \dots\rangle \tag{2.10}$$

$$b_\nu |\dots n_\nu \dots\rangle = \sqrt{n_\nu}\, |\dots n_\nu - 1 \dots\rangle \tag{2.11}$$

The symmetry of the state under particle exchange is encoded in the commutation relations for the creation and annihilation operators

$$[b_\mu, b_\nu] = 0 \tag{2.12}$$

$$[b_\mu^\dagger, b_\nu^\dagger] = 0 \tag{2.13}$$

$$[b_\mu, b_\nu^\dagger] = \delta_{\mu\nu} \tag{2.14}$$

The indices μ and ν are *sets* of quantum numbers. The single particle state ν can for example be $\nu = (\boldsymbol{k}, \alpha)$, where $\boldsymbol{k}$ is a wavevector, and α is a spin component. The recipe for going from first quantization operators, to second quantization opeartors are as follows

$$\hat{H}_0 = \sum_{i=1}^{N} \hat{h}(x_i) \to \sum_{\mu\nu} \langle\mu|\, \hat{h}\, |\nu\rangle\, b_\mu^\dagger b_\nu \tag{2.15}$$

$$\hat{H}_I = \frac{1}{2} \sum_{i \neq j} \hat{v}(x_i, x_j) \to \frac{1}{2} \sum_{\mu\nu\lambda\rho} \langle\mu\nu|\, \hat{v}\, |\lambda\rho\rangle\, b_\nu^\dagger b_\mu^\dagger b_\lambda b_\rho \tag{2.16}$$

The coefficients in the sums are defined as

$$\langle\mu|\, \hat{h}\, |\nu\rangle = \int \phi_\mu^*(x) \hat{h}(x) \phi_\nu(x) \mathrm{d}x \tag{2.17}$$

$$\langle\mu\nu|\, \hat{v}\, |\lambda\rho\rangle = \iint \phi_\mu^*(x) \phi_\nu^*(x') \hat{v}(x, x') \phi_\lambda(x') \phi_\rho(x) \mathrm{d}x \mathrm{d}x' \tag{2.18}$$

The wavefunctions $\phi_\alpha(x) = \langle x|\alpha\rangle$ is the projection from state $|\alpha\rangle$ on $|x\rangle$. Here H_0 and H_I are respectively single and two particle operators. We will also encounter the so called *field operators* $\hat{\psi}^\dagger(x)$ and $\hat{\psi}(x)$, which are creation and annihilation operators in the space $|x\rangle$, where $x = (\boldsymbol{r}, \sigma)$ is the set of quantum numbers containing position $\boldsymbol{r}$ and spin component σ. These create or destroy a particle at position $\boldsymbol{r}$ with spin orientation σ. They also satisfy bosonic commutation relations

$$[\hat{\psi}(x), \hat{\psi}(x')] = [\hat{\psi}^\dagger(x), \hat{\psi}^\dagger(x')] = 0 \tag{2.19}$$

$$[\hat{\psi}(x), \hat{\psi}^\dagger(x')] = \delta(x - x') \tag{2.20}$$

The quantum numbers x and x' are continuous variables, in which the delta function becomes a continuous function of x and x'. The field operators can further be expanded in another basis $\{|\nu\rangle\}$ as

$$\hat{\psi}^\dagger(x) = \sum_\nu \langle x|\nu\rangle\, b_\nu^\dagger = \sum_\nu \phi_\nu(x)^* b_\nu^\dagger \tag{2.21}$$

$$\hat{\psi}(x) = \sum_\nu \langle \nu|x\rangle\, b_\nu = \sum_\nu \phi_\nu(x) b_\nu \tag{2.22}$$

2.4 The Bose-Hubbard model

The system of interest is an ultra-cold, two-component, weakly interacting Bose gas residing on an optical Bravais lattice with synthetic SOC. The Bravais-lattice is assumed to have n primitive lattice vectors $\boldsymbol{v}_i$. We for the moment forget spin-orbit coupling, and present the Hamiltonian for a two-component gas of bosons including single- and two-particle operators. This means physically that we only include two-body scattering, neglecting higher order interactions. Hence we are implicitly assuming that the occupation number for each site is not too large, as this would necissarily require higher orders of interactions. Thus the gas must be *dilute*, which means that the average distance $n^{-1/3}$ must be much larger than the average scattering length a_s, where n is the particle density. Also, it would be an advantage if we could only consider s-wave scattering, requiring that the momentums of the particles are small. Thus this system could be a dilute gas of neutral bosonic atoms, confined to an optical lattice, cooled way below the temperature for which Bose-Einstein condensation occurs.

Without SOC, the Hamiltonian for a collection of bosons with two-components $\alpha \in (\uparrow, \downarrow)$, subject to two-body scattering is given by

$$H = \sum_\alpha \int \hat{\psi}^{\alpha\dagger}(\boldsymbol{r}) \hat{h}^\alpha(\boldsymbol{r}) \hat{\psi}^\alpha(\boldsymbol{r}) \mathrm{d}\boldsymbol{r} \tag{2.23}$$

$$+ \frac{1}{2} \sum_{\alpha\beta} \iint \hat{\psi}^{\alpha\dagger}(\boldsymbol{r}) \hat{\psi}^{\beta\dagger}(\boldsymbol{r'}) v^{\alpha\beta}(|\boldsymbol{r} - \boldsymbol{r'}|) \hat{\psi}^\beta(\boldsymbol{r'}) \hat{\psi}^\alpha(\boldsymbol{r}) \mathrm{d}\boldsymbol{r} \mathrm{d}\boldsymbol{r'} \tag{2.24}$$

where $v^{\alpha\beta}$ is spherically symmetric potential that is assumed to be symmetric under permutation of particle species, that is $v^{\alpha\beta} = v^{\beta\alpha}$. Here, $\hat{\psi}^\dagger$ and $\hat{\psi}$ are field operators; $\hat{\psi}^{\alpha\dagger}(\boldsymbol{r})$ creates a boson at position $\boldsymbol{r}$ with pseudo-spin $\alpha \in (\uparrow, \downarrow)$, and $\hat{\psi}^\beta(\boldsymbol{r'})$ destroys a boson at position $\boldsymbol{r'}$ with pseudo-spin $\beta \in (\uparrow, \downarrow)$. Notice that the above Hamiltonian is the second quantization representation

of a single particle operator plus a two-particle operator. The single particle operator $\hat{h}^\alpha(\boldsymbol{r})$ is given by

$$\hat{h}^\alpha(\boldsymbol{r}) = -\frac{\nabla^2}{2m^\alpha} - \mu^\alpha + V(\boldsymbol{r}) \tag{2.25}$$

where m^α is the mass of a boson with pseudo-spin α, μ^α is a species-dependent chemical potential and $V(\boldsymbol{r})$ is a Bravais potential, which in this case is generated by the optical lattice [40]. The Bravais potential can be assumed to have the generic form[2]

$$V(\boldsymbol{r}) = V_x \sin^2(k_x x) + V_y \sin^2(k_y y) + V_z \sin^2(k_z z) \tag{2.26}$$

where the vectors $\boldsymbol{R}_i = (x_i, y_i, z_i)$ are vectors to a specific lattice site i. The direction j for the wave-vectors k_j is related to the wavelength of laser in the j'th direction by $k_j = 2\pi/\lambda_j$ with $j \in (x, y, z)$. We assume that the bosons spends most of their time in the depths located at each lattice site i, with occational tunneling from site to site, such that we may expand the field operators in the lowest-lying Wannier function basis. In the harmonic approximation [31], [22], one assumes that the bosons have a small probability of being localized far from its site i and also that the higher-energy wavefunctions for each site can be neglected. With this approximation the exact Wannier functions can be replaced by their harmonic-oscillator approximations, giving

$$w^\alpha(\boldsymbol{r} - \boldsymbol{R}_i) = w^\alpha(x - x_i)w^\alpha(y - y_i)w^\alpha(z - z_i) \tag{2.27}$$

and the Wannier function $w^\alpha(x - x_i)$ is given by

$$w^\alpha(x - x_i) = \Big(\frac{m_\alpha \omega_{x,\alpha}}{\pi}\Big)^{1/4} e^{-m_\alpha(x-x_i)^2/2} \tag{2.28}$$

$$\omega_{x,\alpha} = \sqrt{\frac{2V_x k_x^2}{m^\alpha}} \tag{2.29}$$

with similar expressions for $w^\alpha(y - y_i)$ and $w^\alpha(z - z_i)$. Notice that the expressions for the Wannier functions makes physical sense; at each lattice i the bosons are most probably found at that site and the probability of being far away decays exponentially. We next expand the field operators in Wannier functions, attaching to each site i a bosonic creation or annihilation operator

$$\hat{\psi}^{\alpha\dagger}(\boldsymbol{r}) = \sum_i w^{\alpha *}(\boldsymbol{r} - \boldsymbol{R}_i) b_i^{\alpha\dagger} \tag{2.30}$$

$$\hat{\psi}(\boldsymbol{r}) = \sum_i w^{\alpha}(\boldsymbol{r} - \boldsymbol{R}_i) b_i^{\alpha} \tag{2.31}$$

Inserting the expressions for the field operators into the single-particle Hamiltonian gives

$$H_0 = -\sum_{i \neq j} \sum_\alpha t_i j^\alpha b_i^{\alpha\dagger} b_j^\alpha - \sum_i \sum_\alpha \mu_i^\alpha b_i^{\alpha\dagger} b_i^\alpha \tag{2.32}$$

[2] One could also include a Harmonic potential at each site, which leads to a shift in the frequencies $w_{x,\alpha}$. See [40] for details.

where we have defined

$$t_{ij}^{\alpha} = -\int w^{\alpha *}(\boldsymbol{r}-\boldsymbol{R}_i)\hat{h}^{\alpha}(\boldsymbol{r})w^{\alpha}(\boldsymbol{r}-\boldsymbol{R}_j)\mathrm{d}\boldsymbol{r} \tag{2.33}$$

$$\mu_i^{\alpha} = -\int w^{\alpha *}(\boldsymbol{r}-\boldsymbol{R}_i)\hat{h}^{\alpha}(\boldsymbol{r})w^{\alpha}(\boldsymbol{r}-\boldsymbol{R}_i)\mathrm{d}\boldsymbol{r} \tag{2.34}$$

$$= -\int w^{\alpha *}(\boldsymbol{r})\hat{h}^{\alpha}(\boldsymbol{r})w^{\alpha}(\boldsymbol{r})\mathrm{d}\boldsymbol{r} \equiv \mu^{\alpha} \tag{2.35}$$

The number μ^{α} is the *new* effective chemical potential, which is in general different from the chemical potential introduced in the single particle operator $\hat{h}^{\alpha}(\boldsymbol{r})$. Notice that μ^{α} is independent of lattice index i, since $\hat{h}^{\alpha}(\boldsymbol{r}+\boldsymbol{R}_i) = \hat{h}^{\alpha}(\boldsymbol{r})$. The two-body Hamiltonian becomes

$$H_{\mathrm{int}} = \frac{1}{2}\sum_{\alpha\beta}\sum_{ijlm} U_{ijlm}^{\alpha\beta} b_i^{\alpha\dagger} b_j^{\beta\dagger} b_l^{\beta} b_m^{\alpha} \tag{2.36}$$

with the scattering coefficient U given by

$$U_{ijlm}^{\alpha\beta} = \int w^{\alpha *}(\boldsymbol{r}-\boldsymbol{R}_i)w^{\beta *}(\boldsymbol{r}'-\boldsymbol{R}_j)v^{\alpha\beta}(|\boldsymbol{r}-\boldsymbol{r}'|)w^{\beta}(\boldsymbol{r}'-\boldsymbol{R}_l)w^{\alpha}(\boldsymbol{r}-\boldsymbol{R}_m)\mathrm{d}\boldsymbol{r}\mathrm{d}\boldsymbol{r}' \tag{2.37}$$

With these definitions, the Hamiltonian is given by

$$H = -\sum_{\alpha}\sum_{i\neq j} t_{ij}^{\alpha} b_i^{\alpha\dagger} b_j^{\alpha} - \sum_{\alpha}\mu^{\alpha}\sum_i b_i^{\alpha\dagger} b_i^{\alpha} \tag{2.38}$$

$$+ \frac{1}{2}\sum_{\alpha\beta}\sum_{ijlm} U_{ijlm}^{\alpha\beta} b_i^{\alpha\dagger} b_j^{\beta\dagger} b_l^{\beta} b_m^{\alpha} \tag{2.39}$$

The first term gives origin to *hopping* between lattice sites $i \neq j$ with pseudo-spin α, where t_{ij}^{α} is the energy cost of switching lattice sites *and* remain the same pseudo-spin. The second term gives the energy cost of having a total of $n^{\alpha} = \sum_i b_i^{\alpha\dagger} b_i^{\alpha}$ particles of pseudo-spin α in the system. The effective chemical potential μ^{α} gives that energy, and can therefore be thought of as the self-energy for particles of species α. The last term is an interaction term between four lattice sites i, j, l and m.

We will now make two significant physical assumptions. We will assume *nearest neighbour hopping* and *on-site* interactions. This means that an atom on site i can only jump to its nearest neighbours, and only interact with other atoms on the same site. This requires deepening the lattice depths such that the overlap of non-neighbouring Wannier functions are negligable, which is known as the *thight-binding* limit. This implies that the two-body scattering potential $v^{\alpha\beta}$ takes the form of a point-like interaction

$$v^{\alpha\beta}(|\boldsymbol{r}-\boldsymbol{r}'|) = \gamma^{\alpha\beta}\delta(\boldsymbol{r}-\boldsymbol{r}') \tag{2.40}$$

where the coefficient $\gamma^{\alpha\beta}$ is given by [40]

$$\gamma^{\alpha\beta} = \gamma^{\beta\alpha} = \frac{2\pi(m^{\alpha}+m^{\beta})a^{\alpha\beta}}{m^{\alpha}m^{\beta}} \tag{2.41}$$

Hence the particles are subjected to an on-site two-body scattering potenial dependent on the respective masses of the species, and the intra and inter scattering lengths $a^{\alpha\beta}$. This gives the much simpler Hamiltonian

$$H = -\sum_{\alpha}\sum_{\langle i,j\rangle} t_{ij}^{\alpha} b_i^{\alpha\dagger} b_j^{\alpha} - \sum_{\alpha}\mu^{\alpha}\sum_i b_i^{\alpha\dagger} b_i^{\alpha} \tag{2.42}$$

$$+ \frac{1}{2}\sum_{\alpha\beta}\sum_i U_{iiii}^{\alpha\beta} b_i^{\alpha\dagger} b_i^{\beta^\dagger} b_i^{\beta} b_i^{\alpha} \tag{2.43}$$

We sum over $\langle i,j\rangle$ nearest neighbour couples, and replace the sum over $ijlm$ by i after the assumption of on-site interactions. The four-body interaction potential $U_{iiii}^{\alpha\beta}$ becomes:

$$U_{iiii}^{\alpha\beta} = \gamma^{\alpha\beta}\int w^{\alpha*}(\boldsymbol{r}-\boldsymbol{R}_i) w^{\beta*}(\boldsymbol{r}-\boldsymbol{R}_i) w^{\beta}(\boldsymbol{r}-\boldsymbol{R}_i) w^{\alpha}(\boldsymbol{r}-\boldsymbol{R}_i)\mathrm{d}\boldsymbol{r} \tag{2.44}$$

$$= \gamma^{\alpha\beta}\int w^{\alpha*}(\boldsymbol{r}) w^{\beta*}(\boldsymbol{r}) w^{\beta}(\boldsymbol{r}) w^{\alpha}(\boldsymbol{r})\mathrm{d}\boldsymbol{r} \tag{2.45}$$

$$= \gamma^{\alpha\beta}\int |w^{\alpha}(\boldsymbol{r})|^2 |w^{\beta}(\boldsymbol{r})|^2 \boldsymbol{r} \equiv U^{\alpha\beta} = U^{\beta\alpha} > 0 \tag{2.46}$$

Consequently, the on-site interaction strength is repulsive and independent of lattice site i. We will also assume that the hopping parameters t_{ij}^{α} are real and independent of lattice sites (i,j). With these assumptions, the final Hamiltonian with two-body scattering becomes

$$H = -\sum_{\alpha} t^{\alpha}\sum_{\langle i,j\rangle} b_i^{\alpha\dagger} b_j^{\alpha} - \sum_{\alpha}\mu^{\alpha}\sum_i b_i^{\alpha\dagger} b_i^{\alpha} \tag{2.47}$$

$$+ \frac{1}{2}\sum_{\alpha\beta} U^{\alpha\beta}\sum_i b_i^{\alpha\dagger} b_i^{\beta^\dagger} b_i^{\beta} b_i^{\alpha} \tag{2.48}$$

This Hamiltonian is the version of the Bose-Hubbard model [29] that we will use in this thesis. We assume that the sign of t^{α} is positive, such that hopping is energetically favorable. The sign of $U^{\alpha\beta}$ is positive, such that interactions are not energetically favorable. The sign of μ^{α} is yet ambigous, and it will be revealed later that the effective chemical potential only needs to be bounded from below.

2.4.1 Fourier transform

We next assume periodic boundary conditions, which means that $b_{i+N_s} = b_i$ where N_s is the number of lattice sites. We also define the set of displacement vectors to the nearest neigbour pair $\langle i,j\rangle$ as

$$\boldsymbol{\delta}_{\langle i,j\rangle} = \{\pm\boldsymbol{a}_1, \pm\boldsymbol{a}_2 \ldots \pm\boldsymbol{a}_m\} \tag{2.49}$$

where the $\boldsymbol{a}_i$'s are of equal lengths. We next expand the creation and annihilation $b_i^{\alpha\dagger}$ and b_i^{α} in *momentum* space operators $\{A_{\boldsymbol{k}}^{\alpha}\}$, in the following manner [19]

$$b_i^{\alpha\dagger} = \frac{1}{\sqrt{N_s}}\sum_{\boldsymbol{k}} e^{-i\boldsymbol{k}\cdot\boldsymbol{R}_i} A_{\boldsymbol{k}}^{\alpha\dagger} \tag{2.50}$$

$$b_i^{\alpha} = \frac{1}{\sqrt{N_s}}\sum_{\boldsymbol{k}} e^{i\boldsymbol{k}\cdot\boldsymbol{R}_i} A_{\boldsymbol{k}}^{\alpha} \tag{2.51}$$

with the particularly simple inverse relation

$$A_{\boldsymbol{k}}^{\alpha\dagger} = \frac{1}{\sqrt{N_s}} \sum_i e^{i\boldsymbol{k}\cdot\boldsymbol{R}_i} b_i^{\alpha\dagger} \tag{2.52}$$

$$A_{\boldsymbol{k}}^{\alpha} = \frac{1}{\sqrt{N_s}} \sum_i e^{-i\boldsymbol{k}\cdot\boldsymbol{R}_i} b_i^{\alpha} \tag{2.53}$$

The Fourier transformed operators $A_{\boldsymbol{k}}$ are bosonic, as seen by

$$[A_{\boldsymbol{k}}^{\alpha}, A_{\boldsymbol{k}'}^{\beta\dagger}] = \frac{1}{N_s} \sum_{i,j} e^{i(\boldsymbol{k}'\cdot\boldsymbol{r}_j - \boldsymbol{k}\cdot\boldsymbol{r}_i)} [b_i^{\alpha}, b_j^{\beta\dagger}] \tag{2.54}$$

$$= \frac{\delta^{\alpha\beta}}{N_s} \sum_{i,j} e^{i(\boldsymbol{k}'\cdot\boldsymbol{r}_j - \boldsymbol{k}\cdot\boldsymbol{r}_i)} \delta_{ij} \tag{2.55}$$

$$= \delta^{\alpha\beta} \frac{1}{N_s} \sum_i e^{i(\boldsymbol{k}'-\boldsymbol{k})\cdot\boldsymbol{r}_i} \tag{2.56}$$

$$= \delta^{\alpha\beta} \delta_{\boldsymbol{k}\boldsymbol{k}'} \tag{2.57}$$

with the relations $[A_{\boldsymbol{k}}^{\alpha}, A_{\boldsymbol{k}'}^{\beta}] = [A_{\boldsymbol{k}}^{\alpha\dagger}, A_{\boldsymbol{k}'}^{\beta\dagger}] = 0$ proved similarly. The sum over $\langle i,j\rangle$ may be simplified by utilizing the vectors in $\boldsymbol{\delta}_{\langle i,j\rangle}$, where we write $\sum_{\langle i,j\rangle} = \sum_i \sum_{\boldsymbol{\delta}}$, for $\boldsymbol{\delta} \in \boldsymbol{\delta}_{\langle i,j\rangle}$. The nearest neighbour lattice vectors for site i is given by $\boldsymbol{R}_j = \boldsymbol{R}_i + \boldsymbol{\delta}$. We insert the expressions for b_i^{α} and $b_i^{\alpha\dagger}$ into the Bose-Hubbard Hamiltonian in eq. (2.48), giving the hopping term

$$-\sum_{\alpha} t^{\alpha} \sum_{\langle i,j\rangle} b_i^{\alpha\dagger} b_i^{\alpha} = -\sum_{\alpha} t^{\alpha} \sum_{\boldsymbol{k}\boldsymbol{k}'} \left(\sum_{\langle i,j\rangle} \frac{1}{N_s} e^{i(\boldsymbol{k}'\cdot\boldsymbol{R}_j - \boldsymbol{k}\cdot\boldsymbol{R}_i)} \right) A_{\boldsymbol{k}}^{\alpha\dagger} A_{\boldsymbol{k}'}^{\alpha} \tag{2.58}$$

$$= -\sum_{\alpha} t^{\alpha} \sum_{\boldsymbol{k}\boldsymbol{k}'} \sum_i \sum_{\boldsymbol{\delta}} e^{i\boldsymbol{k}'\cdot\boldsymbol{\delta}} \frac{1}{N_s} e^{i(\boldsymbol{k}'-\boldsymbol{k})\cdot\boldsymbol{R}_i} A_{\boldsymbol{k}}^{\alpha\dagger} A_{\boldsymbol{k}'}^{\alpha} \tag{2.59}$$

$$= -\sum_{\alpha} t^{\alpha} \sum_{\boldsymbol{k}\boldsymbol{k}'} \sum_{\boldsymbol{\delta}} e^{i\boldsymbol{k}'\cdot\boldsymbol{\delta}} \delta_{\boldsymbol{k}\boldsymbol{k}'} A_{\boldsymbol{k}}^{\alpha\dagger} A_{\boldsymbol{k}'}^{\alpha} \tag{2.60}$$

$$= -\sum_{\alpha} t^{\alpha} \sum_{\boldsymbol{k}} \sum_{\boldsymbol{\delta}} e^{i\boldsymbol{k}\cdot\boldsymbol{\delta}} A_{\boldsymbol{k}}^{\alpha\dagger} A_{\boldsymbol{k}}^{\alpha} \tag{2.61}$$

$$= -\sum_{\boldsymbol{k}} \sum_{\alpha} \epsilon_{\boldsymbol{k}}^{\alpha} A_{\boldsymbol{k}}^{\alpha\dagger} A_{\boldsymbol{k}}^{\alpha} \tag{2.62}$$

where we have used the important relation

$$\sum_i \frac{1}{N_s} e^{i(\boldsymbol{k}'-\boldsymbol{k})\cdot\boldsymbol{R}_i} = \delta_{\boldsymbol{k},\boldsymbol{k}'} \tag{2.63}$$

and defined the single-particle energies in $\boldsymbol{k}$-space

$$\epsilon_{\boldsymbol{k}}^{\alpha} = t^{\alpha} \sum_{\boldsymbol{\delta}} e^{i\boldsymbol{k}\cdot\boldsymbol{\delta}} \tag{2.64}$$

By a similar analysis, the chemical potential term contributes,

$$-\sum_{\alpha}\mu^{\alpha}\sum_{i}b_{i}^{\alpha\dagger}b_{i}^{\alpha}=-\sum_{\boldsymbol{k}}\sum_{\alpha}\mu^{\alpha}A_{\boldsymbol{k}}^{\alpha\dagger}A_{\boldsymbol{k}}^{\alpha} \tag{2.65}$$

and the interaction term becomes:

$$\frac{1}{2}\sum_{\alpha\beta}U^{\alpha\beta}\sum_{i}b_{i}^{\alpha\dagger}b_{i}^{\beta\dagger}b_{i}^{\beta}b_{i}^{\alpha}=\frac{1}{2N_{s}}\sum_{\alpha\beta}U^{\alpha\beta}\sum_{\boldsymbol{k}\boldsymbol{k}'\boldsymbol{p}\boldsymbol{p}'}\sum_{i}\frac{1}{N_{s}}e^{i\boldsymbol{R}_{i}\cdot(\boldsymbol{p}+\boldsymbol{p}'-(\boldsymbol{k}+\boldsymbol{k}'))} \tag{2.66}$$

$$\times A_{\boldsymbol{k}}^{\alpha\dagger}A_{\boldsymbol{k}'}^{\beta\dagger}A_{\boldsymbol{p}}^{\beta}A_{\boldsymbol{p}'}^{\alpha} \tag{2.67}$$

where the sum over i gives conservation of momentum, leading to

$$H_{\text{int}}=\frac{1}{2N_{s}}\sum_{\alpha\beta}\sum_{\boldsymbol{k}\boldsymbol{k}'\boldsymbol{p}\boldsymbol{p}'}U^{\alpha\beta}A_{\boldsymbol{k}}^{\alpha\dagger}A_{\boldsymbol{k}'}^{\beta\dagger}A_{\boldsymbol{p}}^{\beta}A_{\boldsymbol{p}'}^{\alpha}\delta_{\boldsymbol{k}+\boldsymbol{k}',\boldsymbol{p}+\boldsymbol{p}'} \tag{2.68}$$

Finally, we have the Hamiltonian in momentum space

$$H=-\sum_{\boldsymbol{k}}\sum_{\alpha}(\epsilon_{\boldsymbol{k}}^{\alpha}+\mu^{\alpha})A_{\boldsymbol{k}}^{\alpha\dagger}A_{\boldsymbol{k}}^{\alpha} \tag{2.69}$$

$$+\frac{1}{2N_{s}}\sum_{\alpha\beta}\sum_{\boldsymbol{k}\boldsymbol{k}'\boldsymbol{p}\boldsymbol{p}'}U^{\alpha\beta}A_{\boldsymbol{k}}^{\alpha\dagger}A_{\boldsymbol{k}'}^{\beta\dagger}A_{\boldsymbol{p}}^{\beta}A_{\boldsymbol{p}'}^{\alpha}\delta_{\boldsymbol{k}+\boldsymbol{k}',\boldsymbol{p}+\boldsymbol{p}'} \tag{2.70}$$

We can also simplify the single-particle energies $\epsilon_{\boldsymbol{k}}^{\alpha}$, by using that the displacement vectors $\boldsymbol{a}_i$ come in pairs on the form $(\boldsymbol{a}_n,-\boldsymbol{a}_n)$, giving

$$\epsilon_{\boldsymbol{k}}^{\alpha}=t^{\alpha}\sum_{\boldsymbol{\delta}}e^{i\boldsymbol{k}\cdot\boldsymbol{\delta}} \tag{2.71}$$

$$=t^{\alpha}\sum_{n}\left(e^{i\boldsymbol{k}\cdot\boldsymbol{a}_{n}}+e^{-i\boldsymbol{k}\cdot\boldsymbol{a}_{n}}\right) \tag{2.72}$$

$$=2t^{\alpha}\sum_{n}\cos(\boldsymbol{k}\cdot\boldsymbol{a}_{n}) \tag{2.73}$$

The Hamiltonian in eq. (2.70) is the version which will be used for the weakly interacting Bose gas. In the next section, a heuristic derivation of synthetic spin-orbit coupling is deduced, leading to new terms in the Hamiltonian.

2.5 Synthetic SOC

For a system of electrons moving in a static electric field $\boldsymbol{E}=E_0\boldsymbol{z}$ in two dimensions, the spin-orbit coupling is of the Rashba type [20],[48], giving the Hamiltonian

$$H_{\text{SOC}}=\lambda_R\left(\sigma_x k_y-\sigma_y k_x\right) \tag{2.74}$$

where the coupling strength is given by $\lambda_R=e\hbar^2E_0/4m_e^2c^2$ [48], which we will assume is positive. The following work is based on the derivation from Jansønn in [32], where he derives his work

from Sjømark [47]. The component $k_n \equiv \boldsymbol{k}\cdot\hat{\boldsymbol{a}}_n$ along the non-parallel unit vectors $\hat{\boldsymbol{a}}_n = \boldsymbol{a}_n/\|\boldsymbol{a}_n\|$ of the nearest neighbor lattice displacement vectors contained in $\boldsymbol{\delta}_{\langle i,j\rangle}$ is discretized as follows

$$k_n = -i\sum_i \left(b_i^\dagger b_{i+n} - b_{i+n}^\dagger b_i\right) \tag{2.75}$$

where the index $i+n$ refers to the lattice site displaced by $+\boldsymbol{a}_n$ from $\boldsymbol{r}_i$, and

$$b_i = \begin{pmatrix} b_i^\uparrow \\ b_i^\downarrow \end{pmatrix} \tag{2.76}$$

Next we decompose $\boldsymbol{k}$ in the euclidean unit vectors, and in the non-parallell unit vectors

$$\boldsymbol{k} = \sum_i k_i \boldsymbol{x}_i = \sum_n k_n \hat{\boldsymbol{a}}_n \tag{2.77}$$

Consequently, the component k_i can be expressed by k_n in the following way

$$k_i = \sum_n k_n(\hat{\boldsymbol{a}}_n \cdot \boldsymbol{x}_i) \tag{2.78}$$

This gives that the Rasbha SOC Hamiltonian can be expressed as

$$H_{\text{SOC}} = i\lambda_R \sum_{\alpha\beta}\sum_n\sum_i b_i^{\alpha\dagger}\left(-\sigma_x^{\alpha\beta}(\hat{\boldsymbol{a}}_n\cdot\boldsymbol{y}) + \sigma_y^{\alpha\beta}(\hat{\boldsymbol{a}}_n\cdot\boldsymbol{x})\right) b_{i+n}^\beta - \text{H.c} \tag{2.79}$$

where we have explicitly moved the Pauli matrices between the products of $b_i^\dagger$ and b_{i+n}, to form a matrix product on the form $\boldsymbol{x}^\dagger A\boldsymbol{x} = \sum_{\alpha\beta}\boldsymbol{x}^{\alpha\dagger}A_{\alpha\beta}x^\beta$. This makes the derivation heuristic, not rigorous. It is however a variation of the Kane-Mele model [33]. The Hamiltonian contains a term on the form $\sum_{\alpha\beta} b_i^{\alpha\dagger}\sigma_x^{\alpha\beta}b_{i+n}^\beta$, which written out becomes

$$\sum_{\alpha\beta} b_i^{\alpha\dagger}\sigma_x^{\alpha\beta}b_{i+n}^\beta = \begin{pmatrix} b_i^{\uparrow\dagger} & b_i^{\downarrow\dagger}\end{pmatrix}\begin{pmatrix}0 & 1\\ 1 & 0\end{pmatrix}\begin{pmatrix} b_{i+n}^\uparrow \\ b_{i+n}^\downarrow\end{pmatrix} \tag{2.80}$$

$$= \begin{pmatrix} b_i^{\uparrow\dagger} & b_i^{\downarrow\dagger}\end{pmatrix}\begin{pmatrix} b_{i+n}^\downarrow \\ b_{i+n}^\uparrow\end{pmatrix} \tag{2.81}$$

$$= b_i^{\uparrow\dagger}b_{i+n}^\downarrow + b_i^{\downarrow\dagger}b_{i+n}^\uparrow \tag{2.82}$$

The first term $b_i^{\uparrow\dagger}b_{i+n}^\downarrow$ annihilates a boson at lattice site $i+n$ with pseudo-spin $\downarrow$, and creates a boson at lattice site i with psedo-spin $\uparrow$, while the second term is similar only with opposite spin-orientation. Thus this process consist of hopping from site $i+n$ to i, and flipping the spins. The H.c term in the Hamiltonian then consist of hopping from site i to $i+n$, with a spin-flip.

We next go to momentum space, and expand the bosonic operators b_i^α in the momentum

basis $\{A^{\alpha}_{\boldsymbol{k}}\}$ as in the previous section

$$H_{\text{SOC}} = i\lambda_R \sum_{\alpha\beta}\sum_{n}\sum_{i} b_i^{\alpha\dagger}\Sigma_n^{\alpha\beta} b_{i+n}^{\beta} - \text{H.c} \tag{2.83}$$

$$= i\lambda_R \sum_{\alpha\beta}\sum_{n}\sum_{i} \frac{1}{N_s}\sum_{\boldsymbol{k}\boldsymbol{k}'} A_{\boldsymbol{k}}^{\alpha\dagger}\Sigma_n^{\alpha\beta} A_{\boldsymbol{k}'}^{\beta} e^{i(\boldsymbol{k}'-\boldsymbol{k})\cdot\boldsymbol{R}_i} e^{i\boldsymbol{k}'\cdot\boldsymbol{a}_n} - \text{H.c} \tag{2.84}$$

$$= i\lambda_R \sum_{\alpha\beta}\sum_{n}\sum_{\boldsymbol{k}\boldsymbol{k}'} A_{\boldsymbol{k}}^{\alpha\dagger}\Sigma_n^{\alpha\beta} A_{\boldsymbol{k}'}^{\beta}\delta_{\boldsymbol{k}\boldsymbol{k}'} e^{i\boldsymbol{k}'\cdot\boldsymbol{a}_n} \tag{2.85}$$

$$= i\lambda_R \sum_{\boldsymbol{k}}\sum_{n}\sum_{\alpha\beta} A_{\boldsymbol{k}}^{\alpha\dagger}\Sigma_n^{\alpha\beta} e^{i\boldsymbol{k}\cdot\boldsymbol{a}_n} A_{\boldsymbol{k}}^{\beta} - \text{H.c} \tag{2.86}$$

where we have defined

$$\Sigma_n^{\alpha\beta} = \sigma_y^{\alpha\beta}(\hat{\boldsymbol{a}}_n\cdot\boldsymbol{x}) - \sigma_x^{\alpha\beta}(\hat{\boldsymbol{a}}_n\cdot\boldsymbol{y}) \tag{2.87}$$

Next, explicitly writing out the sum over pseudo-spin indices, one obtains

$$H_{\text{SOC}} = \sum_{\boldsymbol{k}} s_{\boldsymbol{k}} A_{\boldsymbol{k}}^{\uparrow\dagger} A_{\boldsymbol{k}}^{\downarrow} + \text{H.c} \tag{2.88}$$

The spin-orbit coupling $s_{\boldsymbol{k}}$ is given by

$$s_{\boldsymbol{k}} = \pm 2\lambda_R \sum_n \left((\hat{\boldsymbol{a}}_n\cdot\boldsymbol{y}) + i(\hat{\boldsymbol{a}}_n\cdot\boldsymbol{x})\right)\sin(\boldsymbol{k}\cdot\boldsymbol{a}_n) \tag{2.89}$$

where the sign $\pm$ relies on the definition of the transformation from b_i^{α} to $A_{\boldsymbol{k}}^{\alpha}$. If the exponential has a $+\boldsymbol{k}$ sign in the transformation of b_i^{α}, see eq. (2.51), as in this thesis, then one must choose a plus sign above. If however one has a $-\boldsymbol{k}$ in the exponential, as was done in Janssøns thesis, then one must choose a minus sign. To be consistent with Jansønns master thesis, we will choose a minus sign. This should not affect the physics, as the choice is only a matter of definition.

The full Hamiltonian with synthetic SOC and weak interactions, residing on a Bravais lattice now becomes

$$H = \sum_{\boldsymbol{k}} s_{\boldsymbol{k}} A_{\boldsymbol{k}}^{\uparrow\dagger} A_{\boldsymbol{k}}^{\downarrow} + \text{H.c} \tag{2.90}$$

$$- \sum_{\boldsymbol{k}}\sum_{\alpha}(\epsilon_{\boldsymbol{k}}^{\alpha} + \mu^{\alpha}) A_{\boldsymbol{k}}^{\alpha\dagger} A_{\boldsymbol{k}}^{\alpha} \tag{2.91}$$

$$+ \frac{1}{2N_s}\sum_{\alpha\beta}\sum_{\boldsymbol{k}\boldsymbol{k}'\boldsymbol{p}\boldsymbol{p}'} U^{\alpha\beta} A_{\boldsymbol{k}}^{\alpha\dagger} A_{\boldsymbol{k}'}^{\beta^{\dagger}} A_{\boldsymbol{p}}^{\beta} A_{\boldsymbol{p}'}^{\alpha}\delta_{\boldsymbol{k}+\boldsymbol{k}',\boldsymbol{p}+\boldsymbol{p}'} \tag{2.92}$$

$$= \sum_{\boldsymbol{k}}\sum_{\alpha\beta} \eta_{\boldsymbol{k}}^{\alpha\beta} A_{\boldsymbol{k}}^{\alpha\dagger} A_{\boldsymbol{k}}^{\beta} \tag{2.93}$$

$$+ \frac{1}{2N_s}\sum_{\alpha\beta}\sum_{\boldsymbol{k}\boldsymbol{k}'\boldsymbol{p}\boldsymbol{p}'} U^{\alpha\beta} A_{\boldsymbol{k}}^{\alpha\dagger} A_{\boldsymbol{k}'}^{\beta^{\dagger}} A_{\boldsymbol{p}}^{\beta} A_{\boldsymbol{p}'}^{\alpha}\delta_{\boldsymbol{k}+\boldsymbol{k}',\boldsymbol{p}+\boldsymbol{p}'} \tag{2.94}$$

The matrix $\eta_{\boldsymbol{k}}$ is defined as

$$\eta_{\boldsymbol{k}} = \begin{pmatrix} \eta_{\boldsymbol{k}}^{\uparrow\uparrow} & \eta_{\boldsymbol{k}}^{\uparrow\downarrow} \\ \eta_{\boldsymbol{k}}^{\downarrow\uparrow} & \eta_{\boldsymbol{k}}^{\downarrow\downarrow} \end{pmatrix} = \begin{pmatrix} -(\epsilon_{\boldsymbol{k}}^{\uparrow} + \mu^{\uparrow}) & s(\boldsymbol{k}) \\ s^*(\boldsymbol{k}) & -(\epsilon_{\boldsymbol{k}}^{\downarrow} + \mu^{\downarrow}) \end{pmatrix} \tag{2.95}$$

We next construct the Feynman diagrams [18] for the single-particle Hamiltonian and the interacting Hamiltoninan. The single-particle Hamiltonian is given by

$$H_{\text{non-int}} = \sum_{\boldsymbol{k}} \sum_{\alpha\beta} \eta_{\boldsymbol{k}}^{\alpha\beta} A_{\boldsymbol{k}}^{\alpha\dagger} A_{\boldsymbol{k}}^{\beta} \tag{2.96}$$

where the diagonal terms of $\eta_{\boldsymbol{k}}$ is simply the single-particle energies, see fig. 2.1a for the corresponding Feynman diagram. The off-diagonal terms however, corresponds to a spin-flip, which is precisely what the Raman transitions describe. See Feynman diagram in fig. 2.1b for the case where $\alpha = \uparrow$ and $\beta = \downarrow$. In the off-diagonal, a boson with momentum $\boldsymbol{k}$ and pseudo-spin $\beta = \downarrow$ is destroyed and a boson with momentum $\boldsymbol{k}$ and pseudo-spin $\alpha = \uparrow$ is created. Hence, the spin-orbit coupling flips the spin in momentum space.

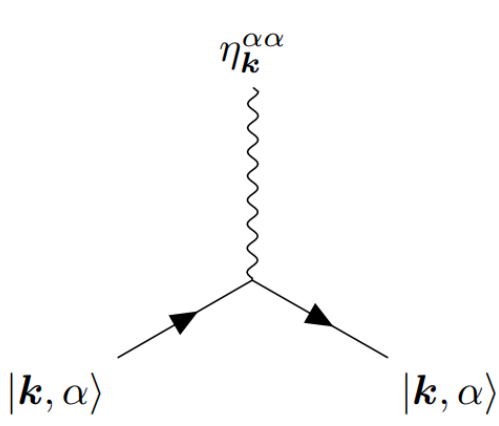

(a) Feynman diagram along diagonal of $\eta_{\boldsymbol{k}}^{\alpha\beta}$

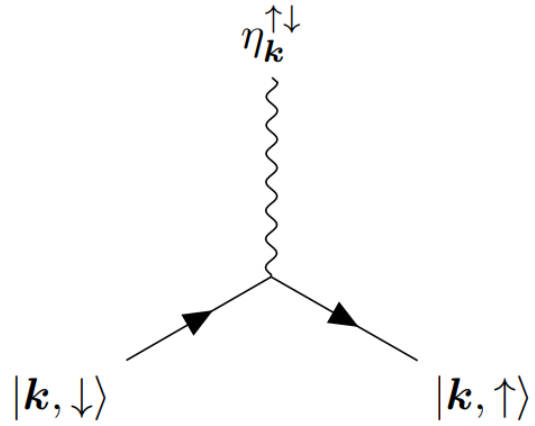

(b) Feynman diagram for the case of $\alpha = \uparrow$, $\beta = \downarrow$ in the single-particle Hamiltonian

Figure 2.1: Feynman diagrams for the single-particle Hamiltonian

The interacting Hamiltonian is given by

$$H_{\text{int}} = \frac{1}{2N_s} \sum_{\alpha\beta} \sum_{\boldsymbol{k}\boldsymbol{k}'\boldsymbol{p}\boldsymbol{p}'} U^{\alpha\beta} A_{\boldsymbol{k}}^{\alpha\dagger} A_{\boldsymbol{k}'}^{\beta\dagger} A_{\boldsymbol{p}}^{\beta} A_{\boldsymbol{p}'}^{\alpha} \delta_{\boldsymbol{k}+\boldsymbol{k}',\boldsymbol{p}+\boldsymbol{p}'} \tag{2.97}$$

where conservation of momentum fixes $\boldsymbol{k} = \boldsymbol{p} + \boldsymbol{p}' - \boldsymbol{k}'$. We introduce the wavevector $\boldsymbol{q} = \boldsymbol{k}' - \boldsymbol{p}$, such that

$$\boldsymbol{k} = \boldsymbol{p}' - \boldsymbol{q} \tag{2.98}$$

$$\boldsymbol{k}' = \boldsymbol{p} + \boldsymbol{q} \tag{2.99}$$

Consequently, we can write the interacting Hamiltonian in the generic way

$$H_{\text{int}} = \sum_{\boldsymbol{q}} \sum_{\alpha\beta} v^{\alpha\beta}(\boldsymbol{q}) \sum_{\boldsymbol{p},\boldsymbol{p}'} A_{\boldsymbol{p}'-\boldsymbol{q}}^{\alpha\dagger} A_{\boldsymbol{p}+\boldsymbol{q}}^{\beta\dagger} A_{\boldsymbol{p}}^{\beta} A_{\boldsymbol{p}'}^{\alpha} \tag{2.100}$$

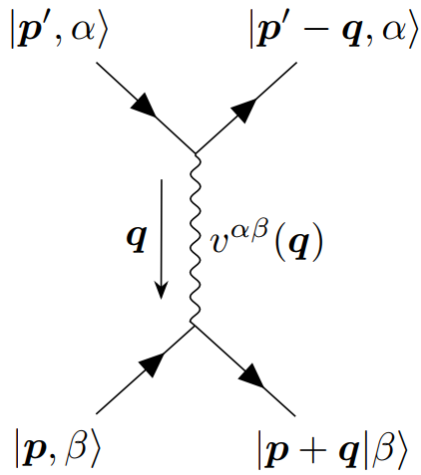

Figure 2.2: Feynman diagram for the interacting Hamiltonian

The potential $v^{\alpha\beta}(\boldsymbol{q})$ is independent of $\boldsymbol{q}$ and is given by

$$v^{\alpha\beta}(\boldsymbol{q}) = \frac{U^{\alpha\beta}}{2N_s} \tag{2.101}$$

The interacting Hamiltonian has the Feynman diagram as shown in fig. 2.2. The process thus describes scattering: two bosons with momentum and pseudo-spin $|\boldsymbol{p}', \alpha\rangle$ and $|\boldsymbol{p}, \beta\rangle$ are annihilated, where the total momentum is $\boldsymbol{p} + \boldsymbol{p}'$. The creation operators then creates two bosons with momentum and spin $|\boldsymbol{p}' - \boldsymbol{q}, \alpha\rangle$ and $|\boldsymbol{p} + \boldsymbol{q}, \beta\rangle$. The interaction is mediated by the therm $v^{\alpha\beta}(\boldsymbol{q})$. Note that the two-body scattering does not change the initial configuration of spins, as spin-orbit coupling does. Also, the total momentum before and after the collosion is of course conserved, since $\boldsymbol{p} + \boldsymbol{q} + \boldsymbol{p}' - \boldsymbol{q} = \boldsymbol{p} + \boldsymbol{p}'$.

Chapter 3

Preliminaries

3.1 Synthetically Spin-Orbit Coupled, Non-Interacting Bose Gas

In this section we will analytically derive the excitation spectrum for a spin-orbit coupled, non-interacting Bose gas. This example will aid our intuition in the main part of the thesis. It is a simplification of the Hamiltonian given in eq. (2.94). We will also review the process of diagonalizing a matrix, where we bring corrections to Janssønns master thesis which produces the wrong basis-transformation. The Hamiltonian in question is given by, where we simply set $U = 0$ in eq. (2.94)

$$H = \sum_{\boldsymbol{k}} \sum_{\alpha\beta} \eta_{\boldsymbol{k}}^{\alpha\beta} A_{\boldsymbol{k}}^{\alpha\dagger} A_{\boldsymbol{k}}^{\beta} \tag{3.1}$$

A square matrix A is said to be *diagonizable* if there exists an invertible matrix T such that $T^{-1}AT$ is diagonal [4]. In this case the matrix T is said to diagonalize A. An important result from linear algebra is that a square $n \times n$ matrix A is diagonizable if and only if A has n linearly independent eigenvectors. The advantage of diagonalizing a Hamiltonian is that it is rewritten as a sum over Harmonic oscillators [23] on the form $\sum_\nu e_\nu n_\nu$, where $n_\nu = B_\nu^\dagger B_\nu$ is the number operator and e_ν is a single-particle energy. Thus the diagonalized Hamiltonian simply sums the energy of each single- particle state ν, multiplied by the number of particles in that state. We call the new set of operators B_ν *quasiparticles*. The list of quasiparticles is long, with a few examples: anyons [54], skyrmions [37], excitons [36] and the familiar phonons [13]. The quasiparticles of a system effectively describe the dynamics.

The above Hamiltonian is not diagonal, but can be brought on diagonal form by changing particle basis from $S = \left\{A_{\boldsymbol{k}}^{\uparrow}, A_{\boldsymbol{k}}^{\downarrow}\right\}$ to $S' = \left\{B_{\boldsymbol{k}}^{+}, B_{\boldsymbol{k}}^{-}\right\}$ where the new operators $B_{\boldsymbol{k}}^{\alpha}$ must satisfy bosonic commutation relations:

$$[B_{\boldsymbol{k}}^{\alpha}, B_{\boldsymbol{k}'}^{\beta\dagger}] = \delta_{\boldsymbol{k}\boldsymbol{k}'}\delta^{\alpha\beta} \tag{3.2}$$

For all $\boldsymbol{k}$ and $\boldsymbol{k}'$ and $\alpha, \beta \in (+, -)$. The diagonalized Hamiltonian can then be written on the

form

$$H = \sum_{\boldsymbol{k}} \sum_{\alpha} \lambda_k^{\alpha\alpha} B_{\boldsymbol{k}}^{\alpha\dagger} B_{\boldsymbol{k}}^{\alpha} \tag{3.3}$$

where $\lambda_{\boldsymbol{k}}^{\alpha\alpha}$ are elements of the diagonal matrix

$$\lambda_{\boldsymbol{k}} = \begin{pmatrix} \lambda_{\boldsymbol{k}}^{++} & \lambda_{\boldsymbol{k}}^{+-} \\ \lambda_{\boldsymbol{k}}^{-+} & \lambda_{\boldsymbol{k}}^{--} \end{pmatrix} = \begin{pmatrix} \lambda_{\boldsymbol{k}}^{+} & 0 \\ 0 & \lambda_{\boldsymbol{k}}^{-} \end{pmatrix} \tag{3.4}$$

To find the new basis, and the corresponding eigenvalues, we observe that the Hamiltonian in (3.1) can be written in the form:

$$H = \sum_{\boldsymbol{k}} \psi_{\boldsymbol{k}}^{\dagger} \eta_{\boldsymbol{k}} \psi_{\boldsymbol{k}} \tag{3.5}$$

Where $\psi_{\boldsymbol{k}} = \begin{pmatrix} A_{\boldsymbol{k}}^{\uparrow} & A_{\boldsymbol{k}}^{\downarrow} \end{pmatrix}^T$ and $\psi_{\boldsymbol{k}}^{\dagger} = \begin{pmatrix} A_{\boldsymbol{k}}^{\uparrow\dagger} & A_{\boldsymbol{k}}^{\downarrow\dagger} \end{pmatrix}$. Linear algebra states that a Hermitian matrix M can be diagonalized on the form $M = PDP^{\dagger}$, where D is the diagonal matrix with the eigenvalues of M along the diagonal, and P is the matrix with the corresponding orthonormalized eigenvectors as columns (such that $PP^{\dagger} = P^{\dagger}P = I$). Writing $\eta_{\boldsymbol{k}} = P_{\boldsymbol{k}} \lambda_{\boldsymbol{k}} P_{\boldsymbol{k}}^{\dagger}$, we get

$$H = \sum_{\boldsymbol{k}} \psi_{\boldsymbol{k}}^{\dagger} P_{\boldsymbol{k}} \lambda_{\boldsymbol{k}} P_{\boldsymbol{k}}^{\dagger} \psi_{\boldsymbol{k}} \equiv \sum_{\boldsymbol{k}} \phi_{\boldsymbol{k}}^{\dagger} \lambda_{\boldsymbol{k}} \phi_{\boldsymbol{k}} \tag{3.6}$$

where we have made a change of basis from $\psi_{\boldsymbol{k}}$ to $\phi_{\boldsymbol{k}}$ by the following relation

$$\phi_{\boldsymbol{k}} = P_{\boldsymbol{k}}^{\dagger} \psi_{\boldsymbol{k}} \tag{3.7}$$

Or, equivalently, by an inversion

$$\psi_{\boldsymbol{k}} = P_{\boldsymbol{k}} \phi_{\boldsymbol{k}} \tag{3.8}$$

Note that this is opposite of the results by Janssønn, where he uses the same $P_{\boldsymbol{k}}$. There it was claimed that $P\eta P^{\dagger}$ was a diagonal matrix, when it is fact $P^{\dagger}\eta P$ which gives the diagonal matrix. The elements of $\phi_{\boldsymbol{k}}$ are given by

$$\phi_{\boldsymbol{k}} = \begin{pmatrix} B_{\boldsymbol{k}}^{+} \\ B_{\boldsymbol{k}}^{-} \end{pmatrix} \tag{3.9}$$

and the transformation matrix $P_{\boldsymbol{k}}$ has the form

$$P_{\boldsymbol{k}} = \begin{pmatrix} \boldsymbol{x}^{+} & \boldsymbol{x}^{-} \end{pmatrix} \tag{3.10}$$

where the columns are the eigenvectors of the eigenvalue problem $\eta_{\boldsymbol{k}} \boldsymbol{x}^{\pm} = \lambda_{\boldsymbol{k}}^{\pm} \boldsymbol{x}^{\pm}$. The eigenvalues are determined by the condition $\det(\eta_{\boldsymbol{k}} - I_2 \lambda_{\boldsymbol{k}})$, and are given by

$$\lambda_{\boldsymbol{k}}^{\pm} = -\bar{\epsilon}_{\boldsymbol{k}} - \bar{\mu} \pm \sqrt{|s_{\boldsymbol{k}}|^2 + \frac{(\delta\epsilon_{\boldsymbol{k}} + \delta\mu)^2}{4}} \tag{3.11}$$

with the definitions

$$\bar{\epsilon}_{\boldsymbol{k}} = \frac{\epsilon_{\boldsymbol{k}}^{\uparrow} + \epsilon_{\boldsymbol{k}}^{\downarrow}}{2}, \quad \delta\epsilon_{\boldsymbol{k}} = \epsilon_{\boldsymbol{k}}^{\uparrow} - \epsilon_{\boldsymbol{k}}^{\downarrow} \tag{3.12}$$

$$\bar{\mu} = \frac{\mu^{\uparrow} + \mu^{\downarrow}}{2}, \quad \delta\mu = \mu^{\uparrow} - \mu^{\downarrow} \tag{3.13}$$

As noted by Janssønn, we get a *Zeeman splitting* at $\boldsymbol{k} = 0$, given by the difference in energies at $\boldsymbol{k} = 0$

$$\lambda_0^+ - \lambda_0^- = |\delta\epsilon_{\boldsymbol{k}} + \delta\mu| \tag{3.14}$$

which is non-zero if the pseduo-spin parameters μ^α and t^α are spin-dependent. For the moment, we treat pseudo-spin parameters equally, which gives no Zeeman splitting

$$\mu^\uparrow = \mu^\downarrow \equiv \mu \tag{3.15}$$

$$t^\uparrow = t^\downarrow \equiv t \tag{3.16}$$

$$\epsilon_{\boldsymbol{k}}^\uparrow = \epsilon_{\boldsymbol{k}}^\downarrow \equiv \epsilon_{\boldsymbol{k}} \tag{3.17}$$

We also restrict our analysis to the case of a square lattice with displacement vectors given as $\boldsymbol{a}_n \in (a\boldsymbol{x}, a\boldsymbol{y})$, where a is the lattice spacing constant. Using the expressions for $s_{\boldsymbol{k}}$ and $\epsilon_{\boldsymbol{k}}$ given in eqs. (2.73) and (2.89), we get

$$s_{\boldsymbol{k}} = -2\lambda_R \left(\sin(k_y a) + i \sin(k_x a)\right) \tag{3.18}$$

$$\epsilon_{\boldsymbol{k}} = 2t \left(\cos(k_x a) + \cos(k_y a)\right) \tag{3.19}$$

which gives the eigenvalues $\lambda_{\boldsymbol{k}}^\pm$ as

$$\lambda_{\boldsymbol{k}}^\pm = -(\epsilon_{\boldsymbol{k}} + \mu) \pm |s_{\boldsymbol{k}}| \tag{3.20}$$

with the corresponding orthonormalized eigenvectors

$$\boldsymbol{x}^\pm = \begin{cases} \frac{1}{\sqrt{2}} \begin{pmatrix} 1 \\ 0 \end{pmatrix}, \frac{1}{\sqrt{2}} \begin{pmatrix} 0 \\ 1 \end{pmatrix} & s_{\boldsymbol{k}} = 0 \\ \frac{1}{\sqrt{2}} \begin{pmatrix} \pm e^{-i\gamma_{\boldsymbol{k}}} \\ 1 \end{pmatrix} & s_{\boldsymbol{k}} \neq 0 \end{cases} \tag{3.21}$$

where the spin-orbit coupling is written as

$$e^{-i\gamma_{\boldsymbol{k}}} \equiv \frac{s_{\boldsymbol{k}}}{|s_{\boldsymbol{k}}|}, \quad s_{\boldsymbol{k}} \neq 0 \wedge \gamma_{\boldsymbol{k}} \in [0, 2\pi) \tag{3.22}$$

and $\gamma_{\boldsymbol{k}}$ is the *helicity* angle. If $s_{\boldsymbol{k}} = 0$, there is no change in basis. This can be seen from the fact that the original Hamiltonian then becomes diagonal. If $s_{\boldsymbol{k}} \neq 0$, the matrix $P_{\boldsymbol{k}}$ takes the form

$$P_{\boldsymbol{k}} = \frac{1}{\sqrt{2}} \begin{pmatrix} e^{-i\gamma_{\boldsymbol{k}}} & -e^{-i\gamma_{\boldsymbol{k}}} \\ 1 & 1 \end{pmatrix} \tag{3.23}$$

giving the new basis as

$$\begin{pmatrix} B_{\boldsymbol{k}}^+ \\ B_{\boldsymbol{k}}^- \end{pmatrix} \overset{(3.7)}{=} \frac{1}{\sqrt{2}} \begin{pmatrix} A_{\boldsymbol{k}}^\downarrow + e^{i\gamma_{\boldsymbol{k}}} A_{\boldsymbol{k}}^\uparrow \\ A_{\boldsymbol{k}}^\downarrow - e^{i\gamma_{\boldsymbol{k}}} A_{\boldsymbol{k}}^\uparrow \end{pmatrix} \tag{3.24}$$

which differs from the eigenvectors given by Janssønn, since there the new basis was defined as $\phi_{\boldsymbol{k}} = P_{\boldsymbol{k}} \phi_{\boldsymbol{k}}$ with the *same* matrix $P_{\boldsymbol{k}}$. The eigenvectors can compactly be written as

$$B_{\boldsymbol{k}}^\alpha = \frac{1}{\sqrt{2}} \left(A_{\boldsymbol{k}}^\downarrow + \alpha e^{i\gamma_{\boldsymbol{k}}} A_{\boldsymbol{k}}^\uparrow\right), \quad \alpha \in (+, -) \tag{3.25}$$

We must further verify that the new basis of operators satisfy bosonic commutation relations

$$\left[B_{\boldsymbol{k}}^{\alpha}, B_{\boldsymbol{k}'}^{\beta\dagger}\right] = \frac{1}{2}\left[A_{\boldsymbol{k}}^{\downarrow} + \alpha e^{i\gamma_{\boldsymbol{k}}} A_{\boldsymbol{k}}^{\uparrow}, A_{\boldsymbol{k}'}^{\downarrow\dagger} + \beta e^{-i\gamma_{\boldsymbol{k}'}} A_{\boldsymbol{k}'}^{\uparrow\dagger}\right] \tag{3.26}$$

$$= \frac{1}{2}\left(\left[A_{\boldsymbol{k}}^{\downarrow}, A_{\boldsymbol{k}'}^{\downarrow\dagger}\right] + \alpha\beta\left[A_{\boldsymbol{k}}^{\uparrow}, A_{\boldsymbol{k}'}^{\uparrow\dagger}\right]\right) \tag{3.27}$$

$$= \frac{\delta_{\boldsymbol{k}\boldsymbol{k}'}}{2}(1+\alpha\beta) \tag{3.28}$$

The $1+\alpha\beta$ term is 2 if $\alpha = \beta = \pm$ or 0 if $\alpha \neq \beta = \pm$, so we can conclude that indeed

$$\left[B_{\boldsymbol{k}}^{\alpha}, B_{\boldsymbol{k}'}^{\beta\dagger}\right] = \delta_{\boldsymbol{k}\boldsymbol{k}'}\delta^{\alpha\beta} \tag{3.29}$$

The old basis $\psi_{\boldsymbol{k}}$ is connected with the new basis $\phi_{\boldsymbol{k}}$ by an inversion

$$\begin{pmatrix} A_{\boldsymbol{k}}^{\uparrow} \\ A_{\boldsymbol{k}}^{\downarrow} \end{pmatrix} \overset{(3.8)}{=} \frac{1}{\sqrt{2}} \begin{pmatrix} e^{-i\gamma_{\boldsymbol{k}}}\left(B_{\boldsymbol{k}}^{+} - B_{\boldsymbol{k}}^{-}\right) \\ B_{\boldsymbol{k}}^{+} + B_{\boldsymbol{k}}^{-} \end{pmatrix} \tag{3.30}$$

One can confirm that the new basis gives a diagonal Hamiltonian by inserting the expressions in (3.30) in the original Hamiltonian, obtaining

$$\begin{aligned}
\mathcal{H} = \sum_{\boldsymbol{k}} & B_{\boldsymbol{k}}^{+\dagger} B_{\boldsymbol{k}}^{+}\left(\frac{\xi}{2} + \frac{\xi}{2} + \frac{|s_{\boldsymbol{k}}|}{2} + \frac{|s_{\boldsymbol{k}}|}{2}\right) \\
& + B_{\boldsymbol{k}}^{+\dagger} B_{\boldsymbol{k}}^{-}\left(-\frac{\xi}{2} + \frac{\xi}{2} + \frac{|s_{\boldsymbol{k}}|}{2} - \frac{|s_{\boldsymbol{k}}|}{2}\right) \\
& + B_{\boldsymbol{k}}^{-\dagger} B_{\boldsymbol{k}}^{+}\left(-\frac{\xi}{2} + \frac{\xi}{2} - \frac{|s_{\boldsymbol{k}}|}{2} + \frac{|s_{\boldsymbol{k}}|}{2}\right) \\
& + B_{\boldsymbol{k}}^{-\dagger} B_{\boldsymbol{k}}^{-}\left(\frac{\xi}{2} + \frac{\xi}{2} - \frac{|s_{\boldsymbol{k}}|}{2} - \frac{|s_{\boldsymbol{k}}|}{2}\right)
\end{aligned}$$

where $\xi \equiv -(\epsilon_{\boldsymbol{k}} + \mu)$. The off-diagonal terms cancel, leaving

$$H = \sum_{\boldsymbol{k}} B_{\boldsymbol{k}}^{+\dagger} B_{\boldsymbol{k}}^{+}(-(\epsilon_{\boldsymbol{k}} + \mu) + |s_{\boldsymbol{k}}|) + B_{\boldsymbol{k}}^{-\dagger} B_{\boldsymbol{k}}^{-}(-(\epsilon_{\boldsymbol{k}} + \mu) - |s_{\boldsymbol{k}}|) \tag{3.31}$$

which is excactly on the diagonal form outlined in equation (3.3) with the correct eigenvalues $\lambda^{\pm}$. Let us further investigate the excitation spectrum given in eq. (3.11). It is evident that $\lambda_{\boldsymbol{k}}^{-}$ has the lowest energy. The minima of $\lambda_{\boldsymbol{k}}^{-}$ is found to be at

$$k_x, k_y = \pm \arcsin \frac{\lambda_R/t}{\sqrt{2 + (\lambda_R/t)^2}} \tag{3.32}$$

where we treat k_x and k_y as continious variables, even though they are discrete as shown later in this section. Ergo, a *finite* SOC always leads to minima displaced from $\boldsymbol{k} = 0$, which is the usual minimum. This is the usual effect of Rashba SOC [20]. There are in total four minima, where the value of the excitation spectrum evaluated at one of these points is given by

$$\lambda_{\min}^{-} = -4t\sqrt{\frac{1}{2}\left(\frac{\lambda_R}{t}\right)^2 + 1} - \mu \tag{3.33}$$

which is *negative*. This is problematic, as then we get a term $-|\lambda_{\min}|B_{\boldsymbol{k}}^{-\dagger}B_{\boldsymbol{k}}^{-}$ in the Hamiltonian, which is minimized by maximizing the number of quasiparticles $n_{\boldsymbol{k}}^{-} = B_{\boldsymbol{k}}^{-\dagger}B_{\boldsymbol{k}}^{-}$, in effect flooding the system. We can avoid this by adding and subtracting a constant term to the Hamiltonian, and consider it as a contribution to the chemical potential. We write

$$\lambda_{\boldsymbol{k}}^{\pm} = \lambda_{\boldsymbol{k}}^{\pm} - \lambda_{\min}^{-} + \lambda_{\min}^{-} \tag{3.34}$$

$$= \Lambda_{\boldsymbol{k}}^{\pm} + \lambda_{\min}^{-} \tag{3.35}$$

$\Lambda_{\boldsymbol{k}}^{-}$ is the new lowest branch, and is bounded from below by 0. The Hamiltonian thus becomes

$$H = \sum_{\boldsymbol{k}}\sum_{\alpha} \lambda_{\boldsymbol{k}}^{\alpha} B_{\boldsymbol{k}}^{\alpha\dagger} B_{\boldsymbol{k}}^{\alpha} \tag{3.36}$$

$$= \sum_{\boldsymbol{k}}\sum_{\alpha} \Lambda_{\boldsymbol{k}}^{\alpha} B_{\boldsymbol{k}}^{\alpha\dagger} B_{\boldsymbol{k}}^{\alpha} + \lambda_{\min}^{-} \sum_{\boldsymbol{k}}\sum_{\alpha} B_{\boldsymbol{k}}^{\alpha\dagger} B_{\boldsymbol{k}}^{\alpha} \tag{3.37}$$

$$= \lambda_{\min}^{-} N_b + \sum_{\boldsymbol{k}}\sum_{\alpha} \Lambda_{\boldsymbol{k}}^{\alpha} B_{\boldsymbol{k}}^{\alpha\dagger} B_{\boldsymbol{k}}^{\alpha} \tag{3.38}$$

where N_b is the total number of quasi-particles in the system. Note that this is generally different from the total number of sites N_s, as pointed out by Janssønn. In fig. 3.1 a plot of the excitation spectrums are shown. Notice the advertised displacement of the minima from $\boldsymbol{k} = 0$, and also that the two branches meet *linearly* at $\boldsymbol{k} = 0$.

Quantization of $\boldsymbol{k}$

The periodic boundary conditions discretizes $\boldsymbol{k} = (k_x, k_y)$ in the following way [17]. Since $e^{ik_x L} = 1$ and $e^{ik_y L} = 1$, where $L = a\sqrt{N_s}$, we get that $k_x = 2\pi m_x/L$ and $k_y = 2\pi m_y/L$ where m is an integer. Since b_i^{α} has N_s independent operators for each value of α, $A_{\boldsymbol{k}}$ also has N_s independent operators for N_s inequivalent values of (k_x, k_y). We choose these N_s inequivalent values for (m_x, m_y) to be

$$m_x = m_y = -N/2, -N/2+1, \ldots, N/2-1 \tag{3.39}$$

$$k_x = k_y = -\pi/a, -\pi/a + 2\pi/L, \ldots, \pi/a - 2\pi/L \tag{3.40}$$

The total size of the system is $N^2 = N_s$. In the limit $N \to \infty$, this is known as the 1st Brillouin zone $[-\pi/a, \pi/a)$ [38]. In the next section we shall ignore SOC, and focus on a weakly interacting, one-component, bose gas. We shall also give physical constraints on the intra-scattering potentials.

3.2 Weakly interacting Bose gas

This section will serve as a warm-up for the case of a two-component weakly interacting Bose gas with synthetic SOC. This will also aid our intuition in the main section of the thesis. The Hamiltonian for a weakly interacting, *single*-component, Bose gas is given by eq. (2.70) when setting all components equal and turning off SOC $\lambda_R = 0$

$$H = -\sum_{\boldsymbol{k}} (\epsilon_{\boldsymbol{k}} + \mu) A_{\boldsymbol{k}}^{\dagger} A_{\boldsymbol{k}} + \frac{U}{2N_s} \sum_{\boldsymbol{k}\boldsymbol{k}'\boldsymbol{p}\boldsymbol{p}'} A_{\boldsymbol{k}}^{\dagger} A_{\boldsymbol{k}'}^{\dagger} A_{\boldsymbol{p}} A_{\boldsymbol{p}'} \delta_{\boldsymbol{k}+\boldsymbol{k}',\boldsymbol{p}+\boldsymbol{p}'} \tag{3.41}$$

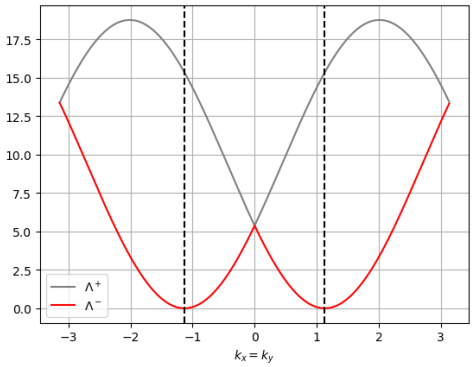

(a) A plot of the excitation spectrum $\Lambda^{\pm}_{\boldsymbol{k}}$ for the SOC, non-interacting Bose gas.

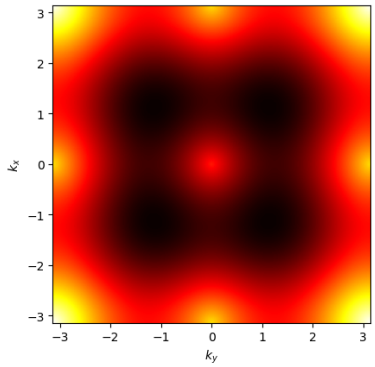

(b) A plot of the excitation spectrum of the lowest branch $\Lambda^-_{\boldsymbol{k}}$

Figure 3.1: The plots of the excitation spectrum for the bosons subjected to synthetic SOC. The physical parameters are $\lambda_R = 3.0$ and $t = a = 1$.

The temperature of the system is assumed to be way below the critical temperature T_c for Bose-Einstein condensation to occur. Thus we can assume that the particles are in the lowest energy state, which is at $\boldsymbol{k} = \boldsymbol{0}$. With this simplification we can utilize *mean field theory*. This requires a transformation on the condensate operators $A_{\boldsymbol{0}}$ and $A^\dagger_{\boldsymbol{0}}$, where we write

$$A_{\boldsymbol{0}} = a_{\boldsymbol{0}} + \delta A_{\boldsymbol{0}} \tag{3.42}$$

The fluctuation $\delta A_{\boldsymbol{0}}$ is an operator representing small fluctuations from the ground state at $\boldsymbol{k} = 0$. $a_{\boldsymbol{0}}$ is a complex number, and is given by

$$a_{\boldsymbol{0}} = \sqrt{N_{\boldsymbol{0}}} e^{-i\theta} \tag{3.43}$$

N_0 and θ are mean-field parameters which may be solved by minimizing the free energy of the system. The parameter θ is normally set to zero, as was done in [51]. However, as Janssønns thesis reveals, there are certain phases in $\boldsymbol{k}$ space which cannot exist without a non-zero mean-field parameter θ. Note that the condensate particle number N_0 is given by the modulos squared of $a_{\boldsymbol{0}}$. We further assume that terms bilinear in *excitation* operators multiplied with a fluctuation operator vanishes, which is reasonable since the excitation operators are small in this approximation. Furthermore, we also assume that the interaction terms are at most bilinear in excitation operators. The table in 3.1 shows the possible configurations in the sum over $\boldsymbol{kk'pp'}$ with these approximations. There are no terms linear in excitation operators, since momentum conservation gives the momentum $\boldsymbol{k} = \boldsymbol{0}$. Using the mentioned approximations, and writing out all terms in the interaction at most bilinear in excitation operators, we get the following Hamiltonian

$$H \approx H_0 + H_{(1)} + H_2 \tag{3.44}$$

$\boldsymbol{k}$	$\boldsymbol{k}'$	$\boldsymbol{p}$	$\boldsymbol{p}'$
0	0	0	0
0	0	$\boldsymbol{p}$	$\boldsymbol{p}'$
0	$\boldsymbol{k}'$	0	$\boldsymbol{p}'$
0	$\boldsymbol{k}'$	$\boldsymbol{p}$	0
$\boldsymbol{k}$	0	$\boldsymbol{p}$	0
$\boldsymbol{k}$	$\boldsymbol{k}'$	0	0
$\boldsymbol{k}$	0	0	$\boldsymbol{p}'$

Table 3.1: Possible momentum configurations for the weakly interacting Bose-Gas

where,

$$H_0 = -(\epsilon_{\mathbf{0}} + \mu)N_{\mathbf{0}} + \frac{U}{2N_s}N_{\mathbf{0}}^2 \tag{3.45}$$

$$H_{(1)} = \sqrt{N_{\mathbf{0}}}\left(\frac{UN_{\mathbf{0}}}{N_s} - (\epsilon_{\mathbf{0}} + \mu)\right)\left[e^{i\theta}\delta A_{\mathbf{0}} + e^{-i\theta}\delta A_{\mathbf{0}}^\dagger\right] \tag{3.46}$$

$$\begin{aligned} H_2 = &\sum_{\boldsymbol{k}}\left(\frac{2UN_{\mathbf{0}}}{N_s} - (\epsilon_{\boldsymbol{k}} + \mu)\right)A_{\boldsymbol{k}}^\dagger A_{\boldsymbol{k}} \\ &+ \frac{UN_{\mathbf{0}}}{2N_s}\sum_{\boldsymbol{k}} e^{2i\theta}A_{\boldsymbol{k}}A_{-\boldsymbol{k}} + e^{-2i\theta}A_{\boldsymbol{k}}^\dagger A_{-\boldsymbol{k}}^\dagger \end{aligned} \tag{3.47}$$

Notice that we have reduced the two-body scattering problem, to an effective single-body problem. Further, the $\boldsymbol{k} = \mathbf{0}$ term in H_2 means that we replace $A_{\boldsymbol{k}}$ by the fluctuation $\delta A_{\mathbf{0}}$. Since the free energy of the system is supposed to be minimized with respect to the mean-field parameters, the terms proportional to a fluctuation must be zero. Consequently, $H_{(1)}$ must be zero, which is achieved by adjusting the chemical potential

$$\mu = \frac{UN_{\mathbf{0}}}{N_s} - \epsilon_{\mathbf{0}} \tag{3.48}$$

giving equivalently an equation for the condensate density in the presense of interactions

$$\frac{N_{\mathbf{0}}}{N_s} = \frac{\epsilon_{\mathbf{0}} + \mu}{U} \tag{3.49}$$

Inserting the equation for μ in H_0 and H_2, we get

$$H_0 = -\frac{UN_{\mathbf{0}}^2}{2N_s} \tag{3.50}$$

$$\begin{aligned} H_2 = &\sum_{\boldsymbol{k}}\left(\epsilon_{\mathbf{0}} - \epsilon_{\boldsymbol{k}} + \frac{UN_{\mathbf{0}}}{N_s}\right)A_{\boldsymbol{k}}^\dagger A_{\boldsymbol{k}} \\ &+ \frac{UN_{\mathbf{0}}}{2N_s}\sum_{\boldsymbol{k}} e^{2i\theta}A_{\boldsymbol{k}}A_{-\boldsymbol{k}} + e^{-2i\theta}A_{\boldsymbol{k}}^\dagger A_{-\boldsymbol{k}}^\dagger \end{aligned} \tag{3.51}$$

Because the sum over $\boldsymbol{k}$ is symmetric in the 1st Brillouin zone, we can make the symmetrization $\sum_{\boldsymbol{k}} f(\boldsymbol{k}) = \frac{1}{2}\sum_{\boldsymbol{k}} f(\boldsymbol{k}) + f(-\boldsymbol{k})$. We also introduce the new operators $a_{\boldsymbol{k}}$ and $b_{\boldsymbol{k}}$

$$a_{\boldsymbol{k}} = e^{i\theta} A_{\boldsymbol{k}} \tag{3.52}$$

$$b_{\boldsymbol{k}} = a_{-\boldsymbol{k}} = e^{i\theta} A_{-\boldsymbol{k}} \tag{3.53}$$

Next, explicitly summing over $-\boldsymbol{k}$, and inserting the expressions for $a_{\boldsymbol{k}}$ and $b_{\boldsymbol{k}}$, we obtain the Hamiltonian

$$H = -\frac{UN_{\mathbf{0}}^2}{2N_s} + \sum_{\boldsymbol{k}} \epsilon_0(\boldsymbol{k})(a_{\boldsymbol{k}}^\dagger a_{\boldsymbol{k}} + b_{\boldsymbol{k}}^\dagger b_{\boldsymbol{k}}) + \epsilon_1(a_{\boldsymbol{k}}^\dagger b_{\boldsymbol{k}}^\dagger + a_{\boldsymbol{k}} b_{\boldsymbol{k}}) \tag{3.54}$$

where,

$$\epsilon_0(\boldsymbol{k}) = \frac{1}{2}\left(\epsilon_{\mathbf{0}} - \epsilon_{\boldsymbol{k}} + \frac{UN_{\mathbf{0}}}{N_s}\right) \tag{3.55}$$

$$\epsilon_1 = \frac{UN_{\mathbf{0}}}{2N_s} \tag{3.56}$$

3.2.1 The Bogoliubov transformation

From the previous section, we see that the Hamiltonian is a sum over independent terms on the form

$$\hat{h} = \epsilon_0(\hat{a}^\dagger \hat{a} + \hat{b}^\dagger \hat{b}) + \epsilon_1(\hat{a}^\dagger \hat{b}^\dagger + \hat{a}\hat{b}) \tag{3.57}$$

where ϵ_0 and ϵ_1 are real. The operators are bosonic, and satisfy the commutation relations

$$[\hat{a}, \hat{a}^\dagger] = [\hat{b}, \hat{b}^\dagger] = 1 \tag{3.58}$$

with the additional bosonic commutation relations

$$[\hat{a}, \hat{b}^\dagger] = [\hat{b}, \hat{a}^\dagger] = [\hat{a}, \hat{b}] = [\hat{a}^\dagger, \hat{b}^\dagger] = 0 \tag{3.59}$$

Our goal is to obtain the eigenvalues of this Hamiltonian. This can be achieved by performing a transformation in the operators such that the Hamiltonian becomes diagonal, as was done with the spin-orbit coupled bose gas in section 3.1. This was achieved by Bogoliubov when treating liquid Helium [7], where he performed a *canonical transformation* to new bosonic operators $\hat{\alpha}$ and $\hat{\beta}$ such that the Hamiltonian describes *free* bosons. We make the transformations

$$\hat{\alpha} = u\hat{a} + v\hat{b}^\dagger \tag{3.60}$$

$$\hat{\beta} = u\hat{b} + v\hat{a}^\dagger \tag{3.61}$$

The coefficients u and v are chosen to be real. The old operators are given by the inverse transformation

$$\hat{a} = u\hat{\alpha} - v\hat{\beta}^\dagger \tag{3.62}$$

$$\hat{b} = u\hat{\beta} - v\hat{\alpha}^\dagger \tag{3.63}$$

To assure that the new operators $\hat{\alpha}$ and $\hat{\beta}$ are bosonic, we must require

$$[\hat{\alpha}, \hat{\alpha}^\dagger] = [\hat{\beta}, \hat{\beta}^\dagger] = 1 \tag{3.64}$$

and also,

$$[\hat{\alpha}, \hat{\beta}^\dagger] = [\hat{\beta}, \hat{\alpha}^\dagger] = [\hat{\alpha}, \hat{\beta}] = [\hat{\alpha}^\dagger, \hat{\beta}^\dagger] = 0 \tag{3.65}$$

Using the expressions for $\hat{\alpha}$ and $\hat{\beta}$ into one of the equations in (3.64), we get the requirement on u and v

$$u^2 - v^2 = 1 \tag{3.66}$$

We now insert the expressions for $\hat{a}$ and $\hat{b}$ in (3.62) and (3.63) into the Hamiltonian given in (3.57), obtaining

$$\begin{aligned}\hat{h} = 2v^2\epsilon_0 - 2uv\epsilon_1 + [\epsilon_0(u^2+v^2) - 2uv\epsilon_1](\hat{\alpha}^\dagger\hat{\alpha} + \hat{\beta}^\dagger\hat{\beta}) \\ + [\epsilon_1(u^2+v^2) - 2uv\epsilon_0](\hat{\alpha}\hat{\beta} + \hat{\beta}^\dagger\hat{\alpha}^\dagger)\end{aligned} \tag{3.67}$$

By the requirement that the Hamiltoian should be diagonal in the operators $\hat{\alpha}$ and $\hat{\beta}$, we must require that the term proportional to $\hat{\alpha}\hat{\beta} + \hat{\beta}^\dagger\hat{\alpha}^\dagger$ vanish. This leads to a condition on u and v

$$\epsilon_1(u^2+v^2) = 2uv\epsilon_0 \tag{3.68}$$

But this have no simple solution for u and v. However, we can make the transformation

$$u = \cosh(t), \quad v = \sinh(t) \tag{3.69}$$

where t is real. This transformation satisfies condition (3.66), since we have the identity

$$\cosh^2(t) - \sinh^2(t) = 1 \tag{3.70}$$

which makes life a *bit* simpler. We will now make use of the following relations

$$u^2 + v^2 = \cosh^2(t) + \sinh^2(t) = \cosh(2t) \tag{3.71}$$

$$uv = \cosh(t)\sinh(t) = \frac{1}{2}\sinh(2t) \tag{3.72}$$

Using the above relations in equation (3.68) thus leads to

$$\frac{\epsilon_1}{\epsilon_0} = \tanh(2t) \tag{3.73}$$

such that

$$2t = \tanh^{-1}\left(\frac{\epsilon_1}{\epsilon_0}\right) \tag{3.74}$$

where $\tanh^{-1}$ is the inverse tanh function. The solution for $2t$ makes the off-diagonal term in the Hamiltonian vanish. The energy of the bosons are given by the term proportional to $\hat{\alpha}^\dagger\hat{\alpha} + \hat{\beta}^\dagger\hat{\beta}$, which gives the energy ϵ

$$\epsilon = \epsilon_0(u^2+v^2) - 2uv\epsilon_1 \tag{3.75}$$

Using the relations given in (3.71) and (3.72), we get

$$\epsilon = \epsilon_0 \cosh(2t) - \epsilon_1 \sinh(2t) \tag{3.76}$$

Further, using the solution for $2t$ and the following relations

$$\cosh(\tanh^{-1}(x)) = \frac{1}{\sqrt{1-x^2}}, \quad \sinh(\tanh^{-1}(x)) = \frac{x}{\sqrt{1-x^2}} \tag{3.77}$$

we finally obtain the Bogoliubov spectrum

$$\epsilon = \text{sign}(\epsilon_0)\sqrt{\epsilon_0^2 - \epsilon_1^2} \tag{3.78}$$

where $\text{sign}(x) = |x|/x$. In addition, we get the expressions for u and v

$$u^2 = \cosh^2(t) = \frac{1}{2}\left(\cosh(2t) + 1\right) = \frac{1}{2}\left(\frac{\epsilon_0}{\epsilon} + 1\right) \tag{3.79}$$

$$v^2 = \sinh^2(t) = \frac{1}{2}\left(\cosh(2t) - 1\right) = \frac{1}{2}\left(\frac{\epsilon_0}{\epsilon} - 1\right) \tag{3.80}$$

For the constant term, which is given by $2v^2\epsilon_0 - 2uv\epsilon_1$, we get $\epsilon - \epsilon_0$. Thus we obtain the Hamiltonian on diagonal form

$$\hat{h} = \epsilon(\hat{\alpha}^\dagger\hat{\alpha} + \hat{\beta}^\dagger\hat{\beta}) + \epsilon - \epsilon_0 \tag{3.81}$$

Furthermore, we must have that ϵ is a positive quantity. Otherwise, we would have a term in the expectation value of the energy $\langle\hat{h}\rangle$ on the form $-|\epsilon|(n_\alpha + n_\beta)$, where n_α and n_β are the expectation values of $\hat{n}_\alpha = \hat{\alpha}^\dagger\hat{\alpha}$ and $\hat{n}_\beta = \hat{\beta}^\dagger\hat{\beta}$. The system will minimize this term by maximizing n_α and n_β, which both can be infinite for bosons, thus flooding the system. The quantity determining the sign of ϵ is ϵ_0, which must be positive. Consequently, we get the energy ϵ as

$$\epsilon = \sqrt{\epsilon_0^2 - \epsilon_1^2} \tag{3.82}$$

We must also have real eigenvalues, which requires that $|\epsilon_0| > |\epsilon_1|$. If this constraint is not met, we will get instabilities in the system [44].

3.2.2 Completing the diagonalization procedure

Let us define the Bogoliubov operators (where $b_{\boldsymbol{k}} = a_{-\boldsymbol{k}}$):

$$\alpha_{\boldsymbol{k}} = u_{\boldsymbol{k}} a_{\boldsymbol{k}} - v_{\boldsymbol{k}} a_{-\boldsymbol{k}}^\dagger \tag{3.83}$$

$$\beta_{\boldsymbol{k}} = \alpha_{-\boldsymbol{k}} = u_{\boldsymbol{k}} a_{-\boldsymbol{k}} - v_{\boldsymbol{k}} a_{\boldsymbol{k}}^\dagger \tag{3.84}$$

Such that we may immedeatly obtain, following the process of the previous section, the diagonalized Hamiltonian given in eq (3.54)

$$H = -\frac{UN_0^2}{2N_s} + \sum_{\boldsymbol{k}} \zeta_{\boldsymbol{k}} - \epsilon_{\boldsymbol{k}} + \sum_{\boldsymbol{k}} \hbar\omega(\boldsymbol{k})\alpha_{\boldsymbol{k}}^\dagger\alpha_{\boldsymbol{k}} \tag{3.85}$$

where we have defined,

$$\zeta_{\boldsymbol{k}} = \sqrt{\epsilon_0^2(\boldsymbol{k}) - \epsilon_1^2} \tag{3.86}$$

Further, $\epsilon_0(\boldsymbol{k})$ and ϵ_1 are given in eqs.(3.55) and (3.56), and the energy $\hbar\omega(\boldsymbol{k})$ for the free bosons $\alpha_{\boldsymbol{k}}$ are given by,

$$\hbar\omega(\boldsymbol{k}) = 2\zeta_{\boldsymbol{k}} = \sqrt{(\epsilon_{\boldsymbol{0}} - \epsilon_{\boldsymbol{k}})\left((\epsilon_{\boldsymbol{0}} - \epsilon_{\boldsymbol{k}}) + \frac{2UN_{\boldsymbol{0}}}{N_s}\right)} \tag{3.87}$$

Which agrees with [32]. Notice here that we have chosen the positive branch, relying on the sign of $\epsilon_0(\boldsymbol{k})$, which is given by the interaction proportional to U plus the term $\epsilon_{\boldsymbol{0}} - \epsilon_{\boldsymbol{k}}$. It can be shown that for a square lattice, $\epsilon_{\boldsymbol{k}}$ has its maximum in $\boldsymbol{k} = \boldsymbol{0}$ within the 1st Brilloin zone. This means that $\epsilon_{\boldsymbol{0}} - \epsilon_{\boldsymbol{k}}$ is never zero, which means that $\zeta_{\boldsymbol{k}}$ indeed has the correct sign. Further, this also enshures that $\hbar\omega(\boldsymbol{k})$ is always real. Thus the energy spectrum of the weakly interacting, single-component, Bose gas is stable for all values in parameter space. It is stated in [44] that when terms cubic and quartic in excitation operators are included in the Hamiltonian, the "excitations are damped and their energies shifted relative to the Bogoliubov spectrum".

Also note that for small $\boldsymbol{k}$, the excitation spectrum becomes *linear* in the presense of interactions $U \neq 0$, resembling the dispersion relation for phonons. See fig. 3.2 for a plot of the excitation spectrum. This is characteristic for a superfluid, and the slope of the dispersion relation in this limit gives the superfluid critical velocity. Also note that the excitation spectrum is quadratic near the end of the 1st Brillouin zone, behaving as free bosons with dispersion relation $p^2/2m^*$, where m^* is an effective mass.

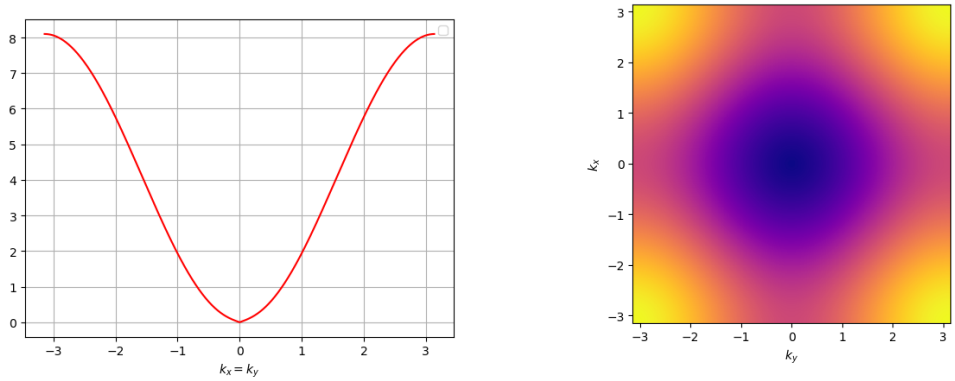

(a) A plot of the excitation spectrum for $k_x = k_y$

(b) A plot of the excitation spectrum for all (k_x, k_y) in the 1st Brillouin zone

Figure 3.2: The plots of the excitation spectrum for weakly interacting bosons. The physical parameters are $t = a = 1$, $U = 0.1$ and $N_0 = N_s$, which means one boson per lattice site.

It is shown in Janssønns master thesis that to avoid severe *ground state depletion*, which means that a significant fraction of condesate particles escape the ground state due to interactions, we must be in the superfluid phase. This physically means that $U/t \ll 1$, which is a

constraint we must apply to our mean-field method. The reason for this is due to only considering two-body scattering. In contrast, to investigate the insulating *Mott* phase, which requires considering higher order interactions, one can use pertubation theory.

3.3 Spin-Orbit Coupled, Weakly Interacting Bose Gas

The work in this section is largely based on Janssønns master thesis [32] in chapter 3. The goal of this section is to give the reader a qualitative summmary *and* intuition for the case of a two-component, weakly interacting Bose gas, which is quite complicated. The short reason for why this is mathematically complicated originates from the fact that with a finite SOC, the condensate can have multiple minima in $\boldsymbol{k}$-space, as opposed to the weakly interacting bose gas, in which the minima was found to be only at $\boldsymbol{k} = \boldsymbol{0}$.

We have the following Hamiltonian for a weakly interacting, two-component, SOC bose gas

$$H = \sum_{\boldsymbol{k}} \sum_{\alpha\beta} \eta_{\boldsymbol{k}}^{\alpha\beta} A_{\boldsymbol{k}}^{\alpha\dagger} A_{\boldsymbol{k}}^{\beta} + \frac{1}{2N_s} \sum_{\boldsymbol{k}\boldsymbol{k}'\boldsymbol{p}\boldsymbol{p}'} \sum_{\alpha\beta} U^{\alpha\beta} A_{\boldsymbol{k}}^{\alpha\dagger} A_{\boldsymbol{k}'}^{\beta\dagger} A_{\boldsymbol{p}}^{\beta} A_{\boldsymbol{p}'}^{\alpha} \delta_{\boldsymbol{k}+\boldsymbol{k}',\boldsymbol{p}+\boldsymbol{p}'} \tag{3.88}$$

We make the same assumptions as in the previous section, namely that the temperature T is way below T_c and that ground state depletion is negligible. This assures that the bosons are mainly occupied in the condensate minima $\boldsymbol{k}_{0i}$ in $\boldsymbol{k}$-space (this means that the energy-spectrum is minimized for these values of $\boldsymbol{k}$). These assumptions requires that we are in the superfluid phase, in which the hopping parameters are much stronger than the interation terms. Here $\boldsymbol{k}_{0i}$ will be referred to as a condensate momenta, where i runs from 1 to n. If $n = 1$, this will be referred to as a *one-fold* case, and if $n > 1$ it will be referred to as a *many-fold* case. Further, if a $\boldsymbol{k}$-dependent operator, e.g $A_{\boldsymbol{k}}$, has $\boldsymbol{k}$ equal to any of the condensate momenta, we call this operator a *condensate operator*, and if not, an *excitation* operator.

We do as in the previous section, and neglect all terms cubic or quartic in *excitation* operators. The table in Tab. 3.2 shows the possible momentum configurations $\boldsymbol{k}\boldsymbol{k}'\boldsymbol{p}\boldsymbol{p}'$ in the interaction terms. See [32] for a detailed analysis of the number of possible configurations, and also the

Constant	Linear	Bilinear
$\boldsymbol{k}_{0i}, \boldsymbol{k}_{0j}, \boldsymbol{k}_{0i'}, \boldsymbol{k}_{0j'}$	$\boldsymbol{k}_{0i}, \boldsymbol{k}_{0j}, \boldsymbol{k}_{0i'}, \boldsymbol{p}'$	$\boldsymbol{k}_{0i}, \boldsymbol{k}_{0j}, \boldsymbol{p}, \boldsymbol{p}'$
	$\boldsymbol{k}_{0i}, \boldsymbol{k}_{0j}, \boldsymbol{p}, \boldsymbol{k}_{0j'}$	$\boldsymbol{k}_{0i}, \boldsymbol{k}', \boldsymbol{k}_{0i}, \boldsymbol{p}'$
	$\boldsymbol{k}_{0i}, \boldsymbol{k}', \boldsymbol{k}_{0i'}, \boldsymbol{k}_{0j'}$	$\boldsymbol{k}_{0i}, \boldsymbol{k}', \boldsymbol{p}, \boldsymbol{k}_{0j'}$
	$\boldsymbol{k}, \boldsymbol{k}_{0j}, \boldsymbol{k}_{0i'}, \boldsymbol{k}_{0j'}$	$\boldsymbol{k}, \boldsymbol{k}', \boldsymbol{k}_{0i'}, \boldsymbol{k}_{0j'}$
		$\boldsymbol{k}, \boldsymbol{k}_{0j}, \boldsymbol{p}, \boldsymbol{k}_{0j'}$
		$\boldsymbol{k}, \boldsymbol{k}_{0j}, \boldsymbol{k}_{0i'}, \boldsymbol{p}'$

Table 3.2: Possible configurations for the momenta in the interaction term for the two-component, spin-orbit coupled, weakly interacting Bose gas.

types of combinations allowed by momentum conservation on a Bravais-lattice. Notice also that we get terms *linear* in excitation operators, which the author, nor Janssønn, has found explored in the literature. The Hamiltonian may now be written as

$$H \approx H_0 + H_1 + H_2 \tag{3.89}$$

where,

$$H_0 = \sum_i \sum_{\alpha\beta} \eta^{\alpha\beta}_{\boldsymbol{k}_{0i}} A^{\alpha\dagger}_{\boldsymbol{k}_{0i}} A^{\beta}_{\boldsymbol{k}_{0i}} + \frac{1}{2N_s} \sum_{iji'j'} \sum_{\alpha\beta} U^{\alpha\beta} A^{\alpha\dagger}_{\boldsymbol{k}_{0i}} A^{\beta\dagger}_{\boldsymbol{k}_{0j}} A^{\beta}_{\boldsymbol{k}_{0i'}} A^{\alpha}_{\boldsymbol{k}'_{0j}} \delta_{\boldsymbol{k}_{0i}+\boldsymbol{k}_{0j},\boldsymbol{k}_{0i'}+\boldsymbol{k}_{0j'}} \tag{3.90}$$

$$H_1 = \frac{1}{N_s} {\sum_{\boldsymbol{k}}}' \sum_{iji'} \sum_{\alpha\beta} U^{\alpha\beta} \Big(A^{\alpha\dagger}_{\boldsymbol{k}_{0i}} A^{\beta\dagger}_{\boldsymbol{k}_{0j}} A^{\beta}_{\boldsymbol{k}_{0i'}} A^{\alpha}_{\boldsymbol{k}} + A^{\alpha\dagger}_{\boldsymbol{k}} A^{\beta\dagger}_{\boldsymbol{k}_{0i'}} A^{\beta}_{\boldsymbol{k}_{0j}} A^{\alpha}_{\boldsymbol{k}_{0i}} \Big) \delta_{\boldsymbol{k}+\boldsymbol{k}'_{0i},\boldsymbol{k}_{0j}+\boldsymbol{k}_{0i}} \tag{3.91}$$

And,

$$H_2 = {\sum_{\boldsymbol{k}}}' \sum_{\alpha\beta} \eta^{\alpha\beta}_{\boldsymbol{k}} A^{\alpha\dagger}_{\boldsymbol{k}} A^{\beta}_{\boldsymbol{k}} \frac{1}{2N_s} {\sum_{\boldsymbol{k}\boldsymbol{k}'}}'' \sum_{ij} \sum_{\alpha\beta} U^{\alpha\beta} \Big((A^{\alpha\dagger}_{\boldsymbol{k}_{0i}} A^{\beta\dagger}_{\boldsymbol{k}_{0j}} A^{\beta}_{\boldsymbol{k}} A^{\alpha}_{\boldsymbol{k}'} + A^{\alpha\dagger}_{\boldsymbol{k}} A^{\beta\dagger}_{\boldsymbol{k}'} A^{\beta}_{\boldsymbol{k}_{0i}} A^{\alpha}_{\boldsymbol{k}_{0j}}) \delta_{\boldsymbol{k}+\boldsymbol{k}',\boldsymbol{k}_{0i}+\boldsymbol{k}_{0j}} + 2(A^{\alpha\dagger}_{\boldsymbol{k}_{0i}} A^{\beta\dagger}_{\boldsymbol{k}} A^{\beta}_{\boldsymbol{k}_{0j}} A^{\alpha}_{\boldsymbol{k}'} + A^{\alpha\dagger}_{\boldsymbol{k}_{0i}} A^{\beta\dagger}_{\boldsymbol{k}} A^{\beta}_{\boldsymbol{k}'} A^{\alpha}_{\boldsymbol{k}_{0j}}) \delta_{\boldsymbol{k}_{0i}+\boldsymbol{k},\boldsymbol{k}'+\boldsymbol{k}_{0j}} \Big) \tag{3.92}$$

Where we have followed the derivation from Janssønn [32], utilizing commutation relations and permuting momentum indices. Here, the sum ${\sum_{\boldsymbol{k}}}'$ excludes all condensate momenta $\boldsymbol{k} = \boldsymbol{k}_{0i}$, $\forall i$, and the sum ${\sum_{\boldsymbol{k}\boldsymbol{k}'}}''$ exludes all pairs $(\boldsymbol{k}, \boldsymbol{k}')$ with at least one condensate momentum; if $\boldsymbol{k}$ is equal to an arbitrary non-condensate momenta, and $\boldsymbol{k}'$ is equal to a condensate momenta, then this pair is excluded. This *can* happen due to conservation of momentum. The Hamiltonian is now ready for mean-field theory.

3.3.1 Mean field theory

Similarly to the weakly-interacting, one-component, Bose gas, we introduce the mean field condensate operators for each condensate momentum $\boldsymbol{k}_{0i}$ and pseudo-spin α

$$A^{\alpha}_{\boldsymbol{k}_{0i}} = a^{\alpha}_{\boldsymbol{k}_{0i}} + \delta A^{\alpha}_{\boldsymbol{k}_{0i}} \tag{3.93}$$

The expectation value $a^{\alpha}_{\boldsymbol{k}_{0i}}$ is a complex number proportional to the root of the condensate number for pseudo-spin α, and $\delta A_{\boldsymbol{k}^{\alpha}_{0i}}$ is a *small* fluctuation with zero expectation value. The subscripts $\boldsymbol{k}_{0i}$ are condensate momenta, and are distinct points in $\boldsymbol{k}$ space where one expects to find a minima. In the literature, it is customary to choose $a^{\alpha}_{\boldsymbol{k}_{0i}}$ to be real and equal to the square root of the condensate particle number $\sqrt{N^{\alpha}_{\boldsymbol{k}_{0i}}}$. It is however necessary for this thesis to parametrise $a^{\alpha}_{\boldsymbol{k}_{0i}}$ by the mean-field parameter $\theta^{\alpha}_{\boldsymbol{k}_{0i}}$, in the following way

$$a^{\alpha}_{\boldsymbol{k}_{0i}} = \sqrt{N^{\alpha}_{\boldsymbol{k}_{0i}}} e^{-i\theta^{\alpha}_{\boldsymbol{k}_{0i}}} \tag{3.94}$$

such that the modulus of $a^{\alpha}_{\boldsymbol{k}_{0i}}$ gives the root of the condensate number for pseudo-spin α. It will become apparent in the ensuing calculations that the mean-field parameters $\theta^{\alpha}_{\boldsymbol{k}_{0i}}$ cannot all be

zero. We now insert the expression for the condensate operators in the Hamiltonian. We only keep terms that are constant or linear in fluctuations, and also terms that are a product of a fluctuation and an excitation operator. The rest of the terms are neglected. This is the same as done in the previous section, and also in D. van Oosten et al [51].

In the mean field approach, we introduce a number of mean-field parameters, namely $a^{\alpha}_{\boldsymbol{k}_{0i}}$. There are two ways of determining these, either by solving a set of self-consistent equations, or by minimizing the free energy F. In this thesis, as was done in Janssønn [32], we will minimize the free-energy F. This implies that the terms linear in condensate fluctuations must vanish, as was done in the previous section with the weakly interacting Bose gas. We will see that the linear terms must be cancelled by tuning the chemical potentials for each pseudo-spin. *Let us for the rest of the chapter make the shortcut $\boldsymbol{k}_{0i} \to i$, for mathematical simplicity. The only place we have this dependence is in the condensate operators and condensate mean field parameters. It will be made clear when this is no longer the case.*

3.3.2 Terms linear in condensate fluctuation operators

The terms that are linear in condensate fluctuations operators are shown in to be

$$\sum_i \sum_{\alpha\beta} \delta A_i^{\beta} \left(\eta_i^{\alpha\beta} a_i^{\alpha *} + \frac{U^{\alpha\beta}}{N_s} \sum_{ji'j'} a_j^{\alpha} a_{i'}^{\alpha *} a_{j'}^{\beta *} \delta_{i+j,i'+j'} \right) + \text{H.c} \tag{3.95}$$

where H.c denotes the complex conjugate. Please note that the arguments in the delta function are not numbers, but indices refering to a specific condensate $\boldsymbol{k}$-vector, the indices are not supposed to be added together. The goal is to cancel this term, by adjusting the chemical potential μ^{α} which is located along the diagonal of the matrix $\eta_{\boldsymbol{k}}$ of the non-interacting Hamiltonian. We assume that the fluctuations for the respective pseudo-spin indices are independent, so that we may set the individual terms in front of these fluctuations zero respectively. Setting each individual term in front of a fluctuation equal to zero, we get the equation for each pseudo-spin index β

$$\sum_{\alpha} \eta_i^{\alpha\beta} a_i^{\alpha *} + \sum_{ji'j'} \sum_{\alpha} \frac{U^{\alpha\beta}}{N_s} a_j^{\alpha} a_{i'}^{\alpha *} a_{j'}^{\beta *} \delta_{i+j,i'+j'} = 0 \tag{3.96}$$

and the corresponding conjugate term. We first find an equation for $\mu^{\uparrow}$, which is given by

$$(\epsilon_i^{\uparrow} + \mu^{\uparrow}) a_i^{\uparrow *} = s_i^* a_i^{\downarrow *} + \sum_{ji'j'} \sum_{\alpha} \frac{U^{\alpha\uparrow}}{N_s} a_j^{\alpha} a_{i'}^{\alpha *} a_{j'}^{\uparrow *} \delta_{i+j,i'+j'} \tag{3.97}$$

Let us assume that $a_i^{\uparrow} \neq 0$. This gives the solution for $\mu^{\uparrow}$

$$\mu^{\uparrow} = -\epsilon_i^{\uparrow} + s_i^* \frac{a_i^{\downarrow *}}{a_i^{\uparrow *}} + \sum_{ji'j'} \sum_{\alpha} \frac{U^{\alpha\uparrow}}{N_s} \left(\frac{a_{j'}^{\uparrow}}{a_i^{\uparrow}} \right)^* a_j^{\alpha} a_{i'}^{\alpha *} \delta_{i+j,i'+j'} \tag{3.98}$$

If $a_i^{\uparrow} = 0$, then we must insist that the fluctuation $\delta A_i^{\uparrow}$ is also zero. In this case, there will be no equation for $\mu^{\uparrow}$ which in principle can be chosen at will. This also applies to $\mu^{\downarrow}$. In addition, we have the complex conjugate version of this equation, which gives an equation for $\mu^{\uparrow *}$. If we

insist that $\mu^{\uparrow}$ is a real number, we get the equation $\mu^{\uparrow} = \mu^{\uparrow *}$. This leads to two conditions, where the first is caused by a non-zero SOC

$$\Im\left(s_i^* \frac{a_i^{\downarrow *}}{a_i^{\uparrow *}}\right) = 0 \tag{3.99}$$

Using the paramatrized versions of s_i, $a_i^{\uparrow}$ and $a_i^{\downarrow}$, we get

$$\Im\left(|s_i|\sqrt{\frac{N_i^{\downarrow}}{N_i^{\uparrow}}}e^{i(\gamma_i - \delta\theta_i)}\right) = 0 \tag{3.100}$$

where we have defined the quantity

$$\delta\theta_i = \theta_i^{\uparrow} - \theta_i^{\downarrow} \tag{3.101}$$

Consequently, we must require

$$\sin(\gamma_i - \delta\theta_i) = 0 \rightarrow \gamma_i - \delta\theta_i = l\pi, l \in \{0, 1\} \tag{3.102}$$

giving for the SOC term the expression

$$s_i^* \frac{a_i^{\downarrow *}}{a_i^{\uparrow *}} = |s_i|\sqrt{\frac{N_i^{\downarrow}}{N_i^{\uparrow}}}e^{il\pi} \tag{3.103}$$

Where we must choose $l = 1$ to get consistent results with literature [32]. Thus we get the very important relation

$$\boxed{\delta\theta_i = \gamma_i - \pi} \tag{3.104}$$

This equation makes it possible to express all pseudo-spin $\uparrow$ mean-field parameters in terms of all pseudo-spin $\downarrow$ mean-field parameters, halfing the number of mean-field parameters in the system. Notice that this condition is *only* valid when the SOC is of finite length, as it is only then that the helicity angle γ_i is well defined.

The second condition for $\mu^{\uparrow}$ to be real requires that the imaginary part of the interaction term for $\mu^{\uparrow}$ is zero

$$\Im\left(\sum_{ji'j'}\sum_{\alpha}\frac{U^{\alpha\uparrow}}{N_s}\left(\frac{a_{j'}^{\uparrow}}{a_i^{\uparrow}}\right)^* a_j^{\alpha} a_{i'}^{\alpha *}\delta_{i+j,i'+j'}\right) = 0 \tag{3.105}$$

which, writing again out the expressions for the variational parameters, becomes

$$\boxed{\sum_{ji'j'}\sum_{\alpha}\frac{U^{\alpha\uparrow}}{N_s}\sqrt{\frac{N_{j'}^{\uparrow}N_j^{\alpha}N_{i'}^{\alpha}}{N_i^{\uparrow}}}\sin\left(\theta_{j'}^{\uparrow} - \theta_i^{\uparrow} - \theta_j^{\alpha} + \theta_{i'}^{\alpha}\right)\delta_{i+j,i'+j'} = 0} \tag{3.106}$$

To summarize, these two conditions makes shure that the chemical potential for pseudo-spin $\uparrow$

is *real*. The expression for $\mu^{\uparrow}$ finally becomes

$$\mu^{\uparrow} = -\epsilon_i^{\uparrow} - |s_i|\sqrt{\frac{N_i^{\downarrow}}{N_i^{\uparrow}}} + \sum_{ji'j'}\sum_{\alpha}\frac{U^{\alpha\uparrow}}{N_s}\sqrt{\frac{N_{j'}^{\uparrow}N_j^{\alpha}N_{i'}^{\alpha}}{N_i^{\uparrow}}}\cos\left(\theta_{j'}^{\uparrow} - \theta_i^{\uparrow} - \theta_j^{\alpha} + \theta_{i'}^{\alpha}\right)\delta_{i+j,i'+j'} \tag{3.107}$$

For the chemical potential in pseudo-spin $\downarrow$ we get, doing the excact same calulcations

$$\mu^{\downarrow} = -\epsilon_i^{\downarrow} - |s_i|\sqrt{\frac{N_i^{\uparrow}}{N_i^{\downarrow}}} + \sum_{ji'j'}\sum_{\alpha}\frac{U^{\alpha\downarrow}}{N_s}\sqrt{\frac{N_{j'}^{\downarrow}N_j^{\alpha}N_{i'}^{\alpha}}{N_i^{\downarrow}}}\cos\left(\theta_{j'}^{\downarrow} - \theta_i^{\downarrow} - \theta_j^{\alpha} + \theta_{i'}^{\alpha}\right)\delta_{i+j,i'+j'} \tag{3.108}$$

The equation for $\delta\theta_i$ is the same, as it should be. To enshure that the imaginary part of the interaction term for $\mu^{\downarrow}$ is zero, we get the constraint

$$\boxed{\sum_{ji'j'}\sum_{\alpha}\frac{U^{\alpha\downarrow}}{N_s}\sqrt{\frac{N_{j'}^{\downarrow}N_j^{\alpha}N_{i'}^{\alpha}}{N_i^{\downarrow}}}\sin\left(\theta_{j'}^{\downarrow} - \theta_i^{\downarrow} - \theta_j^{\alpha} + \theta_{i'}^{\alpha}\right)\delta_{i+j,i'+j'} = 0} \tag{3.109}$$

To summarize, for $\mu^{\uparrow}$ and $\mu^{\downarrow}$ to be *real*, we have in total three conditions:

1. Equation (3.104) expressing $\theta_i^{\uparrow}$ in terms of $\theta_i^{\downarrow}$, connected with spin-orbit coupling.
2. Equation (3.105) making the imaginary part of the interaction term for $\mu^{\uparrow}$ zero.
3. Equation (3.109) making the imaginary part of the interaction term for $\mu^{\downarrow}$ zero.

Janssønn shows that the two constraints in eq. (3.105) and eq. (3.109) only needs to be met for $n \geq 4$-fold cases, e.g it is automatically true for $n = 1$ and $n = 2$ fold cases. The interaction terms can further be simplified, by explicitely writing out the delta function. However, this leads to hairy expressions and will only be mentioned when needed.

The story is not over, however. We must require that the chemical potentials are independent of momentum index i. Bravais symmetry for the square lattice dictates that ϵ_i^{α} and $|s_i|$ are independent of momentum index i, see [32] for details. However, we must require that the interaction terms in the respective expressions for the chemical potentials are independent of momentum index i. This is done in Jansønns master thesis [32], with the main result: if the condensate consists of particles with different condensate momentum, then the fraction of these particles carrying the specific pseudo-spin with a specific condensate momentum, must be equal

$$\boxed{N_{\boldsymbol{k}_{0l}}^{\uparrow} = N_{\boldsymbol{k}_{0l'}}^{\uparrow}, \quad N_{\boldsymbol{k}_{0l}}^{\downarrow} = N_{\boldsymbol{k}_{0l'}}^{\downarrow}} \tag{3.110}$$

for all combinations of l and $l' \neq l$ for which the respective condensate occupation numbers are non-zero. Since the number of up or down pseudo-spin particle numbers is independent of condensate momentum, one may write

$$N_0^{\uparrow}/f \equiv N_{\boldsymbol{k}_{0l}}^{\uparrow} \tag{3.111}$$

$$N_0^{\downarrow}/f \equiv N_{\boldsymbol{k}_{0l}}^{\downarrow} \tag{3.112}$$

where f is the number of distinct condensate momentum, N_0^{α} is the total number of particles carrying pseudo-spin α and l is any of the f condensate momentum indices for which $N_{\boldsymbol{k}_{0l}}^{\alpha} \neq 0$. Thus, when the particle numbers satisifies the above constraints, the chemical potentials are independent of momentum index.

3.3.3 Exceptions to the condensate particle number solution

The solution in (3.110) does not *necessarily* hold if either [32]

$$\frac{(U^{\uparrow\downarrow})^2}{U^{\uparrow\uparrow}U^{\downarrow\downarrow}} = 1 \tag{3.113}$$

in *general*, or

$$\frac{\left(U^{\uparrow\downarrow}\cos\left(\gamma_{l'}-\gamma_l\right)\right)^2}{U^{\uparrow\uparrow}U^{\downarrow\downarrow}} = 1 \tag{3.114}$$

if $\boldsymbol{k}_{0l'}$ and $\boldsymbol{k}_{0l}$ are non-parallel, and either $N_{-\boldsymbol{k}_{0l}}^{\alpha} = 0$ or $N_{-\boldsymbol{k}_{0l'}}^{\alpha} = 0$, or

$$\frac{\left(U^{\uparrow\downarrow}\cos\left(\gamma_{l'}-\gamma_l\right)\right)^2}{U^{\uparrow\uparrow}U^{\downarrow\downarrow}(1-A)(1-B)} = 1, \quad A, B \neq 1 \tag{3.115}$$

if $N_{-\boldsymbol{k}_{0l}}^{\alpha}, N_{-\boldsymbol{k}_{0l'}}^{\alpha} \neq 0$, where A and B are defined by:

$$A = 2\cos\left(\theta_{-\boldsymbol{k}_{0l'}}^{\uparrow} - \theta_{\boldsymbol{k}_{0l}}^{\uparrow} - \theta_{-\boldsymbol{k}_{0l}}^{\uparrow} + \theta_{\boldsymbol{k}_{0l'}}^{\uparrow}\right) \tag{3.116}$$

$$B = 2\cos\left(\theta_{-\boldsymbol{k}_{0l'}}^{\uparrow} - \theta_{\boldsymbol{k}_{0l}}^{\uparrow} - \theta_{-\boldsymbol{k}_{0l}}^{\downarrow} + \theta_{\boldsymbol{k}_{0l'}}^{\downarrow}\right) \tag{3.117}$$

3.3.4 Complete Mean-Field Hamiltonian

If the solution in (3.110) holds, then the expressions for $\mu^{\uparrow}$ and $\mu^{\downarrow}$ can be simplified even further

$$\begin{aligned}\mu^{\uparrow} = &-\epsilon_i^{\uparrow} - |s_i|\sqrt{\frac{N_0^{\downarrow}}{N_0^{\uparrow}}}\Omega(|\boldsymbol{k}_{0i}|, N_i^{\uparrow}) \\ &+ \left(\sum_{ji'j'}\sum_{\alpha}\right)''' \frac{U^{\alpha\uparrow}N_0^{\alpha}}{N_s f}\cos\left(\theta_{j'}^{\uparrow} - \theta_i^{\uparrow} - \theta_j^{\alpha} + \theta_{i'}^{\alpha}\right)\delta_{i+j,i'+j'}\Omega(N_i^{\uparrow})\end{aligned} \tag{3.118}$$

$$\mu^{\downarrow} = -\epsilon_i^{\downarrow} - |s_i|\sqrt{\frac{N_0^{\uparrow}}{N_0^{\downarrow}}}\Omega(|\boldsymbol{k}_{0i}|, N_i^{\downarrow}) + \left(\sum_{ji'j'}\sum_{\alpha}\right)''' \frac{U^{\alpha\downarrow}N_0^{\alpha}}{N_s f}\cos\left(\theta_{j'}^{\downarrow} - \theta_i^{\downarrow} - \theta_j^{\alpha} + \theta_{i'}^{\alpha}\right)\delta_{i+j,i'+j'}\Omega(N_i^{\downarrow}) \tag{3.119}$$

The function $\Omega(x_1, x_2, ..., x_n)$, defined as

$$\Omega(x_1, x_2, ..., x_n) = \begin{cases} 1 & x_1 > 0, x_2 > 0 ... x_n > 0 \\ 0 & \text{otherwise} \end{cases} \tag{3.120}$$

enshures that we dont divide by zero, and forces us to choose a condensate momentum i for which the condensate number is non-zero. The primed sum $\left(\sum_{ji'j'}\sum_{\alpha}\right)'''$ means that we should sum over the subset of values (j, i', j', α) such that $N_j^{\alpha} \neq 0$, $N_{i'}^{\alpha} \neq 0$ and $N_{j'}^{\alpha} \neq 0$. The complete Hamiltonian after applying mean-field theory is derived in detail in Jansønns master thesis [32], with the result

$$H \approx H_0 + H_1 + H_2 \tag{3.121}$$

where the linear terms in condensate fluctuations have been cancelled by tuning $\mu^{\uparrow}$ and $\mu^{\downarrow}$, or equivalently $N_0^{\uparrow}$ and $N_0^{\downarrow}$. This means that the condensate numbers are no longer variational parameters, as they already have been chosen to minimize F through cancelling terms linear in condensate fluctuations. The constant Hamiltonian H_0 is given by

$$H_0 = -\frac{1}{2N_s f^2}\left(\sum_{iji'j'}\sum_{\alpha\beta}\right)''' U^{\alpha\beta}N_0^{\alpha}N_0^{\beta}\cos\left(\theta_{j'}^{\alpha} - \theta_i^{\alpha} - \theta_j^{\beta} + \theta_{i'}^{\beta}\right)\delta_{i+j,i'+j'} \tag{3.122}$$

where the primed sum runs over the subset of values $(i, j, i', j', \alpha, \beta)$ for which $N_i^{\alpha} \neq 0$, $N_j^{\beta} \neq 0$, $N_{i'}^{\beta} \neq 0$ and $N_{j'}^{\alpha} \neq 0$. The next term, H_1, comprises all terms *linear* in *excitation* operators

$$H_1 = \frac{1}{N_s f^{3/2}}{\sum_{\boldsymbol{k}}}'\left(\sum_{iji'}\sum_{\alpha\beta}\right)''' U^{\alpha\beta}N_0\sqrt{N_0^{\beta}} \times \left(e^{-i\left(\theta_{i'}^{\beta} - \theta_i^{\alpha} - \theta_j^{\beta}\right)}A_{\boldsymbol{k}}^{\alpha} + \text{H.c}\right)\delta_{\boldsymbol{k}+\boldsymbol{k}_{0i'},\boldsymbol{k}_{0j}+\boldsymbol{k}_{0i}} \tag{3.123}$$

The first primed sum over $\boldsymbol{k}$ avoids condensate momenta, and the second primed sum runs over the subset of values $(i, j, i', \alpha, \beta)$ such that $N_i^{\alpha} \neq 0$, $N_j^{\beta} \neq 0$ and $N_{i'}^{\beta} \neq 0$. The next term, H_2,

comprises all terms *quadratic* in *excitation* operators

$$\begin{aligned}
H_2 =& \sum_{\boldsymbol{k}} \sum_{\alpha\beta} \eta_{\boldsymbol{k}}^{\alpha\beta} A_{\boldsymbol{k}}^{\alpha\dagger} A_{\boldsymbol{k}}^{\beta} \\
&+ \frac{1}{2N_s f} \sum_{\boldsymbol{k}\boldsymbol{k}'} \left(\sum_{ij} \sum_{\alpha\beta} \right)_1''' U^{\alpha\beta} \sqrt{N_0^{\alpha} N_0^{\beta}} \\
&\times \Big(\left(e^{-i\left(-\theta_i^{\alpha} - \theta_j^{\beta}\right)} A_{\boldsymbol{k}}^{\beta} A_{\boldsymbol{k}'}^{\alpha} + \text{H.c} \right) \delta_{\boldsymbol{k}+\boldsymbol{k}', \boldsymbol{k}_{0i}+\boldsymbol{k}_{0j}} \\
&+ \left(e^{-i\left(-\theta_i^{\alpha} + \theta_j^{\beta}\right)} A_{\boldsymbol{k}}^{\beta\dagger} A_{\boldsymbol{k}'}^{\alpha} + \text{H.c} \right) \delta_{\boldsymbol{k}_{0i}+\boldsymbol{k}, \boldsymbol{k}'+\boldsymbol{k}_{0j}} \Big) \\
&+ \frac{1}{2N_s f} \sum_{\boldsymbol{k}\boldsymbol{k}'} \left(\sum_{ij} \sum_{\alpha\beta} \right)_2''' U^{\alpha\beta} N_0^{\alpha} \\
&\times \left(e^{-i\left(-\theta_i^{\alpha} + \theta_j^{\alpha}\right)} A_{\boldsymbol{k}}^{\beta\dagger} A_{\boldsymbol{k}'}^{\beta} + \text{H.c} \right) \delta_{\boldsymbol{k}_{0i}+\boldsymbol{k}, \boldsymbol{k}'+\boldsymbol{k}_{0j}}
\end{aligned} \tag{3.124}$$

where the first primed sum runs over the subset of values (i, j, α, β) such that $N_i^{\alpha} \neq 0$ and $N_j^{\beta} \neq 0$, and the second goes over the subset of values such that $N_i^{\alpha} \neq 0$ and $N_j^{\alpha} \neq 0$. Note that the second constrained sum gives no restriction on $\beta \in (\uparrow, \downarrow)$. We have also relabeled the condensate fluctuations

$$\delta A_i^{\alpha} \equiv A_i^{\alpha} \tag{3.125}$$

Which is why the sums over $\boldsymbol{k}$ and $\boldsymbol{k}'$ in H_2 are *unconstrained*. We further recast H_2 into a more pleasing form

$$\begin{aligned}
H_2 = H_{\text{non-int}} + H_{\text{int}} =& \sum_{\boldsymbol{k}} \sum_{\alpha\beta} \eta_{\boldsymbol{k}}^{\alpha\beta} A_{\boldsymbol{k}}^{\alpha\dagger} A_{\boldsymbol{k}}^{\beta} \\
&+ \sum_{\boldsymbol{k}\boldsymbol{k}'} \left(\sum_{ij} \sum_{\alpha\beta} \right)_1''' g_{ij}^{\alpha\beta}(\boldsymbol{k}, \boldsymbol{k}') \delta_{\boldsymbol{k}+\boldsymbol{k}', \boldsymbol{k}_{0i}+\boldsymbol{k}_{0j}} + r_{ij}^{\alpha\beta}(\boldsymbol{k}, \boldsymbol{k}') \delta_{\boldsymbol{k}_{0i}+\boldsymbol{k}, \boldsymbol{k}'+\boldsymbol{k}_{0j}} \\
&+ \sum_{\boldsymbol{k}\boldsymbol{k}'} \left(\sum_{ij} \sum_{\alpha\beta} \right)_2''' l_{ij}^{\alpha\beta}(\boldsymbol{k}, \boldsymbol{k}') \delta_{\boldsymbol{k}_{0i}+\boldsymbol{k}, \boldsymbol{k}'+\boldsymbol{k}_{0j}}
\end{aligned} \tag{3.126}$$

The subscipt non-int refers to the single-particle Hamiltonian, with SOC. The first primed sum $\left(\sum_{ij} \sum_{\alpha\beta}\right)_1'''$ goes over the subset of values (i, j, α, β) such that $N_i^{\alpha} \neq 0$ and $N_j^{\beta} \neq 0$, and the second primed sum $\left(\sum_{ij} \sum_{\alpha\beta}\right)_2'''$ goes over the subset of values such that $N_i^{\alpha} \neq 0$ and $N_j^{\alpha} \neq 0$. Here, we have defined

$$g_{ij}^{\alpha\beta}(\boldsymbol{k}, \boldsymbol{k}') = \frac{1}{2} a^{\alpha\beta} e^{i\sigma_{ij}^{\alpha\beta}} \left(A_{\boldsymbol{k}}^{\beta} A_{\boldsymbol{k}'}^{\alpha} + A_{\boldsymbol{k}'}^{\alpha} A_{\boldsymbol{k}}^{\beta} \right) + \text{H.c} \tag{3.127}$$

$$r_{ij}^{\alpha\beta}(\boldsymbol{k}, \boldsymbol{k}') = \frac{1}{2} a^{\alpha\beta} e^{i\delta_{ij}^{\alpha\beta}} \left(A_{\boldsymbol{k}}^{\beta\dagger} A_{\boldsymbol{k}'}^{\alpha} + A_{\boldsymbol{k}'}^{\alpha} A_{\boldsymbol{k}}^{\beta\dagger} - \delta_{\boldsymbol{k}, \boldsymbol{k}'} \delta^{\alpha\beta} \right) + \text{H.c} \tag{3.128}$$

$$l_{ij}^{\alpha\beta}(\boldsymbol{k}, \boldsymbol{k}') = \frac{1}{2} b^{\alpha\beta} e^{i\delta_{ij}^{\alpha\alpha}} \left(A_{\boldsymbol{k}}^{\beta\dagger} A_{\boldsymbol{k}'}^{\beta} + A_{\boldsymbol{k}'}^{\beta} A_{\boldsymbol{k}}^{\beta\dagger} - \delta_{\boldsymbol{k}, \boldsymbol{k}'} \right) + \text{H.c} \tag{3.129}$$

The operators $g_{ij}^{\alpha\beta}(\boldsymbol{k},\boldsymbol{k}')$, $r_{ij}^{\alpha\beta}(\boldsymbol{k},\boldsymbol{k}')$ and $l_{ij}^{\alpha\beta}(\boldsymbol{k},\boldsymbol{k}')$ have already have utilized the bosonic commutation relations

$$A_{\boldsymbol{k}}^{\alpha\dagger}A_{\boldsymbol{k}'}^{\beta} = \frac{1}{2}\left(A_{\boldsymbol{k}}^{\alpha\dagger}A_{\boldsymbol{k}'}^{\beta} + A_{\boldsymbol{k}'}^{\beta}A_{\boldsymbol{k}}^{\alpha\dagger} - \delta_{\boldsymbol{k},\boldsymbol{k}'}\delta^{\alpha\beta}\right) \tag{3.130}$$

$$A_{\boldsymbol{k}}^{\alpha}A_{\boldsymbol{k}'} = \frac{1}{2}\left(A_{\boldsymbol{k}}^{\alpha}A_{\boldsymbol{k}'}^{\beta} + A_{\boldsymbol{k}'}\beta A_{\boldsymbol{k}}^{\alpha}\right) \tag{3.131}$$

which will be helpful for calculating matrix elements in later chapters. The lower indices (i,j) refer to the mean-field parameters, caused by SOC, the upper indices (α,β) refer to a specific pseudo-spin configuration, and the arguments $(\boldsymbol{k},\boldsymbol{k}')$ gives the operator dependence. In addition, the coeffecients are given by

$$a^{\alpha\beta} = \sqrt{N_0^{\alpha}N_0^{\beta}}\frac{U^{\alpha\beta}}{2N_s f}, \quad \sigma_{ij}^{\alpha\beta} \equiv \theta_i^{\alpha} + \theta_j^{\beta} \tag{3.132}$$

$$b^{\alpha\beta} = N_0^{\alpha}\frac{U^{\alpha\beta}}{2N_s f}, \quad \delta_{ij}^{\alpha\beta} \equiv \theta_i^{\alpha} - \theta_j^{\beta} \tag{3.133}$$

Let us also for later, define the quantities G, R and L which are independent of pseudo-spin

$$G_{ij}(\boldsymbol{k},\boldsymbol{k}') = \sum_{\alpha\beta} g_{ij}^{\alpha\beta}(\boldsymbol{k},\boldsymbol{k}') \tag{3.134}$$

$$R_{ij}(\boldsymbol{k},\boldsymbol{k}') = \sum_{\alpha\beta} r_{ij}^{\alpha\beta}(\boldsymbol{k},\boldsymbol{k}') \tag{3.135}$$

$$L_{ij}(\boldsymbol{k},\boldsymbol{k}') = \sum_{\alpha\beta} l_{ij}^{\alpha\beta}(\boldsymbol{k},\boldsymbol{k}') \tag{3.136}$$

which explicitly written out becomes

$$G_{ij}(\boldsymbol{k},\boldsymbol{k}') = \frac{1}{2}a^{\uparrow\uparrow}e^{i\sigma_{ij}^{\uparrow\uparrow}}\left(A_{\boldsymbol{k}}^{\uparrow}A_{\boldsymbol{k}'}^{\uparrow} + A_{\boldsymbol{k}'}^{\uparrow}A_{\boldsymbol{k}}^{\uparrow}\right) + \text{H.c} \tag{3.137}$$

$$+ \frac{1}{2}a^{\uparrow\downarrow}e^{i\sigma_{ij}^{\uparrow\downarrow}}\left(A_{\boldsymbol{k}}^{\downarrow}A_{\boldsymbol{k}'}^{\uparrow} + A_{\boldsymbol{k}'}^{\uparrow}A_{\boldsymbol{k}}^{\downarrow}\right) + \text{H.c} \tag{3.138}$$

$$+ \frac{1}{2}a^{\downarrow\uparrow}e^{i\sigma_{ij}^{\downarrow\uparrow}}\left(A_{\boldsymbol{k}}^{\uparrow}A_{\boldsymbol{k}'}^{\downarrow} + A_{\boldsymbol{k}'}^{\downarrow}A_{\boldsymbol{k}}^{\uparrow}\right) + \text{H.c} \tag{3.139}$$

$$+ \frac{1}{2}a^{\downarrow\downarrow}e^{i\sigma_{ij}^{\downarrow\downarrow}}\left(A_{\boldsymbol{k}}^{\downarrow}A_{\boldsymbol{k}'}^{\downarrow} + A_{\boldsymbol{k}'}^{\downarrow}A_{\boldsymbol{k}}^{\downarrow}\right) + \text{H.c} \tag{3.140}$$

$$R_{ij}(\boldsymbol{k},\boldsymbol{k}') = \frac{1}{2}a^{\uparrow\uparrow}e^{i\delta_{ij}^{\uparrow\uparrow}}\left(A_{\boldsymbol{k}}^{\uparrow\dagger}A_{\boldsymbol{k}'}^{\uparrow} + A_{\boldsymbol{k}'}^{\uparrow}A_{\boldsymbol{k}}^{\uparrow\dagger} - \delta_{\boldsymbol{k},\boldsymbol{k}'}\right) + \text{H.c} \tag{3.141}$$

$$+ \frac{1}{2}a^{\uparrow\downarrow}e^{i\delta_{ij}^{\uparrow\downarrow}}\left(A_{\boldsymbol{k}}^{\downarrow\dagger}A_{\boldsymbol{k}'}^{\uparrow} + A_{\boldsymbol{k}'}^{\uparrow}A_{\boldsymbol{k}}^{\downarrow\dagger}\right) + \text{H.c} \tag{3.142}$$

$$+ \frac{1}{2}a^{\downarrow\uparrow}e^{i\delta_{ij}^{\downarrow\uparrow}}\left(A_{\boldsymbol{k}}^{\uparrow\dagger}A_{\boldsymbol{k}'}^{\downarrow} + A_{\boldsymbol{k}'}^{\downarrow}A_{\boldsymbol{k}}^{\uparrow\dagger}\right) + \text{H.c} \tag{3.143}$$

$$+ \frac{1}{2}a^{\downarrow\downarrow}e^{i\delta_{ij}^{\downarrow\downarrow}}\left(A_{\boldsymbol{k}}^{\downarrow\dagger}A_{\boldsymbol{k}'}^{\downarrow} + A_{\boldsymbol{k}'}^{\downarrow}A_{\boldsymbol{k}}^{\downarrow\dagger} - \delta_{\boldsymbol{k},\boldsymbol{k}'}\right) + \text{H.c} \tag{3.144}$$

$$L_{ij}(\boldsymbol{k},\boldsymbol{k}') = \frac{1}{2}\left(b^{\uparrow\uparrow}e^{i\delta_{ij}^{\uparrow\uparrow}} + b^{\downarrow\uparrow}e^{i\delta_{ij}^{\downarrow\downarrow}}\right)\left(A_{\boldsymbol{k}}^{\uparrow\dagger}A_{\boldsymbol{k}'}^{\uparrow} + A_{\boldsymbol{k}'}^{\uparrow}A_{\boldsymbol{k}}^{\uparrow\dagger} - \delta_{\boldsymbol{k},\boldsymbol{k}'}\right) + \text{H.c} \tag{3.145}$$

$$+ \frac{1}{2}\left(b^{\downarrow\downarrow}e^{i\delta_{ij}^{\downarrow\downarrow}} + b^{\uparrow\downarrow}e^{i\delta_{ij}^{\uparrow\uparrow}}\right)\left(A_{\boldsymbol{k}}^{\downarrow\dagger}A_{\boldsymbol{k}'}^{\downarrow} + A_{\boldsymbol{k}'}^{\downarrow}A_{\boldsymbol{k}}^{\downarrow\dagger} - \delta_{\boldsymbol{k},\boldsymbol{k}'}\right) + \text{H.c} \tag{3.146}$$

3.4 Dynamic matrix method

After mean-field theory, the Hamiltonian is written as a product of bilinear creation and annihilation operators. The hope is now to diagonalize the two-component, spin-orbit coupled, weakly interacting Bose gas, in effect describing the system as an effective free particle problem. Naturally, one would look for a unitary transformation. But, reality is often disappointing, and it will become apparant that a unitary transformation will rarely preserve the physics of the system. We must therefore turn to other diagonalization methods, namely the *dynamic matrix method*. The following work is based heavily on Xiao [53], Hemmen [50] and Tsallis [49]. Let us consider the quadratic Hamiltonian, comprising all types of bilinear terms

$$H = \sum_{i,j}^{n} \alpha_{ij}c_i^\dagger c_j + \frac{1}{2}\gamma_{ij}c_i^\dagger c_j^\dagger + \frac{1}{2}\gamma_{ij}^* c_i c_j \tag{3.147}$$

The operators c_i and $c_i^\dagger$ are bosonic annihilation and creation operators, satisfying bosonic commutation relations

$$[c_i, c_j^\dagger] = \delta_{ij}, \quad [c_i, c_j] = [c_i^\dagger, c_j^\dagger] = 0 \tag{3.148}$$

Since the Hamiltonian is hermitian, $H = H^\dagger$, the coefficients $\alpha_{ij} \in \mathbb{C}$, $\gamma_{ij} \in \mathbb{C}$ have the following properties

$$\alpha_{ij} = \alpha_{ji}^*, \quad \gamma_{ij} = \gamma_{ji} \tag{3.149}$$

Introducing the field operators ψ and $\psi^\dagger$ in $2n$ dimensions as

$$\psi = \begin{pmatrix} c \\ c^{\dagger T} \end{pmatrix}, \quad \psi^\dagger = \begin{pmatrix} c^\dagger & c^T \end{pmatrix} \tag{3.150}$$

where c and $c^\dagger$ are vectors of operators in n dimensions

$$c = \begin{pmatrix} c_1 \\ \vdots \\ c_n \end{pmatrix}, \quad c^\dagger = \begin{pmatrix} c_1^\dagger & \dots & c_n^\dagger \end{pmatrix} \tag{3.151}$$

We can write the Hamiltonian in eq. (3.147) on the form

$$H = \frac{1}{2}\psi^\dagger M \psi - \frac{1}{2}\text{tr}(\alpha) \tag{3.152}$$

The coefficient matrix M is given by

$$M = \begin{pmatrix} \alpha & \gamma \\ \gamma^* & \alpha^* \end{pmatrix} \tag{3.153}$$

where α and γ are the submatrices with α_{ij} and γ_{ij} as entries. We also have,

$$\alpha = \alpha^\dagger, \quad \gamma = \gamma^T, \quad M = M^\dagger \tag{3.154}$$

such that α and M are hermitian matrices, and γ is a symmetric matrix. We next define the matrix J:

$$[\psi_\mu, \psi_\nu^\dagger] = J_{\mu\nu}, \quad 1 \leq \mu, \nu \leq 2n \tag{3.155}$$

The form of J is decided upon using the commutation relations for c_i and $c_i^\dagger$, giving

$$J = \begin{pmatrix} 1_n & 0 \\ 0 & -1_n \end{pmatrix} \tag{3.156}$$

with 1_n as the identity matrix in n-dimensions. To diagonalize the Hamiltonian, Bogoliubov and Valking proposed the following linear transformation

$$c = Ad + B{d^\dagger}^T \tag{3.157}$$

with A and B as square matrices of size n, and d and $d^\dagger$ are vectors of operators in n dimensions

$$d = \begin{pmatrix} d_1 \\ \vdots \\ d_n \end{pmatrix}, \quad d^\dagger = \begin{pmatrix} d_1^\dagger & \dots & d_n^\dagger \end{pmatrix} \tag{3.158}$$

The operators d_i and $d_i^\dagger$ are *new* bosonic annihilation and creation operators satisfying the standard commutation relations,

$$[\phi_\mu, \phi_\nu^\dagger] = J_{\mu\nu} \tag{3.159}$$

with d and $d^\dagger$ as elements in the new basis ϕ in $2n$ dimensions

$$\phi = \begin{pmatrix} d \\ {d^\dagger}^T \end{pmatrix}, \quad \phi^\dagger = \begin{pmatrix} d^\dagger & d^T \end{pmatrix} \tag{3.160}$$

Using that $c = c^\dagger$, we use the proposed linear transformation in the *old* field operators in eq. (3.150), leading to the transformation rule

$$\psi = \begin{pmatrix} c \\ c^{\dagger T} \end{pmatrix} = \begin{pmatrix} Ad + Bd^{\dagger T} \\ \left(d^\dagger A^\dagger + d^T B^\dagger\right)^T \end{pmatrix} = \begin{pmatrix} Ad + Bd^{\dagger T} \\ B^{\dagger T} d + A^{\dagger T} d^{\dagger T} \end{pmatrix} \tag{3.161}$$

$$= \begin{pmatrix} A & B \\ B^* & A^* \end{pmatrix} \begin{pmatrix} d \\ d^{\dagger T} \end{pmatrix} \tag{3.162}$$

$$= T\phi \tag{3.163}$$

The transformation matrix T is defined as

$$\begin{pmatrix} A & B \\ B^* & A^* \end{pmatrix} \tag{3.164}$$

Inserting $\psi = T\phi$ into the Hamiltonian in (3.152), one obtains:

$$H = \frac{1}{2}\phi^\dagger T^\dagger M T \phi - \frac{1}{2}\mathrm{tr}(\alpha) \tag{3.165}$$

The matrix $T^\dagger MT$ is the new coefficient matrix. The first requirement on the transformation matrix T is that $T^\dagger MT$ is *diagonal*, which means

$$T^\dagger MT = \text{diag}(w_1, \ldots, w_{2n}) \tag{3.166}$$

with the constraint that the diagonal entries w_μ's must be real for $\mu = 1, \ldots, 2n$[1]. If this is the case, then the Hamiltonian will be written as a sum over independent harmonic oscillators in the new basis ϕ. We further have another constraint on T, namely that the new quasi-particles are bosonic

$$J_{\mu\nu} = [\psi_\mu, \psi_\nu^\dagger] = \sum_{\alpha\beta}^{2n} T_{\mu\alpha} T^*_{\nu\beta} [\phi_\alpha, \phi_\beta^\dagger] \tag{3.167}$$

$$= \sum_{\alpha\beta}^{2n} T_{\mu\alpha} J_{\alpha\beta} T^*_{\nu\beta} \tag{3.168}$$

$$= (TJT^\dagger)_{\mu\nu} \tag{3.169}$$

which is equivalent to,

$$J = TJT^\dagger \tag{3.170}$$

In summary, the tranformation matrix T must satisfy equations (3.166) and (3.170). The first enshures that T diagonalizes M, which is a mathematical argument, and the second enshures that the system is still bosonic after the transformation, which is a *physical* argument.

Since H is hermitian, it can always be diagonalized by a unitary transformation. One would therefore think that the same unitary transformation could be used to diagonalize the bosonic system. However, a unitary transformation cannot in general be brought on the form in (3.164), or meet the bosonic requirements in (3.170). It is stated in [53] that this is due to the field operators ψ and ϕ being vectors of operators, not complex numbers. The diagonalization of a bosonic system is therefore much more complicated. It is emphasized in [53], that a very efficient way for diagonalizing a quadratic hamiltonian, is to use the Heisenberg equations of motions for the system. It can be shown that for the bosonic system described by equation (3.147), the Heisenberg equations of motion becomes (with $\hbar = c = 1$)

$$i\frac{\mathrm{d}}{\mathrm{d}t}\psi = D\psi \tag{3.171}$$

Where D is *different* from M, and is given by

$$D = JM \tag{3.172}$$

please note that D is in general not hermitian. We say that a dynamic matrix is *physically diagonizable* if it is diagonizable and all its eigenvalues are real. If we can find a T that has the right shape according to (3.164) and satisfies requirements (3.170) and (3.166), then we call the quadratic Hamiltonian BV diagonizable. The relationship between a BV diagonizable Hamiltonian and the associated dynamic matrix is as follows

A quadratic Hamiltonian of bosons is BV diagonizable if and only if its dynamic matrix is

[1] Please note that the w_μ's are not the eigenvalues of M

physically diagonizable.
This is an important result. It means that we should not find the eigenvectors and eigenvalues of M, but rather of $D = JM$. We must also require that the eigenvalues of D are real, which becomes a stability requirement.

3.4.1 Investigating the eigenvalues and eigenvectors of the dynamic matrix

To bring the Hamiltonian on diagonal form, we should look for a T that diagonalizes D

$$T^{-1}DT = \Omega \tag{3.173}$$

where Ω is a diagonal $2n \times 2n$ matrix. We must also meet requirement (3.170), which gives us an equation for T^{-1}

$$J = TJT^{\dagger} \tag{3.174}$$
$$T^{-1} = JT^{\dagger}J \tag{3.175}$$

using that $J^2 = 1$. Expressing $D = JM$ as $D = T\Omega T^{-1}$, we get an equation for the original coefficient matrix M

$$M = JT\Omega T^{-1} \tag{3.176}$$

which gives for the quadratic part of the Hamiltonian $\psi^{\dagger}M\psi$

$$\psi^{\dagger}M\psi = \psi^{\dagger}JT\Omega T^{-1}\psi \tag{3.177}$$
$$= \psi^{\dagger}JTJJ\Omega T^{-1}\psi \tag{3.178}$$
$$= \psi^{\dagger}(T^{-1})^{\dagger}J\Omega T^{-1}\psi \tag{3.179}$$
$$= \phi^{\dagger}J\Omega\phi \tag{3.180}$$

The new basis is defined by the transfomration matrix $\phi = T^{-1}\psi$. Further, the matrix $J\Omega$ is diagonal. Thus, if T diagonalizes D and preserves bosonic commutation relations by eq. (3.170), then the Hamiltonian can be brought on diagonal form. Next we investigate the shape of T and the physical diagonalizability of the dynamic matrix. Following the steps in Hemmen [50], we define the operator K acting on a general vector $\begin{pmatrix}\boldsymbol{u}^T & \boldsymbol{v}^T\end{pmatrix}^T$ in $\mathbb{C}^{2n}$, where $\boldsymbol{u}$ and $\boldsymbol{v}$ are in $\mathbb{C}^n$

$$K\begin{pmatrix}\boldsymbol{u}\\ \boldsymbol{v}\end{pmatrix} = \begin{pmatrix}\boldsymbol{v}^*\\ \boldsymbol{u}^*\end{pmatrix} \tag{3.181}$$

It can be shown that K satisfies the relations $\{J, K\} = 0$ and $[M, K] = 0$ [2]. If $\boldsymbol{x}_i$ is an eigenvector of D with corresponding eigenvalue w_i, then $K\boldsymbol{x}_i$ is also an eigenvector with corresponding eigenvalue $-w_i$

$$D(K\boldsymbol{x}_i) = JMK\boldsymbol{x}_i = JKM\boldsymbol{x}_i = -K(JM\boldsymbol{x}_i) = -w_iK\boldsymbol{x}_i \tag{3.182}$$

[2]The last relation comes from the fact that M has the shape as in eq.(3.153)

thus we only need to find half of the eigenvalues. It is shown in Xiao [53] that the pairs of eigenvectors corresponding to the eigenvalues $(w, -w)$ are linearly independent. One may then construct the diagonal matrix

$$\Omega = \text{diag}(w_1, \ldots, w_n, -w_1, \ldots, -w_n) \tag{3.183}$$

leading to the diagonal matrix associated with M

$$J\Omega = \text{diag}(w_1, \ldots, w_n, w_1, \ldots, w_n) \tag{3.184}$$

We cannot however, determine whether the w_i's are real or not, which depends on the entries in D. The diagonal matrix Ω requires that we construct T as

$$T = \begin{pmatrix} \boldsymbol{x}_1 & \ldots & \boldsymbol{x}_n & K(\boldsymbol{x}_1) & \ldots & K(\boldsymbol{x}_n) \end{pmatrix} \tag{3.185}$$

The form of T is consequently given by

$$T = \begin{pmatrix} T_1 & T_2 \\ T_2^* & T_1^* \end{pmatrix} \tag{3.186}$$

which satisfies the form as outlined in eq. (3.164). Now, equation (3.170) leads to the following constraint on the eigenvectors $\boldsymbol{u}_\mu$

$$(\boldsymbol{u}_\mu, J\boldsymbol{u}_\nu) = J_{\mu\nu} \quad 0 \leq \mu, \nu \leq 2n \tag{3.187}$$

where $(\boldsymbol{x}, \boldsymbol{y}) = \sum_\mu x_\mu^* y_\mu$ is the conventional inner product in $\mathbb{C}^{2n}$. Here $\boldsymbol{u}_\mu$ is an eigenvector of D, either $\boldsymbol{x}_i$ or $K\boldsymbol{x}_i$. We also define the norm of a vector $\boldsymbol{u}_\mu$ as

$$(\boldsymbol{u}_\mu, J\boldsymbol{u}_\mu) = J_{\mu\mu} \tag{3.188}$$

which can be either positive or negative. If $\mu \leq n$, the eigenvectors u_μ must be scaled to have norm 1, and if $\mu > n$ the eigenvectors u_μ must be scaled to have norm -1. Here comes an important point. The norm requirement demands that we must construct the eigenvectors with positive norm on the *left* in T, and the eigenvectors with negative norm on the *right* in T. In addition, *if* M is positive-definite[3], we have

$$w_\mu(\boldsymbol{u}_\mu, J\boldsymbol{u}_\mu) = (\boldsymbol{u}_\mu, Jw_\mu\boldsymbol{u}_\mu) = (\boldsymbol{u}_\mu, M\boldsymbol{u}_\mu) > 0 \tag{3.189}$$

such that

$$w_\mu(\boldsymbol{u}_\mu, J\boldsymbol{u}_\mu) > 0 \tag{3.190}$$

which means that if $\mu \leq n$, the eigenvalues w_μ must be positive, since the norm of eigenvector $\boldsymbol{u}_\mu$ is positive by construction. This makes physical sense, as then the diagonalized Hamiltonian is bounded from below. If however M is indeterminate, which means that M both as positive and negative eigenvalues λ_μ, then we cannot with certainty place the eigenvectors with $w_\mu > 0$ to the left in T. This observation will turn out to be important for later in the thesis. It will for example be the case that an eigenvector with positive eigenvalue w_μ will have a negative

[3]This means that M has strictly positive eigenvalues $\lambda_\mu > 0$, and that $(\boldsymbol{x}_\mu, M\boldsymbol{x}_\mu) > 0$ for an arbitrary vector $\boldsymbol{x}_\mu \neq 0$

norm, while the associated eigenvector with eigenvalue $-w_i$ will have a positive norm. Thus the diagonal matrix associated with the quadratic, intederminate, Hamiltonian becomes

$$J\Omega = \mathrm{diag}(w_1, \ldots, -w_i, \ldots, w_n, w_1, \ldots, -w_i, \ldots, w_n) \tag{3.191}$$

Which is *not* bounded from below by zero (assuming $w_i > 0$). One can however lift the energy-spectrum, absorbing the difference in the chemical potentials, as was done in section 3.1.

When the eigenvalues of the dynamic matrix are zero, it is shown in [53] that the corresponding eigenvectors are linearly independent, and the norm of the eigenvectors come in pairs as $(1, -1)$. Also, the number of zero-eigenvalues should be an even number, as even the zero-eigenvalues comes in pairs $(0, -0)$.

3.5 Free energy and the Metropolis-Hastings algorithm

Depending on the phase, the mean field approach introduces a number of mean-field variational parameters to be determined. These must be decided by minimizing the free energy of the system. The parameters will be shown to be $\{\theta_i\}$ with $i = 1 \ldots m$, where m is the number of *independent* θ parameters, and k_0 which is the finite length of the non-zero SOC-induced minima in $\boldsymbol{k}$-space. We express this dependence by

$$F = F(\{\theta_i\}, k_0) \tag{3.192}$$

The mean-field parameters $\{\theta_i\}$ and k_0 can in principle be functions of the physical parameters of the system, e.g the SOC strength λ_R and the intra and inter scattering strengths $U^{\alpha\beta}$. The Hamiltonian is assumed to be on the diagonal form

$$H = C + \frac{1}{2}\sum_{\boldsymbol{k}}\sum_{\sigma} \hbar\omega_\sigma(\boldsymbol{k}) \left(d^{\sigma\dagger}_{\boldsymbol{k}} d^{\sigma}_{\boldsymbol{k}} + \frac{1}{2} \right) \tag{3.193}$$

where C is an operator independent term, σ labels the branch, $\hbar\omega_\sigma(\boldsymbol{k})$ is the excitation spectrum for branch σ, and the $d^{\sigma}_{\boldsymbol{k}}$'s constitutate a basis for the diagonal Hamiltonian. We next introduce the state $|\mathcal{N}_m\rangle$ in Fock space

$$|\mathcal{N}_m\rangle = |n_1\rangle\,|n_2\rangle \ldots |n_m\rangle \tag{3.194}$$

which is a product of single-particle number states $\hat{n}_i = d^{\dagger}_i d_i$, where i is a set of quantum numbers. To obtain F, where we follow the derivation from Solli [48], we must first find the partition function Z

$$\begin{aligned} Z &= \mathrm{tr}\left(e^{-\beta H}\right) && (3.195)\\ &= \sum_m \langle \mathcal{N}_m |\, e^{-\beta H}\, |\mathcal{N}_m\rangle && (3.196)\\ &= e^{-\beta C} e^{-\beta/4 \sum_{\boldsymbol{k},\sigma} \hbar\omega_\sigma(\boldsymbol{k})} \sum_m \langle \mathcal{N}_m |\, e^{-\beta/2 \sum_{\boldsymbol{k},\sigma} \hbar\omega_\sigma \hat{n}_{\boldsymbol{k},\sigma}}\, |\mathcal{N}_m\rangle && (3.197) \end{aligned}$$

where $\beta = 1/kT$ is the inverse temperature. The average $\langle \mathcal{N}_m | \dots | \mathcal{N}_m \rangle$ becomes

$$\sum_m \langle \mathcal{N}_m | \, e^{-\beta/2 \sum_{\boldsymbol{k},\sigma} \hbar\omega_\sigma \hat{n}_{\boldsymbol{k},\sigma}} \, | \mathcal{N}_m \rangle = \tag{3.198}$$

$$\prod_{\boldsymbol{k},\sigma} \sum_m \langle \mathcal{N}_m | \, e^{-\beta/2 \hbar\omega_\sigma \hat{n}_{\boldsymbol{k},\sigma}} \, | \mathcal{N}_m \rangle = \tag{3.199}$$

$$\prod_{\boldsymbol{k},\sigma} \sum_m \langle \mathcal{N}_m | \, e^{\beta/2 \hbar\omega_\sigma n_{\boldsymbol{k},\sigma}} \, | \mathcal{N}_m \rangle = \tag{3.200}$$

$$\prod_{\boldsymbol{k},\sigma} \sum_{n_{\boldsymbol{k},\sigma}} e^{\beta/2 \hbar\omega_\sigma n_{\boldsymbol{k},\sigma}} = \tag{3.201}$$

$$\prod_{\boldsymbol{k},\sigma} \frac{1}{1 - \exp\left(-\frac{\beta}{2}\hbar\omega_\sigma(\boldsymbol{k})\right)} \tag{3.202}$$

where we recognized the last sum as a geometric series, since the occupation number for any single-particle boson state can be infinite. This gives the free energy $F = -\frac{1}{\beta}\ln(Z)$ as

$$F = C + \frac{1}{4}\sum_{\boldsymbol{k},\sigma} \hbar\omega_\sigma(\boldsymbol{k}) + \frac{1}{\beta}\sum_{\boldsymbol{k},\sigma} \ln\left(1 - \exp\left(\frac{-\beta}{2}\hbar\omega_\sigma(\boldsymbol{k})\right)\right) \tag{3.203}$$

For zero temperature $T \to 0$ ($\beta \to \infty$) the expression becomes

$$F = C + \frac{1}{4}\sum_{\boldsymbol{k},\sigma} \hbar\omega_\sigma(\boldsymbol{k}) \tag{3.204}$$

In order for this limit to be valid it is important that all the branches are positive. We see that the effect of interactions has a finite contribution at $T = 0$, since the excitation spectrum is non-zero. We must now minimize F w.r.t the mean-field parameters $\{\theta_i\}$ and k_0. This *can* be done by taking a first derivative of F w.r.t all mean-field parameters, and setting this to zero. One must also take a second derivative to check that the values of $\{\theta_i\}$ and k_0 gives a *minimum*. This is the preferred method if one has an analytic expression for C and $\hbar\omega_\sigma(\boldsymbol{k})$, as was the case in Janssønn [32] where the *pure* condensate was considered. However, this is rarely the case for more complex phases, and we turn to *Monte Carlo* methods for determining these parameters

3.5.1 Metropolis-Hastings algorithm

A Monte Carlo method is a numerical method which rely on repeated random samplings to obtain numerical results [43]. They are popular methods in physics and mathematics when it is hard or even impossible to obtain analytical results. We will here present the Metropolis-Hastings algorithm which is a Monte Carlo method [28]. The main idea is to try to minimize the free energy $F(\{\theta_i\}, k_0)$ by randomly exploring the phase space $(\{\theta_i\}, k_0)$ available, computing and comparing the free energy at random points hopefully converging to the global minima of F. The following algorithm is based on sec. 3.1.4 in [28], and also from [43]. The *transition probabilities* $\mathcal{P}(\Psi_i \to \Psi_j)$, which is the probability of going to state Ψ_j given that you are in state Ψ_i, are in the Metropolis-Hastings algorithm chosen to satisfy the *detailed balance* constraint

$$p(\Psi_i)\mathcal{P}(\Psi_i \to \Psi_j) = p(\Psi_j)\mathcal{P}(\Psi_j \to \Psi_i) \tag{3.205}$$

The state Ψ_i is particular configuration $\{\{\theta_i\}_{i=1}^m, k_0\}$ of mean-field variatonal parameters at step i. The transition probability is given as $\mathcal{P}(\Psi_i \to \Psi_j) = \mathcal{P}_{\text{sel}}(\Psi_i \to \Psi_j)\mathcal{P}_{\text{acc}}(\Psi_i \to \Psi_j)$, where $\mathcal{P}_{\text{sel}}(\Psi_i \to \Psi_j)$ is the probability of selecting state Ψ_j from Ψ_i, and $\mathcal{P}_{\text{acc}}(\Psi_i \to \Psi_j)$ is the probability of accepting the new state Ψ_j from Ψ_i. In the Metropolis-Hastings algorithm, the selectance probability is symmetric $\mathcal{P}_{\text{sel}}(\Psi_i \to \Psi_j) = \mathcal{P}_{\text{sel}}(\Psi_j \to \Psi_i)$. Further, the acceptance probability of the Metropolis-Hastings algorithm is chosen to be

$$\mathcal{P}_{\text{acc}}(\Psi_i \to \Psi_j) = \min\left\{1, \frac{p(\Psi_j)}{p(\Psi_i)}\right\} \tag{3.206}$$

where,

$$\frac{p(\Psi_j)}{p(\Psi_i)} = e^{-\beta(F[\Psi_j]-F[\Psi_i])} \tag{3.207}$$

The free energy of state Ψ_i is given by $F[\Psi_i]$. The acceptance probability is thus unity if $F[\Psi_j] - F[\Psi_i] < 0$, which means that the new state has lower free energy than the old state. If the new state has higher free energy than the old state, we maybe accept it. The algorithm is as follows

1. Generate an initial state Ψ_i
2. Generate a new state Ψ_j
3. Calculate $\Delta F = F[\Psi_j] - F[\Psi_i]$
4. If $\Delta F < 0$, the acceptance probability is unity, accept the new state Ψ_j
5. If $\Delta F > 0$, calculate $w = p(\Psi_j)/p(\Psi_i) = e^{-\beta(F[\Psi_j]-F[\Psi_i])} < 1$
6. Generate a random number $r \in [0, 1)$. If $r < w$, accept the new state and assign $\Psi_i = \Psi_j$. If not, keep the old state $\Psi_i = \Psi_i$
7. Change Ψ_i by altering its configuration
8. Repeat 1. $\to$ 7. until the state converges

Step 2. requires generating a new state Ψ_j. For this thesis, this will be done by choosing new parameters $\theta_i \in [0, 2\pi)$ and $k_0 \in [0, \pi)$ with a random number generator (RNG). Step 6. requires generating a random number $r \in [0, 1)$ which makes shure that there is some probability of hopping out of a *local* minima. In addition, we make a *sweep* when all parameters have been traversed randomly a selected number of times. Therefore it is customary to repeat steps 1. $\to$ 6. an integer number of sweeps. We also include a *cooling* temperature. The algorithm starts out with high temperature, such that β is small. When the number of iterations increases, we cool the temperature of the system, increasing β. This will hopefully speed up convergence to a minimum. Note that the free energy is still evaluated at zero temperature. The method for cooling temperature will depend on the problem, but for this thesis the cooling temperature was chosen to be

$$kT_{\text{cooling}} = \frac{kT_0}{1 + 10 \times i} \tag{3.208}$$

where i is the number of sweeps and kT_0 is the starting temperature. Thus after a certain number of sweeps (where each sweep contains many iterations) one expects the system to reach equilibrium. For more information about cooling schemes, see 'Simulated Annealing' in e.g [6].

3.6 Determination of phases

Janssønn [32] considered in his thesis a *pure* condensate, in which all terms proportional to an operator was neglected. This means that free energy is simply the constant Hamiltonian, $F = H_0$. We define the mean-field parameter k_0 which is simply a re-scaling of $|\boldsymbol{k}_{0i}|$, and gives the length of the x and y components of a non-zero condensate momentum $\boldsymbol{k}_{0i}$

$$\sqrt{2}k_0 = |\boldsymbol{k}_{0i}| \tag{3.209}$$

The diagonal and off-diagonal terms $\epsilon_{\boldsymbol{k}_{0i}}$ and $|s_{\boldsymbol{k}_{0i}}|$ are given by

$$\epsilon_{\boldsymbol{k}_{0i}} = 4t\cos(k_0 a) \tag{3.210}$$
$$|s_{\boldsymbol{k}_{0i}}| = 2\sqrt{2}\lambda_R|\sin(k_0 a)| \tag{3.211}$$

The intra- and inter component scattering strengths are treated equally

$$U^{\uparrow\uparrow} = U^{\downarrow\downarrow} \equiv U \tag{3.212}$$
$$U^{\uparrow\downarrow} = U^{\downarrow\uparrow} \equiv \alpha U \tag{3.213}$$

Finally, we also assume that eq. (3.110) is valid, which by eq. (3.113) prohibits $\alpha = 1$. This makes it possible to identify certain configurations in $\boldsymbol{k}$-space for which to place the $N^{\alpha}_{\boldsymbol{k}_{0i}}$ bosons, as proposed by mean-field theory. The configurations which are allowed in $\boldsymbol{k}$-space are illustrated in fig 3.3. See chapter 4. in Janssønn for details.

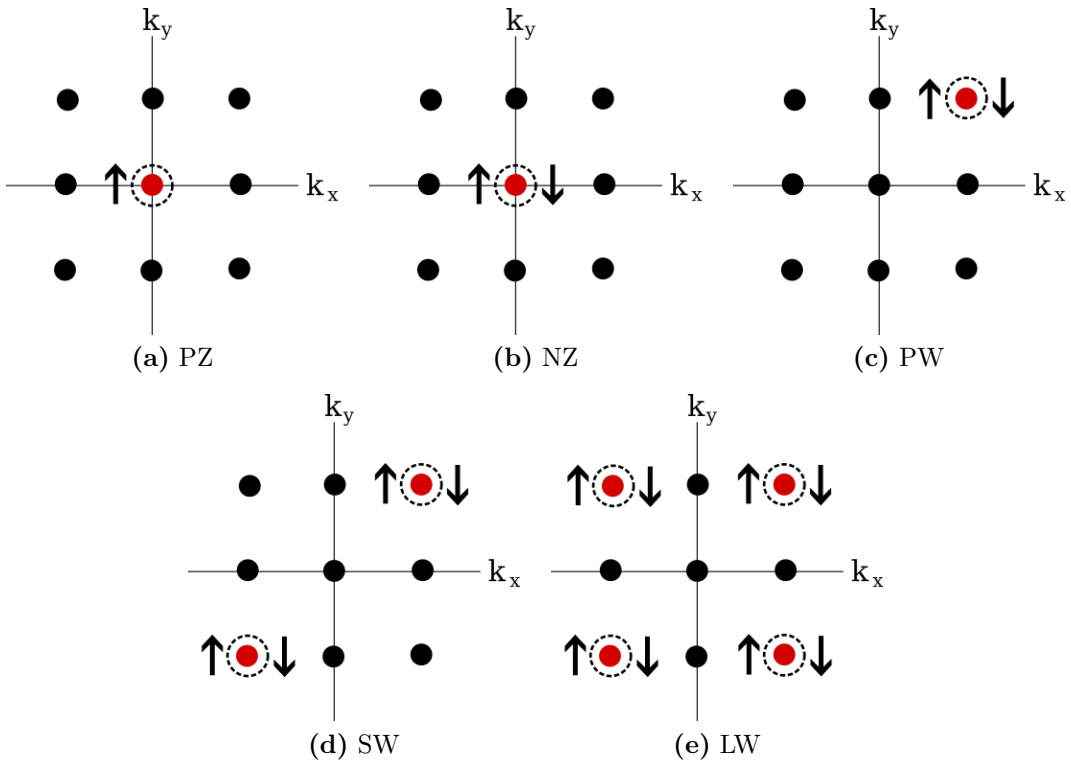

Figure 3.3: Overview of the allowed phases in $\boldsymbol{k}$-space using mean field theory on the two component, spin-orbit coupled, weakly interacting Bose gas. The phases are: **(a)** Polarized (PZ) phase **(b)** Non-Polarized (NZ) phase **(c)** Plane Wave (PW) phase **(d)** Stripe Wave (SW) phase **(e)** Lattice Wave (LW) phase. The red points shows a non-zero condensate number, and the arrows imply wich pseudo-spin component it is filled by. The points are labeled counter-clockwise as 1, 2, 3,4 and so forth

Notice that for the zero-momentum phases (PZ and NZ) the condensate spin-orbit coupling $|s_{\boldsymbol{k}_{0i}}|$ is zero. This means that we can have $N_0^{\uparrow} \neq 0$ and $N_0^{\downarrow} = 0$, as the expressions for the chemical potentials in eqs. (3.118) and (3.119) does not have the problematic SOC term with one of the condensate numbers in the denominator. For all non-zero momentum phases, the condenasate numbers $N_0^{\uparrow}$ and $N_0^{\downarrow}$ for each point must both be non-zero, since the condensate spin-orbit coupling is finite. Janssønn treated all of these phases, but neglected the LW-phase (for reasons which will become appearant later). For the PZ and NZ phases, for which $k_0 = 0$, the free energy was found to be independent of the mean-field parameters $\theta^{\uparrow}$ and $\theta^{\downarrow}$. For the PW and SW phases, the free energy was found to be dependent on k_0. Via minimization of the free energy, both PW and SW must have k_0 fixed to

$$k_0 = \frac{1}{a} \arctan\left(\frac{\sqrt{2}\lambda_R}{2t}\right) \tag{3.214}$$

for the pure condensate. Both PW and SW was found to be independent of the varatinal

parameters θ_i^α, which are therefore only constrained by eq.(3.104). The free energies are found to be, where we assume $\mu^\uparrow = \mu^\downarrow$, $t^\uparrow = t^\downarrow$ and $N_0^\uparrow = N_0^\downarrow = N_0/2$ (except the PZ phase which has $N_0^\uparrow = N_0$ and $\mu^\uparrow = \mu$ with $\mu^\downarrow$ chosen for the moment at will)

$$F_{\mathrm{PZ}} = \frac{-N_s}{2U}\left(4t+\mu\right)^2 \tag{3.215}$$

$$F_{\mathrm{NZ}} = \frac{-N_s}{U(1+\alpha)}\left(4t+\mu\right)^2 \tag{3.216}$$

$$F_{\mathrm{PW}} = \frac{-N_s}{U(1+\alpha)}\left(4t\sqrt{\frac{\lambda_R^2}{2t^2}+1}+\mu\right)^2 \tag{3.217}$$

$$F_{\mathrm{SW}} = \frac{-2N_s}{U(3+\alpha)}\left(4t\sqrt{\frac{\lambda_R^2}{2t^2}+1}+\mu\right)^2 \tag{3.218}$$

These expressions produces the phase-diagram shown in fig. 3.4, where the author has used the Python programming language. The phase-diagram is produced in (α, λ_R) space by comparing

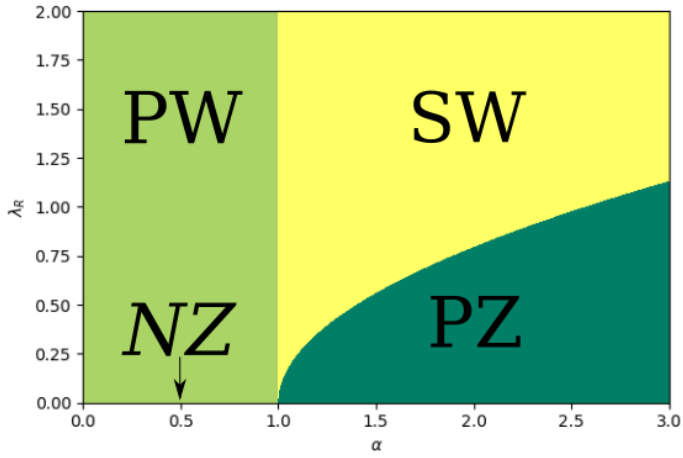

Figure 3.4: Phase diagram for the pure condensate. The NZ region is very small. The physical parameters are $\mu = 1$, $U = 0.1$, $t = 1$, and $N_s = 1000^2$

the free energies $(F_{\mathrm{PZ}}, F_{\mathrm{NZ}}, F_{\mathrm{PW}}, F_{\mathrm{LW}})$ and choosing the smallest value for every combination of (α, λ_R). Notice the bondary at $\alpha = 1$ which separates the PW and SW phase. As mentioned, this value for α is actually problematic, as it violates eq. (3.113). This phase-diagram coincides with the results from [21].

3.6.1 Investigation of condensate densities for the pure condensate

In fig. 3.5 a the phase diagram for two different values for μ are shown, including plots of the condensate densities N_0/N_s. For $\mu = -3.9$, the PZ phase has a constant condensate density which is close to unity. This physically means on average one boson per lattice site. However, for the other phases, the condensate density quickly rises, with maximum value at as high as 60. This would mean on average 60 bosons per lattice site, which makes it unreasonable to only consider two-body scattering. Notice that the condensate densities increases with increasing SOC strength λ_R. For $\mu = 1$, the PZ phase has a constant condensate density at about 50, while the other phases here also increases quicly, with a maximum value at about 150. In this case also, it would seem unreasonable to only consider two-body scattering. The remaining

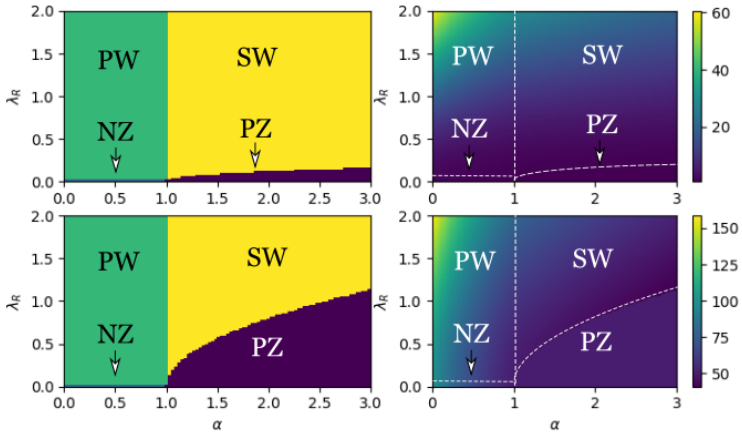

Figure 3.5: Two phase-diagrams (left) with $\mu = -3.9$ (top) and $\mu = 1$ (bottom). On the right the condensate density N_0/N_s is shown for the two-phase diagrams. The physical parameters are $U = 0.1$, $t = 1$ and $N_s = 100^2$

chapters of this thesis will therefore be devoted to consider the operator-dependent terms for each phase, and calculate the associated excitation spectrum. We shall also investigate the solutions to $N_0^{\uparrow}$ and $N_0^{\downarrow}$ for each phase in detail, and investigate stability criteria. We will also, when possible, investigate the excitation spectrums near $\boldsymbol{k}$-minima, in order to calculate a superfluid critical velocity.

Chapter 4

The PZ-phase

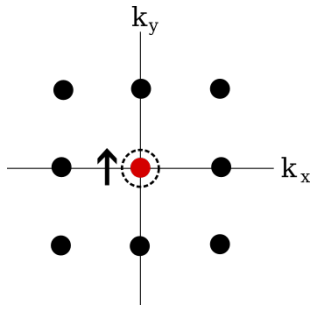

This is the first, and mathematically simplest phase we will encounter. The condensate momenta are $\boldsymbol{k}_{01} = \mathbf{0}$. The first thing to notice is the *imbalance* in the condensate particle numbers $N_0^{\uparrow} \neq 0$ and $N_0^{\downarrow} = 0$, leading to a *strong* zeeman field. In addition, the fluctuation pertaining to $A^{\downarrow}_{\boldsymbol{k}_{01}}$ is considered to be 0. This gives in principle that the chemical potential for the down component $\mu^{\downarrow}$ can be chosen arbitrarily. However, we shall see that the chemical potential difference $\delta \equiv \mu^{\uparrow} - \mu^{\downarrow}$ will be bounded from below from physical arguments. Secondly, since $\boldsymbol{k}_{01} = \mathbf{0}$, we have no condensate spin-orbit coupling.

4.1 Chemical potentials and condensate densities

The fluctuation of the condensate operator $A^{\uparrow}_{\boldsymbol{k}_{01}}$ is *not* zero[1] and the expression for $\mu^{\uparrow}$ is given by eq. (3.118) from the previous chapter. Here we note that $|s_{\boldsymbol{k}_{01}}| = 0$. The primed sum gives the allowed values as $\alpha = \uparrow$ and $(j, i', j') = (1, 1, 1)$. This gives (with $f = 1$) the expression for

[1]Notice that we cannot use the converse equation for $\mu^{\downarrow}$ in this case, as that equation assumed that $a^{\downarrow}_{\boldsymbol{k}_{00}} \neq 0$,which clearly is violated here

$\mu^{\uparrow} \equiv \mu$

$$\mu = -4t + \frac{UN_0}{N_s} \tag{4.1}$$

Notice that μ is negative in most cases. With weak interactions in the superfluid case, and with t normalized to 1, U must be much smaller than one. In addition, the fraction of bosons to lattice sites N_s cannot exceed any value, as then one would probabably have to include more orders of interactions. If for example $N_0/N_s = 10$ then it would mean on average four bosons per lattice site, which would make it unreasonable to only consider two-body scattering. The expression for μ also gives an equation for the condensate density N_0/N_s

$$\frac{N_0}{N_s} = \frac{\mu + 4t}{U} \tag{4.2}$$

which clearly must be positive, giving the lower bound $\mu > -4t$. Note that there is a clear correspondence between having particles in the system and having a finite μ, even with a negative μ. It is also evident that μ actually can be zero, if t is nonzero. One can ask, does a negative μ imply an unstable condensate? For the pure condensate, the free energies for all the phases are *negative* independent of the sign of μ. This implies that the system is *stable* since there is no energy-cost of placing bosons at their respective minima in $\boldsymbol{k}$-space. For the non-pure condensate, the stability of the system will be connected with the energy costs of exciting a particle from the condensate. If the energy of exciting a state is negative then the system will quickly move particles to finite $\boldsymbol{k}$, since this leads towards a new minimum. However, if the energy of exciting a state is positive, the system would rather stay in the condensed state and excitations would then be a result of interactions. We shall investigate the energy costs of exciting a boson in the pseudo-spin up and pseudo-spin down states in section 4.3.1. We also define the difference in chemical potentials δ

$$\mu - \mu^{\downarrow} = \delta \tag{4.3}$$

giving the expression for $\mu^{\downarrow}$

$$\mu^{\downarrow} = \mu - \delta \tag{4.4}$$

It is a reasonable assumption that since $N_0^{\uparrow} > N_0^{\downarrow}$, $\mu^{\uparrow} > \mu^{\downarrow}$, and so $\delta > 0$.

4.2 Constant and linear Hamiltonian

The linear Hamiltonian is given by eq. (3.123), and vanishes in the PZ phase. This is due to the delta-function, giving $\boldsymbol{k} = \boldsymbol{0}$, which is a condensate momentum and is therefore excluded by the sum. The expression for the constant Hamiltonian is given in eq. (3.122), where the primed sum gives the possible values as $(\alpha, \beta) = (\uparrow, \uparrow)$ and $(i, j, i', j') = (1, 1, 1, 1)$. Thus we get the expression for the constant Hamiltonian

$$H_0 = -\frac{UN_0^2}{2N_s} \tag{4.5}$$

which by inserting the expression for N_0/N_s in eq. 4.2 becomes

$$H_0 = -\frac{N_s(\mu + 4t)^2}{2U} \tag{4.6}$$

The expression for H_0 coincides with the expression for the free energy of the PZ phase in eq. (3.215)

4.3 Quadratic Hamiltonian

The quadratic Hamiltonian for the PZ-phase, and indeed all the following phases also, is on the quadratic form outlined in eq. (3.147) in the Dynamic Matrix section. This will become clear in a moment. The non-interacting part of H_2 is given by

$$H_{\text{non-int}} = \sum_{\boldsymbol{k}} \sum_{\alpha\beta} \eta_{\boldsymbol{k}}^{\alpha\beta} A_{\boldsymbol{k}}^{\alpha\dagger} A_{\boldsymbol{k}}^{\beta} \tag{4.7}$$

The sum over (α, β) can be rewritten by using the commutation relations for the bosonic operators $A_{\boldsymbol{k}}^{\alpha}$ and $A_{\boldsymbol{k}}^{\alpha\dagger}$

$$\frac{\eta_{\boldsymbol{k}}^{\uparrow\uparrow}}{2}\left(A_{\boldsymbol{k}}^{\uparrow\dagger}A_{\boldsymbol{k}}^{\uparrow} + A_{\boldsymbol{k}}^{\uparrow}A_{\boldsymbol{k}}^{\uparrow\dagger} - 1\right) + \frac{\eta_{\boldsymbol{k}}^{\uparrow\downarrow}}{2}\left(A_{\boldsymbol{k}}^{\uparrow\dagger}A_{\boldsymbol{k}}^{\downarrow} + A_{\boldsymbol{k}}^{\downarrow}A_{\boldsymbol{k}}^{\uparrow\dagger}\right) \tag{4.8}$$

$$\frac{\eta_{\boldsymbol{k}}^{\downarrow\uparrow}}{2}\left(A_{\boldsymbol{k}}^{\downarrow\dagger}A_{\boldsymbol{k}}^{\uparrow} + A_{\boldsymbol{k}}^{\uparrow}A_{\boldsymbol{k}}^{\downarrow\dagger}\right) + \frac{\eta_{\boldsymbol{k}}^{\downarrow\downarrow}}{2}\left(A_{\boldsymbol{k}}^{\downarrow\dagger}A_{\boldsymbol{k}}^{\downarrow} + A_{\boldsymbol{k}}^{\downarrow}A_{\boldsymbol{k}}^{\downarrow\dagger} - 1\right) \tag{4.9}$$

The above expression is the same for all the ensuing phases as well. The interaction Hamiltonian is given by

$$H_{\text{int}} = \sum_{\boldsymbol{k}} g_{11}^{\uparrow\uparrow}(\boldsymbol{k}, -\boldsymbol{k}) + r_{11}^{\uparrow\uparrow}(\boldsymbol{k}, \boldsymbol{k}) + l_{11}^{\uparrow\uparrow}(\boldsymbol{k}, \boldsymbol{k}) + l_{11}^{\uparrow\downarrow}(\boldsymbol{k}, \boldsymbol{k}) \tag{4.10}$$

The expressions for g, r and l are given by eqs. (3.127), (3.128) and (3.129). Note that we get interactions from pseudo-spin $\downarrow$ from l, as the condensate can interact with *excited* down bosons. The the first primed sum gives the possible values for the indices as $(\alpha, \beta) \in (\uparrow, \uparrow)$ and $(i, j, i', j') = (1, 1, 1, 1)$, and the second primed sum gives $\alpha = \uparrow$, $\beta \in (\uparrow, \downarrow)$ and $(i, j, i', j') = (1, 1, 1, 1)$. The goal is to write H_2 as a matrix product, as in the Dynamic Matrix section

$$H_2 = \psi_{\boldsymbol{k}}^{\dagger} M \psi_{\boldsymbol{k}} + C_2 \tag{4.11}$$

where C_2 is an operator independent term. Let us introduce the vectors of operators $\psi_{\boldsymbol{k}}$ and $\psi_{\boldsymbol{k}}^{\dagger}$ with 8 entries each as

$$\psi_{\boldsymbol{k}} = \begin{pmatrix} A_{\boldsymbol{k}}^{\uparrow} \\ A_{-\boldsymbol{k}}^{\uparrow} \\ A_{\boldsymbol{k}}^{\downarrow} \\ A_{-\boldsymbol{k}}^{\downarrow} \\ A_{\boldsymbol{k}}^{\uparrow\dagger} \\ A_{-\boldsymbol{k}}^{\uparrow\dagger} \\ A_{\boldsymbol{k}}^{\downarrow\dagger} \\ A_{-\boldsymbol{k}}^{\downarrow\dagger} \end{pmatrix}, \quad \psi_{\boldsymbol{k}}^{\dagger} = \begin{pmatrix} A_{\boldsymbol{k}}^{\uparrow\dagger} & A_{-\boldsymbol{k}}^{\uparrow\dagger} & A_{\boldsymbol{k}}^{\downarrow\dagger} & A_{-\boldsymbol{k}}^{\downarrow\dagger} & A_{\boldsymbol{k}}^{\uparrow} & A_{-\boldsymbol{k}}^{\uparrow} & A_{\boldsymbol{k}}^{\downarrow} & A_{-\boldsymbol{k}}^{\downarrow} \end{pmatrix} \tag{4.12}$$

These vectors satisfy bosonic commutation relations

$$[\psi_{\boldsymbol{k}}^{\mu}, \psi_{\boldsymbol{k}}^{\nu\dagger}] = J_{\mu\nu}, \quad 1 \leq \mu, \nu \leq 8 \tag{4.13}$$

with J is defined in eq. (3.156). Notice the order of the operators, if $B_{\boldsymbol{k}}$ is an operator, then the operator $B_{-\boldsymbol{k}}$ is placed to the right of it. This will also apply to the case where we have the operator $B_{\boldsymbol{p}}$, where $\boldsymbol{p}$ is a linear function of $\boldsymbol{k}$. The order will then be $B_{\boldsymbol{p}}$ and to the right $B_{\boldsymbol{p}'}$, where $\boldsymbol{p}' = \boldsymbol{p}(-\boldsymbol{k})$. The reason for this will become apparent in the ensuing calculations. Let $V_{\boldsymbol{k}}$ be a 8×8 matrix. The quadratic Hamiltonian can then be written as a matrix product

$$H_2 = \sum_{\boldsymbol{k}} \psi^\dagger_{\boldsymbol{k}} V_{\boldsymbol{k}} \psi_{\boldsymbol{k}} + C_2 \tag{4.14}$$

The matrix $V_{\boldsymbol{k}}$ is given by

$$V_{\boldsymbol{k}} = \begin{pmatrix} V_1(\boldsymbol{k}) & V_2 \\ V_2^* & V_1^*(\boldsymbol{k}) \end{pmatrix} \tag{4.15}$$

The four-by-four submatrices $V_1(\boldsymbol{k})$ and V_2 are given by

$$V_1(\boldsymbol{k}) = \begin{pmatrix} \frac{\eta^{\uparrow\uparrow}_{\boldsymbol{k}}}{2} + 2a_s & 0 & \frac{\eta^{\uparrow\downarrow}_{\boldsymbol{k}}}{2} & 0 \\ 0 & 0 & 0 & 0 \\ \frac{\eta^{\downarrow\uparrow}_{\boldsymbol{k}}}{2} & 0 & \frac{\eta^{\downarrow\downarrow}_{\boldsymbol{k}}}{2} + \alpha a_s & 0 \\ 0 & 0 & 0 & 0 \end{pmatrix} \tag{4.16}$$

$$V_2 = \begin{pmatrix} 0 & \frac{1}{2}a_s e^{-2i\theta} & 0 & 0 \\ \frac{1}{2}a_s e^{-2i\theta} & 0 & 0 & 0 \\ 0 & 0 & 0 & 0 \\ 0 & 0 & 0 & 0 \end{pmatrix} \tag{4.17}$$

We have defined $\theta = \theta_1^\uparrow$ as the mean-field parameter. In addition, the frequent number a_s is given by

$$a_s = \frac{UN_0}{2N_s} \tag{4.18}$$

We would also like to explicitly sum over $-\boldsymbol{k}$, in order to symmetrize the Hamiltonian, and give equal importance for the $\boldsymbol{k}$ and $-\boldsymbol{k}$ terms. This is allowed since the $\sum_{\boldsymbol{k}}$ is symmetric in the first Brilluoin zone, such that we may write $\sum_{\boldsymbol{k}} f(\boldsymbol{k}) = \frac{1}{2}\sum_{\boldsymbol{k}}(f(\boldsymbol{k}) + f(-\boldsymbol{k}))$, where $f(\boldsymbol{k})$ is an arbitrary function of $\boldsymbol{k}$. Consequently, H_2 becomes

$$H_2 = C_2 + \frac{1}{2}\sum_{\boldsymbol{k}} \psi^\dagger_{\boldsymbol{k}} V_{\boldsymbol{k}} \psi_{\boldsymbol{k}} + \psi^\dagger_{-\boldsymbol{k}} V_{-\boldsymbol{k}} \psi_{-\boldsymbol{k}} \tag{4.19}$$

The constant term C_2 becomes

$$C_2 = \frac{N_s}{2}(2\mu - \delta) - UN_0\left(1 + \frac{\alpha}{2}\right) \tag{4.20}$$

where we have used that $\sum_{\boldsymbol{k}} \eta^{\alpha\alpha}_{\boldsymbol{k}} = -N_s\mu^\alpha$ for $\alpha = (\uparrow, \downarrow)$, as given in the appendix. The troubling term is now $\psi^\dagger_{-\boldsymbol{k}} V_{-\boldsymbol{k}} \psi_{-\boldsymbol{k}}$. However, since $\psi_{-\boldsymbol{k}}$ is only different from $\psi_{\boldsymbol{k}}$ by a pairwise exchange of the operators, hope is not lost. The vector of operators $\psi_{\boldsymbol{k}}$ is constructed such that all $\boldsymbol{k}$ operators fall on a *odd* number, and all $-\boldsymbol{k}$ operators fall on an *even* number. The shifted vector of operators $\psi_{-\boldsymbol{k}}$ will therefore have the *opposite* pattern, with $\boldsymbol{k}$ operators falling

on a *odd* number and $-\boldsymbol{k}$ operators falling on an *even* number. This means that we can write $\psi^\dagger_{-\boldsymbol{k}} V_{-\boldsymbol{k}} \psi_{-\boldsymbol{k}}$ on the form

$$\psi^\dagger_{-\boldsymbol{k}} V_{-\boldsymbol{k}} \psi_{-\boldsymbol{k}} = \psi^\dagger_{\boldsymbol{k}} V'_{\boldsymbol{k}} \psi_{\boldsymbol{k}} \tag{4.21}$$

where $V'_{\boldsymbol{k}}$ is the *shifted* matrix defined as

$$V'_{ij}(\boldsymbol{k}) = \begin{cases} V(-\boldsymbol{k})_{i+1,j+1} & (i,j) = \text{odd} \\ V(-\boldsymbol{k})_{i+1,j-1} & (i,j) = \text{odd, even} \\ V(-\boldsymbol{k})_{i-1,j+1} & (i,j) = \text{even, odd} \\ V(-\boldsymbol{k})_{i-1,j-1} & (i,j) = \text{even} \end{cases} \tag{4.22}$$

The matrix $V'_{\boldsymbol{k}}$ is on the form:

$$V'_{\boldsymbol{k}} = \begin{pmatrix} V'_1(\boldsymbol{k}) & V'_2 \\ V'^*_2 & V'^*_1(\boldsymbol{k}) \end{pmatrix} \tag{4.23}$$

The shifted submatrices $V'_1(\boldsymbol{k})$ and V'_2 are given by

$$V'_1(\boldsymbol{k}) = \begin{pmatrix} 0 & 0 & 0 & 0 \\ 0 & \frac{\eta^{\uparrow\uparrow}_{\boldsymbol{k}}}{2} + 2a_s & 0 & -\frac{\eta^{\uparrow\downarrow}_{\boldsymbol{k}}}{2} \\ 0 & 0 & 0 & 0 \\ 0 & -\frac{\eta^{\downarrow\uparrow}_{\boldsymbol{k}}}{2} & 0 & \frac{\eta^{\downarrow\downarrow}_{\boldsymbol{k}}}{2} + \alpha a_s \end{pmatrix} \tag{4.24}$$

$$V'_2 = \begin{pmatrix} 0 & \frac{1}{2}a_s e^{-2i\theta} & 0 & 0 \\ \frac{1}{2}a_s e^{-2i\theta} & 0 & 0 & 0 \\ 0 & 0 & 0 & 0 \\ 0 & 0 & 0 & 0 \end{pmatrix} \tag{4.25}$$

we have used that $s(-\boldsymbol{k}) = -s(\boldsymbol{k})$ and $\epsilon(-\boldsymbol{k}) = \epsilon(\boldsymbol{k})$. The symmetrized expression for the quadratic Hamiltonian becomes

$$H_2 = C_2 + \frac{1}{2}\sum_{\boldsymbol{k}} \psi^\dagger_{\boldsymbol{k}} M_{\boldsymbol{k}} \psi_{\boldsymbol{k}} \tag{4.26}$$

where $M_{\boldsymbol{k}} = V_{\boldsymbol{k}} + V'_{\boldsymbol{k}}$, and is on the form

$$M_{\boldsymbol{k}} = \begin{pmatrix} M_1(\boldsymbol{k}) & M_2 \\ M_2^* & M_1^*(\boldsymbol{k}) \end{pmatrix} \tag{4.27}$$

The entries of submatrix $M_1(\boldsymbol{k})$ are given by

$$M_1(\boldsymbol{k}) = \begin{pmatrix} \frac{\eta^{\uparrow\uparrow}_{\boldsymbol{k}}}{2} + 2a_s & 0 & \frac{\eta^{\uparrow\downarrow}_{\boldsymbol{k}}}{2} & 0 \\ 0 & \frac{\eta^{\uparrow\uparrow}_{\boldsymbol{k}}}{2} + 2a_s & 0 & -\frac{\eta^{\uparrow\downarrow}_{\boldsymbol{k}}}{2} \\ \frac{\eta^{\downarrow\uparrow}_{\boldsymbol{k}}}{2} & 0 & \frac{\eta^{\downarrow\downarrow}_{\boldsymbol{k}}}{2} + \alpha a_s & 0 \\ 0 & -\frac{\eta^{\downarrow\uparrow}_{\boldsymbol{k}}}{2} & 0 & \frac{\eta^{\downarrow\downarrow}_{\boldsymbol{k}}}{2} + \alpha a_s \end{pmatrix} \tag{4.28}$$

and the entries of sumatrix M_2 are given by

$$M_2 = \begin{pmatrix} 0 & a_s e^{-2i\theta} & 0 & 0 \\ a_s e^{-2i\theta} & 0 & 0 & 0 \\ 0 & 0 & 0 & 0 \\ 0 & 0 & 0 & 0 \end{pmatrix} \tag{4.29}$$

The procedure with shifting the sum with $-\boldsymbol{k}$, introducing a shifted matrix, is the one which will be used throughout this thesis. This is allowed since all the $\boldsymbol{k}$ dependence on the operators turns out to come in explicit pairs $(\boldsymbol{p}(\boldsymbol{k}), \boldsymbol{p}(-\boldsymbol{k}))$ with *linear* dependence of $\boldsymbol{k}$ for all the phases. The exception is the PW phase, which requires symmetrization with another vector.

4.3.1 Physical constraints on the chemical potential difference

Let us invesigate the signs of $M_{1,1}$ and $M_{3,3}$, as they give the energy cost/gain of exciting a particle from the condensate to a finite $\boldsymbol{k}$ wavevector in the pseudo-spins up and down respectively. The reason for this is because the matrix product becomes $M_{1,1}A^{\uparrow\dagger}_{\boldsymbol{k}}A^{\uparrow}_{\boldsymbol{k}} = M_{1,1}n^{\uparrow}_{\boldsymbol{k}}$ when written out, and likewise for $M_{3,3}$. Thus to increase the number of particles in either state, one must pay with the energies $M_{1,1}$ and $M_{3,3}$. The matrix-element for excitation to pseudo-spin *up* is given by

$$M_{1,1} = \frac{\eta^{\uparrow\uparrow}_{\boldsymbol{k}}}{2} + 2a_s \tag{4.30}$$

$$= (4t - \epsilon_{\boldsymbol{k}}) + \frac{3UN_0}{2N_s} > 0, \quad \forall \boldsymbol{k} \tag{4.31}$$

where we have used that $\epsilon_{\boldsymbol{k}}$ has a maximum at $4t$, such that $4t - \epsilon_{\boldsymbol{k}} \geq 0$ for all $\boldsymbol{k}$, and we have used the definitions $\eta^{\uparrow}_{\boldsymbol{k}}$ and a_s as given in equations (2.95) and (4.18). We have also inserted the explicit expression for μ, as given by eq. (4.1). Thus the energy cost of exciting a boson with pseudo-spin up is positive, which means that it is energetically unfavorable. The same is true for $M_{3,3}$, by a similar analysis.

The matrix element $M_{1,1}$ gives the energy cost of increasing the number of bosons with pseudo-spin up in the excited state with wavevector $\boldsymbol{k}$. Similarly, the matrix element $M_{3,3}$ gives the energy cost of increasing the number of bosons with pseudo-spin down in the excited state with wavevector $\boldsymbol{k}$. It makes physical sense that since there are only bosons with pseudo-spin up in the condensed state and no bosons in the pseudo-spin down state, it should be easier to increase the number of bosons with pseudo-spin up in the excited state. Therefore we must have the constraint

$$M_{1,1} < M_{3,3} \tag{4.32}$$

$$\frac{\eta^{\uparrow\uparrow}_{\boldsymbol{k}}}{2} + 2a_s < \frac{\eta^{\downarrow\downarrow}_{\boldsymbol{k}}}{2} + \alpha a_s \tag{4.33}$$

$$\frac{-(\epsilon_{\boldsymbol{k}} + \mu^{\uparrow})}{2} + 2a_s < \frac{-(\epsilon_{\boldsymbol{k}} + \mu^{\downarrow})}{2} + \alpha a_s \tag{4.34}$$

$$\delta > \frac{UN_0}{N_s}(2 - \alpha) = (\mu + 4t)(2 - \alpha) \tag{4.35}$$

where we have used the expression for the condensate density N_0/N_s in eq. (4.2). Thus the chemical potential difference is bounded from below by physical arguments. With $U = 0.1$, $\alpha = 0.5$ and one boson per lattice site $N_0/N_s = 1$ this lower bound becomes $\delta > 0.15$.

4.4 Explicit expression for the excitation spectrum for the PZ-phase

Maple[2] is able to find eight eigenvalues, with two independent positive branches for the dynamic matrix $D = JM_{\boldsymbol{k}}$, labeled by w_+ and w_-. The eigenvalues are given by, as advertised in the Dynamic Matrix section:

$$w_1 = w_+, \quad w_5 = -w_+ \tag{4.36}$$
$$w_2 = w_+, \quad w_6 = -w_+ \tag{4.37}$$
$$w_3 = w_-, \quad w_7 = -w_- \tag{4.38}$$
$$w_4 = w_-, \quad w_8 = -w_- \tag{4.39}$$

Confirming the fact that the eigenvalues comes in pairs $(w, -w)$. Maple is however not able to find the eigenvectors. The explicit expression for the branches are given by

$$w_+(\boldsymbol{k}) = \frac{1}{2}\sqrt{A_{\boldsymbol{k}} + 2\sqrt{B_{\boldsymbol{k}}}} \tag{4.40}$$
$$w_-(\boldsymbol{k}) = \frac{1}{2}\sqrt{A_{\boldsymbol{k}} - 2\sqrt{B_{\boldsymbol{k}}}} \tag{4.41}$$

where $A_{\boldsymbol{k}}$ and $B_{\boldsymbol{k}}$ are given by

$$A_{\boldsymbol{k}} = 2E_1(\boldsymbol{k})^2 + 2E_2(\boldsymbol{k})^2 + |s(\boldsymbol{k})|^2 - 2a_s^2 \tag{4.42}$$
$$B_{\boldsymbol{k}} = \left(E_2(\boldsymbol{k})^2 - E_1(\boldsymbol{k})^2 + a_s^2\right)^2 \tag{4.43}$$
$$- |s(\boldsymbol{k})|^2 \left(a_s + E_1(\boldsymbol{k}) + E_2(\boldsymbol{k})\right)\left(a_s - E_1(\boldsymbol{k}) - E_2(\boldsymbol{k})\right) \tag{4.44}$$

We see that the spin-orbit coupling can cause imaginary eigenvalues from $B_{\boldsymbol{k}}$. The energies $E_1(\boldsymbol{k})$ and $E_2(\boldsymbol{k})$ are given by

$$E_1(\boldsymbol{k}) = \frac{\eta_{\boldsymbol{k}}^{\uparrow\uparrow}}{2} + 2a_s \tag{4.45}$$
$$E_2(\boldsymbol{k}) = \frac{\eta_{\boldsymbol{k}}^{\downarrow\downarrow}}{2} + \alpha a_s \tag{4.46}$$

and comprises the expressions for the chemical potentials. We note that the branches are independent of the variational parameter θ, which may thefore be set to zero. In fig. 4.1 the plot of the excitation spectrum for the PZ-phase is shown. Note that we get two branches, versus the case of a weakly interacting bose gas, which only had one. This will be explained in the next chapter, when comparing this phase to the NZ phase. We see that $w_1(\boldsymbol{k})$ is quadratic

[2]Maple is a symbolic math software. See `https://www.maplesoft.com/` for more information.

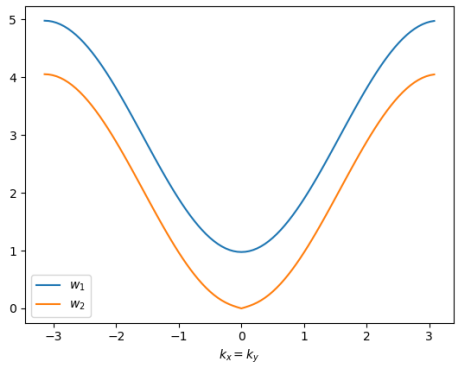

(a) A plot of the excitation spectrum for the PZ phase when $k_x = k_y$

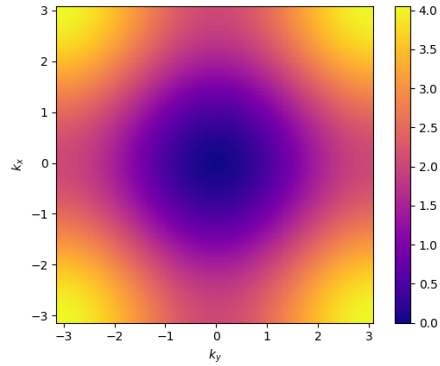

(b) Plot of the lowest energy branch w^- in the first Brilloin zone

Figure 4.1: Plot of the excitation spectrum for the PZ phase. The physical parameters are $U = 0.1$, $N_s = 100^2$, $N_0/N_s = 1$, $t = 1$, $\lambda_R = 1$, $\alpha = 0.1$ and $\delta = 2$

near $\boldsymbol{k} = 0$, while $w_2(\boldsymbol{k})$ is reminiscent of the Bogoliubov spectrum given in fig. 3.2. We also include a plot of the maximum absolute value of the imaginary part of (w^+, w^-) for all (k_x, k_y) in the 1st Brillouin zone and for different values of δ, see fig. 4.2. The imaginary part is mainly concetrated around $\boldsymbol{k} = 0$, which is true for the other phases as well, the imaginary part appears around a minima in $\boldsymbol{k}$ space. Note that the imaginary part in fig. 4.2 quickly vanishes below a certain line in (α, λ_R) space. Above this line, the eigenvalues are imaginary, and the dynamic matrix JM is not physically diagonizable. This means that the Hamiltonian H can not be BV-diagonalized.

4.5 Dispersion relation

From the excitation spectrum, we see that the minimum is at $\boldsymbol{k} = \boldsymbol{0}$. At this value, $A_{\boldsymbol{k}}$ becomes

$$A_{\boldsymbol{0}} = \frac{((\alpha - 1)(\mu + 4t) + \delta)^2}{2} \tag{4.47}$$

and $\sqrt{B_{\boldsymbol{0}}}$ becomes

$$\sqrt{B_{\boldsymbol{0}}} = \frac{((\alpha - 1)(\mu + 4t) + \delta)^2}{4} \tag{4.48}$$

where we have inserted the explicit expression for the condensate density in eq. (4.2). Consequently, the two branches each take the values

$$w_+(\boldsymbol{0}) = |(\alpha - 1)(\mu + 4t) + \delta| \tag{4.49}$$

$$w_-(\boldsymbol{0}) = 0 \tag{4.50}$$

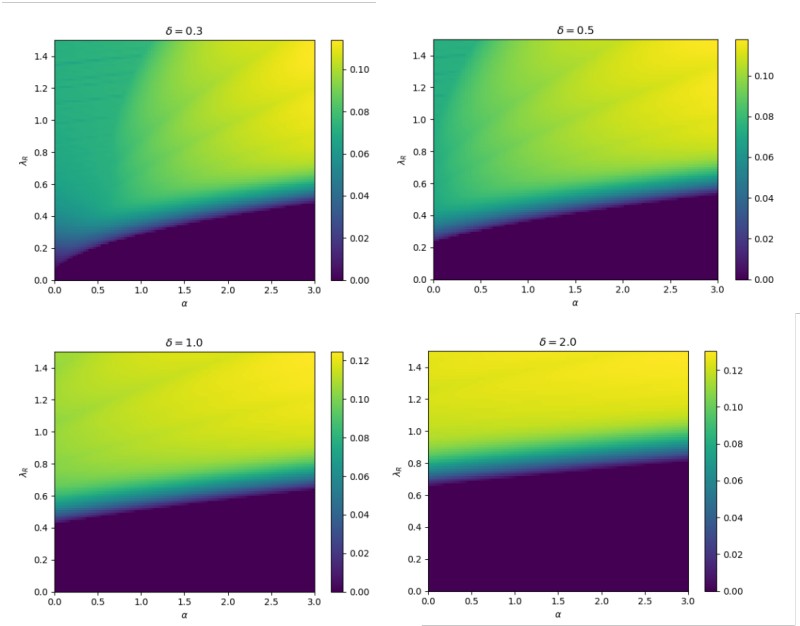

Figure 4.2: The plot of the maximum absolute value of the imaginary part of the branches in the PZ phase, with constant condensate density $N_0/N_s = 1$, and varying μ.

This means that we get a Zeeman splitting at $\boldsymbol{k} = 0$, given by

$$\Delta w(\mathbf{0}) = |(\alpha - 1)(\mu + 4t) + \delta| \tag{4.51}$$

We can remove the absolute sign, since $\delta > (2-\alpha)(\mu + 4t)$ by eq. (4.35). The Zeeman splitting can be made arbitrarily large by tuning the difference in chemical potentials δ, which is only bounded from below by eq. (4.35). Numerical analysis shows that increasing δ increases the parameter space for which the branches are real, see fig. 4.2. Further, we calculate the gradient in $\boldsymbol{k}$ space for each branch

$$\frac{\partial w_\sigma}{\partial \boldsymbol{k}}|_{\boldsymbol{k}=\mathbf{0}} \equiv \nabla_{\boldsymbol{k}} w_\sigma(\boldsymbol{k})|_{\boldsymbol{k}=\mathbf{0}} \tag{4.52}$$

If the gradient is linear on the form $v_g \hat{\boldsymbol{k}}$, then v_g gives the *superfluid* critical velocity. Calculating the gradient we obtain

$$\frac{\partial w_\pm}{\partial \boldsymbol{k}} = \frac{1}{2w_\pm(\boldsymbol{k})}\left(\frac{\partial A_{\boldsymbol{k}}}{\partial \boldsymbol{k}} \pm \frac{1}{\sqrt{B_{\boldsymbol{k}}}}\frac{\partial B_{\boldsymbol{k}}}{\partial \boldsymbol{k}}\right) \tag{4.53}$$

The derivative is well defined for the $(+)$ branch, since $w_+(\mathbf{0}) \neq 0$ because of the Zeeman shift. The derivative must be handled more carefully for the $(-)$ branch, as we get 0 in the

denominator. The partial derivatives are given by

$$\frac{\partial A_{\boldsymbol{k}}}{\partial \boldsymbol{k}} = \frac{\partial}{\partial \boldsymbol{k}} \left(2E_1(\boldsymbol{k})^2 + 2E_2(\boldsymbol{k})^2 + |s(\boldsymbol{k})|^2 - 2a_s^2\right) \tag{4.54}$$

$$\boldsymbol{k} \to \boldsymbol{0} = 4\left(E_1(\boldsymbol{k})\frac{\partial E_1}{\partial \boldsymbol{k}} + E_2(\boldsymbol{k})\frac{\partial E_2}{\partial \boldsymbol{k}}\right) \tag{4.55}$$

where we have used that

$$\frac{\partial}{\partial \boldsymbol{k}}|s(\boldsymbol{k})|^2 = 2|s(\boldsymbol{k})|\frac{\partial |s(\boldsymbol{k})|}{\partial \boldsymbol{k}} \to 0 \tag{4.56}$$

in the limit $\boldsymbol{k} \to 0$, as $s(\boldsymbol{0}) = 0$. For $B_{\boldsymbol{k}}$, we get, were we also remove any terms proportional to $|s(\boldsymbol{k})|^2$

$$\frac{\partial B_{\boldsymbol{k}}}{\partial \boldsymbol{k}} = \frac{\partial}{\partial \boldsymbol{k}} \left(E_2(\boldsymbol{k})^2 - E_1(\boldsymbol{k})^2 + a_s^2\right)^2 \tag{4.57}$$

$$= 2^2\left(E_2^2(\boldsymbol{k}) - E_1^2(\boldsymbol{k}) + a_s^2\right)\left(E_2(\boldsymbol{k})\frac{\partial E_2}{\partial \boldsymbol{k}} - E_1(\boldsymbol{k})\frac{\partial E_1}{\partial \boldsymbol{k}}\right) \tag{4.58}$$

We see that the prefactor is proportional to $B_{\boldsymbol{0}} \neq 0$ in the limit $\boldsymbol{k} \to \boldsymbol{0}$. Using the definitions of E_1 and E_2 given in eqs. (4.45) and (4.46), and that $\eta_{\boldsymbol{k}}^{\beta} = -(\epsilon(\boldsymbol{k})^{\beta} + \mu^{\beta})$ for $\beta = (\uparrow, \downarrow)$, we get

$$\frac{\partial E_1}{\partial \boldsymbol{k}} = -\frac{1}{2}\frac{\partial \epsilon_{\boldsymbol{k}}^{\uparrow}}{\partial \boldsymbol{k}} = at^{\uparrow}\left(\sin(k_x a), \sin(k_y a)\right)_{\boldsymbol{k}} \tag{4.59}$$

$$\frac{\partial E_2}{\partial \boldsymbol{k}} = -\frac{1}{2}\frac{\partial \epsilon_{\boldsymbol{k}}^{\downarrow}}{\partial \boldsymbol{k}} = at^{\downarrow}\left(\sin(k_x a), \sin(k_y, a)\right)_{\boldsymbol{k}} \tag{4.60}$$

Consequently, the derivatives of $A_{\boldsymbol{k}}$ and $B_{\boldsymbol{k}}$ goes to 0 as $\boldsymbol{k} \to \boldsymbol{0}$. For $\partial/\partial \boldsymbol{k}(w_+)$ we get $\boldsymbol{0}$ in this limit, as $w_+(\boldsymbol{0}) \neq 0$ making the denominator well defined. We therefore get no superfluid for the + branch. For w_- however, we get a indeterminate "0/0" expression, which requires more care. Taking the limit will be cumbersome, and one must most likely make a Taylor expansion of both the numerator and the denominator. To avoid unnecessary work, we can rather make a multi-variate Taylor expansion of $w_-(\boldsymbol{k})$ around $\boldsymbol{k} = \boldsymbol{0}$, and investigate the slope in that domain. We neglect terms that are higher than bilinear, for example terms like $k_x^2 k_y^2$. Using Maple, we Taylor expand $w_-(\boldsymbol{k})$ in the variables k_x and k_y, obtaining

$$w_-^2(\boldsymbol{k}) = a_0\left(p(t) - \lambda_R^2\right)\boldsymbol{k}^2 \tag{4.61}$$

where a_0 and $p(t)$ are given by

$$a_0 = \frac{2a^2(\mu + 4t)}{(\alpha - 1)(\mu + 4t) + \delta} \tag{4.62}$$

$$p(t) = (\alpha - 1)t^2 + \frac{1}{4}\left((\alpha - 1)\mu + \delta\right)t \tag{4.63}$$

$$= \frac{t}{4}\Delta w(\boldsymbol{0}) \tag{4.64}$$

where $\Delta w(\boldsymbol{0})$ is the Zeeman splitting. Thus $w_-(\boldsymbol{k})$ is *linear* around $\boldsymbol{k} \to 0$

$$w_-(\boldsymbol{k}) = v_g|\boldsymbol{k}| \tag{4.65}$$

The gradient is therefore

$$\frac{\partial w_-}{\partial \boldsymbol{k}} = v_g \frac{\partial |\boldsymbol{k}|}{\partial \boldsymbol{k}} \tag{4.66}$$

$$= v_g \frac{\partial}{\partial \boldsymbol{k}} \left(\sqrt{\boldsymbol{k}^2} \right) \tag{4.67}$$

$$= v_g \frac{1}{2\sqrt{\boldsymbol{k}^2}} \frac{\partial}{\partial \boldsymbol{k}} \left(\boldsymbol{k}^2 \right) \tag{4.68}$$

$$= v_g \frac{2\boldsymbol{k}}{2|\boldsymbol{k}|} = v_g \hat{\boldsymbol{k}} \tag{4.69}$$

giving the superfluid critical velocity as

$$v_g = \sqrt{a_0 \left(p(t) - \lambda_R^2 \right)} \tag{4.70}$$

The superfluid velocity is a decreasing function of the SOC-strength λ_R, as long as $p(t) - \lambda_R^2 > 0$. The number a_0 is always positive, since $\delta > (2-\alpha)(\mu+4t)$. The superfluid velocity as a function of λ_R is shown in fig. 4.3, which verifies that the superfluid velocity is indeed a decreasing

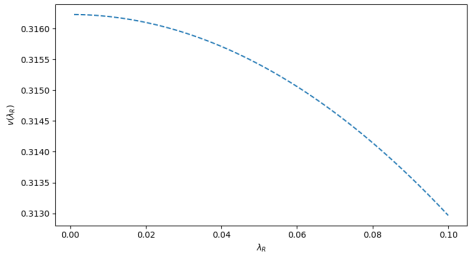

Figure 4.3: The superfluid velocity v_g as a function of λ_R. The physical parameters are $\alpha = 0.5$, $N_0 = N_s = 100^2$, $t = 1$, $U = 0.1$ and $\delta = 2t$

function of λ_R. The reason for this is that the SOC tries to bring the minima of the excitation spectrum out on finite $\boldsymbol{k}$. When this happens, the PZ phase is no longer defined, and the velocity becomes ill-defined. The critical value $\lambda_{R,\text{crit}}$ for when this happens is given by

$$\lambda_R \geq \lambda_{R,\text{crit}} = \frac{\sqrt{t}}{2} \sqrt{\Delta w(\boldsymbol{0})} \tag{4.71}$$

When λ_R is greater than $\lambda_{R,\text{crit}}$, the lowest lying branch w_- becomes imaginary. If we have on average one boson per lattice site $N_0/N_s = 1$, $\alpha = 0.5$ and $\delta = 2$, the critical value for λ_R is given by $\lambda_{R,\text{crit}} \approx 0.7$. The Zeeman field, generated in part by δ, is fully responsible for keeping a well-defined superfluid critical velocity, as $\lambda_{R,\text{crit}} \neq 0$ when $\Delta w(\boldsymbol{0}) \neq 0$, and by extension keeping the eigenvalues of the PZ phase real. We note that $\Delta w(\boldsymbol{0})$ is always positive when δ satisfies eq. (4.35). Ergo, we always have real eigenvalues for the PZ phase when δ is tuned appropriately, and $\lambda_R < \lambda_{R,\text{crit}} \neq 0$.

4.6 Free energy for the PZ-phase

The PZ containts no variational parameters, as θ could be set to zero. There is therefore no need to minimize the free energy with respect to the variational parameters. It will however be calculated and then compared to the other phases, creating a phase diagram.

Since the coefficient matrix M is positive-definite, we can choose the positive branches w_+ and w_- along the first diagonal of Ω, giving

$$\Omega = (w_1, w_2, w_3, w_4, -w_1, -w_2, -w_3, -w_4) \tag{4.72}$$

$$J\Omega = (w_1, w_2, w_3, w_4, w_1, w_2, w_3, w_4) \tag{4.73}$$

With $w_1 = w_2 = w_+$ and $w_3 = w_4 = w_-$. The vector of operators in the new basis is given by

$$\phi_{\boldsymbol{k}} = \begin{pmatrix} d^1_{\boldsymbol{k}} \\ d^2_{\boldsymbol{k}} \\ d^3_{\boldsymbol{k}} \\ d^4_{\boldsymbol{k}} \\ d^{1\dagger}_{\boldsymbol{k}} \\ d^{2\dagger}_{\boldsymbol{k}} \\ d^{3\dagger}_{\boldsymbol{k}} \\ d^{4\dagger}_{\boldsymbol{k}} \end{pmatrix}, \quad \phi^\dagger_{\boldsymbol{k}} = \begin{pmatrix} d^{1\dagger}_{\boldsymbol{k}} & d^{2\dagger}_{\boldsymbol{k}} & d^{3\dagger}_{\boldsymbol{k}} & d^{4\dagger}_{\boldsymbol{k}} & d^1_{\boldsymbol{k}} & d^2_{\boldsymbol{k}} & d^3_{\boldsymbol{k}} & d^4_{\boldsymbol{k}} \end{pmatrix} \tag{4.74}$$

Note that even though $w_1 = w_2 = w_+$, we cannot say that $d^1_{\boldsymbol{k}} = d^2_{\boldsymbol{k}} = d^+_{\boldsymbol{k}}$. The $d^i_{\boldsymbol{k}}$ operators are linearly independent, and they must satisfy $[\phi^\mu_{\boldsymbol{k}}, \phi^{\nu\dagger}_{\boldsymbol{k}}] = J_{\mu\nu}$, which could not be possible if two or more operators were linearly dependent. The diagonalized Hamiltonian is given by

$$H_2 = C_2 + {\sum_{\boldsymbol{k}}}' \sum_{i=1}^{4} w_i(\boldsymbol{k}) \left(d^{i\dagger}_{\boldsymbol{k}} d^i_{\boldsymbol{k}} + \frac{1}{2} \right) \tag{4.75}$$

where the primed sum avoids $\boldsymbol{k}$ in which $w_i(\boldsymbol{k}) = 0$. The Hamiltonian is on the form as outlined in section 3.5, and the free energy is thus given by

$$F = H_0 + C_2 + {\sum_{\boldsymbol{k}}}' w_+(\boldsymbol{k}) + w_-(\boldsymbol{k}) \tag{4.76}$$

$$+ \frac{2}{\beta} {\sum_{\boldsymbol{k}}}' \ln\left(1 - e^{-\beta w_+}\right) + \ln\left(1 - e^{-\beta w_-}\right) \tag{4.77}$$

The operator-independent terms H_0 and C_2 are given by eqs. (4.5) and (4.20) respectively.

Chapter 5

The NZ-phase

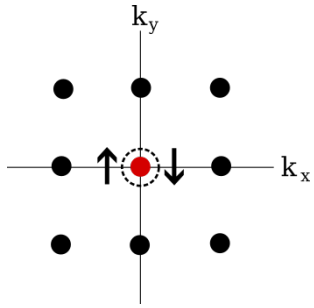

The NZ phase is different from the PZ phase by a finite $N_0^{\downarrow}$ condensate number. This will not lead to the same Zeeman field, as the chemical potential in pseudo-spin down are no longer independent of system parameters. We will be general, and assume that $N_0^{\uparrow}$ and $N_0^{\downarrow}$ can be different. This is in contrast with the treatment in [32], where it was assumed that $N_0^{\uparrow} = N_0^{\downarrow}$. Also, the mean-field parameters $\theta_1^{\uparrow}$ and $\theta_1^{\downarrow}$ are independent, due to zero condensate SOC.

5.1 Chemical potentials and condensate densities for the NZ-phase

The chemical potential for the pseudo-spin $\uparrow$ component is given by eq. (3.118), where the primed sum gives the allowed configurations as $(j, i', j') = (1, 1, 1)$ and $\alpha = (\uparrow, \downarrow)$. Writing out the primed sum, we get the expression for $\mu^{\uparrow}$

$$\mu^{\uparrow} = -4t + \frac{UN_0^{\uparrow}}{N_s f} + \alpha \frac{UN_0^{\downarrow}}{N_s f} \tag{5.1}$$

and conversely for $\mu^\downarrow$

$$\mu^\downarrow = -4t + \frac{UN_0^\downarrow}{N_s f} + \alpha\frac{UN_0^\uparrow}{N_s f} \tag{5.2}$$

Introducing the quantities $x \propto N_0^\uparrow$ and $y \propto N_0^\downarrow$ as

$$x = \frac{UN_0^\uparrow}{N_s f}, \quad y = \frac{UN_0^\downarrow}{N_s f} \tag{5.3}$$

we get the *linear* set of equations in x and y

$$\mu^\uparrow = -4t + x + \alpha y \tag{5.4}$$

$$\mu^\downarrow = -4t + y + \alpha x \tag{5.5}$$

This allows us to obtain expressions for $N_0^\uparrow$ and $N_0^\downarrow$ in terms of the given parameters $\mu^\uparrow$ and $\mu^\downarrow$. We can write the above equation on matrix form, obtaining

$$\begin{pmatrix} 1 & \alpha \\ \alpha & 1 \end{pmatrix} \begin{pmatrix} x \\ y \end{pmatrix} = \begin{pmatrix} \mu^\uparrow + 4t \\ \mu^\downarrow + 4t \end{pmatrix} \tag{5.6}$$

which has the unique solutions

$$x = \frac{\mu^\uparrow - \alpha\mu^\downarrow + 4t(1-\alpha)}{1-\alpha^2}, \quad y = \frac{\mu^\downarrow - \alpha\mu^\uparrow + 4t(1-\alpha)}{1-\alpha^2} \tag{5.7}$$

Notice that one can obtain the solution for $y \propto N_0^\downarrow$ simply by flipping the spins from $\uparrow$ to $\downarrow$ and visa versa in the expression for $x \propto N_0^\uparrow$. For a given α and t, one must be careful to choose $\mu^\uparrow$ and $\mu^\downarrow$ such that x and y becomes positive.

5.2 Constant, linear and quadratic Hamiltonian

Again, as in the PZ phase, the linear Hamiltonian vanishes. The constant Hamiltonian, for any phase, is given by eq. (3.122), where the primed sum gives the possible configurations as $(i, j, i', j') = (1, 1, 1, 1)$, $\alpha = (\uparrow, \downarrow)$ and $\beta = (\uparrow, \downarrow)$. Thus, we simply get

$$H_0 = -\frac{1}{2N_s f^2} \sum_{\alpha\beta} U^{\alpha\beta} N_0^\alpha N_0^\beta \tag{5.8}$$

$$= -\frac{U}{2N_s f^2} \left(N_0^{\uparrow 2} + 2\alpha N_0^\uparrow N_0^\downarrow + N_0^{\downarrow 2} \right) \tag{5.9}$$

The interacting part of the Hamiltonian is given by

$$H_{\text{int}} = \sum_{\boldsymbol{k}} G_{11}(\boldsymbol{k}, -\boldsymbol{k}) + R_{11}(\boldsymbol{k}, \boldsymbol{k}) + L_{11}(\boldsymbol{k}, \boldsymbol{k}) \tag{5.10}$$

The quantities G, R and L are defined in eqs. (3.134), (3.135) and (3.136). The first and second primed sum both give the possible configurations as $(i, j) = (1, 1)$, $\alpha \in (\uparrow, \downarrow)$ and $\beta \in (\uparrow, \downarrow)$. We

also define the vector of operators $\psi_{\boldsymbol{k}}^\dagger$ and $\psi_{\boldsymbol{k}}$ exactly as in the PZ-phase. We also explicitly sum over $-\boldsymbol{k}$, in order to symmetrize the Hamiltonian. The quadratic Hamiltonian can then be written

$$H_2 = C_2 + \frac{1}{2}\sum_{\boldsymbol{k}} \psi_{\boldsymbol{k}}^\dagger M_{\boldsymbol{k}} \psi_{\boldsymbol{k}} \tag{5.11}$$

The constant term is given by,

$$C_2 = \frac{\mu^\uparrow + \mu^\downarrow}{2} N_s - \frac{U(N_0^\uparrow + N_0^\downarrow)}{f}\left(1 + \frac{\alpha}{2}\right) \tag{5.12}$$

and the coefficient matrix $M_{\boldsymbol{k}}$ has the form

$$M_{\boldsymbol{k}} = \begin{pmatrix} M_1(\boldsymbol{k}) & M_2 \\ M_2^* & M_1^*(\boldsymbol{k}) \end{pmatrix} \tag{5.13}$$

where the four-by-four, Hermitian submatrix $M_1(\boldsymbol{k})$ is given by

$$M_1(\boldsymbol{k}) = \begin{pmatrix} E_1(\boldsymbol{k}) & 0 & b(\boldsymbol{k}) & 0 \\ 0 & E_1(\boldsymbol{k}) & 0 & b(-\boldsymbol{k}) \\ b^*(\boldsymbol{k}) & 0 & E_2(\boldsymbol{k}) & 0 \\ 0 & b^*(-\boldsymbol{k}) & 0 & E_2(\boldsymbol{k}) \end{pmatrix} \tag{5.14}$$

The matrix-elements has the values

$$E_1(\boldsymbol{k}) = \frac{\eta_{\boldsymbol{k}}^{\uparrow\uparrow}}{2} + \frac{UN_0^\uparrow}{N_s f} + \frac{\alpha U N_0^\downarrow}{2N_s f} \tag{5.15}$$

$$b(\boldsymbol{k}) = \frac{\eta_{\boldsymbol{k}}^{\uparrow\downarrow}}{2} + \frac{\alpha U\sqrt{N_0^\uparrow N_0^\downarrow}}{2N_s f} e^{-i(\theta_1^\uparrow - \theta_1^\downarrow)} \tag{5.16}$$

$$E_2(\boldsymbol{k}) = \frac{\eta_{\boldsymbol{k}}^{\downarrow\downarrow}}{2} + \frac{UN_0^\downarrow}{N_s f} + \frac{\alpha U N_0^\uparrow}{2N_s f} \tag{5.17}$$

and the symmetric four-by-four submatrix M_2 is given by

$$M_2 = \begin{pmatrix} 0 & c^\uparrow & 0 & d \\ c^\uparrow & 0 & d & 0 \\ 0 & d & 0 & c^\downarrow \\ d & 0 & c^\downarrow & 0 \end{pmatrix} \tag{5.18}$$

with matrix-elements defined as

$$c^\uparrow = \frac{UN_0^\uparrow}{2N_s f} e^{-2i\theta_1^\uparrow} \tag{5.19}$$

$$d = \frac{\alpha U\sqrt{N_0^\uparrow N_0^\downarrow}}{2N_s f} e^{-i(\theta_1^\uparrow + \theta_1^\downarrow)} \tag{5.20}$$

$$c^\downarrow = \frac{UN_0^\downarrow}{2N_s f} e^{-2i\theta_1^\downarrow} \tag{5.21}$$

The author is not able to find explicit expressions for the excitation spectrum, and the eigenvalues found numerically are *imaginary*. For the case of equal condensate particle numbers $N_0^\uparrow = N_0^\downarrow$, this is due to a zero Zeeman field. The spin-orbit coupling therefore forces the minima out on finite $\boldsymbol{k}$, making the NZ phase ill-defined. We next compare the PZ and NZ phases, and explore the effect of an imbalance in condensate numbers for the NZ phase, as this intuitively could make the NZ phase stable.

5.3 Comparison of the PZ and NZ phases

The PZ phase has an extreme imbalance in condensate numbers, $N_0^\uparrow \neq 0$ and $N_0^\downarrow = 0$. We found in the PZ chapter that to obtain real eigenvalues, one had to include a Zeeman shift which was proportional to $\delta = \mu^\uparrow - \mu^\downarrow$. The advantage of the PZ phase was that since $N_0^\downarrow = 0$, one could in principle choose $\mu^\downarrow$ to any value. Thus the difference δ could be tuned to give real eigenvalues. We can understand the PZ phase better by analyzing the spin-orbit coupled, single-particle problem in section 3.1 including a finite Zeeman shift. The eigenvalues are given by

$$\lambda_{\boldsymbol{k}}^{\pm} = -\epsilon_{\boldsymbol{k}} - \bar{\mu} \pm \sqrt{|s_{\boldsymbol{k}}|^2 + \delta^2/4} \tag{5.22}$$

$$\bar{\mu} = \frac{\mu^\uparrow + \mu^\downarrow}{2} \tag{5.23}$$

$$\delta = \mu^\uparrow - \mu^\downarrow \tag{5.24}$$

The minima of the $\lambda_{\boldsymbol{k}}^-$ branch is found at the values

$$k_x, k_y = \pm \frac{1}{2a} \arccos(z) \tag{5.25}$$

$$z = \frac{t^2/\lambda_R^2 - 1/2 + t^2\delta^2/16\lambda_R^4}{t^2/\lambda_R^2 + 1/2} \tag{5.26}$$

The value of $\lambda_{\boldsymbol{k}}^-$ evaluated at any one of these points is given by

$$\lambda_{\min}^- = -2\sqrt{2}t\sqrt{z+1} - \bar{\mu} - \sqrt{4\lambda_R^2(1-z) + \delta^2/4} \tag{5.27}$$

which is negative. Following the same logic as in the zero Zeeman field case, we must shift the branches *up* and absorb the difference in the chemical potentials. In fig. 5.1 the plot of the excitation spectrum for intreasing values of δ is shown. At $\delta = 0$ the two branches meet linearly at $\boldsymbol{k} = 0$, with minima at finite $\boldsymbol{k}$. When δ is increased, the two branches are seperated at $\boldsymbol{k} = 0$ by the Zeeman field, and the behaviour at $\boldsymbol{k} = 0$ is not longer linear. Also, the minima at finite $\boldsymbol{k}$ moves closer to the origin. When the minima meet at the origin, the Zeeman field has effectively overtaken the influence from SOC. This happens when $z = 1$, since $\arccos(1) = 0$, which gives the critial value for δ

$$\delta_m = \frac{4\lambda_R^2}{t} \tag{5.28}$$

For $\delta \geq \delta_m$ the minima of $\Lambda_{\boldsymbol{k}}^-$ will be at $\boldsymbol{k} = 0$, even with SOC. This is reminiscent of the PZ phase. The PZ phase *has* a Zeeman field, and has real eigenvalues with a finite λ_R. Also note

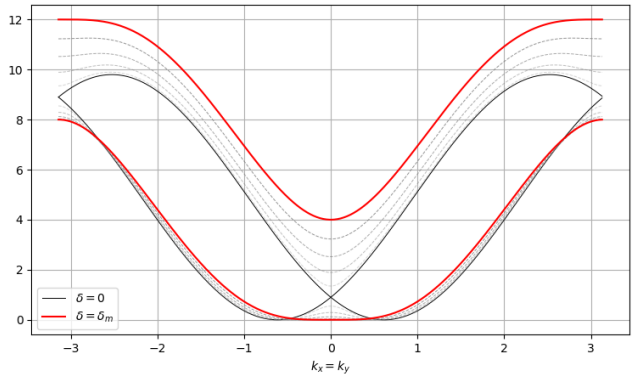

Figure 5.1: Plot of the single-particle excitation spectrum with spin-orbit coupling. The black lines are the excitation spectrum with $\delta = 0$, the dotted lines are with increasing δ, and the red lines are with $\delta = \delta_m$.

that the excitation spectrum for the PZ phase is similar to fig. 5.1, only with the Bogoliubov spectrum in the lowest branch, which makes the behaviour around $\boldsymbol{k} = 0$ linear. We can try to understand the spin-orbit coupled, weakly interacting, two-component Bose gas, by superimposing the single-particle excitation spectrum with SOC, and the one-component weakly interacting Bogoliubov spectrum. Thus we can understand why the NZ phase is unstable for $N_0^{\uparrow} = N_0^{\downarrow}$; there is no Zeeman field which can overtake the influence from SOC. We can however try to create a Zeeman field for the NZ phase by introducing an inbalance in the condensate numbers $\Delta N_0 = N_0^{\uparrow} - N_0^{\downarrow}$. Using the equations for $\mu^{\uparrow}$ and $\mu^{\downarrow}$ given in eqs. (5.5), we get

$$\Delta N_0 = \frac{\delta}{U(1-\alpha)} N_s \tag{5.29}$$

We can, as a zeroth order approximation, expect that the eigenvalues of the NZ phase becomes real when $\delta = \delta_m$, which gives

$$\Delta N_0 = \frac{4\lambda_R^2}{Ut(1-\alpha)} N_s \tag{5.30}$$

However, the numerical results reveal that the eigenvalues of NZ are still imaginary, even with the ΔN_0 as defined above. The reason for this is that the expressions for the chemical potentials are linked in a way that gives no Zeeman splitting, as opposed to the PZ phase where $\mu^{\downarrow}$ can be chosen appropriately. The author *was* able to introduce a Zeeman shift if an independent fluctuation μ^* was added to either of the chemical potentials, but this does not follow the equations of the mean-field approach, and is simply an illustration that the equations for the chemical potentials leads to zero Zeeman field.

Chapter 6

The PW-phase

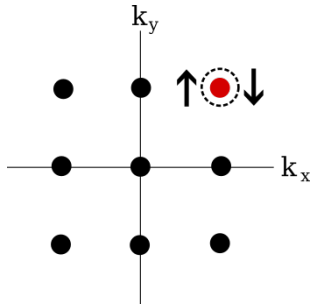

This phase looks similar to the NZ-phase, it is simply a shift in coordinate systems. One would think that this phase should be equivalent, because of galilean invariance. However, SOC *breaks* galilean invariance, and we must treat this phase seperately. We will see that a finite $\boldsymbol{k}_{01}$ leads to complications when solving for the condensate densities $N_0^{\uparrow}$ and $N_0^{\downarrow}$ in terms of the chemical potentials $\mu^{\uparrow}$ and $\mu^{\downarrow}$. Also, spin-orbit coupling makes the mean-field parameters $\theta_1^{\uparrow}$ and $\theta_1^{\downarrow}$ *dependent*. Lastly, we must choose a *different* symmetrization of H to obtain real eigenvalues.

6.1 Finding condensate densities

We will assume that $N_0^\uparrow$ and $N_0^\downarrow$ in general can be different. The expression for $\mu^\uparrow$ is given by eq. (3.118)

$$\mu^\uparrow = -\epsilon_i^\uparrow - |s_i|\sqrt{\frac{N_0^\downarrow}{N_0^\uparrow}}\Omega(|\boldsymbol{k}_{0i}|, N_i^\uparrow) + \left(\sum_{ji'j'}\sum_{\alpha}\right)''' \frac{U^{\alpha\uparrow}N_0^\alpha}{N_s f}\cos\left(\theta_{j'}^\uparrow - \theta_i^\uparrow - \theta_j^\alpha + \theta_{i'}^\alpha\right)\delta_{i+j,i'+j'}\Omega(N_i^\uparrow) \tag{6.1}$$

Because of finite $\boldsymbol{k}_{01}$, we must include the SOC term. The possible configurations from the primed sum is given by $(j, i', j') = (1, 1, 1)$ and $\alpha = (\uparrow, \downarrow)$, and we must choose $i = 1$. The primed sum gives the same contribution as the NZ-phase, and the final expression for $\mu^\uparrow$ is given by

$$\mu^\uparrow = -\epsilon_{\boldsymbol{k}_{01}} - |s_{\boldsymbol{k}_{01}}|\sqrt{\frac{N_0^\downarrow}{N_0^\uparrow}} + \frac{UN_0^\uparrow}{N_s f} + \frac{\alpha U N_0^\downarrow}{N_s f} \tag{6.2}$$

and conversely for $\mu^\downarrow$

$$\mu^\downarrow = -\epsilon_{\boldsymbol{k}_{01}} - |s_{\boldsymbol{k}_{01}}|\sqrt{\frac{N_0^\uparrow}{N_0^\downarrow}} + \frac{UN_0^\downarrow}{N_s f} + \frac{\alpha U N_0^\uparrow}{N_s f} \tag{6.3}$$

We see that the SOC-term introduces the condensate densities N_0^α in the *denominator* of the expression for μ^α. This makes the equations non-linear in the condensate densities. Let us treat, for the moment, the chemical potentials as known parameters. The unknowns are then the condensate densities $N_0^\uparrow$ and $N_0^\downarrow$. We introduce the quantities x and y

$$x = \sqrt{\frac{U}{N_s f}}\sqrt{N_0^\uparrow}, \quad y = \sqrt{\frac{U}{N_s f}}\sqrt{N_0^\downarrow} \tag{6.4}$$

for which we get the coupled set of third-degree equations in x and y

$$x^3 + \alpha y^2 x - sy - u_1 x = 0 \tag{6.5}$$

$$y^3 + \alpha x^2 y - sx - u_2 y = 0 \tag{6.6}$$

where the coefficients are given by

$$s = |s_{\boldsymbol{k}_{01}}| = 2\sqrt{2}\lambda_R|\sin(k_0 a)| \tag{6.7}$$

$$u_1 = \mu^\uparrow + \epsilon_{\boldsymbol{k}_{01}} = \mu^\uparrow + 4t\cos(k_0 a) \tag{6.8}$$

$$u_2 = \mu^\downarrow + \epsilon_{\boldsymbol{k}_{01}} = \mu^\downarrow + 4t\cos(k_0 a) \tag{6.9}$$

Using Maple, the author tried to find an analytic solution for the condensate densities, but was unsuccessful.

6.1.1 Numerical solution to condensate densities

We choose k_0 as $k_0 = 1/a \arctan(\sqrt{2}\lambda_R/2t)$, which is the k_0 found by minimizing the *pure* condensate for the PZ phase. One may find an numerical approximation for the condensate densities by finding the roots (x, y) of the above equations. This is done using Python, using Numpys SOLVE function. In figure 6.1 the simultaneous solution for x and y is shown for SOC strength λ_R varying from 0.2 to 2.5. The plot also includes the difference in chemical potentials, defined as $\delta = \mu^\uparrow - \mu^\downarrow$. The choice $\mu^\uparrow = 1$ has also been made. We see that for $\delta = 0$, y behaves as a linear function of x. This simply implies that if the chemical potentials are equal, the number of particles in the condensate for both pseudo-spins are also equal $N_0^\uparrow = N_0^\downarrow$. This makes physical sense, as the chemical potential for a specific pseudo-spin regulates the average number of particles for the specific pseudo-spin. Also, $\delta < 0$ shows that $y > x$. Thus $\mu^\downarrow > \mu^\uparrow$ leads to $N_0^\downarrow > N_0^\uparrow$, which is what we expect. From figure 6.2, which shows x as a function of λ_R, we see that x is an increasing function of δ for all λ_R. This is opposite for the solution for y, which is a decreasing function of δ for all λ_R. This makes physical sense; when δ ranges from -1 to 1, $\mu^\downarrow$ decreases from 2 to 0 respectively. We expect that a high value for $\mu^\downarrow$ leads to a high value for y, as the numerical solutions show.

There is also other interesting features from figures 6.2 and 6.3. We see in fig. 6.2 that x behaves linearly when λ_R is increasing. Also, this seems to be independent of the value of δ. This behaviour is also similar in fig. 6.3, where y behaves linearly for increasing λ_R, but here the intersection with the y-axis is seen dependent on the value of δ. This is due to keeping $\mu^\uparrow = 1$ (which regulates x), and varying $\mu^\downarrow$ from 0 to 2 (which regulates y).

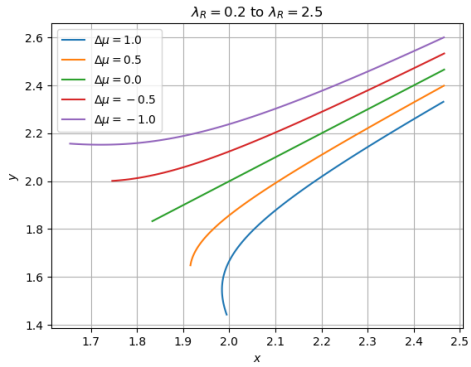

Figure 6.1: Plot over the simultaneous solutions for the condensate densities (x, y). The SOC strength is increasing from $\lambda_R = 0.2$ to $\lambda_R = 2.5$. The plot includes differences in the chemical potentials, ranging from 1 to -1, and is defined as $\delta\mu = \mu^\uparrow - \mu^\downarrow$. The upper-most curve is $\delta > 0$. Other physical variables are given the values $t = 1$, $\mu^\uparrow = 1$ and $\alpha = 0.5$

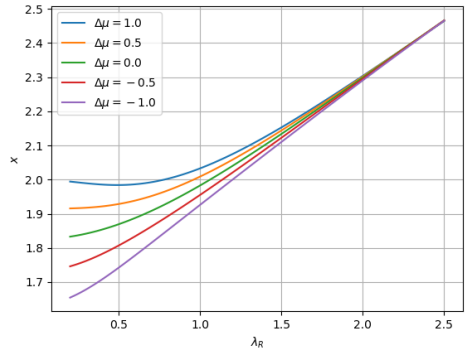

Figure 6.2: Plot over the solution for x in terms of λ_R. The plot includes differences in the chemical potentials, ranging from 1 to -1, and is defined as $\delta = \mu^{\uparrow} - \mu^{\downarrow}$. Other physical variables are given the values $t = 1$, $\mu^{\uparrow} = 1$ and $\alpha = 0.5$

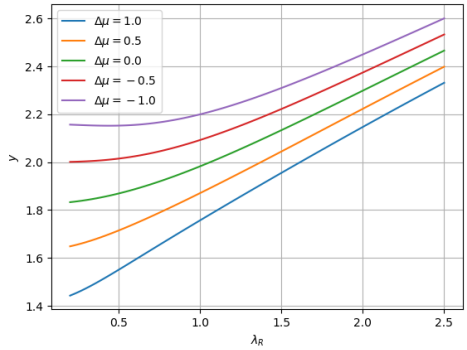

Figure 6.3: Plot over the solution for y in terms of λ_R. The plot includes differences in the chemical potentials, ranging from 1 to -1, and is defined as $\delta = \mu^{\uparrow} - \mu^{\downarrow}$. The upper-most curve is $\delta > 0$. Other physical variables are given the values $t = 1$, $\mu^{\uparrow} = 1$ and $\alpha = 0.5$

6.2 Constant and linear Hamiltonian

We now have the constraint on the variational parameters $\theta_1^{\uparrow}$ and $\theta_1^{\downarrow}$, from equation (3.104):

$$\delta\theta_1 = \gamma_1 - \pi \tag{6.10}$$

Where γ_1 is given by $-\pi - \pi/4$, due to finite SOC. We will in the following assume that $N_0^{\uparrow}$ can be different from $N_0^{\downarrow}$. Using the expression for H_0 in (3.122), and that the possible values for $(i, j, i', j', \alpha, \beta)$ are given by $(i, j, i', j') = (1, 1, 1, 1)$, $\alpha \in (\uparrow, \downarrow)$ and $\beta \in (\uparrow, \downarrow)$, we get

$$H_0 = -\frac{U}{2N_s f^2}\left(N_0^{\uparrow 2} + 2\alpha N_0^{\uparrow} N_0^{\downarrow} + N_0^{\downarrow 2}\right) \tag{6.11}$$

From the expression for the linear Hamiltonian H_1, in eq. (3.123), we get that the possible configurations for the momentum indices are $(i, j, i') = (1, 1, 1)$. Conservation of momentum constraints $\boldsymbol{k}$ to the value $\boldsymbol{k} = \boldsymbol{k}_{01}$, which is excluded from the sum since it is a condensate momentum.

6.3 Quadratic Hamiltonian

The expression for H_2 is given in eq. (3.126). The contribution from the interaction Hamiltonian is given by

$$H_{\text{int}} = \sum_{\boldsymbol{k}} G_{11}(\boldsymbol{k}, \boldsymbol{p}) + R_{11}(\boldsymbol{k}, \boldsymbol{k}) + L_{11}(\boldsymbol{k}, \boldsymbol{k}) \tag{6.12}$$

The quantities G, R and L are defined in eqs. (3.134), (3.135) and (3.136). The vector $\boldsymbol{p}$ is given by $\boldsymbol{p} = 2\boldsymbol{k}_{01} - \boldsymbol{k}$. Notice that this is very similar to the NZ-phase, which gives the same expressions when $\boldsymbol{k}_{01} = 0$. This suggests that instead of symmetrizing H_2 with $\sum_{\boldsymbol{k}} f(\boldsymbol{k}) = 1/2 \sum_{\boldsymbol{k}} (f(\boldsymbol{k}) + f(-\boldsymbol{k}))$, we should rather symmetrize with $\sum_{\boldsymbol{k}} f(\boldsymbol{k}) = 1/2 \sum_{\boldsymbol{k}} (f(\boldsymbol{k}) + f(\boldsymbol{p}))$. This is allowed since the 1st Brilloin zone is periodic, and shifting the sum by a finite $\boldsymbol{p}$ only moves the Brilloin zone. The interaction Hamiltonian with $\boldsymbol{k} \to \boldsymbol{p}$ becomes $G_{11}(\boldsymbol{p}, \boldsymbol{k}) + R_{11}(\boldsymbol{p}, \boldsymbol{p}) + L_{11}(\boldsymbol{p}, \boldsymbol{p})$, leading to no new operators. The author tried at first, and naively, to symmetrize with $-\boldsymbol{k}$. This led to imaginary eigenvalues. It may be a troubling thought that different symmetrizations leads to different answers. However, the choice of symmetrization actually defines the coefficient matrix, as well as the vector of operators. Consequently, different symmetrizations leads to different particle basises. In addition, the PW phase is not inversion symmetric around $\boldsymbol{k} = 0$. We define the vectors of operators

$$\psi_{\boldsymbol{k}} = \begin{pmatrix} A^{\uparrow}_{\boldsymbol{k}} \\ A^{\uparrow}_{\boldsymbol{p}} \\ A^{\downarrow}_{\boldsymbol{k}} \\ A^{\downarrow}_{\boldsymbol{p}} \\ A^{\uparrow\dagger}_{\boldsymbol{k}} \\ A^{\uparrow\dagger}_{\boldsymbol{p}} \\ A^{\downarrow\dagger}_{\boldsymbol{k}} \\ A^{\downarrow\dagger}_{\boldsymbol{p}} \end{pmatrix}, \quad \psi^{\dagger}_{\boldsymbol{k}} = \begin{pmatrix} A^{\uparrow\dagger}_{\boldsymbol{k}} & A^{\uparrow\dagger}_{\boldsymbol{p}} & A^{\downarrow\dagger}_{\boldsymbol{k}} & A^{\downarrow\dagger}_{\boldsymbol{p}} & A^{\uparrow}_{\boldsymbol{k}} & A^{\uparrow}_{\boldsymbol{p}} & A^{\downarrow}_{\boldsymbol{k}} & A^{\downarrow}_{\boldsymbol{p}} \end{pmatrix} \tag{6.13}$$

which has the same structure as in the PZ and NZ phases, only with $-\boldsymbol{k} \to \boldsymbol{p}$. Forming H_2 as a matrix product, and symmetrizing over $\boldsymbol{p}$, we get

$$H_2 = C_2 + \frac{1}{2} \sum_{\boldsymbol{k}} \psi^{\dagger}_{\boldsymbol{k}} M_{\boldsymbol{k}} \psi_{\boldsymbol{k}} \tag{6.14}$$

$$C_2 = \frac{\mu^{\uparrow} + \mu^{\downarrow}}{2} N_s - \frac{U(N_0^{\uparrow} + N_0^{\downarrow})}{f} \left(1 + \frac{\alpha}{2}\right) \tag{6.15}$$

with the coefficient matrix $M_{\boldsymbol{k}}$ given by

$$M_{\boldsymbol{k}} = \begin{pmatrix} M_1(\boldsymbol{k}) & M_2 \\ M_2^* & M_1^*(\boldsymbol{k}) \end{pmatrix} \tag{6.16}$$

The submatrices $M_1(\boldsymbol{k})$ and M_2 are almost exactly the same as in the NZ phase, only with the replacement $-\boldsymbol{k} \to \boldsymbol{p}$, which is due to the symmetrization with $\boldsymbol{p}$. Thus $M_1(\boldsymbol{k})$ and M_2 are given by

$$M_1(\boldsymbol{k}) = \begin{pmatrix} E_1(\boldsymbol{k}) & 0 & b(\boldsymbol{k}) & 0 \\ 0 & E_1(\boldsymbol{p}) & 0 & b(\boldsymbol{p}) \\ b^*(\boldsymbol{k}) & 0 & E_2(\boldsymbol{k}) & 0 \\ 0 & b^*(\boldsymbol{p}) & 0 & E_2(\boldsymbol{p}) \end{pmatrix} \quad M_2 = \begin{pmatrix} 0 & c^{\uparrow} & 0 & d \\ c^{\uparrow} & 0 & d & 0 \\ 0 & d & 0 & c^{\downarrow} \\ d & 0 & c^{\downarrow} & 0 \end{pmatrix} \tag{6.17}$$

The definition of the matrix elements are *excactly* the same as in the NZ phase. The author is not able to find explicit expressions for the excitation spectrum, but is able to find them numerically as long as $\alpha < 1$. The spectrum is shown in fig. 6.4. There is no unbalance in

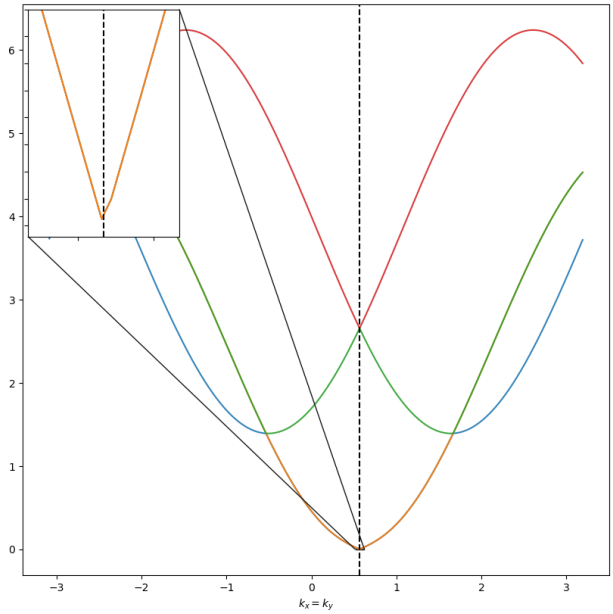

Figure 6.4: The excitation spectrum for the PW phase with $N_0^{\uparrow} = N_0^{\downarrow}$. The black dotted line is the value for k_0 as given in the pure condensate phase.

condensate numbers, still leading to real eigenvalues, which is a clear difference from the NZ phase. This is due to the fact that we need no Zeeman splitting to overcome the influence from SOC, since the condensate already lies on a finite $\boldsymbol{k}$ vector. We get in total four branches. The lowest branch is Bogoliubov-like with a superfluid critical velocity around k_0. This makes physical sense. The condensate lies on a finite $\boldsymbol{k}$ vector, where the interacting Bogoliubov spectrum kicks in, similar with the lowest branch of the PZ phase. We also have two parabolas shifted due to SOC, lying above the lowest branch, similar to fig. 3.1.

The excitation spectrum resembles the overlap between the spin-orbit coupled, non-interacting excitation spectrum, and the single-component, interacting excitation spectrum. Also, the spectrum is periodic in the shifted Brilloin zone $[-\pi/a + k_0, \pi/a + k_0)$, which originates from the symmetrization with $\boldsymbol{p}$. This demonstrates that the PW phase is not inversion symmetric around $\boldsymbol{k} = 0$.

Chapter 7

The SW-Phase

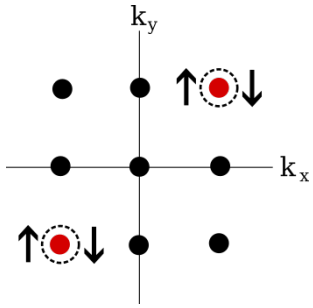

In this phase there are *two* condensate momenta, $\boldsymbol{k}_{01}$ and $\boldsymbol{k}_{03}$. Our intuition would suggest that we get Bogoliubov spectra around these points. However, numerical analysis will later reveal that this is not the case. We note that Jansønns assumption that the helicity angle γ_i is in general equal with the angle of $\boldsymbol{k}_{0i}$ with the k_x-axis, is wrong. This can be seen by investigating the expression for $s_{\boldsymbol{k}}$

$$s_{\boldsymbol{k}} = -2\lambda_R \left(\sin(k_y a) + i \sin(k_x a)\right) = |s_{\boldsymbol{k}}| e^{-i\gamma_{\boldsymbol{k}}} \tag{7.1}$$

By using that $\boldsymbol{k}_{01} = (k_0, k_0)$ and $\boldsymbol{k}_{03} = -\boldsymbol{k}_{01}$, we get

$$s_{\boldsymbol{k}_{01}} \propto -(1+i) \tag{7.2}$$
$$s_{\boldsymbol{k}_{03}} \propto (1+i) \tag{7.3}$$

which gives the angles $\gamma_{\boldsymbol{k}}$

$$\gamma_{\boldsymbol{k}_{03}} = -\frac{\pi}{4}, \quad \gamma_{\boldsymbol{k}_{01}} = -\pi + \gamma_{\boldsymbol{k}_{03}} \tag{7.4}$$

Note that the difference between the two angles is $\gamma_{\boldsymbol{k}_{03}} - \gamma_{\boldsymbol{k}_{01}} = -\pi$, which is opposite of Janssønns master thesis. However, since this difference often appears as an argument in a cosine function, the sign does not matter. Also, we can presume that the γ's are the angle with

some direction in $\boldsymbol{k}$ space. In addition, we have the SOC induced constraints on the variational parameters

$$\delta\theta_1 = \gamma_1 - \pi, \quad \delta\theta_3 = \gamma_3 - \pi \tag{7.5}$$

7.1 Finding condensate densities for the SW phase

Similarly as for the PW phase, we assume that $N_0^{\uparrow} \neq N_0^{\downarrow}$ in general. The chemical potential for pseudo-spin $\uparrow$ is again given by eq. (3.118). We choose $\boldsymbol{k}_{0i} = \boldsymbol{k}_{01}$. The primed sum gives the possible momentum configurations as $(j, i', j') = (1,1,1), (3,1,3), (3,3,1)$ and $\alpha \in (\uparrow, \downarrow)$. Writing out the sum gives

$$\sum_{\alpha} \frac{U^{\alpha\uparrow} N_0^{\alpha}}{N_s f} \left(2 + \cos\left(\theta_3^{\uparrow} - \theta_1^{\uparrow} - \theta_3^{\alpha} + \theta_1^{\alpha}\right)\right) \tag{7.6}$$

$$= \frac{3UN_0^{\uparrow}}{N_s f} + \frac{\alpha U N_0^{\downarrow}}{N_s f} \left(2 + \cos(\delta\theta_3 - \delta\theta_1)\right) \tag{7.7}$$

$$= \frac{3UN_0^{\uparrow}}{N_s f} + \frac{\alpha U N_0^{\downarrow}}{N_s f} \left(2 + \cos(\gamma_3 - \gamma_1)\right) \tag{7.8}$$

$$= \frac{3UN_0^{\uparrow}}{N_s f} + \frac{\alpha U N_0^{\downarrow}}{N_s f} \tag{7.9}$$

where we have used that $\gamma_1 = \gamma_3 + \pi$. This gives the expression for $\mu^{\uparrow}$

$$\mu^{\uparrow} = -\epsilon_{\boldsymbol{k}_{01}} - |s_{\boldsymbol{k}_{01}}| \sqrt{\frac{N_0^{\downarrow}}{N_0^{\uparrow}}} + \frac{3UN_0^{\uparrow}}{N_s f} + \frac{\alpha U N_0^{\downarrow}}{N_s f} \tag{7.10}$$

and conversely for $\mu^{\downarrow}$

$$\mu^{\downarrow} = -\epsilon_{\boldsymbol{k}_{01}} - |s_{\boldsymbol{k}_{01}}| \sqrt{\frac{N_0^{\uparrow}}{N_0^{\downarrow}}} + \frac{3UN_0^{\downarrow}}{N_s f} + \frac{\alpha U N_0^{\uparrow}}{N_s f} \tag{7.11}$$

which is very similar to the expressions for the chemical potentials in the PW-phase, only different by a factor of 3. Let us again introduce the quantities x and y as in the PW phase

$$x = \sqrt{\frac{U}{N_s f}} \sqrt{N_0^{\uparrow}}, \quad y = \sqrt{\frac{U}{N_s f}} \sqrt{N_0^{\downarrow}} \tag{7.12}$$

leading to the coupled set of third-degree equations in x and y

$$3x^3 + \alpha y^2 x - sy - u_1 x = 0 \tag{7.13}$$

$$3y^3 + \alpha x^2 y - sx - u_2 y = 0 \tag{7.14}$$

where the coefficients are given by

$$s = |s_{\boldsymbol{k}_{01}}| = 2\sqrt{2}\lambda_R |\sin(k_0 a)| \tag{7.15}$$

$$u_1 = \mu^{\uparrow} + \epsilon_{\boldsymbol{k}_{01}} = \mu^{\uparrow} + 4t\cos(k_0 a) \tag{7.16}$$

$$u_2 = \mu^{\downarrow} + \epsilon_{\boldsymbol{k}_{01}} = \mu^{\downarrow} + 4t\cos(k_0 a) \tag{7.17}$$

We remind ourselves that k_0 is still a variational parameter. Notice that this system of third-degree equations is very similar to the system of third-degree equations in the PW phase. The plots of the solutions will therefore not be included.

7.2 Constant and quadratic Hamiltonian

H_0 is again given by eq. (3.122). The primed sum together with the delta-function gives the possible configurations for the momentum indices $(i,j,i',j') = (1,1,1,1),(1,3,1,3),(1,3,3,1),(3,1,1,3),(3,1,3,1),(3,3,3,3)$, $\alpha \in (\uparrow,\downarrow)$, and $\beta \in (\uparrow,\downarrow)$. The constant Hamiltonian is thus given by

$$H_0 = -\frac{1}{2N_s f^2}\sum_{\alpha\beta} N_0^\alpha N_0^\beta U^{\alpha\beta}\left(4+2\cos\left(\theta_3^\alpha-\theta_1^\alpha-\theta_3^\beta+\theta_1^\beta\right)\right) \tag{7.18}$$

$$= -\frac{U}{2N_s f^2}\left(6N_0^{\uparrow 2}+6N_0^{\downarrow 2}+2\alpha N_0^\uparrow N_0^\downarrow\left(4+2\cos\left(\delta\theta_3-\delta\theta_1\right)\right)\right) \tag{7.19}$$

$$= -\frac{U}{2N_s f^2}\left(6N_0^{\uparrow 2}+4\alpha N_0^\uparrow N_0^\downarrow+6N_0^{\downarrow 2}\right) \tag{7.20}$$

$$= -\frac{U}{N_s f^2}\left(3N_0^{\uparrow 2}+2\alpha N_0^\uparrow N_0^\downarrow+3N_0^{\downarrow 2}\right) \tag{7.21}$$

The linear Hamiltonian is finite, and treated in the appendix. The author has outlined a method for dealing with these terms, but will not use them for the rest of the thesis, due to the uncertainty of the method. The interaction Hamiltonian is given by[1]

$$H_{\text{int}} = \sum_{\boldsymbol{k}} G_{11}(\boldsymbol{k},\boldsymbol{p}) + G_{13}(\boldsymbol{k},-\boldsymbol{k}) + G_{31}(\boldsymbol{k},-\boldsymbol{k}) + G_{33}(\boldsymbol{k},\boldsymbol{q}) \tag{7.22}$$

$$+ R_{11}(\boldsymbol{k},\boldsymbol{k}) + R_{13}(\boldsymbol{k},\boldsymbol{p}') + R_{31}(\boldsymbol{k},\boldsymbol{q}') + R_{33}(\boldsymbol{k},\boldsymbol{k}) \tag{7.23}$$

$$+ L_{11}(\boldsymbol{k},\boldsymbol{k}) + L_{13}(\boldsymbol{k},\boldsymbol{p}') + L_{31}(\boldsymbol{k},\boldsymbol{q}') + L_{33}(\boldsymbol{k},\boldsymbol{k}) \tag{7.24}$$

The vectors $\boldsymbol{q}$, $\boldsymbol{q}'$, $\boldsymbol{p}$ and $\boldsymbol{p}'$ comes from momentum conservation and are given by

$$\boldsymbol{p} = 2\boldsymbol{k}_{01} - \boldsymbol{k}, \quad \boldsymbol{q} = -2\boldsymbol{k}_{01} - \boldsymbol{k} \tag{7.25}$$

$$\boldsymbol{p}' = 2\boldsymbol{k}_{01} + \boldsymbol{k}, \quad \boldsymbol{q}' = -2\boldsymbol{k}_{01} + \boldsymbol{k} \tag{7.26}$$

such that $\boldsymbol{p}' = \boldsymbol{p}(-\boldsymbol{k})$ and $\boldsymbol{q}' = \boldsymbol{q}(-\boldsymbol{k})$. We see that the SW is symmetric around $\boldsymbol{k} = 0$, in contrast with the PW phase, which only had the vector $\boldsymbol{p}$. We introduce the vector of operators $\Psi_{\boldsymbol{k}}^\dagger$ and $\Psi_{\boldsymbol{k}}$ with 24 elements each

$$\Psi_{\boldsymbol{k}}^\dagger = \Big(A_{\boldsymbol{k}}^{\uparrow\dagger}A_{-\boldsymbol{k}}^{\uparrow\dagger}A_{\boldsymbol{p}}^{\uparrow\dagger}A_{\boldsymbol{p}'}^{\uparrow\dagger}A_{\boldsymbol{q}}^{\uparrow\dagger}A_{\boldsymbol{q}'}^{\uparrow\dagger}A_{\boldsymbol{k}}^{\downarrow\dagger}A_{-\boldsymbol{k}}^{\downarrow\dagger}A_{\boldsymbol{p}}^{\downarrow\dagger}A_{\boldsymbol{p}'}^{\downarrow\dagger}A_{\boldsymbol{q}}^{\downarrow\dagger}A_{\boldsymbol{q}'}^{\downarrow\dagger} \tag{7.27}$$

$$A_{\boldsymbol{k}}^{\uparrow}A_{-\boldsymbol{k}}^{\uparrow}A_{\boldsymbol{p}}^{\uparrow}A_{\boldsymbol{p}'}^{\uparrow}A_{\boldsymbol{q}}^{\uparrow}A_{\boldsymbol{q}'}^{\uparrow}A_{\boldsymbol{k}}^{\downarrow}A_{-\boldsymbol{k}}^{\downarrow}A_{\boldsymbol{p}}^{\downarrow}A_{\boldsymbol{p}'}^{\downarrow}A_{\boldsymbol{q}}^{\downarrow}A_{\boldsymbol{q}'}^{\downarrow}\Big)^T \tag{7.28}$$

[1] The quantities G, R and L are defined in eqs. (3.134), (3.135) and (3.136).

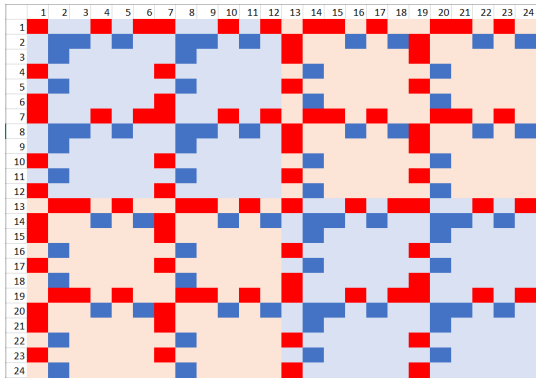

Figure 7.1: The entries of the matrix $M_{\boldsymbol{k}}$ in the SW-phase. The red entries show the matrix elements of the sum over $\boldsymbol{k}$, and the blue entries show the shifted entries of the sum over $-\boldsymbol{k}$

and,

$$\Psi_{\boldsymbol{k}} = \Big(A^{\uparrow}_{\boldsymbol{k}} A^{\uparrow}_{-\boldsymbol{k}} A^{\uparrow}_{\boldsymbol{p}} A^{\uparrow}_{\boldsymbol{p}'} A^{\uparrow}_{\boldsymbol{q}} A^{\uparrow}_{\boldsymbol{q}'} A^{\downarrow}_{\boldsymbol{k}} A^{\downarrow}_{-\boldsymbol{k}} A^{\downarrow}_{\boldsymbol{p}} A^{\downarrow}_{\boldsymbol{p}'} A^{\downarrow}_{\boldsymbol{q}} A^{\downarrow}_{\boldsymbol{q}'} \tag{7.29}$$

$$A^{\uparrow\dagger}_{\boldsymbol{k}} A^{\uparrow\dagger}_{-\boldsymbol{k}} A^{\uparrow\dagger}_{\boldsymbol{p}} A^{\uparrow\dagger}_{\boldsymbol{p}'} A^{\uparrow\dagger}_{\boldsymbol{q}} A^{\uparrow\dagger}_{\boldsymbol{q}'} A^{\downarrow\dagger}_{\boldsymbol{k}} A^{\downarrow\dagger}_{-\boldsymbol{k}} A^{\downarrow\dagger}_{\boldsymbol{p}} A^{\downarrow\dagger}_{\boldsymbol{p}'} A^{\downarrow\dagger}_{\boldsymbol{q}} A^{\downarrow\dagger}_{\boldsymbol{q}'} \Big) \tag{7.30}$$

Forming the quadratic Hamiltonian H_2 as a matrix product $H_2 = \frac{1}{2} \sum_{\boldsymbol{k}} \Psi^{\dagger}_{\boldsymbol{k}} M \Psi_{\boldsymbol{k}}$, we get the pattern outlined in fig. 7.1 for the 24×24 matrix M. The elements on the upper diagonal of the Hermitian submatrix $A(\boldsymbol{k})$ are given by the entries

$$A_{11} = A_{22} = \frac{\eta_{\boldsymbol{k}}^{\uparrow\uparrow}}{2} + 2a^{\uparrow\uparrow} + 2b^{\uparrow\uparrow} + 2b^{\downarrow\uparrow} \tag{7.31}$$

$$A_{14} = A_{23} = \frac{a^{\uparrow\uparrow}}{2} e^{i\delta_{13}^{\uparrow\uparrow}} + \frac{1}{2}\left(b^{\uparrow\uparrow} e^{i\delta_{13}^{\uparrow\uparrow}} + b^{\downarrow\uparrow} e^{i\delta_{13}^{\downarrow\downarrow}}\right) \tag{7.32}$$

$$A_{16} = A_{25} = \frac{a^{\uparrow\uparrow}}{2} e^{i\delta_{31}^{\uparrow\uparrow}} + \frac{1}{2}\left(b^{\uparrow\uparrow} e^{i\delta_{31}^{\uparrow\uparrow}} + b^{\downarrow\uparrow} e^{i\delta_{31}^{\downarrow\downarrow}}\right) \tag{7.33}$$

$$A_{17} = \frac{\eta_{\boldsymbol{k}}^{\uparrow\downarrow}}{2} + \frac{a^{\downarrow\uparrow}}{2}\left(e^{i\delta_{11}^{\downarrow\uparrow}} + e^{i\delta_{33}^{\downarrow\uparrow}}\right) \tag{7.34}$$

$$A_{28} = -\frac{\eta_{\boldsymbol{k}}^{\uparrow\downarrow}}{2} + \frac{a^{\downarrow\uparrow}}{2}\left(e^{i\delta_{11}^{\downarrow\uparrow}} + e^{i\delta_{33}^{\downarrow\uparrow}}\right) \tag{7.35}$$

$$A_{1,10} = A_{29} = \frac{a^{\downarrow\uparrow}}{2} e^{i\delta_{13}^{\downarrow\uparrow}} \tag{7.36}$$

$$A_{1,12} = A_{2,11} = \frac{a^{\downarrow\uparrow}}{2} e^{i\delta_{31}^{\downarrow\uparrow}} \tag{7.37}$$

$$A_{47} = A_{38} = \frac{a^{\uparrow\downarrow}}{2} e^{-i\delta_{13}^{\uparrow\downarrow}} \tag{7.38}$$

$$A_{67} = A_{58} = \frac{a^{\uparrow\downarrow}}{2} e^{-i\delta_{31}^{\uparrow\downarrow}} \tag{7.39}$$

$$A_{77} = A_{88} = \frac{\eta_{\boldsymbol{k}}^{\downarrow\downarrow}}{2} + 2a^{\downarrow\downarrow} + 2b^{\downarrow\downarrow} + 2b^{\uparrow\downarrow} \tag{7.40}$$

$$A_{7,10} = A_{89} = \frac{a^{\downarrow\downarrow}}{2} e^{i\delta_{13}^{\uparrow\uparrow}} + \frac{1}{2}\left(b^{\downarrow\downarrow} e^{i\delta_{13}^{\downarrow\downarrow}} + b^{\uparrow\downarrow} e^{i\delta_{13}^{\uparrow\uparrow}}\right) \tag{7.41}$$

$$A_{7,12} = A_{8,11} = \frac{a^{\downarrow\downarrow}}{2} e^{i\delta_{31}^{\downarrow\downarrow}} + \frac{1}{2}\left(b^{\downarrow\downarrow} e^{i\delta_{31}^{\downarrow\downarrow}} + b^{\uparrow\downarrow} e^{i\delta_{31}^{\uparrow\uparrow}}\right) \tag{7.42}$$

and the elements on the upper diagonal of the symmetric submatrix B is given by

$$B_{1,2} = a^{\uparrow\uparrow} e^{-i\sigma_{13}^{\uparrow\uparrow}} + a^{\uparrow\uparrow} e^{-i\sigma_{31}^{\uparrow\uparrow}} \tag{7.43}$$

$$B_{1,3} = B_{2,4} = \frac{a^{\uparrow\uparrow}}{2} e^{-i\sigma_{11}^{\uparrow\uparrow}} \tag{7.44}$$

$$B_{1,5} = B_{2,6} = \frac{a^{\uparrow\uparrow}}{2} e^{-i\sigma_{33}^{\uparrow\uparrow}} \tag{7.45}$$

$$B_{1,8} = B_{2,7} = \frac{a^{\downarrow\uparrow}}{2} \left(e^{-i\sigma_{13}^{\downarrow\uparrow}} + e^{-i\sigma_{31}^{\downarrow\uparrow}} \right) + \frac{a^{\uparrow\downarrow}}{2} \left(e^{-i\sigma_{13}^{\uparrow\downarrow}} + e^{-i\sigma_{31}^{\uparrow\downarrow}} \right) \tag{7.46}$$

$$B_{1,9} = B_{2,10} = \frac{a^{\downarrow\uparrow}}{2} e^{-i\sigma_{11}^{\downarrow}\uparrow} \tag{7.47}$$

$$B_{1,11} = B_{2,12} = \frac{a^{\downarrow\uparrow}}{2} e^{-i\sigma_{33}^{\downarrow}\uparrow} \tag{7.48}$$

$$B_{3,7} = B_{4,8} = \frac{a^{\uparrow\downarrow}}{2} e^{-i\sigma_{11}^{\uparrow}\downarrow} \tag{7.49}$$

$$B_{5,7} = B_{6,8} = \frac{a^{\uparrow\downarrow}}{2} e^{-i\sigma_{33}^{\uparrow}\downarrow} \tag{7.50}$$

$$B_{7,8} = a^{\downarrow\downarrow} e^{-i\sigma_{13}^{\downarrow\downarrow}} + a^{\downarrow\downarrow} e^{-i\sigma_{31}^{\downarrow\downarrow}} \tag{7.51}$$

$$B_{7,9} = B_{8,10} = \frac{a^{\downarrow\downarrow}}{2} e^{-i\sigma_{11}^{\downarrow\uparrow}} \tag{7.52}$$

$$B_{7,11} = B_{8,12} = \frac{a^{\downarrow\downarrow}}{2} e^{-i\sigma_{33}^{\downarrow\downarrow}} \tag{7.53}$$

Again, the author is unable to find an analytic expression for the eigenvalues of the dynamic matrix D. In addition, the constant terms originating from the delta-function $\delta_{\boldsymbol{k},\boldsymbol{k}'}$ are given by

$$C_2 = \frac{N_s \left(\mu^{\uparrow} + \mu^{\downarrow} \right)}{2} - U \left(N_0^{\uparrow} + N_0^{\downarrow} \right) \left(1 + \frac{\alpha}{2} \right) \tag{7.54}$$

7.3 Numerical determination of the eigenvalues

We assume as in Jansønns master thesis that $N_0^{\uparrow} = N_0^{\downarrow} = N_0/2$, as we get *real* eigenvalues for the dynamic matrix JM with this choice. The expressions for $\mu^{\uparrow}$ and $\mu^{\downarrow}$ thus reduce to (with $f = 2$)

$$\mu^{\uparrow} = \mu^{\downarrow} \equiv \mu = -\epsilon_{\boldsymbol{k}_{01}} - |s_{\boldsymbol{k}_{01}}| + \frac{UN_0}{4N_s} (3 + \alpha) \tag{7.55}$$

Giving the expression for the condensate density

$$\frac{N_0}{N_s} = \frac{4}{U} \frac{\epsilon_{\boldsymbol{k}_{01}} + |s_{\boldsymbol{k}_{01}}| + \mu}{3 + \alpha} \tag{7.56}$$

and the constant Hamiltonian reduces to

$$H_0 = -\frac{UN_0^2}{8N_s} (3 + \alpha) \tag{7.57}$$

Inserting the epxression for the condensate density, and choosing $k_0 = \frac{1}{a}\arctan(\sqrt{2}\lambda_R/2t)$, H_0 becomes

$$H_0 = \frac{-2N_s}{U(3+\alpha)}\left(4t\sqrt{\frac{\lambda_R^2}{2t^2}+1}+\mu\right)^2 \tag{7.58}$$

which agrees with the free energy F_{SW} for the *pure* condensate given in eq. (3.218). The constant C_2 is given by

$$C_2 = N_s\mu - UN_0\left(1+\frac{\alpha}{2}\right) \tag{7.59}$$

In figure 7.3 the eigenvalues λ_i of M is shown. This plot reveals that the coefficient matrix M is indeterminate, since it has $\lambda_i < 0$, $\lambda_i = 0$ *and* $\lambda_i > 0$. This means that we cannot simply choose the positive eigenvalues of JM as the first $n = 12$ entries of the diagonal matrix Ω. We refer the reader to the Dynamic Matrix section. The rule according to eq. (3.170) is to choose the first n eigenvalues in Ω according to the positivity of the norm of the eigenvectors. We must therefore:

1. Calculate the 24 eigenvalues w_μ for each k_x and k_y.
2. Check the norm of the 24 corresponding eigenvectors for each k_x and k_y, note that this norm is defined as (x_μ, Jx_μ) where $(x,y) = \sum_i x_i^* y_i$ is the inner product in $\mathbb{C}^{2n}$. This norm must be finite.
3. Find the 12 eigenvectors positive norm for all k_x and k_y. The most important quantity is the sign of the norm, since the eigenvectors can be scaled arbitrarily.
4. Place the eigenvalues corresponding to these eigenvectors along the first 12 entries in the diagonal matrix Ω.

We must also check that the norms of the eigenvectors are *finite*, and that all the eigenvectors are linearly independent. In fig. 7.4 the plot of the *smallest* norm of all the eigenvalues for each pair (k_x, k_y) is shown, with minimum norm taken over all points equal to $\approx 1.9 \times 10^{-8}$. The distribution of points appears to be random, and most importantly, we have no vanishing norms. In fig. 7.5 the plot over the absolute value of the determinant $|\det(JM_{\boldsymbol{k}})|$ over all the eigenvalues for each pair (k_x, k_y) is shown, with minimum determinant over all points equal to $\approx 4.7 \times 10^{-10}$. If the determinant vanishes, then the eigenvectors of JM are not linearly independent, which they must be. Notice the marked ring with radius $r = k_0$, originating from spin-orbit coupling.

In fig. 7.2 the excitation spectrum for $k_x = k_y$ is shown, with *real* eigenvalues, or at least with a maximum eigenvalue of $\approx 2.4 \times 10^{-15}$. Numerical analysis show that 8 of the eigenvalues are approximately zero, 8 of the eigenvalues are positive with 4 independent branches, and 8 of the eigenvalues are negative with 4 independent branches. The stapled eigenvalues are the ones where the corresponding eigenvectors has a negative norm, and the hard-color lines are the ones with positive $+1$ norm. We can clearly see that if w_i is an eigenvalue, then $-w_i$ is also an eigenvalue. The zoomed in picture shows the excitation spectrum that is not 0, is negative, and has a *positive* $+1$ norm. This means that we must include these negative eigenvalues in the first entries of Ω. The negative eigenvalues are in fact small, and or of order 10^{-3} in fig. 7.2. The vertical lines are placed at $k_x = k_y = \pm k_0$. Notice that the minima of the excitation spectrum is in fact at $k_x = k_y = \pm k_0$, which is what we expect physically. Incidentally, if we had

chosen only positive eigenvalues for the first 12 entries of Ω we would have obtained a minima at $k = 0$. We also see from the zoomed in picture that the minima-branch is not linear around $\pm k_0$, which means no superfluid critical velocity. This is not what we would expect intuitively, as we anticipated the Bogoliubov spectrum at these points. However, we to get two shifted parabolas, which is the effect of spin-orbit coupling, similar to the SOC spectrum in fig. 3.1.

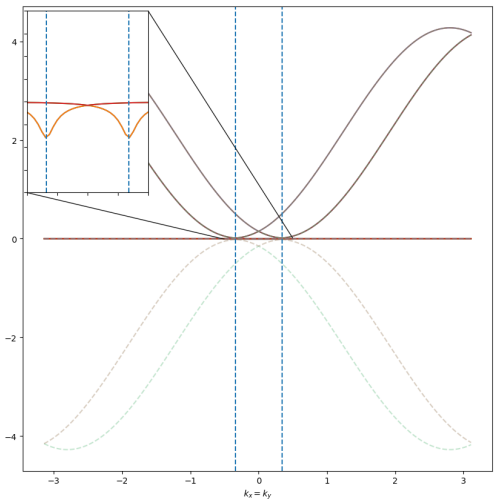

Figure 7.2: The eigenvalues of JM in the SW phase. The physical parameters are $N_x = N_y = 200$, $N_0/N_s = 1$, $\lambda_R = 0.5$, $\alpha = 1.5$ and $U = 0.1$.

From the section on the dynamic matrix method, we expect that we should have 12 eigenvectors with norm $+1$, and 12 eigenvectors with norm -1. For the eigenvalues that are non-zero, we get 8 eigenvectors with norm $+1$ and 8 eigenvectors with norm -1, as expected. We expect then for the zero eigenvalues to get 4 eigenvectors with norm 1 and 4 eigenvectors with norm -1. However, for the approximately zero eigenvalues, we get either. The number of $+1$ norms fluctuates between 0 and 8, and similarly for -1 norms. The reason for this is most probably numerical errors. In reality, no eigenvalue is *exactly* zero. For example, consider the eigenvalue 1.13×10^{-18}, it is highly unlikely that we should also get the eigenvalue -1.13×10^{-18}.

7.4 Free energy for the SW-phase

After making a change of basis from $\Psi_{\boldsymbol{k}}$ to $\phi_{\boldsymbol{k}}$, the quadratic Hamiltonian is given by

$$H_2 = \sum_{\boldsymbol{k}} \sum_{i=1}^{12} w_i(\boldsymbol{k}) \left(d^{i\dagger}_{\boldsymbol{k}} d^i_{\boldsymbol{k}} + \frac{1}{2} \right) \tag{7.60}$$

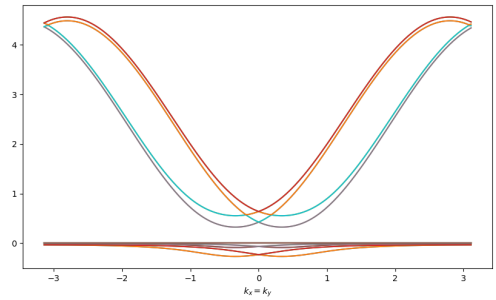

Figure 7.3: The eigenvalues of M in the SW phase. The physical parameters are $N_x = N_y = 200$, $N_0/N_s = 1$, $\lambda_R = 0.5$, $\alpha = 1.5$ and $U = 0.1$.

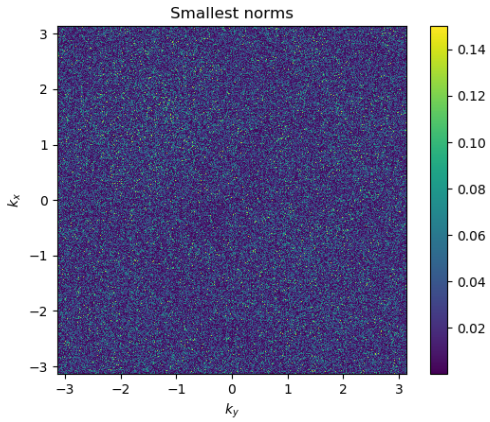

Figure 7.4: The diagram for the smallest norms in the SW phase. Notice the seemingly random distribution of points.

where we have cancelled the 1/2 factor in front of the sum. Here $\phi_{\boldsymbol{k}}$ is given as in eq. (3.160), with components d_i and $d_i^\dagger$, with $i = 1, ..., 12$. The eigenvalues $w_i(\boldsymbol{k})$ are given as follows

$$w_1(\boldsymbol{k}) = w_2(\boldsymbol{k}) = -E_1(\boldsymbol{k}), \quad E_1(\boldsymbol{k}) \geq 0 \tag{7.61}$$
$$w_3(\boldsymbol{k}) = w_4(\boldsymbol{k}) = -E_2(\boldsymbol{k}), \quad E_2(\boldsymbol{k}) \geq E_1(\boldsymbol{k}) \tag{7.62}$$
$$w_5(\boldsymbol{k}) = w_6(\boldsymbol{k}) = E_3(\boldsymbol{k}), \quad E_3(\boldsymbol{k}) \geq 0 \tag{7.63}$$
$$w_7(\boldsymbol{k}) = w_8(\boldsymbol{k}) = E_4(\boldsymbol{k}), \quad E_4(\boldsymbol{k}) \geq 0 \tag{7.64}$$

And the last 4 eigenvalues are approximately equal to zero. Let us neglect these from our calculation, as they give zero contribtution to the Hamiltonian. Consequently, the sum over i goes from 1 to 8. The problem with a quadratic Hamiltonian with negative w's is that we get terms proportional to $-|w|n_i$, where n_i is a number operator. Nature will thus try to maximize

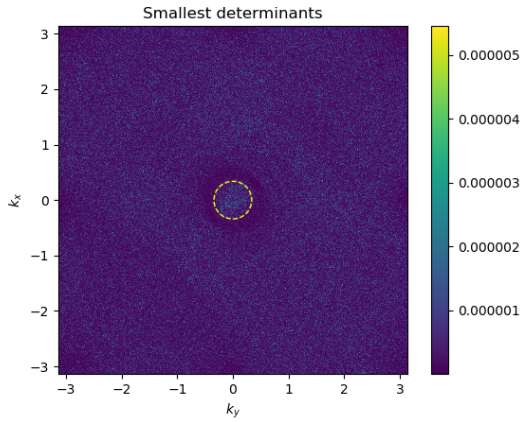

Figure 7.5: The diagram for the smallest determinants in the SW phase. The ring has radius $r = k_0$, which suggest that it is caused by spin-orbit coupling.

n_i, flooding the system. We can however bypass this issue by adding a constant to the quadratic Hamiltonian, considering it as a contribution to the chemical potentials. We shift the branches in the following way

$$w_i(\boldsymbol{k}) = w_i(\boldsymbol{k}) + \lambda - \lambda \tag{7.65}$$

where λ is given by

$$\lambda = |\min_{i,\boldsymbol{k}} w_i(\boldsymbol{k})| \tag{7.66}$$

λ is the absolute value of the smallest value in the excitation spectrum for all $\boldsymbol{k}$ in the 1st Brillouin zone and $i = 1, ..., 12$, which is in our case given by $|w_1(k_0, k_0)|$. Thus the quadratic Hamiltonian becomes

$$H_2 = {\sum_{\boldsymbol{k}}}' \sum_{i=1}^{8} \Lambda_i(\boldsymbol{k}) \left(d_{\boldsymbol{k}}^{i\dagger} d_{\boldsymbol{k}}^{i} + \frac{1}{2} \right) - \lambda \sum_{i=1}^{8} \left(N_i + \frac{1}{2} \right) \tag{7.67}$$

We have defined $\Lambda_i(\boldsymbol{k}) = w_i(\boldsymbol{k}) + \lambda$, and the primed sum over $\boldsymbol{k}$ means that we avoid all $\boldsymbol{k}$ for which $\lambda_{\boldsymbol{k}} = 0$. The number $N_i = \sum_{\boldsymbol{k}} d_{\boldsymbol{k}}^{i\dagger} d_{\boldsymbol{k}}^{i}$ is the total number of pseudo-particles with number i in the system. This will be assumed to be small, as ground state depletion is assumed to be negligible. In addition, λ is in this case also small. The free energy is thus given by

$$F = H_0' - \lambda \sum_{i=1}^{8} \left(N_i + \frac{1}{2} \right) + \frac{1}{2} {\sum_{\boldsymbol{k}}}' \sum_{i=1}^{8} \Lambda_i(\boldsymbol{k}) + \frac{1}{\beta} {\sum_{\boldsymbol{k}}}' \sum_{i=1}^{8} \ln \left(1 - e^{-2\beta \Lambda_i(\boldsymbol{k})} \right) \tag{7.68}$$

where β is the inverse temperature, and $H_0' = H_0 + C_2$.

7.4.1 Metroplis Hastings results for the SW phase

We use the Metropolis Hastings algorithm described in sec. 3.5.1 to determine the variational parameters k_0, $\theta_1^{\downarrow}$ and $\theta_3^{\downarrow}$. The parameters $\theta_1^{\uparrow}$ and $\theta_3^{\uparrow}$ are functions of $\theta_1^{\downarrow}$ and $\theta_3^{\downarrow}$, given by eq.

(3.104). The starting configuration was $\Psi_0 = [\theta_1^{\downarrow}, \theta_3^{\downarrow}, k_0] = [0, 0, \pi]$.

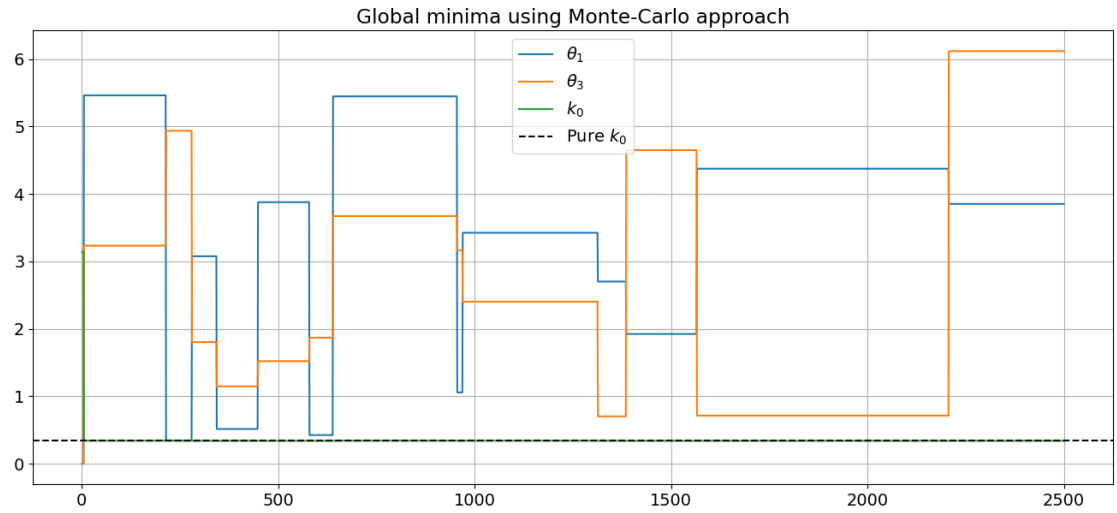

Figure 7.6: The Metropolis algorithm results applied on the SW-phase. The physical parameters are $U = 0.1$, $\lambda_R = 0.5$ and $\alpha = 1.5$. The x-axis labels the number of iterations. The blue line (top) shows the value for $\theta_1^{\downarrow}$, the orange line (middle) shows the value for $\theta_3^{\downarrow}$ and the bottom line shows the value for k_0. The stapled black line shows the value for k_0 as given in the pure condensate by eq. (3.214). Note that the configuration of $(\theta_1^{\downarrow}, \theta_3^{\downarrow})$ seems to be random, while k_0 seems to converge to the pure k_0. The axis gives the value for the mean-field parameters, for every 10th iteration.

The algorithm used 2500 iterations for each of the 10 sweeps. Also, if the excitation spectrum was imaginary, the free energy was automatically set to a NaN value, which limited the phase space available. The θ-parameters were allowed to explore values in $[0, 2\pi)$, while k_0 was allowed to explore to the end of the positive 1st Brillouin zone $[0, \pi)$. In fig. 7.6 we see that the estimated k_0 value is close to the pure k_0 value, as given in eq. (3.214), even with the starting value at π. It would be an advantage if we could use the explicit expression for k_0, as then we could use the explicit expressions for the condensate density N_0/N_s for the pure phases, to later construct a phase diagram where the free energy is a function of (α, λ_R). If not, we would have to do the metropolis algorithm on every point in (α, λ_R) space, to find k_0 as a function of (α, λ_R). This would take a lot of time, as for each point in (α, λ_R) we would have to calculate the excitation spectrum for the entire 1st Brilloiun zone, and sum them together to find the free energy. The Metropolis algorithm for *one* point in (α, λ_R) space is in addition very time-consuming, as one should enshure that the algorithm is *ergodic*, that is, one should be able to find the global minimum from any point in phase space. The final configuration was found to be $\Psi \approx [3.85, 6.12, 0.34]$. We see from fig. 7.7 that the free energy reaches a minima as the number of iterations increases. The effect of the random number r[2] can also be observed, as the free energy increases at a given number of iterations. Also, comparing fig. 7.6 with fig. 7.7, we see

[2]For an explanation of the r-value, see section 3.5.1

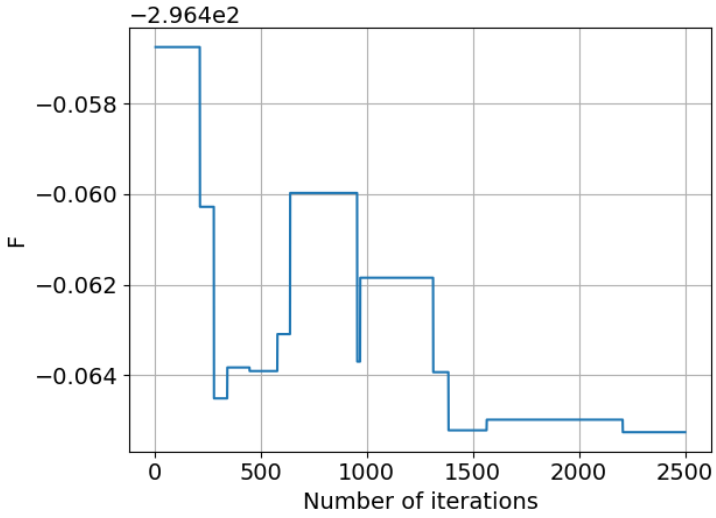

Figure 7.7: The free energy as a function number of iterations for the Metroplis algorithm. The y-axis is the free energy, while the x-axis is the number of iterations. The physical parameters are the same as in fig. 7.6. Notice the jumps in the free energy, this is caused by the r factor in the Metropolis algorithm, to avoid getting stuck in a local minima.

that the free energy is maybe independent of the mean-field angles. Furthermore, the values of these angles seem to be somewhat random, as seen in fig. 7.6, where they do not converge to a specific value. Note that even though the free energy changes as the angles change, this does not imply that they are dependent, as the r value can in principle accept *any* configuration of $(\theta^{\uparrow}, \theta^{\downarrow})$. We for the rest of the thesis assume that k_0 take the value as in the pure condensate. In addition, k_0 as given by the pure condensate was shown to be the minimum of the excitation spectrum for at least one value of $(\alpha, \lambda_R) = (1.5, 0.5)$, see fig. 7.2, strengthening the claim that this is in fact the correct value which minimizes the free energy.

7.5 Phase diagram for the PZ, PW and SW phases

The phases which have shown to have real eigenvalues for many parameters of (α, λ_R) are the PZ, PW and SW phases. We have neglected the term $\lambda \sum_i (N_i + 1/2)$, as λ is of order 10^{-3} and the number of excited bosons N_i cannot be to big, in order to avoid severe ground state depletion. Also, the free energy was set to NaN if the imaginary part of the eigenvalues was larger than 10^{-9}. In fig. 7.8 the phase diagram is shown. We have used the value for k_0 which minimizes the free energy in the *pure* condensate PW and SW phases. The phase diagram is generated by varying N_0, and keeping μ constant. The expressions for the condensate densities for the PZ, PW and SW phases are given in eqs. This is in order to see the effect of spin-orbit coupling on the system. One could accordingly keep N_0 constant, and vary μ instead. This would create a different phase diagram, especially for the pure condensate, as the constant

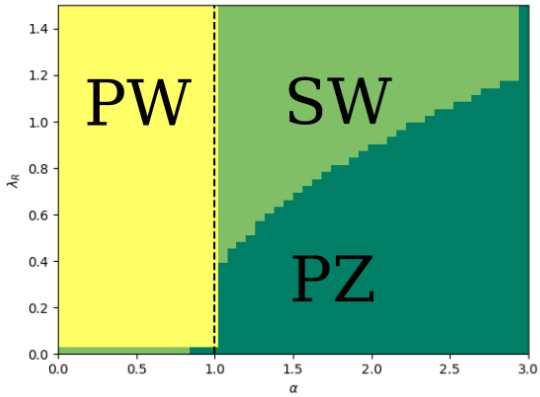

Figure 7.8: Phase diagram for the PZ, PW and SW phases with excitations. The physical parameters are $U = 0.1$, $t = 1$ and $\mu = 1$

terms for all the phases are only dependent on N_0, α and U. Keeping N_0 constant would then create a phase diagram dependent on α and U. Let us also compare this phase diagram with

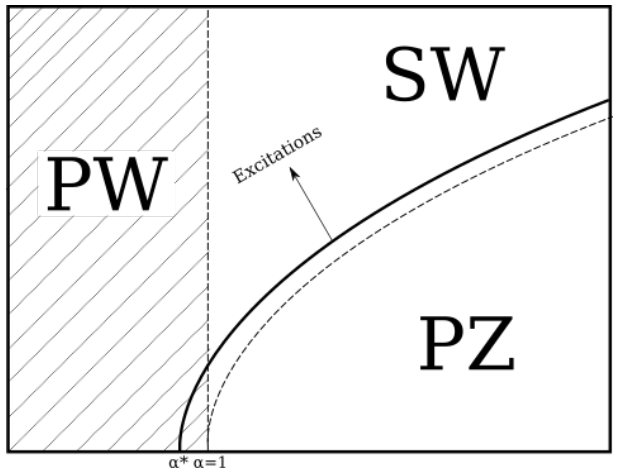

Figure 7.9: A sketch of the process of turning on interactions. Based on the pure phase diagram in fig. 3.4 and the interacting phase diagram in fig. 7.8.

the one obtained from the pure condensate given in fig. 3.4, which has the same values for the physical parameters. It is reassuring that all phases are at the same location in (α, λ_R) space. Also, it would appear that the line seperating the SW and PZ phase has moved to the left. See the sketch in fig. 7.9. The line at $\alpha = 1$ seperating the PW from the SW phase is still there, and one could imagine the curve seperating the SW and PZ phases to intersect at a new point α^* on the α-axis. In terms of the interaction strength $U^{\alpha\beta}$, the condition seperating the SW

and phases is $U^{\uparrow\downarrow} > U$, which agrees with the literature.

Thus, introducing interactions seems to give the PZ phase more room in phase space. This may be due to the fact that including excitations causes more energetic scattering at a finite $\boldsymbol{k}$-vector, in stead of scattering with the zero momentum vector.

Chapter 8

The LW-phase

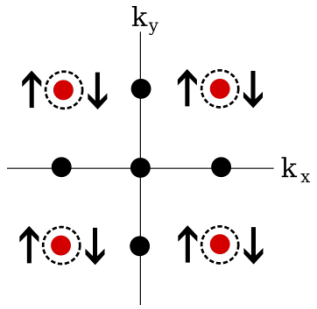

This is the final phase we will encounter, and was previously abandoned by Jansønn. For this phase we have four condensate momenta $\boldsymbol{k}_{01}$, $\boldsymbol{k}_{02}$, $\boldsymbol{k}_{03}$ and $\boldsymbol{k}_{04}$. We will derive the equations for the condensate densities, and find the peculiar result that when $N_0^{\uparrow} = N_0^{\downarrow}$ the chemical potentials are unequal, $\mu^{\uparrow} \neq \mu^{\downarrow}$. We shall also calculate the free energy for the *pure* LW phase, where we find that it has no impact on the phase diagram shown in fig. 3.5.

8.1 Constraints on variational parameters

We now have in principle $8+1 = 9$ variational parameters. There is the length of the condensate momentum $\boldsymbol{k}_{0i}$, given by k_0, and there's the order parameters θ_i^{α}, where $i \in (1, 2, 3, 4)$ and $\alpha \in (\uparrow, \downarrow)$. For the imaginary part of the chemical potential for $\mu^{\uparrow}$ and $\mu^{\downarrow}$ to be zero, we have in total three equations, given by eqs. (3.104), (3.105) and (3.109). The first constraint is caused by the SOC-term, and *halves* the number of order parameters to be determined. This leads to

j	Momentum conservation	Allowed configurations (j, i', j')
$j=1$	$\boldsymbol{k}_{01}+\boldsymbol{k}_{01}=\boldsymbol{k}_{0i'}+\boldsymbol{k}_{0j'}$	$(1,1,1)$
$j=2$	$\boldsymbol{k}_{01}+\boldsymbol{k}_{02}=\boldsymbol{k}_{0i'}+\boldsymbol{k}_{0j'}$	$(2,1,2)$, $(2,2,1)$
$j=3$	$\boldsymbol{k}_{01}+\boldsymbol{k}_{03}=\boldsymbol{k}_{0i'}+\boldsymbol{k}_{0j'}$	$(3,1,3)$, $(3,3,1)$, $(3,2,4)$, $(3,4,2)$
$j=4$	$\boldsymbol{k}_{01}+\boldsymbol{k}_{04}=\boldsymbol{k}_{0i'}+\boldsymbol{k}_{0j'}$	$(4,1,4)$, $(4,4,1)$

Table 8.1: Allowed configurations in the sum for the chemical potentials

four constraints

$$\delta\theta_1 = \gamma_1 - \pi \tag{8.1}$$
$$\delta\theta_2 = \gamma_2 - \pi \tag{8.2}$$
$$\delta\theta_3 = \gamma_3 - \pi \tag{8.3}$$
$$\delta\theta_4 = \gamma_4 - \pi \tag{8.4}$$

These constraints makes it possible to express all mean-field $\uparrow$ parameters in terms of the mean-field $\downarrow$ parameters. The γ's are given by

$$s_{\boldsymbol{k}_{01}} \propto -(1+i), \quad \gamma_1 = -\frac{5\pi}{4} \tag{8.5}$$
$$s_{\boldsymbol{k}_{02}} \propto -(1+i), \quad \gamma_2 = -\frac{3\pi}{4} \tag{8.6}$$
$$s_{\boldsymbol{k}_{03}} \propto -(1+i), \quad \gamma_3 = -\frac{\pi}{4} \tag{8.7}$$
$$s_{\boldsymbol{k}_{04}} \propto -(1+i), \quad \gamma_4 = -\frac{7\pi}{4} \tag{8.8}$$

The two next constraints pertains to each pseudo-spin induvidually, and assures that the imaginary part of the interaction term for the associated chemical potential is zero. For $\mu^{\uparrow}$, the constraint is given by eq. (3.105), and can be simplified to

$$\sum_{ji'j'}\sum_{\alpha}\frac{U^{\alpha\uparrow}N_0^{\alpha}}{N_s f}\sin\left(\theta_{j'}^{\uparrow}-\theta_1^{\uparrow}-\theta_j^{\alpha}+\theta_{i'}^{\alpha}\right)\delta_{i+j,i'+j'}=0 \tag{8.9}$$

where we have used that $N_l^{\uparrow}=N_0^{\uparrow}/f$ and $N_l^{\downarrow}=N_0^{\downarrow}/f$, and chosen $i=1$. The permissable momentum indices are thus $(j,i',j')\in(1,2,3,4)$, and pseudo-spin indices $\alpha\in(\uparrow,\downarrow)$. IN addition, momentum conservation restricts the momentum indices further to the values given in table 8.1. Thus the expression in eq. (8.9) can be simplified to

$$\sum_{\alpha}\frac{U^{\alpha\uparrow}N_0^{\alpha}}{N_s f}S^{\alpha}=0 \tag{8.10}$$

with S^α defined as

$$\begin{aligned} S^\alpha =& \sin\left(\theta_2^\uparrow - \theta_2^\alpha - \left(\theta_1^\uparrow - \theta_1^\alpha\right)\right) && (8.11)\\ &+ \sin\left(\theta_3^\uparrow - \theta_3^\alpha - \left(\theta_1^\uparrow - \theta_1^\alpha\right)\right) && (8.12)\\ &+ \sin\left(\theta_4^\uparrow - \theta_4^\alpha - \left(\theta_1^\uparrow - \theta_1^\alpha\right)\right) && (8.13)\\ &+ \sin\left(\theta_4^\uparrow - \theta_1^\uparrow - \theta_3^\alpha + \theta_2^\alpha\right) && (8.14)\\ &+ \sin\left(\theta_2^\uparrow - \theta_1^\uparrow - \theta_3^\alpha + \theta_4^\alpha\right) && (8.15) \end{aligned}$$

The possible values for S^α are

$$\begin{aligned} S^\uparrow =& 2\sin\left(\theta_4^\uparrow - \theta_1^\uparrow - \theta_3^\uparrow + \theta_2^\uparrow\right) && (8.16)\\ S^\downarrow =& \sin\left(\gamma_2 - \gamma_1\right) && (8.17)\\ &+ \sin\left(\gamma_3 - \gamma_1\right) && (8.18)\\ &+ \sin\left(\gamma_4 - \gamma_1\right) && (8.19)\\ &+ \sin\left(\theta_4^\uparrow - \theta_1^\uparrow - \theta_3^\downarrow + \theta_2^\downarrow\right) && (8.20)\\ &+ \sin\left(\theta_2^\uparrow - \theta_1^\uparrow - \theta_3^\downarrow + \theta_4^\downarrow\right) && (8.21) \end{aligned}$$

where we have used that $\delta\theta_i - \delta\theta_j = \gamma_i - \gamma_j$. In addition,

$$\begin{aligned} \sin(\gamma_2 - \gamma_1) =& 1 && (8.22)\\ \sin(\gamma_3 - \gamma_1) =& 0 && (8.23)\\ \sin(\gamma_4 - \gamma_1) =& -1 && (8.24) \end{aligned}$$

such that

$$\begin{aligned} S^\downarrow =& \sin\left(\theta_4^\uparrow - \theta_1^\uparrow - \theta_3^\downarrow + \theta_2^\downarrow\right) && (8.25)\\ &+ \sin\left(\theta_2^\uparrow - \theta_1^\uparrow - \theta_3^\downarrow + \theta_4^\downarrow\right) && (8.26) \end{aligned}$$

Next, we express the pseudo-spin up order parameters in terms of the pseudo-spin down order parameters, using $\theta_i^\uparrow = \theta_i^\downarrow + \gamma_i - \pi$. This gives us the simplifications

$$\begin{aligned} \theta_4^\uparrow - \theta_1^\uparrow - \theta_3^\downarrow + \theta_2^\downarrow =& \theta_4^\downarrow - \theta_1^\downarrow - \theta_3^\downarrow + \theta_2^\downarrow + (\gamma_4 - \gamma_1) = \Sigma^\downarrow + (\gamma_4 - \gamma_1) && (8.27)\\ \theta_2^\uparrow - \theta_1^\uparrow - \theta_3^\downarrow + \theta_4^\downarrow =& \theta_2^\downarrow - \theta_1^\downarrow - \theta_3^\downarrow + \theta_4^\downarrow + (\gamma_2 - \gamma_1) = \Sigma^\downarrow + (\gamma_2 - \gamma_1) && (8.28) \end{aligned}$$

The value for $S^\downarrow$ therefore becomes

$$\begin{aligned} S^\downarrow =& \sin\left(\Sigma^\downarrow + (\gamma_4 - \gamma_1)\right) + \sin\left(\Sigma^\downarrow + (\gamma_2 - \gamma_1)\right) && (8.29)\\ =& \cos\left(\Sigma^\downarrow\right)\sin(\gamma_4 - \gamma_1) + \sin\left(\Sigma^\downarrow\right)\cos(\gamma_4 - \gamma_1) && (8.30)\\ &+ \cos\left(\Sigma^\downarrow\right)\sin(\gamma_2 - \gamma_1) + \sin\left(\Sigma^\downarrow\right)\cos(\gamma_2 - \gamma_1) && (8.31)\\ =& \cos\left(\Sigma^\downarrow\right) - \cos\left(\Sigma^\downarrow\right) = 0 && (8.32) \end{aligned}$$

So, in fact, $S^{\downarrow} = 0$. Thus, for the imaginary part of the chemical potential for the pseudo-spin up component to be zero, we get the additional constraint

$$S^{\uparrow} = 2\sin\left(\theta_4^{\uparrow} - \theta_1^{\uparrow} - \theta_3^{\uparrow} + \theta_2^{\uparrow}\right) = 0 \tag{8.33}$$

$$\rightarrow \theta_4^{\uparrow} - \theta_1^{\uparrow} - \theta_3^{\uparrow} + \theta_2^{\uparrow} = m^{\uparrow}\pi, \quad m^{\uparrow} \in (0,1) \tag{8.34}$$

This is an important relation, reducing the number of independent pseudo-spin up mean-field parameters from four to three

$$\theta_4^{\uparrow} - \theta_1^{\uparrow} - \theta_3^{\uparrow} + \theta_2^{\uparrow} = m^{\uparrow}\pi, \quad m^{\uparrow} \in (0,1) \tag{8.35}$$

Now we turn to the pseudo-spin down chemical potential. For the imaginary part of the interaction term for $\mu^{\downarrow}$ to be zero, we have the analogous equation given in eq. (3.109). Following the exact same procedure as for $\mu^{\uparrow}$, we obtain the constraint on the pseudo-spin down order parameters

$$\theta_4^{\downarrow} - \theta_1^{\downarrow} - \theta_3^{\downarrow} + \theta_2^{\downarrow} = m^{\downarrow}\pi, \quad m^{\downarrow} \in (0,1) \tag{8.36}$$

Next we derive the relationship between $m^{\uparrow}$ and $m^{\downarrow}$, originating from a finite spin-orbit coupling in the condensate momentum

$$m^{\uparrow}\pi = \theta_4^{\uparrow} - \theta_1^{\uparrow} - \theta_3^{\uparrow} + \theta_2^{\uparrow} \tag{8.37}$$

$$= \theta_4^{\downarrow} - \theta_1^{\downarrow} - \theta_3^{\downarrow} + \theta_2^{\downarrow} + (\gamma_4 - \gamma_1) - (\gamma_3 - \gamma_2) \tag{8.38}$$

$$= m^{\downarrow}\pi - \frac{\pi}{2} - \frac{\pi}{2} \tag{8.39}$$

$$= m^{\downarrow}\pi - \pi \tag{8.40}$$

$$= (m^{\downarrow} - 1)\pi \tag{8.41}$$

Such that we get the peculiar relation between $m^{\uparrow}$ and $m^{\downarrow}$:

$$\boxed{m^{\uparrow} = m^{\downarrow} - 1 \mod 2} \tag{8.42}$$

In summary, to keep the chemical potentials real, we get the following constraints:

- The equations in eq. (8.1)-(8.4), halving the number of order parameters to be determined. This is a finite spin-orbit coupling effect.
- Equation (8.35) determining one pseudo-spin *up* order parameter
- Equation (8.36) determining one pseudo-spin *down* order parameter
- Equation (8.42) relating the binary numbers $m^{\uparrow}$ and $m^{\downarrow}$.

Exceptions to the condensate solutions

As mentioned in the preliminaries, the solution $N_l^{\uparrow} = N_0^{\uparrow}/f$ and $N_{l'}^{\downarrow} = N_0^{\downarrow}/f$ is not unique if $\alpha = 1$ in general, or for our purpose if

$$\frac{\alpha^2 \cos(\gamma_{l'} - \gamma_l)^2}{U^2(1-A)(1-B)} = 1 \tag{8.43}$$

where $\boldsymbol{k}_{0l}$ and $\boldsymbol{k}_{0l'}$ are non-parallel condensate momentum. Let us choose $l = 1$ and $l' = 2$. We then get $\cos(\gamma_2 - \gamma_1) = 0$, which is not unity. We must also check that the denominator is non-zero

$$A = 2\cos(\theta_4^\uparrow - \theta_1^\uparrow - \theta_3^\uparrow + \theta_2^\uparrow) = 2\cos(m^\uparrow \pi) = \pm 2 \tag{8.44}$$

so $1 - A$ is non-zero. B is given by

$$B = 2\cos\left(\theta_4^\uparrow - \theta_1^\uparrow - \theta_3^\downarrow + \theta_2^\downarrow\right) \tag{8.45}$$

$$= 2\cos\left(\theta_4^\downarrow - \theta_1^\downarrow - \theta_3^\downarrow + \theta_2^\downarrow + (\gamma_4 - \gamma_1)\right) \tag{8.46}$$

$$= 2\left(\cos(m^\downarrow \pi)\cos(\gamma_4 - \gamma_1) - \sin(m^\downarrow \pi)\sin(\gamma_4 - \gamma_1)\right) = 0 \tag{8.47}$$

where we have used that $\cos(\gamma_4 - \gamma_1) = 0$ and $\sin(m^\downarrow \pi) = 0$. Consequently, the denominator is well defined, and the uniqueness of $N_l^\uparrow = N_0^\uparrow / f$ and $N_{l'}^\downarrow = N_0^\downarrow / f$ is consistent.

8.2 Chemical potentials and condensate densities for the LW phase

The chemical potential for the pseudo-spin up component is given by eq. (3.118), where the primed sum in the interaction term permits the indices $\alpha \in (\uparrow, \downarrow)$ and $(j, i', j') \in (1, 2, 3, 4)$. The interaction term is given by (where we choose $\boldsymbol{k}_{0i} = \boldsymbol{k}_{01}$)

$$\mu_{\text{int}}^\uparrow = \sum_{ji'j'} \sum_\alpha \frac{U^{\alpha\uparrow} N_0^\alpha}{N_s f} \cos\left(\theta_{j'}^\uparrow - \theta_1^\uparrow - \theta_j^\alpha + \theta_{i'}^\alpha\right) \delta_{i+j, i'+j'} \tag{8.48}$$

Conservation of momentum gives the same indices (j, i', j') as in table 8.1. Thus we can write

$$\mu_{\text{int}}^\uparrow = \sum_\alpha \frac{U^{\alpha\uparrow} N_0^\alpha}{N_s f} C^\alpha \tag{8.49}$$

where C^α is given by

$$C^\alpha = 4 + \cos\left(\theta_2^\uparrow - \theta_2^\alpha - \left(\theta_1^\uparrow - \theta_1^\alpha\right)\right) \tag{8.50}$$

$$+ \cos\left(\theta_3^\uparrow - \theta_3^\alpha - \left(\theta_1^\uparrow - \theta_1^\alpha\right)\right) \tag{8.51}$$

$$+ \cos\left(\theta_4^\uparrow - \theta_4^\alpha - \left(\theta_1^\uparrow - \theta_1^\alpha\right)\right) \tag{8.52}$$

$$+ \cos\left(\theta_4^\uparrow - \theta_1^\uparrow - \theta_3^\alpha + \theta_2^\alpha\right) \tag{8.53}$$

$$+ \cos\left(\theta_2^\uparrow - \theta_1^\uparrow - \theta_3^\alpha + \theta_4^\alpha\right) \tag{8.54}$$

The possible values for C^α are

$$C^\uparrow = 7 + 2\cos\left(\theta_4^\uparrow - \theta_1^\uparrow - \theta_3^\uparrow + \theta_2^\uparrow\right) \tag{8.55}$$

$$= 7 + 2\cos(m^\uparrow \pi) \tag{8.56}$$

and,

$$C^{\downarrow} = 4 + \cos(\gamma_2 - \gamma_1) \tag{8.57}$$
$$+ \cos(\gamma_3 - \gamma_1) \tag{8.58}$$
$$+ \cos(\gamma_4 - \gamma_1) \tag{8.59}$$
$$+ \cos\left(m^{\downarrow}\pi + (\gamma_4 - \gamma_1)\right) \tag{8.60}$$
$$+ \cos\left(m^{\downarrow}\pi + (\gamma_2 - \gamma_1)\right) \tag{8.61}$$

Next we use that $\cos(\gamma_2 - \gamma_1) = \cos(\gamma_4 - \gamma_1) = \sin(m^{\downarrow}\pi) = 0$ and $\cos(\gamma_3 - \gamma_1) = -1$ to obtain

$$C^{\downarrow} = 3 \tag{8.62}$$

which is a cute result. Thus the interaction term in $\mu^{\uparrow}$ becomes

$$\mu^{\uparrow}_{\text{int}} = \sum_{\alpha} \frac{U^{\alpha\uparrow}}{N_s f} C^{\alpha} \tag{8.63}$$
$$= \frac{UN_0^{\uparrow}}{N_s f}\left(7 + 2\cos(m^{\uparrow}\pi)\right) + \frac{3\alpha U N_0^{\downarrow}}{N_s f} \tag{8.64}$$

Hence, the expression for $\mu^{\uparrow}$ is

$$\mu^{\uparrow} = -4t\cos(k_0 a) - |s_1|\sqrt{\frac{N_0^{\downarrow}}{N_0^{\uparrow}}} \tag{8.65}$$
$$+ \frac{UN_0^{\uparrow}}{N_s f}\left(7 + 2\cos(m\pi)\right) + \frac{3\alpha U N_0^{\downarrow}}{N_s f} \tag{8.66}$$

where we have defined $m^{\uparrow} \equiv m \in (0, 1)$. Doing the excact same calculations for $\mu^{\downarrow}$ yields the analogous result

$$\mu^{\downarrow} = -4t\cos(k_0 a) - |s_1|\sqrt{\frac{N_0^{\uparrow}}{N_0^{\downarrow}}} \tag{8.67}$$
$$+ \frac{UN_0^{\downarrow}}{N_s f}\left(7 - 2\cos(m\pi)\right) + \frac{3\alpha U N_0^{\uparrow}}{N_s f} \tag{8.68}$$

We have used eq. (8.42) to express $m^{\downarrow}$ in terms of m, where the term proportional to $N_0^{\downarrow}$ in $\mu^{\downarrow}$ originally was $7 + 2\cos(m^{\downarrow}\pi)$. Now, Janssønns [32] reason for abandoning the LW phase was due to the fact that if you insist $\mu^{\uparrow} = \mu^{\downarrow}$ *and* $N_0^{\uparrow} = N_0^{\downarrow}$ (which makes physical sense), you get an inconsistensy

$$7 + 2\cos(m\pi) = 7 - 2\cos(m\pi) \tag{8.69}$$

giving $2 = -2$, which is impossible. Now, one has two options. One can either assume that $N_0^{\uparrow} = N_0^{\downarrow}$, and find an equation for the *difference* in the chemical potentials, or one can find a general expression for $N_0^{\uparrow}$ and $N_0^{\downarrow}$ as a function of $\mu^{\uparrow}$ and $\mu^{\downarrow}$. We will start with the first. Defining $N_0^{\uparrow} = N_0^{\downarrow} = N_0/2$, and taking the difference $\delta\mu \equiv \mu^{\uparrow} - \mu^{\downarrow}$, we get (with $f = 4$)

$$\delta\mu = \frac{UN_0}{2N_s}\cos(m\pi) \tag{8.70}$$

This shows that even if you insist that the condensate particle numbers are equal, you get a difference in chemical potentials, proportional to the condensate density and the intra-potential scattering strength. The physical interpretation of this is that the diagonalized Hamiltonian, where the helicity angle γ_i are well defined for the condensate bosons, can have a ... (this is still difficult to interpret). Notice that the value of $m \in (0,1)$ chooses a "direction" for $\mu^\uparrow$ and $\mu^\downarrow$. If $m = 0$, we get $\mu^\uparrow > \mu^\downarrow$, and if $m = 1$, we get $\mu^\downarrow > \mu^\uparrow$. We next insist that $N_0^\uparrow$ and $N_0^\downarrow$ in principle can be different. We, as in the PW and SW phases, introduce the quantities $x \propto \sqrt{N_0^\uparrow} > 0$ and $y \propto \sqrt{N_0^\downarrow} > 0$, as follows

$$x = \sqrt{\frac{U}{N_s f}}\sqrt{N_0^\uparrow}, \quad y = \sqrt{\frac{U}{N_s f}}\sqrt{N_0^\downarrow} \tag{8.71}$$

leading to the coupled set of third-degree equations for x and y

$$(7 + 2\cos(m\pi))x^3 + 3\alpha y^2 x - |s_1|y - (\mu^\uparrow + 4t\cos(k_0 a))x = 0 \tag{8.72}$$

$$(7 - 2\cos(m\pi))y^3 + 3\alpha x^2 y - |s_1|x - (\mu^\downarrow + 4t\cos(k_0 a))y = 0 \tag{8.73}$$

Which is the same type of system of equations as in the PW and SW phases as well. The difference is that the prefactor in front of x^3 and y^3 are different, either 9 or 5. The solution to the above system of equations for $N_0^\uparrow$ and $N_0^\downarrow$ was found numerically with $m = 0$, and is given in fig. 8.1. Note that $\mu^\uparrow$ and $\mu^\downarrow$ are input parameters, with $\mu^\uparrow = 1$. We see that for $\delta = 0$, x and y are not linearly dependent, as was the case for the other phases. However, we see that x is still an increasing function of δ, and y is a decreasing function of δ. Thus the chemical potentials can still be thought of as regulating the average number of particles in the system.

8.3 Constant Hamiltonian

The constant Hamiltonian is given by eq. (3.122), where $(i, j, i', j') \in (1, 2, 3, 4)$ and $(\alpha, \beta) \in (\uparrow, \downarrow)$. Momentum conservation further gives the possible configurations (i, j, i', j') as

$$(1,1,1,1), (1,2,1,2), (1,2,2,1) \tag{8.74}$$

$$(1,3,1,3), (1,3,3,1), (1,3,2,4) \tag{8.75}$$

$$(1,3,4,2), (1,4,1,4), (1,4,4,1) \tag{8.76}$$

$$+(1 \leftrightarrow 2, 3 \leftrightarrow 4) \tag{8.77}$$

$$+(1 \leftrightarrow 3, 2 \leftrightarrow 4) \tag{8.78}$$

$$+(1 \leftrightarrow 4, 2 \leftrightarrow 3) \tag{8.79}$$

The notation $(i \leftrightarrow j, l \leftrightarrow m)$ means add the previous calculation, with the indices interchanged. The constant Hamiltonian is given by

$$H_0 = -\frac{1}{2N_s f^2}\sum_{\alpha\beta} U^{\alpha\beta} N_0^\alpha N_0^\beta C^{\alpha\beta} \tag{8.80}$$

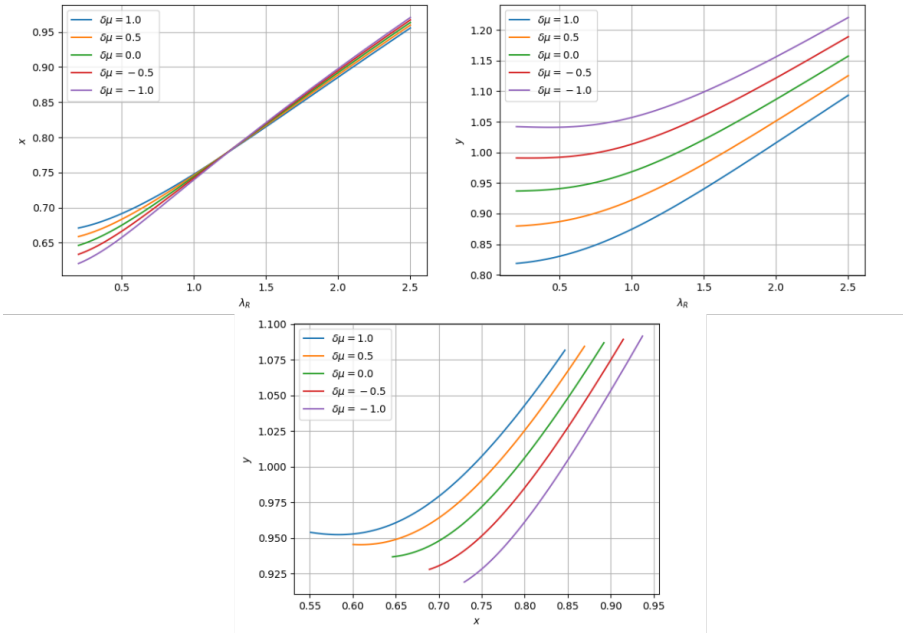

Figure 8.1: Plots of the solutions for $x \propto \sqrt{N_0^{\uparrow}}$ and $y \propto \sqrt{N_0^{\downarrow}}$ for the LW phase. From left to right: plot of $x(\lambda_R)$, plot of $y(\lambda_R)$. The bottom plot is the simultaneous solutions for x and y.

where $C^{\alpha\beta}$ is defined as

$$C^{\alpha\beta} = 4 + \cos\left(\delta_{22}^{\alpha\beta} - \delta_{11}^{\alpha\beta}\right) + \cos\left(\delta_{33}^{\alpha\beta} - \delta_{11}^{\alpha\beta}\right) + \cos\left(\delta_{44}^{\alpha\beta} - \delta_{11}^{\alpha\beta}\right) \tag{8.81}$$

$$+ \cos\left(\theta_4^{\alpha} - \theta_1^{\alpha} - \theta_3^{\beta} + \theta_2^{\beta}\right) + \cos\left(\theta_2^{\alpha} - \theta_1^{\alpha} - \theta_3^{\beta} + \theta_4^{\beta}\right) \tag{8.82}$$

$$+ (1 \leftrightarrow 2, 3 \leftrightarrow 4) + (1 \leftrightarrow 3, 2 \leftrightarrow 4) + (1 \leftrightarrow 4, 2 \leftrightarrow 3) \tag{8.83}$$

and takes the values

$$C^{\uparrow\uparrow} = 4 \times (7 + 2\cos(m\pi)) \tag{8.84}$$

$$C^{\uparrow\downarrow} = 4 \times 3 \tag{8.85}$$

$$C^{\downarrow\uparrow} = 4 \times 3 \tag{8.86}$$

$$C^{\downarrow\downarrow} = 4 \times (7 - 2\cos(m\pi)) \tag{8.87}$$

giving the expression for the constant Hamiltonian

$$H_0 = -\frac{2U}{N_s f^2}\left((7 + 2\cos(m\pi))N_0^{\uparrow 2} + 6\alpha N_0^{\uparrow} N_0^{\downarrow} + (7 - 2\cos(m\pi))N_0^{\downarrow 2}\right) \tag{8.88}$$

It is interesting that when $N_0^{\uparrow} = N_0^{\downarrow}$, the term with $m \in (0, 1)$ disappears.

8.4 Quadratic Hamiltonian

The first and second primed sum in the interaction Hamiltonian are no longer constrained, giving the expression

$$H_{\text{int}} = \sum_{\boldsymbol{k}} G_{\boldsymbol{k}} + R_{\boldsymbol{k}} + L_{\boldsymbol{k}} \tag{8.89}$$

where $G_{\boldsymbol{k}}$ is a sum over all G_{ij}

$$\begin{aligned}
G_{\boldsymbol{k}} &= G_{11}(\boldsymbol{k}, \boldsymbol{q}_1) + G_{12}(\boldsymbol{k}, \boldsymbol{p}_1) + G_{13}(\boldsymbol{k}, -\boldsymbol{k}) + G_{14}(\boldsymbol{k}, \boldsymbol{p}_4) && (8.90)\\
&+ G_{21}(\boldsymbol{k}, \boldsymbol{p}_1) + G_{22}(\boldsymbol{k}, \boldsymbol{q}_2) + G_{23}(\boldsymbol{k}, \boldsymbol{p}_2) + G_{24}(\boldsymbol{k}, -\boldsymbol{k}) && (8.91)\\
&+ G_{31}(\boldsymbol{k}, -\boldsymbol{k}) + G_{32}(\boldsymbol{k}, \boldsymbol{p}_2) + G_{33}(\boldsymbol{k}, \boldsymbol{q}_3) + G_{34}(\boldsymbol{k}, \boldsymbol{p}_3) && (8.92)\\
&+ G_{41}(\boldsymbol{k}, \boldsymbol{p}_4) + G_{42}(\boldsymbol{k}, -\boldsymbol{k}) + G_{43}(\boldsymbol{k}, \boldsymbol{p}_3) + G_{44}(\boldsymbol{k}, \boldsymbol{q}_4) && (8.93)
\end{aligned}$$

and $R_{\boldsymbol{k}}$ and $L_{\boldsymbol{k}}$ take the values

$$\begin{aligned}
R_{\boldsymbol{k}} &= R_{11}(\boldsymbol{k}, \boldsymbol{k}) + R_{12}(\boldsymbol{k}, \boldsymbol{p}'_4) + R_{13}(\boldsymbol{k}, \boldsymbol{q}'_1) + R_{14}(\boldsymbol{k}, \boldsymbol{p}'_1) && (8.94)\\
&+ R_{21}(\boldsymbol{k}, \boldsymbol{p}'_2) + R_{22}(\boldsymbol{k}, \boldsymbol{k}) + R_{23}(\boldsymbol{k}, \boldsymbol{p}'_1) + R_{24}(\boldsymbol{k}, \boldsymbol{q}'_2) && (8.95)\\
&+ R_{31}(\boldsymbol{k}, \boldsymbol{q}'_3) + R_{32}(\boldsymbol{k}, \boldsymbol{p}'_3) + R_{33}(\boldsymbol{k}, \boldsymbol{k}) + R_{34}(\boldsymbol{k}, \boldsymbol{p}'_2) && (8.96)\\
&+ R_{41}(\boldsymbol{k}, \boldsymbol{p}'_3) + R_{42}(\boldsymbol{k}, \boldsymbol{q}'_4) + R_{43}(\boldsymbol{k}, \boldsymbol{p}'_4) + R_{44}(\boldsymbol{k}, \boldsymbol{k}) && (8.97)\\
L_{\boldsymbol{k}} &= L_{11}(\boldsymbol{k}, \boldsymbol{k}) + L_{12}(\boldsymbol{k}, \boldsymbol{p}'_4) + L_{13}(\boldsymbol{k}, \boldsymbol{q}'_1) + L_{14}(\boldsymbol{k}, \boldsymbol{p}'_1) && (8.98)\\
&+ L_{21}(\boldsymbol{k}, \boldsymbol{p}'_2) + L_{22}(\boldsymbol{k}, \boldsymbol{k}) + L_{23}(\boldsymbol{k}, \boldsymbol{p}'_1) + L_{24}(\boldsymbol{k}, \boldsymbol{q}'_2) && (8.99)\\
&+ L_{31}(\boldsymbol{k}, \boldsymbol{q}'_3) + L_{32}(\boldsymbol{k}, \boldsymbol{p}'_3) + L_{33}(\boldsymbol{k}, \boldsymbol{k}) + L_{34}(\boldsymbol{k}, \boldsymbol{p}'_2) && (8.100)\\
&+ L_{41}(\boldsymbol{k}, \boldsymbol{p}'_3) + L_{42}(\boldsymbol{k}, \boldsymbol{q}'_4) + L_{43}(\boldsymbol{k}, \boldsymbol{p}'_4) + L_{44}(\boldsymbol{k}, \boldsymbol{k}) && (8.101)
\end{aligned}$$

Conservation of momentum gives the following wavevectors which must be included in the particle basis, see fig. 8.3 for an overview of these when $\boldsymbol{k} = 0$

$$\begin{aligned}
&\boldsymbol{q}_1 = 2\boldsymbol{k}_{01} - \boldsymbol{k}, \quad \boldsymbol{q}_2 = 2\boldsymbol{k}_{02} - \boldsymbol{k}, \quad \boldsymbol{q}_3 = 2\boldsymbol{k}_{03} - \boldsymbol{k}, \quad \boldsymbol{q}_4 = 2\boldsymbol{k}_{04} - \boldsymbol{k} && (8.102)\\
&\boldsymbol{q}'_1 = 2\boldsymbol{k}_{01} + \boldsymbol{k}, \quad \boldsymbol{q}'_2 = 2\boldsymbol{k}_{02} + \boldsymbol{k}, \quad \boldsymbol{q}'_3 = 2\boldsymbol{k}_{03} + \boldsymbol{k}, \quad \boldsymbol{q}'_4 = 2\boldsymbol{k}_{04} + \boldsymbol{k} && (8.103)\\
&\boldsymbol{p}_1 = 2k_0\hat{\boldsymbol{y}} - \boldsymbol{k}, \quad \boldsymbol{p}_2 = -2k_0\hat{\boldsymbol{x}} - \boldsymbol{k}, \quad \boldsymbol{p}_3 = -2k_0\hat{\boldsymbol{y}} - \boldsymbol{k}, \quad \boldsymbol{p}_4 = 2k_0\hat{\boldsymbol{x}} - \boldsymbol{k} && (8.104)\\
&\boldsymbol{p}'_1 = 2k_0\hat{\boldsymbol{y}} + \boldsymbol{k}, \quad \boldsymbol{p}'_2 = -2k_0\hat{\boldsymbol{x}} + \boldsymbol{k}, \quad \boldsymbol{p}'_3 = -2k_0\hat{\boldsymbol{y}} + \boldsymbol{k}, \quad \boldsymbol{p}'_4 = 2k_0\hat{\boldsymbol{x}} + \boldsymbol{k} && (8.105)\\
& && (8.106)
\end{aligned}$$

We next introduce the vectors of operators $\psi_{\boldsymbol{k}}$ and $\psi^\dagger_{\boldsymbol{k}}$ as

$$\begin{aligned}
\psi_{\boldsymbol{k}} &= \begin{pmatrix} \boldsymbol{A}^{\uparrow}_{\boldsymbol{k}} & \boldsymbol{A}^{\downarrow}_{\boldsymbol{k}} & \boldsymbol{A}^{\uparrow\dagger}_{\boldsymbol{k}} & \boldsymbol{A}^{\downarrow\dagger}_{\boldsymbol{k}} \end{pmatrix}^T && (8.107)\\
\psi^\dagger_{\boldsymbol{k}} &= \begin{pmatrix} \boldsymbol{A}^{\uparrow\dagger}_{\boldsymbol{k}} & \boldsymbol{A}^{\downarrow\dagger}_{\boldsymbol{k}} & \boldsymbol{A}^{\uparrow}_{\boldsymbol{k}} & \boldsymbol{A}^{\downarrow}_{\boldsymbol{k}} \end{pmatrix} && (8.108)
\end{aligned}$$

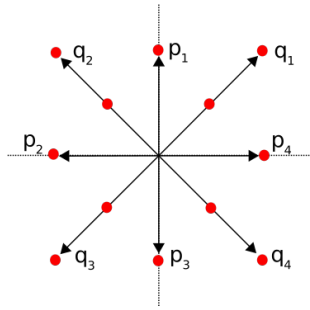

Figure 8.2: Overview of the vectors allowed by conservation of momentum when $\boldsymbol{k} = 0$

where the vectors of operators $\boldsymbol{A}^{\alpha}_{\boldsymbol{k}}$ and $\boldsymbol{A}^{\alpha\dagger}_{\boldsymbol{k}}$ are defined as

$$\boldsymbol{A}^{\alpha}_{\boldsymbol{k}} = \Big(A^{\alpha}_{\boldsymbol{k}} A^{\alpha}_{-\boldsymbol{k}} A^{\alpha}_{\boldsymbol{q}_1} A^{\alpha}_{\boldsymbol{q}'_1} A^{\alpha}_{\boldsymbol{q}_2} A^{\alpha}_{\boldsymbol{q}'_2} A^{\alpha}_{\boldsymbol{q}_3} A^{\alpha}_{\boldsymbol{q}'_3} A^{\alpha}_{\boldsymbol{q}_4} A^{\alpha}_{\boldsymbol{q}'_4} A^{\alpha}_{\boldsymbol{p}_1} A^{\alpha}_{\boldsymbol{p}'_1} \tag{8.109}$$

$$A^{\alpha}_{\boldsymbol{p}_2} A^{\alpha}_{\boldsymbol{p}'_2} A^{\alpha}_{\boldsymbol{p}_3} A^{\alpha}_{\boldsymbol{p}'_3} A^{\alpha}_{\boldsymbol{p}_4} A^{\alpha}_{\boldsymbol{p}'_4} \Big) \tag{8.110}$$

$$\boldsymbol{A}^{\alpha\dagger}_{\boldsymbol{k}} = \Big(A^{\alpha\dagger}_{\boldsymbol{k}} A^{\alpha\dagger}_{-\boldsymbol{k}} A^{\alpha\dagger}_{\boldsymbol{q}_1} A^{\alpha\dagger}_{\boldsymbol{q}'_1} A^{\alpha\dagger}_{\boldsymbol{q}_2} A^{\alpha\dagger}_{\boldsymbol{q}'_2} A^{\alpha\dagger}_{\boldsymbol{q}_3} A^{\alpha\dagger}_{\boldsymbol{q}'_3} A^{\alpha\dagger}_{\boldsymbol{q}_4} A^{\alpha\dagger}_{\boldsymbol{q}'_4} A^{\alpha\dagger}_{\boldsymbol{p}_1} A^{\alpha\dagger}_{\boldsymbol{p}'_1} \tag{8.111}$$

$$A^{\alpha\dagger}_{\boldsymbol{p}_2} A^{\alpha\dagger}_{\boldsymbol{p}'_2} A^{\alpha\dagger}_{\boldsymbol{p}_3} A^{\alpha\dagger}_{\boldsymbol{p}'_3} A^{\alpha\dagger}_{\boldsymbol{p}_4} A^{\alpha\dagger}_{\boldsymbol{p}'_4} \Big) \tag{8.112}$$

$$\tag{8.113}$$

We follow the standard routine and write the quadratic Hamiltonian as a matrix product

$$H_2 = C_2 + \frac{1}{2} \sum_{\boldsymbol{k}} \psi^{\dagger}_{\boldsymbol{k}} M \psi_{\boldsymbol{k}} \tag{8.114}$$

The 72×72 coefficient matrix M has the familiar form

$$M = \begin{pmatrix} A & B \\ B^* & A^* \end{pmatrix} \tag{8.115}$$

Where A is Hermitian, and B is symmetric. The elements for the coefficient matrix M are shown in fig. 8.3 The matrix elements on the upper diagonal of sub-matrix B is given by

$$B_{1,2} = a^{\uparrow} \left(e^{-i\sigma^{\uparrow\uparrow}_{13}} + e^{-i\sigma^{\uparrow\uparrow}_{24}} \right) \tag{8.116}$$

$$B_{1,3} = B_{2,4} = \frac{a^{\uparrow}}{2} e^{-2i\theta^{\uparrow}_1} \tag{8.117}$$

$$B_{1,5} = B_{2,6} = \frac{a^{\uparrow}}{2} e^{-2i\theta^{\uparrow}_2} \tag{8.118}$$

$$B_{1,7} = B_{2,8} = \frac{a^{\uparrow}}{2} e^{-2i\theta^{\uparrow}_3} \tag{8.119}$$

$$B_{1,9} = B_{2,10} = \frac{a^{\uparrow}}{2} e^{-2i\theta^{\uparrow}_4} \tag{8.120}$$

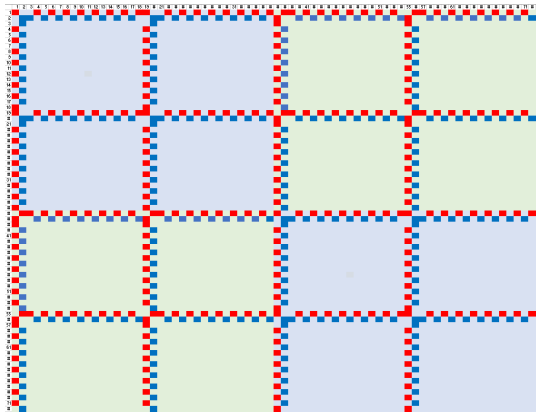

Figure 8.3: Overview of the matrix elements of the coefficient matrix M in the LW-phase. The red entries marks elements of the $\boldsymbol{k}$ sum, and the blue entries show the shifted elements in the $-\boldsymbol{k}$ sum

$$B_{1,11} = B_{2,12} = a^{\uparrow} e^{-2i\sigma_{12}^{\uparrow\uparrow}} \tag{8.121}$$

$$B_{1,13} = B_{2,14} = a^{\uparrow} e^{-2i\sigma_{23}^{\uparrow\uparrow}} \tag{8.122}$$

$$B_{1,15} = B_{2,16} = a^{\uparrow} e^{-2i\sigma_{34}^{\uparrow\uparrow}} \tag{8.123}$$

$$B_{1,17} = B_{2,18} = a^{\uparrow} e^{-2i\sigma_{41}^{\uparrow\uparrow}} \tag{8.124}$$

$$B_{1,20} = B_{2,19} = \alpha\sqrt{a^{\uparrow}a^{\downarrow}}\left(e^{-i\sigma_{31}^{\uparrow\downarrow}} + e^{-i\sigma_{42}^{\uparrow\downarrow}} + e^{-i\sigma_{13}^{\uparrow\downarrow}} + e^{-i\sigma_{24}^{\uparrow\downarrow}}\right) \tag{8.125}$$

$$B_{1,21} = B_{2,22} = \frac{\alpha}{2}\sqrt{a^{\uparrow}a^{\downarrow}}e^{-i\sigma_{11}^{\uparrow\downarrow}} \tag{8.126}$$

$$B_{1,23} = B_{2,24} = \frac{\alpha}{2}\sqrt{a^{\uparrow}a^{\downarrow}}e^{-i\sigma_{22}^{\uparrow\downarrow}} \tag{8.127}$$

$$B_{1,25} = B_{2,26} = \frac{\alpha}{2}\sqrt{a^{\uparrow}a^{\downarrow}}e^{-i\sigma_{33}^{\uparrow\downarrow}} \tag{8.128}$$

$$B_{1,27} = B_{2,28} = \frac{\alpha}{2}\sqrt{a^{\uparrow}a^{\downarrow}}e^{-i\sigma_{44}^{\uparrow\downarrow}} \tag{8.129}$$

$$B_{1,29} = B_{2,30} = \frac{\alpha}{2}\sqrt{a^{\uparrow}a^{\downarrow}}\left(e^{-i\sigma_{21}^{\uparrow\downarrow}} + e^{-i\sigma_{12}^{\uparrow\downarrow}}\right) \tag{8.130}$$

$$B_{1,31} = B_{2,32} = \frac{\alpha}{2}\sqrt{a^{\uparrow}a^{\downarrow}}\left(e^{-i\sigma_{32}^{\uparrow\downarrow}} + e^{-i\sigma_{23}^{\uparrow\downarrow}}\right) \tag{8.131}$$

$$B_{1,33} = B_{2,34} = \frac{\alpha}{2}\sqrt{a^{\uparrow}a^{\downarrow}}\left(e^{-i\sigma_{43}^{\uparrow\downarrow}} + e^{-i\sigma_{34}^{\uparrow\downarrow}}\right) \tag{8.132}$$

$$B_{1,35} = B_{2,36} = \frac{\alpha}{2}\sqrt{a^{\uparrow}a^{\downarrow}}\left(e^{-i\sigma_{14}^{\uparrow\downarrow}} + e^{-i\sigma_{41}^{\uparrow\downarrow}}\right) \tag{8.133}$$

$$B_{3,19} = B_{4,20} = \frac{\alpha}{2}\sqrt{a^{\uparrow}a^{\downarrow}}e^{-i\sigma_{11}^{\uparrow\downarrow}} \tag{8.134}$$

$$B_{5,19} = B_{6,20} = \frac{\alpha}{2}\sqrt{a^{a\downarrow}}e^{-i\sigma_{22}^{\uparrow\downarrow}} \tag{8.135}$$

$$B_{7,19} = B_{8,20} = \frac{\alpha}{2}\sqrt{a^{\uparrow}a^{\downarrow}}e^{-i\sigma_{33}^{\uparrow\downarrow}} \tag{8.136}$$

$$B_{9,19} = B_{10,20} = \frac{\alpha}{2}\sqrt{a^{\uparrow}a^{\downarrow}}e^{-i\sigma_{44}^{\uparrow\downarrow}} \tag{8.137}$$

$$B_{11,19} = B_{12,20} = \frac{\alpha}{2}\sqrt{a^{\uparrow}a^{\downarrow}}\left(e^{-i\sigma_{21}^{\uparrow\downarrow}} + e^{-i\sigma_{12}^{\uparrow\downarrow}}\right) \tag{8.138}$$

$$B_{13,19} = B_{14,20} = \frac{\alpha}{2}\sqrt{a^{\uparrow}a^{\downarrow}}\left(e^{-i\sigma_{32}^{\uparrow\downarrow}} + e^{-i\sigma_{23}^{\uparrow\downarrow}}\right) \tag{8.139}$$

$$B_{15,19} = B_{16,20} = \frac{\alpha}{2}\sqrt{a^{\uparrow}a^{\downarrow}}\left(e^{-i\sigma_{43}^{\uparrow\downarrow}} + e^{-i\sigma_{34}^{\uparrow\downarrow}}\right) \tag{8.140}$$

$$B_{17,19} = B_{18,20} = \frac{\alpha}{2}\sqrt{a^{\uparrow}a^{\downarrow}}\left(e^{-i\sigma_{14}^{\uparrow\downarrow}} + e^{-i\sigma_{41}^{\uparrow\downarrow}}\right) \tag{8.141}$$

$$B_{19,20} = a^{\downarrow}\left(e^{-i\sigma_{13}^{\downarrow\downarrow}} + e^{-i\sigma_{24}^{\downarrow\downarrow}}\right) \tag{8.142}$$

$$B_{19,21} = B_{20,22} = \frac{a^{\uparrow}}{2}e^{-2i\theta_1^{\uparrow}} \tag{8.143}$$

$$B_{19,23} = B_{20,24} = \frac{a^{\uparrow}}{2}e^{-2i\theta_2^{\uparrow}} \tag{8.144}$$

$$B_{19,25} = B_{20,26} = \frac{a^{\uparrow}}{2}e^{-2i\theta_3^{\uparrow}} \tag{8.145}$$

$$B_{19,27} = B_{20,28} = \frac{a^{\uparrow}}{2}e^{-2i\theta_4^{\uparrow}} \tag{8.146}$$

$$B_{19,29} = B_{20,30} = a^{\uparrow}e^{-2i\sigma_{12}^{\uparrow\uparrow}} \tag{8.147}$$

$$B_{19,31} = B_{20,32} = a^{\uparrow}e^{-2i\sigma_{23}^{\uparrow\uparrow}} \tag{8.148}$$

$$B_{19,33} = B_{20,34} = a^{\uparrow}e^{-2i\sigma_{34}^{\uparrow\uparrow}} \tag{8.149}$$

$$B_{19,35} = B_{20,36} = a^{\uparrow}e^{-2i\sigma_{41}^{\uparrow\uparrow}} \tag{8.150}$$

and the matrix elements on the upper diagonal of submatrix A is given by

$$A_{1,1} = A_{2,2} = \frac{\eta_{\boldsymbol{k}}^{\uparrow\uparrow}}{2} + 4(2a^{\uparrow} + \alpha a^{\downarrow}) \tag{8.151}$$

$$A_{1,4} = A_{2,3} = \frac{2a^{\uparrow}e^{i\delta_{13}^{\uparrow\uparrow}} + \alpha a^{\downarrow}e^{i\delta_{13}^{\downarrow\downarrow}}}{2} \tag{8.152}$$

$$A_{1,6} = A_{2,5} = \frac{2a^{\uparrow}e^{i\delta_{24}^{\uparrow\uparrow}} + \alpha a^{\downarrow}e^{i\delta_{24}^{\downarrow\downarrow}}}{2} \tag{8.153}$$

$$A_{1,8} = A_{2,7} = \frac{2a^{\uparrow}e^{i\delta_{31}^{\uparrow\uparrow}} + \alpha a^{\downarrow}e^{i\delta_{31}^{\downarrow\downarrow}}}{2} \tag{8.154}$$

$$A_{1,10} = A_{2,9} = \frac{2a^{\uparrow}e^{i\delta_{42}^{\uparrow\uparrow}} + \alpha a^{\downarrow}e^{i\delta_{42}^{\downarrow\downarrow}}}{2} \tag{8.155}$$

$$A_{1,12} = A_{2,11} = \frac{2a^{\uparrow}\left(e^{i\delta_{14}^{\uparrow\uparrow}} + e^{i\delta_{23}^{\uparrow\uparrow}}\right) + \alpha a^{\downarrow}\left(e^{i\delta_{14}^{\downarrow\downarrow}} + e^{i\delta_{23}^{\downarrow\downarrow}}\right)}{2} \tag{8.156}$$

$$A_{1,14} = A_{2,13} = \frac{2a^{\uparrow}\left(e^{i\delta_{21}^{\uparrow\uparrow}} + e^{i\delta_{34}^{\uparrow\uparrow}}\right) + \alpha a^{\downarrow}\left(e^{i\delta_{21}^{\downarrow\downarrow}} + e^{i\delta_{34}^{\downarrow\downarrow}}\right)}{2} \tag{8.157}$$

$$A_{1,16} = A_{2,15} = \frac{2a^{\uparrow}\left(e^{i\delta_{32}^{\uparrow\uparrow}} + e^{i\delta_{41}^{\uparrow\uparrow}}\right) + \alpha a^{\downarrow}\left(e^{i\delta_{32}^{\downarrow\downarrow}} + e^{i\delta_{41}^{\downarrow\downarrow}}\right)}{2} \tag{8.158}$$

$$A_{1,18} = A_{2,17} = \frac{2a^{\uparrow}\left(e^{i\delta_{43}^{\uparrow\uparrow}} + e^{i\delta_{12}^{\uparrow\uparrow}}\right) + \alpha a^{\downarrow}\left(e^{i\delta_{43}^{\downarrow\downarrow}} + e^{i\delta_{12}^{\downarrow\downarrow}}\right)}{2} \tag{8.159}$$

$$A_{1,19} = \frac{s(\boldsymbol{k})}{2} \tag{8.160}$$

$$A_{2,20} = -\frac{s(\boldsymbol{k})}{2} \tag{8.161}$$

$$A_{1,22} = A_{2,21} = \frac{\alpha\sqrt{a^{\uparrow}a^{\downarrow}}}{2} e^{-i\delta_{31}^{\uparrow\downarrow}} \tag{8.162}$$

$$A_{1,24} = A_{2,23} = \frac{\alpha\sqrt{a^{\uparrow}a^{\downarrow}}}{2} e^{-i\delta_{42}^{\uparrow\downarrow}} \tag{8.163}$$

$$A_{1,26} = A_{2,25} = \frac{\alpha\sqrt{a^{\uparrow}a^{\downarrow}}}{2} e^{-i\delta_{13}^{\uparrow\downarrow}} \tag{8.164}$$

$$A_{1,28} = A_{2,27} = \frac{\alpha\sqrt{a^{\uparrow}a^{\downarrow}}}{2} e^{-i\delta_{24}^{\uparrow\downarrow}} \tag{8.165}$$

$$A_{1,30} = A_{2,29} = \frac{\alpha\sqrt{a^{\uparrow}a^{\downarrow}}}{2}\left(e^{-i\delta_{41}^{\uparrow\downarrow}} + e^{-i\delta_{32}^{\uparrow\downarrow}}\right) \tag{8.166}$$

$$A_{1,32} = A_{2,31} = \frac{\alpha\sqrt{a^{\uparrow}a^{\downarrow}}}{2}\left(e^{-i\delta_{12}^{\uparrow\downarrow}} + e^{-i\delta_{43}^{\uparrow\downarrow}}\right) \tag{8.167}$$

$$A_{1,34} = A_{2,33} = \frac{\alpha\sqrt{a^{\uparrow}a^{\downarrow}}}{2}\left(e^{-i\delta_{23}^{\uparrow\downarrow}} + e^{-i\delta_{14}^{\uparrow\downarrow}}\right) \tag{8.168}$$

$$A_{1,36} = A_{2,35} = \frac{\alpha\sqrt{a^{\uparrow}a^{\downarrow}}}{2}\left(e^{-i\delta_{34}^{\uparrow\downarrow}} + e^{-i\delta_{21}^{\uparrow\downarrow}}\right) \tag{8.169}$$

$$A_{4,19} = A_{3,20} = \frac{\alpha\sqrt{a^{\uparrow}a^{\downarrow}}}{2} e^{-i\delta_{13}^{\uparrow\downarrow}} \tag{8.170}$$

$$A_{6,19} = A_{5,20} = \frac{\alpha\sqrt{a^{\uparrow}a^{\downarrow}}}{2} e^{-i\delta_{24}^{\uparrow\downarrow}} \tag{8.171}$$

$$A_{8,19} = A_{7,20} = \frac{\alpha\sqrt{a^{\uparrow}a^{\downarrow}}}{2} e^{-i\delta_{31}^{\uparrow\downarrow}} \tag{8.172}$$

$$A_{10,19} = A_{9,20} = \frac{\alpha\sqrt{a^{\uparrow}a^{\downarrow}}}{2} e^{-i\delta_{42}^{\uparrow\downarrow}} \tag{8.173}$$

$$A_{12,19} = A_{11,20} = \frac{\alpha\sqrt{a^{\uparrow}a^{\downarrow}}}{2}\left(e^{-i\delta_{14}^{\uparrow\downarrow}} + e^{-i\delta_{23}^{\uparrow\downarrow}}\right) \tag{8.174}$$

$$A_{14,19} = A_{13,20} = \frac{\alpha\sqrt{a^{\uparrow}a^{\downarrow}}}{2}\left(e^{-i\delta_{21}^{\uparrow\downarrow}} + e^{-i\delta_{34}^{\uparrow\downarrow}}\right) \tag{8.175}$$

$$A_{16,19} = A_{15,20} = \frac{\alpha\sqrt{a^{\uparrow}a^{\downarrow}}}{2}\left(e^{-i\delta_{32}^{\uparrow\downarrow}} + e^{-i\delta_{41}^{\uparrow\downarrow}}\right) \tag{8.176}$$

$$A_{18,19} = A_{17,20} = \frac{\alpha\sqrt{a^{\uparrow}a^{\downarrow}}}{2}\left(e^{-i\delta_{43}^{\uparrow\downarrow}} + e^{-i\delta_{12}^{\uparrow\downarrow}}\right) \tag{8.177}$$

$$A_{19,19} = A_{20,20} = \frac{\eta_{\boldsymbol{k}}^{\downarrow\downarrow}}{2} + 4(2a^{\downarrow} + \alpha a^{\uparrow}) \tag{8.178}$$

$$A_{19,22} = A_{20,21} = \frac{2a^{\downarrow}e^{i\delta_{13}^{\downarrow\downarrow}} + \alpha a^{\uparrow}e^{i\delta_{13}^{\uparrow\uparrow}}}{2} \tag{8.179}$$

$$A_{19,24} = A_{20,23} = \frac{2a^{\downarrow}e^{i\delta_{24}^{\downarrow\downarrow}} + \alpha a^{\uparrow}e^{i\delta_{24}^{\uparrow\uparrow}}}{2} \tag{8.180}$$

$$A_{19,26} = A_{20,25} = \frac{2a^{\downarrow}e^{i\delta_{31}^{\downarrow\downarrow}} + \alpha a^{\uparrow}e^{i\delta_{31}^{\uparrow\uparrow}}}{2} \tag{8.181}$$

$$A_{19,28} = A_{20,27} = \frac{2a^{\downarrow}e^{i\delta_{42}^{\downarrow\downarrow}} + \alpha a^{\uparrow}e^{i\delta_{42}^{\uparrow\uparrow}}}{2} \tag{8.182}$$

$$A_{19,30} = A_{20,29} = \frac{2a^{\downarrow}\left(e^{i\delta_{14}^{\downarrow\downarrow}} + e^{i\delta_{23}^{\downarrow\downarrow}}\right) + \alpha a^{\uparrow}\left(e^{i\delta_{14}^{\uparrow\uparrow}} + e^{i\delta_{23}^{\uparrow\uparrow}}\right)}{2} \tag{8.183}$$

$$A_{19,32} = A_{20,31} = \frac{2a^{\downarrow}\left(e^{i\delta_{21}^{\downarrow\downarrow}} + e^{i\delta_{34}^{\downarrow\downarrow}}\right) + \alpha a^{\uparrow}\left(e^{i\delta_{21}^{\uparrow\uparrow}} + e^{i\delta_{34}^{\uparrow\uparrow}}\right)}{2} \tag{8.184}$$

$$A_{19,34} = A_{20,33} = \frac{2a^{\downarrow}\left(e^{i\delta_{32}^{\downarrow\downarrow}} + e^{i\delta_{41}^{\downarrow\downarrow}}\right) + \alpha a^{\uparrow}\left(e^{i\delta_{32}^{\uparrow\uparrow}} + e^{i\delta_{41}^{\uparrow\uparrow}}\right)}{2} \tag{8.185}$$

$$A_{19,36} = A_{20,35} = \frac{2a^{\downarrow}\left(e^{i\delta_{43}^{\downarrow\downarrow}} + e^{i\delta_{12}^{\downarrow\downarrow}}\right) + \alpha a^{\uparrow}\left(e^{i\delta_{43}^{\uparrow\uparrow}} + e^{i\delta_{12}^{\uparrow\uparrow}}\right)}{2} \tag{8.186}$$

Where $a^{\uparrow} \equiv a^{\uparrow\uparrow}$ and $a^{\downarrow} = a^{\downarrow\downarrow}$. The author is able to find real eigenvalues for some values of (α, λ_R), see fig. 8.4 for the excitation spectrum. The plot reveals that there is no stable minima, except for the zero eigenvalue. Thus for this choice of physical parameters, the LW phase will not be stable. This is also reflected in the next section, where we find that the *pure* LW-phase does not appear in the phase-diagram in (α, λ_R) space.

8.4.1 Pure LW phase

In this section we provide the expression for the free energy of the *pure* LW phase. This means that we neglect any terms proportional to an excitation operator. We assume that $N_0^{\uparrow} = N_0^{\downarrow} = N_0/2$. Using the expression for $\mu^{\uparrow}$ in eq. (8.66), and that $s_1 = 2\sqrt{2}\lambda_R|\sin(k_0 a)|$, we get an expression for N_0/N_s

$$\frac{N_0}{N_s} = \frac{2f}{3U(3+\alpha)}\left(\mu^{\uparrow} + 4t\cos(k_0 a) + 2\sqrt{2}\lambda_R|\sin(k_0 a)|\right) \tag{8.187}$$

which inserted into the expression for the constant Hamiltonian gives

$$H_0 = -\frac{4N_s(7+3\alpha)}{9U(3+\alpha)^2}\left(\mu^{\uparrow} + 4t\cos(k_0 a) + 2\sqrt{2}\lambda_R|\sin(k_0 a)|\right)^2 \tag{8.188}$$

giving the free energy as $F = H_0$. The free energy is on the form

$$C\left(\mu^{\uparrow} + 4t\cos(k_0 a) + 2\sqrt{2}\lambda_R|\sin(k_0 a)|\right)^2 \tag{8.189}$$

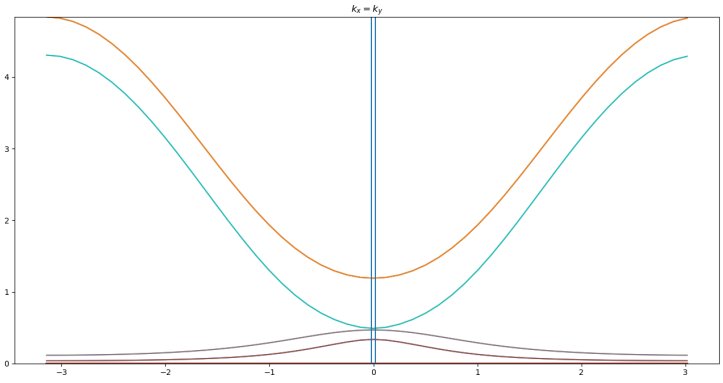

Figure 8.4: Excitation spectrum for the LW phase. The physical parameters are $U = 0.1$, $\delta = 0.9$, $N = 50^2$, $\lambda_R = 0.02$ and $\alpha = 3.43$. The value for k_0 is given in eq. 3.214.

which has a minima for k_0 equal to

$$k_0 = \frac{1}{a} \arctan\left(\frac{\sqrt{2}\lambda_R}{2t}\right) \tag{8.190}$$

which is the same k_0 as in the PW and SW phases. Thus the free energy is given by

$$F_{\text{LW}} = -\frac{4N_s(7+3\alpha)}{9U(3+\alpha)^2}\left(\mu^{\uparrow} + 4t\sqrt{\frac{\lambda_R^2}{2t}+1}\right)^2 \tag{8.191}$$

when $\mu^{\uparrow} = \mu$, as in the other phases, the free energy for the LW phase is actually larger than any of the free energies for the other phases. Consequently, it does not show up in the phase diagram in (α, λ_R) space. The reason for this will be discussed in the Miscellaneous Discussion chapter.

Chapter 9

Miscellaneous Discussion, Summary and Outlook

In this chapter we shall discuss some results from the previous chapters.

9.1 Free energy for the pure LW phase

As noted in at the end of the LW chapter, the free energy for the *pure* LW phase was higher than any of the other phases. As a first guess to why, we may guess that it has something to do with kinetic energy. This cannot be the case however, as we assume for each phase that there are N_0 bosons, which will distribute themselves equally at the condensate momentum points. It was in addition shown that the length of the $\boldsymbol{k}_{0i}$ vector in the LW phase was minimized for the *same* value as for the SW and PW phases. Thus the kinetic energy is the same for the non-zero momentum phases. Thus there must be another explination. The constant Hamiltonian, which gives the free energy, is before simplifying anything given by [32]

$$H_0 = \sum_i \sum_{\alpha\beta} \eta_i^{\alpha\beta} (a_i^\alpha)^* a_i^\beta \tag{9.1}$$

$$+ \frac{1}{2Ns} \sum_{iji'j'} \sum_{\alpha\beta} U^{\alpha\beta} (a_i^\alpha)^* (a_j^\beta)^* a_{i'}^\beta a_{j'}^\alpha \delta_{i+j,i'+j'} \tag{9.2}$$

where the a_i's are the mean-field parameters. The above equation can be written on the form

$$H_0 = -\Lambda + \text{condensate interactions}, \quad \Lambda > 0 \tag{9.3}$$

This means that the free energy has a negative "baseline" at Λ, and the interactions, which are mathematically described as two-body scattering between two incoming wavevectors with indices (i, j), and two outgoing wavevectors with indices (i', j'), causes the energy to rise. Thus we can understand that the *pure* LW phase has higher free energy than the other phases because it has a higher number of condensate momenta $\boldsymbol{k}_{0i}$ in $\boldsymbol{k}$-space. This interpration cannot be *exactly* correct, as the *sign* of the interaction is dependent on the phase differences $\theta_i^\alpha + \theta_j^\beta - \theta_{i'}^\beta - \theta_{j'}^\alpha$.

9.1.1 Chemical potential difference for the LW phase

It was shown in the LW chapter that an equal number of particles in the condensate $N_0^\uparrow = N_0^\downarrow$, led to an imbalance in the chemical potentials δ, which sign relied on the value for $m \in (0, 1)$. Similarly, if $\mu^\uparrow = \mu^\downarrow$, this led to an imbalance in condensate numbers ΔN_0. This is *strange*, and is a direct result of spin-orbit coupling. We can try to understand this by looking at the characteristics of spin-orbit coupling. For a simple quadratic dispersion relation $w(\boldsymbol{k}) = \boldsymbol{k}^2/2m$, Rashba SOC will move the minima at $\boldsymbol{k} = \boldsymbol{0}$ to finite $\boldsymbol{k}$, creating to two bands with definite helicity. Now, it may be the case for the LW phase that to achieve definite helicity bands, one *must* have an imbalance in the condensate parameters, either N_0 or μ, or both at the same time.

Mathematically, the difference in chemical potentials comes from the fact that at $N_0^\uparrow = N_0^\downarrow$, $\mu^\uparrow$ has a term proportional to $7 + 2\cos(m\pi)$, and $\mu^\downarrow$ has a term proportional to $7 - 2\cos(m\pi)$. The m terms originate from $\theta_4^\alpha - \theta_1^\alpha - \theta_3^\alpha + \theta_2^\alpha = m^\alpha \pi$, $\alpha \in (\uparrow, \downarrow)$ which is due to keeping μ^α real. Further, to reduce the expressions for the imaginary part of the chemical potentials to only $\sin(\theta_4^\alpha - \theta_1^\alpha - \theta_3^\alpha + \theta_2^\alpha)$, one had to use the explicit values for the spin-orbit coupling γ's, and also that $\delta\theta_i = \gamma_i - \pi$, which is caused by spin-orbit coupling. So in fact, the reason for why the m's appear, and also that $m^\uparrow \neq m^\downarrow$ is completely due to a finite SOC. Thus the finite $\delta\mu$ at $N_0^\uparrow = N_0^\downarrow$ is because of SOC.

9.2 Finite temperature phase diagram

In fig. 7.8 the phase diagram for the PZ, PW and SW phases are shown, at $T = 0$, with excitations. There is in principle little trouble of calculating the phase diagram at *finite* T, as the excitation spectra are not explicitly dependent on temperature. Thus to create the phase-diagram at finite T, one would simply *add* the finite temperature term from the free energy in eq. (3.203). *However*, it may be that the mean-field parameters θ_i^α and k_0 are in fact dependent on the temperature of the system. To investigate this one could use the Metropolis Algorithm outlined in sec 3.5.1 on a finite temperature system, and look for temperature dependencies in the mean-field parameters.

Further, one could maybe get an intuition for the finite temperature phase diagram by studying the phase diagram in fig. 7.8, which is at $T = 0$, but includes excitations. Here we see that the zero-momentum PZ phase moves into the SW phase, reducing the phase space available for the SW phase. When turning on increasing the temperature, one could therefore expect that the PZ phase moves further into the SW phase, decreasing the phase space available. The fact that the PZ phase becomes more energetically favorable when including interactions may originate from the fact that there is less energetic scattering around $\boldsymbol{k} = \boldsymbol{0}$.

9.3 Higher order interactions and other lattice geometries

We saw in the case of a *pure* condensate in fig. 3.5 that the condensate densities for the phases was, even at $\mu = -3.9$, significantly larger than 1. This means that on average, there are many bosons per lattice sites. This could implicitly break the assumption that two-body scattering is the only non-negligible contribution, and one may have to include higher order interactions. This also begs the question if mean-field theory is the correct approach if one must include higher-order interactions, and one may consider pertubation theory instead.

One could also develop a mean-field approach for other lattice geometries, for example the honey-comb lattice (which is not a Bravais lattice). This could be interesting to study, but it would lead to more complex expressions, as we considered the simplest square lattice case.

9.4 Summary and Outlook

In this master's thesis, the theory outlined in Janssønns master's thesis [32] has been used exstensively on different phases in $\boldsymbol{k}$ space, namely the PZ, NZ, PW, SW and LW phases. The expressions for the chemical potentials for pseudo-spin up an down have been derived for each phase, and the associated equations for the condensate densities $N_0^{\uparrow}$ and $N_0^{\downarrow}$ have been analyzed, both analytically and numerically.

For the PZ phase, we found that the extreme imbalance in the condensate numbers led to a Zeeman field which made the eigenvalues real, and by extension keeping the PZ phase stable. The analytical excitation spectrum resembled the spin-orbit coupled, non-interacting, Bose gas with a Zeeman field, with the lowest branch being Bogoliubov-like with *linear* dispersion relation around $\boldsymbol{k} = \boldsymbol{0}$, as an effect of the weak interactions. The associated superfluid critical velocity was analytically derived, kept finite by the Zeeman field.

For the NZ phase, the zero-momentum minima was incompatible with a finite spin-orbit coupling, as the numerical results revaled that there was no Zeeman field, even with an imbalance in condensate numbers.

For the PW phase, we found that the Hamiltonian had to be appropriately symmetrized to obtain physically meaningful, and real, excitation spectra. The numerically found excitation spectrum was shown to be Bogoliubov-like with a finite superfluid critical velocity for the lowest branch, with two parabolas shifted by SOC lying above.

The SW phase was the first phase containing *linear* excitation operators, whereby a method for dealing with these terms is given in the appendix. Also, as the coefficient matrix of the SW phase was indeterminate, choosing the correct eigenvalues was non-trivial. The excitation spectrum was not Bogoliubov-like around minima in $\boldsymbol{k}$-space, which led to no superfluid critical velocity. However, the excitation spectrum resembled the case of a spin-orbit coupled, non-interacting, Bose gas, demonstrating the influence of a finite SOC. Also, a Monte Carlo method was demonstrated and used to determine the mean-field parameters, which coincided with the mean-field parameters determined for the pure SW phase.

The LW phase showed some strange behaviour, namely the finite difference in chemical potentials when assuming that there are an equal amount of condensed bosons for each pseudo-spin. The excitation spectrum was found to have no stable minima. In addition, the free energy for the *pure* LW phase was derived, and shown to be larger than any of the other free energies for the other phases.

Lastly, a phase diagram for $T = 0$ with excitations was created from the PZ, PW and SW phases, resembling the case of a pure condensate, which agrees with results from the literature. The effect of excitations seemed to give the PZ phase more available phase-space, and decreased the available phase-space for the SW phase.

For future work, it may be interesting to study the phase diagram for the PZ, PW and SW phases at *finite* T, discussed in section 9.2. It could also be interesting to consider a different lattice geometry, for example the honeycomb-lattice.

Bibliography

[1] J. F. Allen and A. D. Misener. Flow phenomena in liquid helium ii. *Nature*, 142, 1938.

[2] J. O. Andersen. *Introduction to Statistical Mechanics*. Fagbokforlaget, 2017.

[3] M. H. Anderson, J. R. Ensher, M. R. Matthews, C. E. Wieman, and E. A. Cornell. Observation of bose-einstein condensation in a dilute atomic vapor. *Science*, 269(5221):198–201, 1995.

[4] H. Anton and C. Rorres. *Elementary Linear Algebra: Applications Version*. Wiley, eleventh edition, 2014.

[5] L. Balents. Spin liquids in frustrated magnets. *Nature*, 464, 2010.

[6] L. Bedini, I. Gerace, E. Salerno, and A. Tonazzini. Models and algorithms for edge-preserving image reconstruction. volume 97 of *Advances in Imaging and Electron Physics*, pages 85 – 189. Elsevier, 1996.

[7] N. N. Bogolyubov. On the theory of superfluidity. *J. Phys.(USSR)*, 11:23–32, 1947. [Izv. Akad. Nauk Ser. Fiz.11,77(1947)].

[8] S. N. Bose. *Z.Phys*, 26, 1924.

[9] C. C. Bradley, C. A. Sackett, and R. G. Hulet. Bose-einstein condensation of lithium: Observation of limited condensate number. *Phys. Rev. Lett.*, 78:985–989, Feb 1997.

[10] A. A. Burkov and L. Balents. Weyl semimetal in a topological insulator multilayer. *Phys. Rev. Lett.*, 107:127205, Sep 2011.

[11] Y. A. Bychkov and E. I. Rashba. Oscillatory effects and the magnetic susceptibility of carriers in inversion layers. *Journal of Physics C Solid State Physics*, 17(33):6039–6045, Nov. 1984.

[12] K. B. Davis, M. O. Mewes, M. R. Andrews, N. J. van Druten, D. S. Durfee, D. M. Kurn, and W. Ketterle. Bose-einstein condensation in a gas of sodium atoms. *Phys. Rev. Lett.*, 75:3969–3973, Nov 1995.

[13] K. Dorn, A. De Martino, and R. Egger. Phase diagram and phonon-induced backscattering in topological insulator nanowires. *Phys. Rev. B*, 101:045402, Jan 2020.

[14] D. S. Durfee and W. Ketterle. Experimental studies of bose-einstein condensation. *Opt. Express*, 2(8):299–313, Apr ts , url = http://www.opticsexpress.org/abstract.cfm?URI=oe-2-8-299, doi = 10.1364/OE.2.000299, abstract = We describe several experimental studies of Bose-Einstein condensation in a dilute gas of sodium atoms. These include studies of static and dynamic behavior of the condensate, and of its coherence properties.,.

[15] A. Einstein. *Sitzungberichte der Preussischen Akademie der Wissenschaften, Physikalisch-mathematische Klasse*, page 261, 1924.

[16] A. Einstein. *Sitzungberichte der Preussischen Akademie der Wissenschaften, Physikalisch-mathematische Klasse*, page 3, 1925.

[17] J. O. Fjærestad. Second quantization - lecture notes. 2014.

[18] J. O. Fjærestad. Second-quantization representation of the hamiltonian of an interacting electron gas in an external potential - lecture notes. 2014.

[19] J. O. Fjærestad. Tight-binding model for electrons in a crystal - lecture notes. 2014.

[20] V. Galitski and I. Spielman. Spin-orbit coupling in quantum gases. *Nature*, 494(7435):49–54, 2 2013.

[21] P. N. Galteland and A. Sudbø. Competing interactions in population-imbalanced two-component bose-einstein condensates. *Phys. Rev. B*, 94:054510, Aug 2016.

[22] S. M. Giampaolo, F. Illuminati, G. Mazzarella, and S. De Siena. Influence of trapping potentials on the phase diagram of bosonic atoms in optical lattices. *Phys. Rev. A*, 70:061601, Dec 2004.

[23] D. Griffiths and P. Griffiths. *Introduction to Quantum Mechanics*. Pearson international edition. Pearson Prentice Hall, 2005.

[24] D. J. Griffiths. *Introduction to elementary particles; 2nd rev. version*. Physics textbook. Wiley, New York, NY, 2008.

[25] M. Z. Hasan and C. L. Kane. Colloquium: Topological insulators. *Rev. Mod. Phys.*, 82:3045–3067, Nov 2010.

[26] E. Hecht. *Optics*. Pearson, 2012.

[27] P. Hemmer. *Kvantemekanikk*. Tapir akademisk forlag, 2005.

[28] E. V. Herland. *Theoretical studies of twocomponent superfluids and superconductors*. PhD thesis, NTNU, 2012.

[29] P. P. Hofer, C. Bruder, and V. M. Stojanović. Superfluid drag of two-species bose-einstein condensates in optical lattices. *Phys. Rev. A*, 86:033627, Sep 2012.

[30] I. Žutić, J. Fabian, and S. Das Sarma. Spintronics: Fundamentals and applications. *Rev. Mod. Phys.*, 76:323–410, Apr 2004.

[31] D. Jaksch, C. Bruder, J. I. Cirac, C. W. Gardiner, and P. Zoller. Cold bosonic atoms in optical lattices. *Phys. Rev. Lett.*, 81:3108–3111, Oct 1998.

[32] A. T. G. Janssønn. Analytic Study of Ultracold, Synthetically Spin–Orbit Coupled, Weakly Interacting, Two-Component Bose Gases Residing on Bravais Lattices. Master's thesis, NTNU, Trondheim, 2018.

[33] C. L. Kane and E. J. Mele. Quantum spin hall effect in graphene. *Phys. Rev. Lett.*, 95:226801, Nov 2005.

[34] P. Kapitza. Viscosity of liquid helium below the λ-point. *Nature*, 141:0, 1938.

[35] Y. K. Kato, R. C. Myers, A. C. Gossard, and D. D. Awschalom. Observation of the spin hall effect in semiconductors. *Science*, 306(5703):1910–1913, 2004.

[36] B. Kaviraj and D. Sahoo. Physics of excitons and their transport in two dimensional transition metal dichalcogenide semiconductors. *RSC Adv.*, 9:25439–25461, 2019.

[37] R. Khoshlahni, A. Qaiumzadeh, A. Bergman, and A. Brataas. Ultrafast generation and dynamics of isolated skyrmions in antiferromagnetic insulators. *Phys. Rev. B*, 99:054423, Feb 2019.

[38] C. Kittel. *Introduction to Solid State Physics*. Wiley, 8 edition, 2004.

[39] J. Linder. Intermediate quantum mechanics. 2017.

[40] J. Linder and A. Sudbø. Calculation of drag and superfluid velocity from the microscopic parameters and excitation energies of a two-component bose-einstein condensate in an optical lattice. *Phys. Rev. A*, 79:063610, Jun 2009.

[41] F. London. The λ-phenomenon of liquid helium and the bose-einstein degeneracy. *Nature*, 141, 1938.

[42] F. London. On the bose-einstein condensation. *Phys. Rev.*, 54:947–954, Dec 1938.

[43] M. E. J. Newman and G. T. Barkema. *Monte Carlo methods in statistical physics*. Clarendon Press, Oxford, 1999.

[44] C. Pethick and H.Smith. *Bose-Einstein Condensation in Dilute Gases, Second Edition*. Cambridge University Press, 2008.

[45] J. D. Sau, R. M. Lutchyn, S. Tewari, and S. Das Sarma. Generic new platform for topological quantum computation using semiconductor heterostructures. *Phys. Rev. Lett.*, 104:040502, Jan 2010.

[46] J. Sinova, D. Culcer, Q. Niu, N. A. Sinitsyn, T. Jungwirth, and A. H. MacDonald. Universal intrinsic spin hall effect. *Phys. Rev. Lett.*, 92:126603, Mar 2004.

[47] S. B. Sjømark. Superconductivity in Dirac Materials . Master's thesis, NTNU, Trondheim, 2016.

[48] S. Solli. Investigating the excitation spectrum of a spin-orbit coupled Bose-Einstein condensate . Master's thesis, NTNU, Trondheim, 2017.

[49] C. Tsallis. Diagonalization methods for the general bilinear hamiltonian of an assembly of bosons. *Journal of Mathematical Physics*, 19(1):277–286, 1978.

[50] J. L. van Hemmen. A note on the diagonalization of quadratic boson and fermion hamiltonians. *Zeitschrift für Physik B Condensed Matter*, 38, 1980.

[51] D. van Oosten, P. van der Straten, and H. T. C. Stoof. Quantum phases in an optical lattice. *Phys. Rev. A*, 63:053601, Apr 2001.

[52] V.S.Letekhov. *JETP Letters*, 7, 1968.

[53] M. wen Xiao. Theory of transformation for the diagonalization of quadratic hamiltonians. 2009.

[54] E. Yakaboylu and M. Lemeshko. Anyonic statistics of quantum impurities in two dimensions. *Phys. Rev. B*, 98:045402, Jul 2018.

Appendix

We will frequently encounter the sum

$$S^\beta = \sum_{\boldsymbol{k}} \eta_{\boldsymbol{k}}^{\beta\beta} \tag{9.4}$$

for $\beta = (\uparrow, \downarrow)$ and $\boldsymbol{k} \in$1BZ. The energy $\eta_{\boldsymbol{k}}^{\beta\beta}$ is given by

$$\eta_{\boldsymbol{k}}^{\beta\beta} = -(\mu^\beta + \epsilon^\beta(\boldsymbol{k})) \tag{9.5}$$

where the energy $\epsilon^\beta(\boldsymbol{k})$ is given by

$$\epsilon^\beta(\boldsymbol{k}) = 2t^\beta \left(\cos(k_x a_l) + \cos(k_y a_l)\right) \tag{9.6}$$

thus, S^β becomes

$$S^\beta = -\sum_{\boldsymbol{k}} \mu^\beta - \sum_{\boldsymbol{k}} \epsilon_{\boldsymbol{k}}^\beta \tag{9.7}$$

The first sum is simply $-\mu^\beta N_s$, as $\sum_{\boldsymbol{k}} = N_s$. The second sum requires more care

$$\sum_{\boldsymbol{k}} \epsilon_{\boldsymbol{k}}^\beta = 2t^\beta \left(\sum_{\boldsymbol{k}} \cos(k_x a_l) + \sum_{\boldsymbol{k}} \cos(k_y a_l)\right) \tag{9.8}$$

$$= 2t^\beta \left(\sqrt{N_s} \sum_{k_x} \cos(k_x a_l) + \sqrt{N_s} \sum_{k_y} \cos(k_y a_l)\right) \tag{9.9}$$

$$= 4t^\beta \sqrt{N_s} \sum_{k_x} \cos(k_x a_l) \tag{9.10}$$

Where we have used that k_x and k_y runs over the same values, so that the two sums are equal. Also, we have used that $\sum_{k_x} = \sum_{k_y} = \sqrt{N_s}$. We further focus on the sum $\sum_{k_x} \cos(k_x a_l)$. The k_x and k_y are in the 1BZ, and we choose k_x on the form [17]

$$k_x = \frac{2\pi m}{L_x} \tag{9.11}$$

where $L_x = \sqrt{N_s} a_l \equiv N_x a_l$, and $m = -N_x/2, -N_x/2 + 1, ..., N_x/2 - 1$ (where we assume that N_x is an even number). This gives $k_x = -\pi/a_l, -\pi/a_l + 2\pi/L_x, ..., \pi/a_l - 2\pi/L_x$. We thus get

$$\sum_{k_x} \cos(k_x a_l) = \sum_{m=-\frac{N_x}{2}}^{\frac{N_x}{2}-1} \cos\left(\frac{2\pi}{N_x} m\right) \tag{9.12}$$

Now we turn to a more general form of the sum above, given by:

$$\sum_{m=a}^{b} \cos(cm) = \frac{1}{2 - 2\cos(c)} \left[\cos(ac) + \cos(bc) - \cos(c(a-1)) - \cos(c(b+1))\right] \tag{9.13}$$

Which can be derived by writing $\cos(cm)$ on exponential form, and realising that you get a geometric series. Using this formula, we get

$$\sum_{m=-\frac{N_x}{2}}^{\frac{N_x}{2}-1} \cos\left(\frac{2\pi}{N_x} m\right) = 0 \tag{9.14}$$

Such that $S^\beta = -\mu^\beta N_s$.

9.5 Hamiltonian linear in excitation operators for the SW phase

The linear Hamiltonian H_1 for the SW phase is given by the equation [32]

$$H_1 = \frac{1}{N_s f^{3/2}} {\sum_{\boldsymbol{k}}}' \left(\sum_{iji'} \sum_{\alpha\beta}\right)''' U^{\alpha\beta} N_0^\beta \sqrt{N_0^\alpha} \times \left(e^{-i(\theta^\beta_{\boldsymbol{k}_{0i'}} - \theta^\alpha_{\boldsymbol{k}_{0i}} - \theta_{\boldsymbol{k}_{0j}})^\beta} A^\alpha_{\boldsymbol{k}} + \text{H.c}\right) \delta_{\boldsymbol{k}+\boldsymbol{k}_{0i'}, \boldsymbol{k}_{0i}+\boldsymbol{k}_{0j}}$$

where the constrained sum $\sum'_{\boldsymbol{k}}$ excludes all condensate momenta, and the primed sum $\left(\sum_{iji'} \sum_{\alpha\beta}\right)'''$ goes over the values in the subset $(i, j, i', \alpha, \beta)$ such that $N^\alpha_{\boldsymbol{k}_{0i}} \neq 0$, $N^\beta_{\boldsymbol{k}_{0j}} \neq 0$ and $N^\alpha_{\boldsymbol{k}_{0i'}} \neq 0$. The dirac-delta function limits the possible values for $\boldsymbol{k}$, by the equation

$$\boldsymbol{k} = \boldsymbol{k}_{0j} + \boldsymbol{k}_{0i} - \boldsymbol{k}_{0i'} \tag{9.15}$$

In addition, we have that $i = (1, 3)$, $j = (1, 3)$ and $i' = (1, 3)$. We have two configurations for (i, j, i') which gives a non-condensate $\boldsymbol{k}$. These are given by

$$(i, j, i') = (1, 1, 3) \rightarrow \quad \boldsymbol{k} = 2k_{01} - k_{03} = 3k_{01} \tag{9.16}$$

$$(i, j, i') = (3, 3, 1) \rightarrow \quad \boldsymbol{k} = 2k_{03} - k_{01} = -3k_{01} \tag{9.17}$$

Hence, the non-condensate momenta are given by

$$\boldsymbol{k}_1 \equiv 3\boldsymbol{k}_{01} \tag{9.18}$$

$$\boldsymbol{k}_2 \equiv -3\boldsymbol{k}_{01} \tag{9.19}$$

We assume that $N_0^\uparrow = N_0^\downarrow = N_0/2$. The linear Hamiltonian thus becomes

$$H_1 = \frac{N_0^{3/2}}{2\sqrt{2} f^{3/2} N_s} \left(S_1(\uparrow\uparrow) + S_2(\uparrow\downarrow) + S_3(\downarrow\uparrow) + S_4(\downarrow\downarrow)\right) \tag{9.20}$$

where the S terms are given by

$$S_1(\uparrow\uparrow) = U\left(e^{-i(\theta_3^\uparrow - 2\theta_1^\uparrow)}A^\uparrow_{\boldsymbol{k}_1} + e^{-i(\theta_1^\uparrow - 2\theta_3^\uparrow)}A^\uparrow_{\boldsymbol{k}_2} + \text{H.c}\right) \tag{9.21}$$

$$S_2(\uparrow\downarrow) = \alpha U\left(e^{-i(\theta_3^\downarrow - \theta_1^\uparrow - \theta_1^\downarrow)}A^\uparrow_{\boldsymbol{k}_1} + e^{-i(\theta_1^\downarrow - \theta_3^\uparrow - \theta_3^\downarrow)}A^\uparrow_{\boldsymbol{k}_2} + \text{H.c}\right) \tag{9.22}$$

$$S_3(\downarrow\uparrow) = \alpha U\left(e^{-i(\theta_3^\uparrow - \theta_1^\downarrow - \theta_1^\uparrow)}A^\downarrow_{\boldsymbol{k}_1} + e^{-i(\theta_1^\uparrow - \theta_3^\downarrow - \theta_3^\uparrow)}A^\downarrow_{\boldsymbol{k}_2} + \text{H.c}\right) \tag{9.23}$$

$$S_4(\downarrow\downarrow) = U\left(e^{-i(\theta_3^\downarrow - 2\theta_1^\downarrow)}A^\downarrow_{\boldsymbol{k}_1} + e^{-i(\theta_1^\downarrow - 2\theta_3^\downarrow)}A^\downarrow_{\boldsymbol{k}_2} + \text{H.c}\right) \tag{9.24}$$

The linear Hamiltonian can be written on the form

$$\begin{aligned} H_1 = {} & c_1^\uparrow A^\uparrow_{\boldsymbol{k}_1} + \text{H.c} \\ & + c_1^\downarrow A^\downarrow_{\boldsymbol{k}_1} + \text{H.c} \\ & + c_2^\uparrow A^\uparrow_{\boldsymbol{k}_2} + \text{H.c} \\ & + c_2^\downarrow A^\downarrow_{\boldsymbol{k}_2} + \text{H.c} \end{aligned}$$

The coefficients are complex, and are given by

$$c_1^\uparrow = \frac{UN_0^{3/2}}{2\sqrt{2}f^{3/2}N_s}\left(e^{-i(\theta_3^\uparrow - 2\theta_1^\uparrow)} + \alpha e^{-i(\theta_3^\downarrow - \theta_1^\uparrow - \theta_1^\downarrow)}\right) \tag{9.25}$$

$$c_1^\downarrow = \frac{UN_0^{3/2}}{2\sqrt{2}f^{3/2}N_s}\left(e^{-i(\theta_3^\downarrow - 2\theta_1^\downarrow)} + \alpha e^{-i(\theta_3^\uparrow - \theta_1^\downarrow - \theta_1^\uparrow)}\right) \tag{9.26}$$

$$c_2^\uparrow = \frac{UN_0^{3/2}}{2\sqrt{2}f^{3/2}N_s}\left(e^{-i(\theta_1^\uparrow - 2\theta_3^\uparrow)} + \alpha e^{-i(\theta_1^\downarrow - \theta_3^\downarrow - \theta_3^\uparrow)}\right) \tag{9.27}$$

$$c_2^\downarrow = \frac{UN_0^{3/2}}{2\sqrt{2}f^{3/2}N_s}\left(e^{-i(\theta_1^\downarrow - 2\theta_3^\downarrow)} + \alpha e^{-i(\theta_1^\uparrow - \theta_3^\downarrow - \theta_3^\uparrow)}\right) \tag{9.28}$$

9.5.1 Dealing with linear terms

We want to remove the linear terms from the diagonalisation problem. Consider having a quadratic Hamiltonian $H_2 = \boldsymbol{A}_0^\dagger M_0 \boldsymbol{A}_0$, where $\boldsymbol{A}_0$ is a vector of operators. Consider also a linear Hamiltonian given by H_1 above. Define the matrix M on block diagonal form:

$$M = \begin{pmatrix} M_0 & 0 \\ 0 & M_n \end{pmatrix} \tag{9.29}$$

where the label n stands for "new". The matrix M_n can be chosen to be a diagonal matrix, as we will see. Also define a vector of operators

$$\boldsymbol{A} = \begin{pmatrix} \boldsymbol{A}_0 & \boldsymbol{A}_n \end{pmatrix}^T \tag{9.30}$$

where $\boldsymbol{A}_n$ is a *new* vector of operators, given by the non-condensate momenta in H_1. The product $\boldsymbol{A}^\dagger M \boldsymbol{A}$ is then

$$\boldsymbol{A}^\dagger M \boldsymbol{A} = \boldsymbol{A}_0^\dagger M_0 \boldsymbol{A}_0 + \boldsymbol{A}_n^\dagger M_n \boldsymbol{A}_n \tag{9.31}$$

Define also a vector of complex numbers χ. Consider the product

$$(\boldsymbol{A}^\dagger + \chi^\dagger)M(\boldsymbol{A} + \chi) = \boldsymbol{A}_0^\dagger M_0 \boldsymbol{A}_0 + \boldsymbol{A}_n^\dagger M_n \boldsymbol{A}_n \tag{9.32}$$

$$+ \chi^\dagger M \boldsymbol{A} + \boldsymbol{A}^\dagger M \chi + \chi^\dagger M \chi \tag{9.33}$$

and define χ as

$$\chi = \begin{pmatrix} 0 & \chi_n \end{pmatrix}^T \tag{9.34}$$

such that we get the products

$$\chi^\dagger M \boldsymbol{A} = \chi_n^\dagger M_n \boldsymbol{A}_n \tag{9.35}$$

$$\boldsymbol{A}^\dagger M \chi = \boldsymbol{A}_n^\dagger M_n \chi_n \tag{9.36}$$

Identifying H_2 as $\boldsymbol{A}_0^\dagger M_0 \boldsymbol{A}_0$ and H_1 as $\chi_n^\dagger M_n \boldsymbol{A}_n + \boldsymbol{A}_n^\dagger M_n \chi_n$ (this assumes that the linear excitation operators contained in H_1 are not in $\boldsymbol{A}_0$), we get

$$(\boldsymbol{A}^\dagger + \chi^\dagger)M(\boldsymbol{A} + \chi) - \boldsymbol{A}_n^\dagger M_n \boldsymbol{A}_n - \chi_n^\dagger M_n \chi_n = H_1 + H_2 \tag{9.37}$$

The left hand side of this equation consists of no linear terms. Now is the question, how do we choose M_n and χ_n? Let us look at the conrecte example of the SW-phase. Define

$$\boldsymbol{A}_n = \left(A^\uparrow_{\boldsymbol{k}_1} A^\downarrow_{\boldsymbol{k}_1} A^\uparrow_{\boldsymbol{k}_2} A^\downarrow_{\boldsymbol{k}_2} A^{\uparrow\dagger}_{\boldsymbol{k}_1} A^{\downarrow\dagger}_{\boldsymbol{k}_1} A^{\uparrow\dagger}_{\boldsymbol{k}_2} A^{\downarrow\dagger}_{\boldsymbol{k}_2} \right)^T \tag{9.38}$$

H_1 is again given by

$$H_1 = c_1^\uparrow A^\uparrow_{\boldsymbol{k}_1} + c_1^{\uparrow *} A^{\uparrow\dagger}_{\boldsymbol{k}_1} + c_1^\downarrow A^\downarrow_{\boldsymbol{k}_1} + c_1^{\downarrow *} A^{\downarrow\dagger}_{\boldsymbol{k}_1} \tag{9.39}$$

$$+ c_2^\uparrow A^\uparrow_{\boldsymbol{k}_2} + c_2^{\uparrow *} A^{\uparrow\dagger}_{\boldsymbol{k}_2} + c_2^\downarrow A^\downarrow_{\boldsymbol{k}_2} + c_2^{\downarrow *} A^{\downarrow\dagger}_{\boldsymbol{k}_2} \tag{9.40}$$

Let χ_n be given by

$$\chi_n = \left(e^{i\eta_1^\uparrow} \quad e^{i\eta_1^\downarrow} \quad e^{i\eta_2^\uparrow} \quad e^{i\eta_2^\downarrow} \quad 0 \quad 0 \quad 0 \quad 0 \right)^T \tag{9.41}$$

and M_n defined as

$$M_n = \mathrm{diag}(w_1^\uparrow, w_1^\downarrow, w_2^\uparrow, w_2^\downarrow, w_1^\uparrow, w_1^\downarrow, w_2^\uparrow, w_2^\downarrow) \tag{9.42}$$

then we get

$$\chi_n^\dagger M_n \boldsymbol{A}_n = w_1^\uparrow e^{-i\eta_1^\uparrow} A^\uparrow_{\boldsymbol{k}_1} + w_1^\downarrow e^{-i\eta_1^\downarrow} A^\downarrow_{\boldsymbol{k}_1} \tag{9.43}$$

$$+ w_2^\uparrow e^{-i\eta_2^\uparrow} A^\uparrow_{\boldsymbol{k}_2} + w_2^\downarrow e^{-i\eta_2^\downarrow} A^\downarrow_{\boldsymbol{k}_2} \tag{9.44}$$

and,

$$\boldsymbol{A}_n^\dagger M_n \chi_n = w_1^\uparrow e^{i\eta_1^\uparrow} A^{\uparrow\dagger}_{\boldsymbol{k}_1} + w_1^\downarrow e^{i\eta_1^\downarrow} A^{\downarrow\dagger}_{\boldsymbol{k}_1} \tag{9.45}$$

$$+ w_2^\uparrow e^{i\eta_2^\uparrow} A^{\uparrow\dagger}_{\boldsymbol{k}_2} + w_2^\downarrow e^{i\eta_2^\downarrow} A^{\downarrow\dagger}_{\boldsymbol{k}_2} \tag{9.46}$$

If we define

$$w_1^\uparrow e^{-i\eta_1^\uparrow} \equiv c_1^\uparrow \tag{9.47}$$

$$w_1^{\downarrow} e^{-i\eta_1^{\downarrow}} \equiv c_1^{\downarrow} \tag{9.48}$$

$$w_2^{\uparrow} e^{-i\eta_2^{\uparrow}} \equiv c_2^{\uparrow} \tag{9.49}$$

$$w_2^{\downarrow} e^{-i\eta_2^{\downarrow}} \equiv c_2^{\downarrow} \tag{9.50}$$

we are able to construct H_1 on the form $\chi_n^\dagger M_n \boldsymbol{A}_n + \boldsymbol{A}_n^\dagger M_n \chi_n$. Furthermore, the w's are real and given by the lenghts of the respective c's. In addition, we have

$$\chi_n^\dagger M_n \chi_n = w_1^{\uparrow} + w_1^{\downarrow} + w_2^{\uparrow} + w_2^{\downarrow} \tag{9.51}$$

We have therefore removed the linear terms, by introducing a shift to the operators and subtracting $\boldsymbol{A}_n^\dagger M_n \boldsymbol{A}_n + \chi_n^\dagger M_n \chi_n$. The term $\boldsymbol{A}_n^\dagger M_n \boldsymbol{A}_n$ is not problematic, as M_n is diagonal. The contribution to the free energy from this term is therefore easily obtained. The term $\chi_n^\dagger M_n \chi$ is operator independent, and can be absorbed into H_0. However, the diagonalisation problem has changed to finding the eigenvalues of the matrix JM, not JM_0. The problem with this method is that the matrix J will be changed. This is due to the relation

$$J_{ij} = [\boldsymbol{A}_i, \boldsymbol{A}_j^\dagger] \tag{9.52}$$

which will lead to a J on the block diagonal form

$$J = \begin{pmatrix} J_0 & 0 \\ 0 & J_n \end{pmatrix} \tag{9.53}$$

where J_0 is the matrix of 1's and -1's along the diagonal pertaining to the operators in $\boldsymbol{A}_0$, and $J_1 = \mathrm{diag}(1,1,1,1,-1,-1,-1,-1)$ pertaining to the operators in $\boldsymbol{A}_n$. Thus this method is not in accordance with the Dynamic Matrix section, since the new matrix J is block-diagonal with 1's and -1's. However, it may be possible to generalize the work done in the Dynamic Matrix section to J's on block-diagonal form

$$J = \begin{pmatrix} J_1 & 0 & 0 & 0 \\ 0 & J_2 & 0 & 0 \\ & & & \\ 0 & 0 & \ddots & 0 \\ 0 & 0 & 0 & J_n \end{pmatrix} \tag{9.54}$$

where J_i is a matix of evenly many 1's and -1's

$$J_i = \begin{pmatrix} 1_m & 0 \\ 0 & -1_m \end{pmatrix} \tag{9.55}$$

The author has not found any papers outlining a method for dealing with linear excitation operators. In addition, since the matrix M is block-diagonal, the eigenvalues of JM are the eigenvalues of $J_0 M_0$, which gives the excitation spectrum, and the eigenvalues of $J_n M_n$, which are only the diagonal entries of $J_n M_n$. Thus the author suspects that the linear terms only contributes with a constant term C_{lin} to the total Hamiltonian.

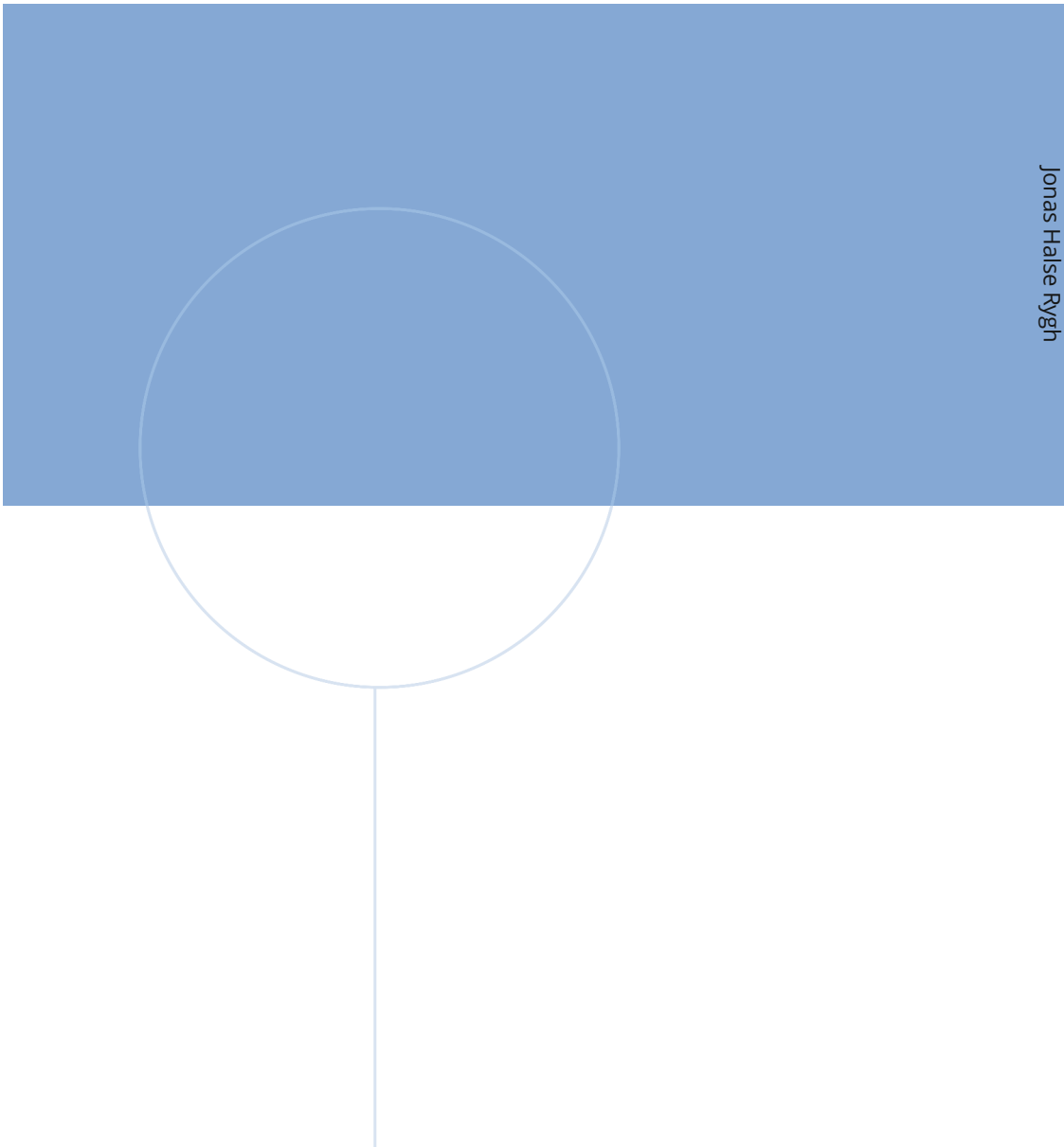

Jonas Halse Rygh

NTNU
Norwegian University of
Science and Technology